2019

Effects Of Tumor-Related Factors And Chemotherapy On Skeletal Muscle And The Protective Effects Of Exercise

Blas Anselmo Guigni
University of Vermont

EFFECTS OF TUMOR-RELATED FACTORS AND CHEMOTHERAPY ON SKELETAL MUSCLE AND THE PROTECTIVE EFFECTS OF EXERCISE

A Dissertation Presented

by

Blas Anselmo Guigni

to

The Faculty of the Graduate College

of

The University of Vermont

In Partial Fulfillment of the Requirements
for the Degree of Doctor of Philosophy
Specializing in Cellular, Molecular and Biomedical Sciences

August, 2019

Defense Date: April 16th, 2019
Dissertation Examination Committee:

Michael Toth, Ph.D., Advisor
Vikas Anathy, Ph.D., Chairperson
Bruce Beynnon, Ph.D.
Jason Stumpff, Ph.D.
Cynthia J. Forehand, Ph.D., Dean of the Graduate College

Abstract

Cancer patients often experience cachexia, a form of weight loss consisting mostly of skeletal muscle wasting. Muscle wasting leads to physical disability, poor quality of life, reduced tolerance to treatments and shorter survival. Although the causes of cancer-related muscle atrophy have been studied for decades, the exact mechanisms through which cancer and its treatments promote muscle wasting have yet to be defined.

The overall aim of this dissertation is to examine the mediators of muscle wasting in cancer patients during their treatment and examine the modulatory role of exercise to maintain muscle size and function. To address these aims, we studied two different populations of cancer patients to examine the effects of tumor-related factors and chemotherapy to cause muscle atrophy using an *in vitro* skeletal muscle system.

We examined whether tumor cells secrete factors to promote atrophy by evaluating the effects of tumor-conditioned media (CM) from murine and human lung tumor cells (hTCM) on cultured muscle myotubes. We hypothesized that conditioned media from murine and human tumor cells would reduce myotube myosin content a marker for atrophy, decrease mitochondrial content, and increase mitochondrial reactive oxygen species production (ROS), all of which have been reported in model systems using murine tumor cell CM.

Cancer patients frequently receive chemotherapy, some of which are known to be myotoxic. Whether these drugs promote muscle wasting, however, is not clear. To address this question, we assessed skeletal muscle structure and protein expression in 13 women diagnosed with breast cancer, who were receiving adjuvant chemotherapy following tumor resection, and 12 non-diseased controls. Furthermore, we evaluated the role of individual chemotherapeutics (doxorubicin and paclitaxel) to cause atrophy, mitochondrial loss and increased reactive oxygen species production in C2C12 cultured muscle myotubes, as well as the modifying effects of a mitochondrial-targeted anti-oxidant.

Pre-clinical models show that exercise protects against the deleterious effects of chemotherapy, although the mechanisms underlying these effects are not known. To address this question, we utilized an *in vitro* model of exercise by treating C2C12 myotubes with doxorubicin (DOX; 0.2 μM for 3 days) with or without daily bouts of electrical field stimulation (STIM).

Our results advance the field by showing that the treatments, and not tumor-related factors, promote skeletal muscle atrophy. Moreover, exercise is effective at countering the deleterious effects of chemotherapy and acts via mechanotransductive signaling pathways.

Citations

Material from this dissertation has been published in the following form:

Guigni, B. A., Callahan, D. M., Tourville, T. W., Miller, M. S., Fiske, B., Voigt, T., . . . Toth, M. J.. (2018). Skeletal muscle atrophy and dysfunction in breast cancer patients: role for chemotherapy-derived oxidant stress. Am J Physiol Cell Physiol, 315(5), C744-C756. doi:10.1152/ajpcell.00002.2018

Acknowledgments

It is difficult to acknowledge all the people who made all this possible. However, I will try to do my best to extend my great appreciation to everyone who helped me scientifically and emotionally throughout this study. Firstly, I would like to express my sincere gratitude to my advisor Dr. Michael Toth for the continuous support of my Ph.D. study and related research, for his patience, motivation, and immense knowledge. I could not have imagined having a better advisor and mentor for my Ph.D. study. I thank all the volunteers for donating their hopes, muscle, and tears, this work was inspired and contributed by you and could not be completed without you. I would like to thank my committee for their insightful comments, encouragement, and various perspectives that widen my research. I thank my parents Fior and Leo, my siblings and the rest of my family, who have always encouraged me and patiently followed my progress. My extended family and friends, who kept an eye on me and occasionally forced me to have fun, my army family for being an interesting distraction, and keeping things in perspective, with constant reminders that my robotic nature and cool demeanor are assets worth exploiting. I thank colleagues from the Toth lab past and present that contributed their time and knowledge to this work. Additionally, I thank my friends and colleagues from the CMB program here at UVM, the members of the COBRE facility and other core facilities that provided their insight, knowledge, and stories over the years. Finally, I thank Lori, whose patience and understanding are beyond reproach, I am blessed to have someone as wonderful as her beside me.

Table of contents

List of tables

List of figures

CHAPTER 1: COMPREHENSIVE LITERATURE REVIEW

A Review on Mediators of Cancer Related Skeletal Muscle Atrophy and the Role of Electrical Stimulation as a Surrogate for Exercise

Blas Guigni and Michael Toth

Department of Molecular Physiology and Biophysics, Department of Medicine, Larner College of Medicine, University of Vermont, Burlington, VT, 05405

Introduction

Cancer-related muscle wasting is a multifactorial condition that negatively affects patients' prognosis and quality of life (84, 113, 164). Traditionally, cachexia has been defined by a specified percentage of weight loss over time (i.e., 5% weight loss in the preceding 6-12 months). However, the assessment of weight loss alone does not reflect the complete scope of pathophysiologic changes or the clinical impact. The severity and phenotypic presentation of cancer-related atrophy may vary, and often muscle wasting may not be diagnosed (5, 42). Regardless, skeletal muscle loss is considered a meaningful prognostic factor during cancer (7) and has been associated with higher incidence of therapy toxicity, increased morbidity, and mortality (129, 156).

The pathogenesis and molecular mechanisms underlying cancer-related muscle wasting have not been fully elucidated. Available evidence suggests an imbalance between the rate of synthesis and protein degradation, although impaired defective myogenesis may contribute as well. In addition, alterations in energy metabolism involving mitochondrial dysfunction have been implicated in the wasting process (2, 41).

Skeletal muscle structure and function

Skeletal muscle fibers (muscle cells) are composed of intracellular contractile proteins called the myofilaments. These myofilaments are made up of bundles of thick and thin filaments that form myofibrils; bundles of myofibrils form muscle fibers; and finally, bundles of muscle fibers are skeletal muscle tissue. The thick myofilaments contain myosin protein and thin myofilaments contain actin protein (Figure 1). The thin and thick filaments, respectively, provide contractility to the cell and are spatially arranged in regular and repetitive structures called the sarcomeres. The interaction of these two myofibrillar proteins allows muscles to contract, and the mechanics of contracture can be classified into fiber types based on different myosin structures (isoforms) or physiologic capabilities (152). The three myosin isoforms that were originally identified in humans were MHCI, MHCIIa, and MHCIIx/d, and they corresponded to the isoforms identified by myosin ATPase staining as types I, IIA, and IIX, respectively (125). In older literature what was originally identified in humans as MHCIIb is actually MHCIIx/d, as humans do not express a fourth and fastest myosin heavy chain isoform (MHCIIb) (65). Although rare, a fiber can have both the MHC I and the MHC IIa isoform and is classified as a hybrid type I/IIa fiber. Similarly, some may have MHC IIa and MHC IIx isoforms termed a hybrid type IIa/IIx fiber. (Table 1) summarizes the properties of the three muscle fiber types found in human skeletal muscle.

Muscle contracture occurs by a process called excitation contracture coupling (EC Coupling), when the release of acetylcholine from the axon ending into the synaptic cleft at the neuromuscular junction, initiates the depolarization of sarcolemma (muscle fiber

membrane), and leads to release of Ca^{2+} ions from the sarcoplasmic reticulum into the sarcoplasm (cytoplasm). Ca^{2+} binds the troponin proteins found on the thin myofilaments, initiating the attachment of actin to the binding site of myosin allowing the muscle contraction process to occur, generating force. There are various molecular signals that mediate skeletal muscle remodeling that will be discussed in the following sections.

Pathways regulating skeletal muscle mass

Muscle atrophy involves the shrinkage of myofibers (decreased muscle fiber cross-sectional area (mCSA)) due to a net loss of proteins partly related to upregulation of degradation pathways, such as the ubiquitin-proteasome system. Recent studies have shown these catabolic pathways modulate one another at different levels, and are coupled to anabolic pathways. The result is a balance between protein breakdown and synthesis that reflects the physiological state of the muscle fiber.

1.1.1 Protein breakdown

Muscle atrophy occurs with a change in the normal balance between protein synthesis and protein degradation. The particular protein degradation pathway, which seems to be responsible for much of the muscle loss seen in atrophy, is the ATP-dependent ubiquitin-proteasome pathway. In muscle, the ubiquitin-proteasome system is required to remove sarcomeric proteins in response to changes in muscle health (13, 26). Skeletal muscle-specific ubiquitin E3 ligases Muscle RING finger 1 (MuRF1) and muscle atrophy F-box (MAFbx)/atrogin-1 have been studied widely and play an essential role during skeletal muscle atrophy (47, 105). This link is further supported by animal studies in mice lacking atrogin-1/MAFbx and MuRF1 (15) that show both are needed for atrophy, with other more recent studies showing MuRF1 not atrogin-1 knockout mice to be resistant to dexamethasone-induced muscle atrophy (6). Additionally, MuRF1 has been reported to interact with and control the half-life of important muscle structural proteins such as myosin (25, 26, 43), suggesting that MuRF1 plays a dominant role in various skeletal muscle atrophy conditions. It has also been reported that upregulation of

these proteins is time-dependent, with no changes in MuRF1 expression seen with a prolonged catabolic stimulus (119). Forkhead box class O family member proteins (FoxOs) are transcription factors that play important roles in regulating the expression of genes involved in cell growth. Four FoxO members in humans, FoxO1, FoxO3, FoxO4, and FoxO6, are all expressed in skeletal muscle, but FoxO1, FoxO3 members are the most studied in muscle. FoxO1 and FoxO3 are key factors of muscle protein breakdown, as the major transcription factors regulating both the MuRF1 and MAFbx expressions (142, 153), with FoxO3a implicated as a major regulator in several disease states (1, 120, 182, 183). FoxO/MuRF1 signaling proteins are regulated on several fronts. In skeletal muscle, the most studied post-translational modification of FoxOs is phosphorylation. 5' adenosine monophosphate-activated protein kinase (AMPK) and Protein kinase B (PKB), also known as (Akt) have opposite effects on FoxO3 localization and activity.

AMPK plays a role in cellular energy homeostasis when cellular energy is low it phosphorylates FoxO3 at two regulatory sites (Ser-413/588) in skeletal muscle, leading to its activation under stress conditions (115, 118, 140). Moreover, AMPK activation is associated with increasing levels of FoxO1 and FoxO3 mRNAs and protein content (118).

Akt is a serine/threonine protein kinase that plays a key role in insulin and PI3K/Akt/mTOR signaling pathways, contributing to the regulation of energy metabolism and protein synthesis. An essential regulator of FoxO activity, it inhibits FoxO1, 3 and 4 by phosphorylation (Ser-253/315, Thr 32) under mitogenic activation

(153) (Figure 2), preventing up-regulation of numerous ubiquitin–proteasome and autophagy-related genes in muscle.

Another regulator of skeletal muscle atrophy is nuclear factor-kappaB (NF-κB), which is a major regulator of gene transcription in response to oxidative, energetic, and mechanical stress in skeletal muscle. Chronic activation of this signaling pathway has been implicated in the development of various pathologies, such as cancer-related muscle wasting. NF-κB transcription factors, which are expressed in skeletal muscle, mediate the effect of inflammatory cytokines, particularly tumor necrosis factor-α (TNFα), on muscle wasting (124). TNFα is thought to act via Mitogen-activated protein kinases (MAPKs) to stimulate expression of the ubiquitin ligase atrogin1/MAFbx and MuRF1in skeletal muscle (71, 89). Indeed, muscle-specific overexpression of NF-κB regulators in mice has led to severe muscle wasting mediated, at least in part, by MuRF1activity (16, 101).

Other degradation pathways in skeletal muscle include the Ca2+-dependent proteases, lysosomal system, and caspases, these pathways will not be covered in this review. However, Akt regulates both the ubiquitin-proteasome system and the autophagy-lysosome pathway, and this action is mediated by FoxO transcription factors.

1.1.2 Protein synthesis

The growth of skeletal muscle mass, like the mass of any other tissue, depends on protein turnover and cell turnover (143). Cellular turnover plays a major role during muscle development in the embryo. Moreover, satellite cell incorporation into the

growing fibers takes place during postnatal muscle growth (110) simultaneously with increased protein synthesis. However, the contribution of cellular turnover in adult fibers is minor, and its role in hypertrophy has been recently debated (80, 96). In adult muscle, the physiological conditions promoting muscle growth are mainly related to increasing protein synthesis and decreasing protein degradation. However, satellite cells are activated in compensatory hypertrophy (80, 110), and the addition of new nuclei to the growing fiber seems to be required for extreme hypertrophy and therefore cannot be completely discounted as a contributing mechanism. The pathways controlling cellular and protein turnover are different, and their contribution to muscle hypertrophy has to be considered.

Under normal physiological condition, the IGF-1-Akt-mTOR pathway is a key regulator of protein synthesis in skeletal muscle (59, 145) with downstream of Akt that include glycogen synthase kinase 3, the mammalian target of rapamycin (mTOR), $p70^{S6K}$, and PHAS-1 (4EBP-1), all key regulatory proteins involved in translation and protein synthesis (56, 135). Changes in the Akt/mTOR and Akt/GSK3 pathways induced skeletal myotube hypertrophy (135). Indeed, genetic models that overexpress or code constitutively active forms Akt induced muscle fiber hypertrophy both *in vivo* (122) and *in vitro* (83, 136). Knockout models of Akt display growth defects (133), and those in which Akt and a related gene, Akt2, are both disrupted undergo skeletal muscle atrophy (137).

1.1.3 Skeletal muscle mitochondrial homeostasis

Several metabolic adaptations occur in atrophying muscles. In many forms of muscle wasting, expression of a variety of enzymes important for oxidative phosphorylation is suppressed (29). Dysfunctional mitochondria, in particular, are thought to play a key role in muscle function decline, as the mitochondria are the main producers of both cellular energy and free radicals. Mitochondrial dysfunction has been tightly associated with excess production of reactive oxygen species (ROS) (97). Chronically elevated ROS can initiate DNA damage, protein oxidation, increased oxidative damage and reduced oxidative capacity. These biochemical changes are accompanied by changes in skeletal muscle dynamics, such as a decrease in mitochondrial biogenesis and an increase in autophagy/mitophagy (Figure 3). Mitochondria are dynamic, existing in networks that are constantly being remodeled by biogenesis, fusion and fission, and degradative processes.

Recent studies have shown that PGC-1α, the master regulatory gene for mitochondrial biogenesis, is downregulated in different models of muscle wasting (74). Indeed, when the levels of PGC-1α are maintained, either by the use of transgenic mice or by transfecting adult muscle fibers, muscles are protected from the atrophy induced by denervation, fasting, or expression of FoxO3 (74, 75, 165). PGC-1α is triggered when the energy demand exceeds respiratory capacity, in response to exercise, stress, and ROS production (66). PGC-1α also activates the nuclear respiratory factors 2 (Nrf-2) (76), thereby driving the transcription of other proteins that are linked with mitochondrial health and skeletal muscle homeostasis via the regulation of ROS (79). Excessive

mitochondrial ROS are associated with oxidative damage and disease states (150, 167). This is supported by studies that utilize mitochondria-targeted antioxidants that have been shown to be beneficial against skeletal muscle atrophy and mitochondrial dysfunction (17, 104).

1.1.4 Tumor Factors

For the last seven decades, there have been attempts to identify and understand what secreted factors from tumors signal skeletal muscle atrophy. In this search, various cytokines and catabolic factors that could regulate the loss of skeletal muscle mass have been identified (108, 112). These pro-inflammatory and pro-catabolic factors are thought to be produced by the tumor cells and have important roles in the development of cancer-related atrophy. For instance, pro-inflammatory cytokines, such as tumor necrosis factor alpha (TNF)-α, interleukin (IL)-1, IL-6, and anti-inflammatory cytokine such as IL-10, promote the activation of factors associated with muscle wasting. These factors cooperate with each other or act alone as drivers of systemic inflammation. The molecular mechanisms by which these pro-inflammatory factors may contribute to the development of skeletal muscle atrophy have been linked to the activation of various downstream molecules in muscle and fat.

1.1.4.1 Increase Protein break down

TNF-α has been reported to be upregulated in several forms of cancer (46, 48) and is linked to the catabolism of various myofibrillar proteins in the myotubes via activation of nuclear transcription factor-kappaB (NF-κB) through IkB kinase signaling (71). The activated NF-κB increases the transcription of genes such as MuRF1 that specifically degrades myofibrillar proteins such as myosin, contributing to the loss of lean body mass during cancer-related atrophy (23, 30, 95). Similarly, IL-6 induces

apoptosis in skeletal muscles by increased caspase activity via activation MAPK cascades (61, 159).

1.1.4.2 Reduce protein synthesis

Along with the TNF-α and IL-6, recent preclinical studies in murine models of cancer-related muscle wasting demonstrated that higher levels of IL-10 inhibited protein synthesis in skeletal muscles via increased levels of Myc and activation of mTOR signaling (4, 134). This link to cancer-related muscle wasting is predominantly based on the concept of tumors reprograming host metabolism (44).

Metabolic reprogramming has been linked with proteolysis-inducing factor (PIF) which acts by decreasing protein synthesis through phosphorylation of eukaryotic translation initiation factor 2α and accelerating protein degradation through the ubiquitin-proteasome pathway promoting skeletal muscle atrophy (160, 166). In addition to pro-inflammatory cytokines, myostatin is another muscle-wasting factor that is secreted by the skeletal muscles, adipose tissue, and tumor cells (60, 149, 178). Myostatin acts via activin receptor type II-mediated signaling and regulates muscle wasting (37, 109, 161). Further to the pro-inflammatory and atrophic factors, cancer-related muscle wasting is associated with other host factors such as neuroendocrine stress responses via the release of glucocorticoids (158, 163). Though the muscle cells and nervous system crosstalk is not fully elucidated, it is thought that this mechanism is complex, and further studies are needed to understand the role of pituitary hormones in inducing muscle wasting and lipolysis.

1.1.5 Chemotherapy

Chemotherapy treatments are a combination of drugs administered in a standardized treatment regimen, specific for the cancer type. Various interactive effects of different drugs could occur; leading to numerous deleterious consequences to normal tissues, including pulmonary toxicity, myotoxicity, mitotoxicity, and cardiotoxicity. How these various compounds may induce atrophy in cancer patients is poorly characterized, and the breadth of literature on the topic is significantly less than tumor factors. However, the direct effects of systemically administered chemotherapeutic agents, which circulate to all tissues in the blood, are prime candidates. Non-tumor tissues, including skeletal muscle, are exposed to a variety of chemotherapy-related toxic effects over the course of treatment with most standard chemotherapy regimens. These include repeated cycles of acute exposure to high levels of oxidative stress (24) which disrupt a wide range of cellular functions.

1.1.5.1 Doxorubicin

Anthracyclines such as doxorubicin are thought to produce their biologic activity principally via interaction with topoisomerase II and subsequent double-stranded DNA breaks (28, 68, 155), however, defects in mitochondrial biogenesis and the production of reactive oxygen (68, 155) has been reported in several studies. Muscle toxicity of anthracyclines is mediated through increased production of reactive oxygen species (ROS) by muscle mitochondria and increased catabolic processes that upregulate MuRF1and impair contractile function (77, 179).

Different tissues accumulate anthracycline-induced mitochondrial damage at varying rates, in rats defective mitochondrial respiratory enzyme activity and increased ROS production are observed in renal (86) tissues, 6–7 months after the end of treatment. Existing studies in tissue culture, rodents, and humans show acute negative effects of anthracyclines such as doxorubicin on skeletal muscle. Administration of doxorubicin induces skeletal muscle mitochondrial ROS, increases proteolysis and leads to muscle weakness (53-55). Direct injection of doxorubicin into skeletal muscle causes atrophy, and altered myofilament structure humans and rodents (98, 172).

Cardiac toxicity is also a well-known side effect of anthracycline chemotherapy and has been the subject of numerous investigations (85), showing that this cardiotoxicity is increased with higher cumulative doses (40). Cardiotoxicity is a dose-limiting side effect of doxorubicin (22).

1.1.5.2 Cisplatin

Cisplatin is a platinum-based anti-cancer drug common in breast, and lung cancers (35), and is thought to interfere with DNA replication, targeting the fastest proliferating cells. It has a number of side effects that can limit its use to include nephrotoxicity and neurotoxicity, with the former being a dose-limiting side effect (103). The mechanisms by which cisplatin affects skeletal muscle, however, are less well described. Cisplatin produces significant muscle atrophy in mice, via the activation of NF-κB; however, other studies have demonstrated that F-box, MuRF1, and FoxO3 are significantly increased with cisplatin treatment (138, 175). These increases of catabolic markers have also been linked to transient and acute reduction of protein synthesis in both healthy and tumor-

bearing mice (139). Both these types of cellular toxicity are potentially relevant in initiating changes in muscle tissue which lead to the long-term functional deficits.

1.1.5.3 Paclitaxel

Taxane drugs, such as paclitaxel and docetaxel, are chemotherapeutic agents, which work by disrupting microtubule function to inhibit cell division. Taxanes have become a common agent primarily against breast cancer, metastatic prostate cancer, and non-small cell lung cancer due to its efficacy in solid tumors. These drugs are believed to induce sensory and motor neuropathy by impairing axon structure and function, most specifically by inducing mitochondrial and vascular dysfunction (127). Other side effects of taxane treatment are pain in the joints and muscles, occurring 2 to 3 days after paclitaxel treatment (52). There are currently no comprehensive studies looking at the mechanisms for which paclitaxel or other taxanes may induce skeletal muscle atrophy. However, studies have looked at the consequences of impairing microtubule dynamics in skeletal muscle. The microtubule cytoskeleton in skeletal muscle resists mechanical perturbation acting as a mechanotransducer (27, 151) allowing the cell to respond mechanically to the environment. Animal studies have shown that disrupting the tubulin dynamics with paclitaxel in skeletal muscle increases cellular ROS and oxidase-dependent production of ROS (78). Indeed tubulin has been implicated regulating mitochondrial bioenergetics and that paclitaxel treatment impaired mitochondrial ADP/ATP exchange resulting in greater H2O2 emission kinetics.

1.1.5.4 Glucocorticoids

Drugs such as dexamethasone and prednisone are frequently used for their anti-emetic properties around the time of chemotherapy (90, 116, 148). During the administration of glucocorticoids, especially prolonged courses or higher doses, skeletal muscle atrophy can be expected (8, 14). Additionally, glucocorticoid treatment-related myopathy is reported to be more pronounced in proximal muscles and fast twitch (type II) fibers (144). There is still research as to whether high dose glucocorticoids contribute to long-term muscle dysfunction, there is evidence that prolonged corticosteroid use can induce muscle mitochondrial dysfunction and increased oxidative damage to both nuclear and mtDNA (106).

1.1.5.5 Other chemotherapies

Other chemotherapy drugs have also been associated with skeletal muscle dysfunction, but evidence of a direct effect on skeletal muscle is currently less characterized than the agents discussed above (35, 70). However, there is not yet enough clinical follow-up data to know whether these newer drugs also have deleterious long-term impacts on skeletal muscle or other tissues. Thus, it remains possible that the specific agents discussed above, used in the treatment of cancer have a synergistic impact on muscle, distinguishing the role of each drug in causing muscle dysfunction in an *in vivo* setting is extremely challenging. Nevertheless, models to help elucidate these mechanisms are being utilized.

With the current treatment regimens leading to higher cancer survival rates, we can anticipate that these agents will continue to be used, increasing the number of cancer survivors. Deficits in skeletal muscle and function have been reported to persist many years after successful treatment (19, 176), implicating anti-cancer treatments themselves as the likely cause of long-term muscle dysfunction.

Exercise

Although cancer treatments, such as chemotherapy, can be efficacious, they can lead to long-term side effects such as fatigue, muscle loss, and reductions in functional capacity (31). However, currently, there are no effective treatments specifically targeting cancer related skeletal muscle atrophy. Cancer-related muscle atrophy is a multi-factorial syndrome that may require an approach that targets the different factors involved. Historically, clinical interventions and studies have focused on stabilizing and improving the nutritional status, finding novel biomarkers, and developing better techniques for the estimation of muscle mass. However, there is new interest in exercise training and muscle loss prevention in cancer patients (100, 128, 171). Exercise training has an important role in skeletal muscle plasticity, acting on several pathways and possessing multifactorial effects. Within the muscle, it has anabolic and catabolic effects, it exerts anti-inflammatory effects, and it has anti-oxidative implications (88).

1.1.6 Exercise-related mechanisms

For a skeletal muscle to undergo exercise-specific adaptations, it must both sense and transmit the information that is unique to each type of exercise stimulus. The force generated in sarcomeres is transferred to the extracellular matrix via focal adhesions, where the actin cytoskeleton is connected via linker proteins to the extracellular-matrix-bound trans-membranous integrins (Figure 5). Changes in mechanical stress are responsible for changes in the multiprotein complexes called costameres in skeletal muscle involved in mechanotransduction and mechano-sensing (167). The transmission

of this information is mediated by signaling pathways that rely on the use of reversible posttranslational modifications to transmit information. Physiological stressors that are active during exercise have been identified: mechanical load, neuronal activation, hormonal adjustments and metabolic disturbances (45). During exercise at a specific intensity and over a defined period of time, muscle tissue experiences a particular blend of these fundamental stressors (63). With strength training, the mechanical stress is dominant, while during endurance exercise, mechanical stress is low but metabolic disturbances can protract. A single bout of physical activity/exercise induces muscle molecular signaling pathways linked to anabolic/catabolic processes that have documented effects on muscle health. Furthermore, repeated bouts of activity can stimulate beneficial mechanical adaptations (102). These acute responses and chronic adaptations to exercise have utility for improving muscle function (62).

In healthy groups, a single bout of exercise mechanical stress can stimulate protein synthesis, which remains elevated for several hours following contraction (34). The duration and extent of this induction can be affected by exercise type (endurance vs resistance), intensity and workload of muscle, but have been shown to induce signaling through extracellular regulated kinase, stress-activated protein kinase and protein kinase such as Akt, and ribosomal S6 kinase (3, 38, 170, 173). In preclinical studies, the ability of muscle contraction to induce protein synthesis has implications for cancer-related muscle wasting in which Akt/mTORC1 signaling may be disrupted (169). Skeletal muscle mass depends on mechanical stresses induced during specific exercise types.

Acute exercise can accelerate protein turnover and may serve to replace damaged proteins, which is necessary for the maintenance of muscle homeostasis. Repeated exercise training can decrease the indices of protein breakdown in muscle, which may be related to improved protein quality (16). Additionally, muscle protein breakdown is stimulated by both acute endurance and resistance exercise (162, 174) related to the need to clear damaged proteins induced by contraction or mechanical loading. Protein turnover and homeostasis have been shown in animal models were voluntary running decreased Murf1 expression and autophagy protein expression when induced via catabolic compounds (126).

Muscle oxidative metabolism is also modified with acute and repeated exercise, expression of several mitochondrial proteins such as PGC-1α, and Nrf (57) have been reported. Evidence also suggests that resistance exercise can improve mitochondrial quality and function via mTORC1 inducing muscle PGC-1α protein expression (33) increasing mitochondrial gene expression and oxidative function (181). Endurance exercise can also positively regulate mitochondrial dynamics through modification of fusion and fission protein expression (36). Damaged or dysfunctional mitochondria removal has also been identified as an important exercise benefit (180).

1.1.7 Neuromuscular electrical stimulation

Exercise is not always possible due to treatment complications or contraindications to aerobic exercise and resistive training. Reports suggest that only ~ 35% of cancer survivors achieve current recommendations (94, 154) with breathlessness, fatigue, weakness, and poor balance cited as common issues affecting

basic exercise participation such as walking (92). Thus, pragmatic alternatives to traditional exercise methods are required.

Neuromuscular electrical stimulation (NMES) involves controlled muscular contractions generated by electrical impulses delivered through surface electrodes, usually placed on major muscle groups such as the quadriceps and hamstrings (69). The evoked contractions have proven efficacy in improving muscle strength and cardiorespiratory fitness across a variety of populations (9, 20, 21, 32). Thus, physician-supervised NMES exercise to enhance the neuromuscular systems has applicability within the cancer population to prevent the complications associated with treatment and improve health-related quality of life. However, NMES uptake clinically is low (93) and currently, no published, high-level evidence supports its application in cancer survivorship. Although experimental evidence in different populations highlights the efficacy of NMES, there is a need to evaluate the efficacy in cancer patients and cancer survivors before it can be implemented into cancer care pathways. Previous work in NMES and cancer has focused on tetanic, muscle strengthening protocols, nonetheless, the mechanisms that lead to the reported beneficial effects of NMES is poorly characterized, leaving a gap in the field that needs to be filled.

Models

Although atrophy is a common outcome of experimental and human cancer cachexia, discrepancies in the mechanisms underlying cancer-related muscle wasting have been reported between different experimental models as well as in patients with different tumor types, with limited available data in humans (71, 111). These differences in experimental design and clinical outcomes hinders the development of therapeutic strategies and underscore the need for more research on patients and the development of pre-clinical models that closely emulate the clinical scenario (123). Currently, most clinical trials on cancer-related atrophy have been conducted in patients very advanced in their disease trajectory, or in animal models with exaggerated clinical phenotypes lacking physiological relevance. This leads to speculation that some reported outcomes are an artifact of experimental design or limited clinical evaluation (130). Using a simplified system such as a cell line offers advantages in experimental design such as consistency, availability, robust cell growth, and simple manipulation. There is the caveat that immortalized cell lines often have been cultured for very long periods of time, which may lead to changes in normal function. However, these deviations are limited and can be mitigated with proper controls, with the additional advantages of reducing animals use and easy transfection. Another option for cell culture is the use of primary human skeletal cells, however; there are several issues that need to be considered. With primary skeletal muscle cells, the amount and source of the tissue can vary, leading to varying results in mechanical and biochemical results depending on the fiber types, there is also the limited passage capacity of primary cells, and the difficulty in keeping a primary line going.

However, the commercially available mouse-derived muscle cell line C2C12 is frequently used to study intracellular signaling and function in skeletal muscle cells.

1.1.8 C2C12 model

The immortalized cell line designated C2C12 were generated by Blau, Chiu, and Webster (11) as a subclone of the C2 cell line isolated by Yaffe and Saxel at the Weizmann Institute of Science in Israel in 1977 (177). C2C12 cells were originally derived from satellite cells from the thigh muscle of 2-month old female C3H dystrophic mice 70 h after a crush injury. The C2C12 cell line differentiates rapidly, forming contractile myotubes and producing characteristic muscle proteins. These proteins include slow- and fast-twitch skeletal muscle myosin isoforms (132) with fast myosin Type IIx the most dominant isoform (18, 146), along with other important sarcomeric proteins involved with contracture (121, 168). These cells have similar characteristics to those of isolated human skeletal muscle cells (51, 87, 91), and have been utilized in several experiments as a model of contraction.

C2C12 cells are capable of rapid proliferation under high serum conditions and can later fuse to form multinucleated myotubes under low serum conditions or starvation, leading to the precursors of contractile skeletal muscle cells in the process of myogenesis (12). Myogenesis in C2C12 can be controlled by genetic manipulation, making it a powerful system for studying muscle development (10). The molecular regulators of myogenic differentiation in C2C12 including the paired box transcription factors Pax7 and the myogenic regulatory factors Myf5, MyoD, myogenin (49, 81), that have been used as early markers of differentiation and maturity in myotubes. Studies have shown

that within two days of differentiation, the normal cells form spindle-shaped mononucleated myoblasts that are in the process of cell migration and fusion (168). By 4-5 days, multinucleated myotube networks formed and some ultrastructure such as unorganized precursor to sarcomeres are visible (82). By 6-8 days sarcomeres and Z-lines could be observed (168) the myofibril content appear to be increased, and the sarcomeres are present across the width of myotubes (Figure 4) (99). By this point in their development C2C12 cells demonstrate maturation into functional muscle having the ability to contract and generate force (99).

C2C12 *in vitro* cells are also a great model for testing physiological stresses, determining their relevance and functions to humans (73). Through literature review, it was found that the most effective functional assay, due to their differentiation and contractile dynamics, is their response to electrical stimulation, since C2C12 myotubes when mature express calcium ion channels and are able to trigger the contraction/relaxation cycle at various voltages (58). These known characteristics of the C2C12 make it a viable cell line to test the effects of exercise/NMES against various catabolic environments present during cancer-related atrophy.

1.1.9 Electrical stimulation in a model system

C2C12 myotubes can grow on various surfaces when appropriate matrix proteins are in place and electrically stimulated with commercially available carbon electrodes (50, 117). This system is easy to manipulate and is useful for analyzing the biochemical and molecular biological phenomena induced by muscle contraction. However, there are fundamental differences between physiological contractions and those evoked by some *in*

vitro STIM protocols. During exercise, muscle contractions are generated due to the activation of motor units by action potentials. Moreover, the frequency is modulated to match the requested power output, and the motor units in a contracting muscle are not simultaneous but alternately activated (107), making it difficult to estimate the duration of each stimulus. It is difficult to evaluate which STIM protocol mimics more an endurance-type or resistance-type *in vivo* exercise. An approach to overcome the limitation of an undefined STIM protocol was presented by Sciancalepore *et al.* who recorded electromyographs of human gastrocnemius medialis during activity (147) and then applied this stochastic STIM pattern to primary myotubes with varied results. As novel as this approach was most current STIM studies have used two different approaches of either high-frequency protocols with rest periods in-between short pulses or with a constant frequency over several hours up to 48 h without resting period (157). Either of which does not accurately reflect the *in vivo* conditions patient muscles are exposed to during exercise but do emulate extreme weight lifting or ultra-long distance running. Others have applied more exercise relevant STIM methodology of low volts and frequency for 30- 60 minutes (72, 114) however, most have not applied it over a multi-day period, providing only acute results. A STIM protocol that could be implemented over several days, to test the chronic effects of exercise, and best emulate *in vivo* exercise conditions was lacking in the literature, and development of one was needed for future studies.

With all the controls in place, there are still limitations to an *in vitro* STIM system, blood flow, and innervation, which are important for feedback regulations to meet the metabolic demands of working muscle *in vivo* cannot be emulated *in vitro*. In

addition, muscle fibers *in vivo* are in a 3D environment surrounded by connective tissue and extracellular matrix, which might affect transcriptional activation of genes in contracting cells, as well as protein release (39) which are difficult to replicate *in vitro,* as the exact substrate demand of myotubes subjected to STIM is unknown. Moreover, *In vivo* skeletal muscle is also connected to the skeleton via tendons, and during contractions, the mechanical load is applied to the myofibers. Using inappropriate conditions or too long stimulation might result in detachment of myotubes, compromised cellular integrity, and damage of cells, as outlined above. Although cultured myotubes are attached to the surface of the culture dish during STIM, the mechanical load is not comparable nevertheless, cell culture allows for the standardization of all these conditions allotting for reproducibility. Finally, some side effects of STIM have to be considered, in particular when long-term stimulation is performed.

Conclusion

Although the factors that lead to cancer-related muscle wasting are still debated, the current paradigm is focused on the pathophysiological state of anabolism and catabolism dysregulation, with decreased protein synthesis and increased MuRF1 expression. Physical activity and exercise are already thought to be beneficial during cancer treatment and holds clear potential as a nonpharmacological treatment for muscle wasting conditions. Emerging evidence from preclinical models suggests an interaction between increased physical activity/exercise and improvements in muscle mass and mitochondrial function, possibly mediated via the contracture of muscle. However, the complexity of etiology and the manifestation of the symptoms will likely need a multimodal format approach to treatment. Further research is warranted to determine the mechanistic basis of these improvements and if these benefits can be achieved with surrogates of exercise such as with NMES.

References:

1. **Al-Nassan S, and Fujino H**. Exercise preconditioning attenuates atrophic mediators and preserves muscle mass in acute sepsis. *Gen Physiol Biophys* 37: 433-441, 2018.

2. **Argiles JM, Busquets S, Stemmler B, and Lopez-Soriano FJ**. Cancer cachexia: understanding the molecular basis. *Nat Rev Cancer* 14: 754-762, 2014.

3. **Atherton PJ, and Smith K**. Muscle protein synthesis in response to nutrition and exercise. *J Physiol* 590: 1049-1057, 2012.

4. **Aust S, Knogler T, Pils D, Obermayr E, Reinthaller A, Zahn L, Radlgruber I, Mayerhoefer ME, Grimm C, and Polterauer S**. Skeletal Muscle Depletion and Markers for Cancer Cachexia Are Strong Prognostic Factors in Epithelial Ovarian Cancer. *PLoS One* 10: e0140403, 2015.

5. **Aversa Z, Costelli P, and Muscaritoli M**. Cancer-induced muscle wasting: latest findings in prevention and treatment. *Ther Adv Med Oncol* 9: 369-382, 2017.

6. **Baehr LM, Furlow JD, and Bodine SC**. Muscle sparing in muscle RING finger 1 null mice: response to synthetic glucocorticoids. *J Physiol* 589: 4759-4776, 2011.

7. **Baracos VE, Martin L, Korc M, Guttridge DC, and Fearon KCH**. Cancer-associated cachexia. *Nat Rev Dis Primers* 4: 17105, 2018.

8. **Batchelor TT, Taylor LP, Thaler HT, Posner JB, and DeAngelis LM**. Steroid myopathy in cancer patients. *Neurology* 48: 1234-1238, 1997.

9. **Bax L, Staes F, and Verhagen A**. Does neuromuscular electrical stimulation strengthen the quadriceps femoris? A systematic review of randomised controlled trials. *Sports Med* 35: 191-212, 2005.

10. **Bi P, Ramirez-Martinez A, Li H, Cannavino J, McAnally JR, Shelton JM, Sanchez-Ortiz E, Bassel-Duby R, and Olson EN**. Control of muscle formation by the fusogenic micropeptide myomixer. *Science* 356: 323-327, 2017.

11. **Blau HM, Chiu CP, and Webster C**. Cytoplasmic activation of human nuclear genes in stable heterocaryons. *Cell* 32: 1171-1180, 1983.

12. **Blau HM, Pavlath GK, Hardeman EC, Chiu CP, Silberstein L, Webster SG, Miller SC, and Webster C**. Plasticity of the differentiated state. *Science* 230: 758-766, 1985.

13. **Bodine SC, and Baehr LM**. Skeletal muscle atrophy and the E3 ubiquitin ligases MuRF1 and MAFbx/atrogin-1. *Am J Physiol Endocrinol Metab* 307: E469-484, 2014.

14. **Bodine SC, and Furlow JD**. Glucocorticoids and Skeletal Muscle. *Adv Exp Med Biol* 872: 145-176, 2015.

15. **Bodine SC, Latres E, Baumhueter S, Lai VK, Nunez L, Clarke BA, Poueymirou WT, Panaro FJ, Na E, Dharmarajan K, Pan ZQ, Valenzuela DM, DeChiara TM, Stitt TN, Yancopoulos GD, and Glass DJ**. Identification of ubiquitin ligases required for skeletal muscle atrophy. *Science* 294: 1704-1708, 2001.

16. **Bonaldo P, and Sandri M**. Cellular and molecular mechanisms of muscle atrophy. *Dis Model Mech* 6: 25-39, 2013.

17. **Broome SC, Woodhead JST, and Merry TL**. Mitochondria-Targeted Antioxidants and Skeletal Muscle Function. *Antioxidants (Basel)* 7: 2018.

18. **Brown DM, Parr T, and Brameld JM**. Myosin heavy chain mRNA isoforms are expressed in two distinct cohorts during C2C12 myogenesis. *J Muscle Res Cell Motil* 32: 383-390, 2012.

19. **Brown JC, and Schmitz KH**. Weight lifting and appendicular skeletal muscle mass among breast cancer survivors: a randomized controlled trial. *Breast Cancer Res Treat* 151: 385-392, 2015.

20. **Carty A, McCormack K, Coughlan GF, Crowe L, and Caulfield B**. Increased aerobic fitness after neuromuscular electrical stimulation training in adults with spinal cord injury. *Arch Phys Med Rehabil* 93: 790-795, 2012.

21. **Caulfield B, Prendergast A, Rainsford G, and Minogue C**. Self directed home based electrical muscle stimulation training improves exercise tolerance and strength in healthy elderly. *Conf Proc IEEE Eng Med Biol Soc* 2013: 7036-7039, 2013.

22. **Chatterjee K, Zhang J, Honbo N, and Karliner JS**. Doxorubicin cardiomyopathy. *Cardiology* 115: 155-162, 2010.

23. **Chen C, Ju R, Zhu L, Li J, Chen W, Zhang DC, Ye CY, and Guo L**. Carboxyamidotriazole alleviates muscle atrophy in tumor-bearing mice by inhibiting NF-kappaB and activating SIRT1. *Naunyn Schmiedebergs Arch Pharmacol* 390: 423-433, 2017.

24. **Chen CY, Liu TZ, Chen CH, Wu CC, Cheng JT, Yiin SJ, Shih MK, Wu MJ, and Chern CL**. Isoobtusilactone A-induced apoptosis in human hepatoma Hep G2 cells is mediated via increased NADPH oxidase-derived reactive oxygen species (ROS) production and the mitochondria-associated apoptotic mechanisms. *Food Chem Toxicol* 45: 1268-1276, 2007.

25. **Clarke BA, Drujan D, Willis MS, Murphy LO, Corpina RA, Burova E, Rakhilin SV, Stitt TN, Patterson C, Latres E, and Glass DJ**. The E3 Ligase MuRF1 degrades myosin heavy chain protein in dexamethasone-treated skeletal muscle. *Cell Metab* 6: 376-385, 2007.

26. **Cohen S, Brault JJ, Gygi SP, Glass DJ, Valenzuela DM, Gartner C, Latres E, and Goldberg AL**. During muscle atrophy, thick, but not thin, filament components are degraded by MuRF1-dependent ubiquitylation. *J Cell Biol* 185: 1083-1095, 2009.

27. **Collinsworth AM, Zhang S, Kraus WE, and Truskey GA**. Apparent elastic modulus and hysteresis of skeletal muscle cells throughout differentiation. *Am J Physiol Cell Physiol* 283: C1219-1227, 2002.

28. **Congras A, Caillet N, Torossian N, Quelen C, Daugrois C, Brousset P, Lamant L, Meggetto F, and Hoareau-Aveilla C**. Doxorubicin-induced loss of DNA topoisomerase II and DNMT1- dependent suppression of MiR-125b induces chemoresistance in ALK-positive cells. *Oncotarget* 9: 14539-14551, 2018.

29. **Constantinou C, Fontes de Oliveira CC, Mintzopoulos D, Busquets S, He J, Kesarwani M, Mindrinos M, Rahme LG, Argiles JM, and Tzika AA**. Nuclear magnetic resonance in conjunction with functional genomics suggests mitochondrial dysfunction in a murine model of cancer cachexia. *Int J Mol Med* 27: 15-24, 2011.

30. **Costelli P, Muscaritoli M, Bossola M, Penna F, Reffo P, Bonetto A, Busquets S, Bonelli G, Lopez-Soriano FJ, Doglietto GB, Argiles JM, Baccino FM, and Rossi Fanelli F**. IGF-1 is downregulated in experimental cancer cachexia. *Am J Physiol Regul Integr Comp Physiol* 291: R674-683, 2006.

31. **Courneya KS, and Friedenreich CM**. Framework PEACE: an organizational model for examining physical exercise across the cancer experience. *Ann Behav Med* 23: 263-272, 2001.

32. **Crognale D, Vito GD, Grosset JF, Crowe L, Minogue C, and Caulfield B**. Neuromuscular electrical stimulation can elicit aerobic exercise response without undue discomfort in healthy physically active adults. *J Strength Cond Res* 27: 208-215, 2013.

33. **Cunningham JT, Rodgers JT, Arlow DH, Vazquez F, Mootha VK, and Puigserver P**. mTOR controls mitochondrial oxidative function through a YY1-PGC-1alpha transcriptional complex. *Nature* 450: 736-740, 2007.

34. **Cuthbertson DJ, Babraj J, Smith K, Wilkes E, Fedele MJ, Esser K, and Rennie M**. Anabolic signaling and protein synthesis in human skeletal muscle after dynamic shortening or lengthening exercise. *Am J Physiol Endocrinol Metab* 290: E731-738, 2006.

35. **Damrauer JS, Stadler ME, Acharyya S, Baldwin AS, Couch ME, and Guttridge DC**. Chemotherapy-induced muscle wasting: association with NF-kappaB and cancer cachexia. *Eur J Transl Myol* 28: 7590, 2018.

36. **Ding H, Jiang N, Liu H, Liu X, Liu D, Zhao F, Wen L, Liu S, Ji LL, and Zhang Y**. Response of mitochondrial fusion and fission protein gene expression to exercise in rat skeletal muscle. *Biochim Biophys Acta* 1800: 250-256, 2010.

37. **Ding H, Zhang G, Sin KW, Liu Z, Lin RK, Li M, and Li YP**. Activin A induces skeletal muscle catabolism via p38beta mitogen-activated protein kinase. *J Cachexia Sarcopenia Muscle* 8: 202-212, 2017.

38. **Egan B, and Zierath JR**. Exercise metabolism and the molecular regulation of skeletal muscle adaptation. *Cell Metab* 17: 162-184, 2013.

39. **Engler AJ, Griffin MA, Sen S, Bonnemann CG, Sweeney HL, and Discher DE**. Myotubes differentiate optimally on substrates with tissue-like stiffness: pathological implications for soft or stiff microenvironments. *J Cell Biol* 166: 877-887, 2004.

40. **Ewer MS, and Ewer SM**. Cardiotoxicity of anticancer treatments: what the cardiologist needs to know. *Nat Rev Cardiol* 7: 564-575, 2010.

41. **Fearon K, Arends J, and Baracos V**. Understanding the mechanisms and treatment options in cancer cachexia. *Nat Rev Clin Oncol* 10: 90-99, 2013.

42. **Fearon KC, Glass DJ, and Guttridge DC**. Cancer cachexia: mediators, signaling, and metabolic pathways. *Cell Metab* 16: 153-166, 2012.

43. **Fielitz J, Kim MS, Shelton JM, Latif S, Spencer JA, Glass DJ, Richardson JA, Bassel-Duby R, and Olson EN**. Myosin accumulation and striated muscle myopathy result from the loss of muscle RING finger 1 and 3. *J Clin Invest* 117: 2486-2495, 2007.

44. **Flint TR, Janowitz T, Connell CM, Roberts EW, Denton AE, Coll AP, Jodrell DI, and Fearon DT**. Tumor-Induced IL-6 Reprograms Host Metabolism to Suppress Anti-tumor Immunity. *Cell Metab* 24: 672-684, 2016.

45. **Fluck M, and Hoppeler H**. Molecular basis of skeletal muscle plasticity--from gene to form and function. *Rev Physiol Biochem Pharmacol* 146: 159-216, 2003.

46. **Fogelman DR, Morris J, Xiao L, Hassan M, Vadhan S, Overman M, Javle S, Shroff R, Varadhachary G, Wolff R, Vence L, Maitra A, Cleeland C, and Wang XS**. A predictive model of inflammatory markers and patient-reported symptoms for cachexia in newly diagnosed pancreatic cancer patients. *Support Care Cancer* 25: 1809-1817, 2017.

47. **Foletta VC, White LJ, Larsen AE, Leger B, and Russell AP**. The role and regulation of MAFbx/atrogin-1 and MuRF1 in skeletal muscle atrophy. *Pflugers Arch* 461: 325-335, 2011.

48. **Fong Y, Lowry SF, and Cerami A**. Cachetin/TNF: a macrophage protein that induces cachexia and shock. *JPEN J Parenter Enteral Nutr* 12: 72S-77S, 1988.

49. **Formigli L, Meacci E, Sassoli C, Squecco R, Nosi D, Chellini F, Naro F, Francini F, and Zecchi-Orlandini S**. Cytoskeleton/stretch-activated ion channel interaction regulates myogenic differentiation of skeletal myoblasts. *J Cell Physiol* 211: 296-306, 2007.

50. **Fujita H, Nedachi T, and Kanzaki M**. Accelerated de novo sarcomere assembly by electric pulse stimulation in C2C12 myotubes. *Exp Cell Res* 313: 1853-1865, 2007.

51. **Gajsek N, Jevsek M, Mars T, Mis K, Pirkmajer S, Brecelj J, and Grubic Z**. Synaptogenetic mechanisms controlling postsynaptic differentiation of the neuromuscular junction are nerve-dependent in human and nerve-independent in mouse C2C12 muscle cultures. *Chem Biol Interact* 175: 50-57, 2008.

52. **Garrison JA, McCune JS, Livingston RB, Linden HM, Gralow JR, Ellis GK, and West HL**. Myalgias and arthralgias associated with paclitaxel. *Oncology (Williston Park)* 17: 271-277; discussion 281-272, 286-278, 2003.

53. **Gilliam LA, Ferreira LF, Bruton JD, Moylan JS, Westerblad H, St Clair DK, and Reid MB**. Doxorubicin acts through tumor necrosis factor receptor subtype 1 to cause dysfunction of murine skeletal muscle. *J Appl Physiol (1985)* 107: 1935-1942, 2009.

54. **Gilliam LA, Moylan JS, Patterson EW, Smith JD, Wilson AS, Rabbani Z, and Reid MB**. Doxorubicin acts via mitochondrial ROS to stimulate catabolism in C2C12 myotubes. *Am J Physiol Cell Physiol* 302: C195-202, 2012.

55. **Gilliam LA, and St Clair DK**. Chemotherapy-induced weakness and fatigue in skeletal muscle: the role of oxidative stress. *Antioxid Redox Signal* 15: 2543-2563, 2011.

56. **Glass DJ**. Signalling pathways that mediate skeletal muscle hypertrophy and atrophy. *Nat Cell Biol* 5: 87-90, 2003.

57. **Gordon JW, Rungi AA, Inagaki H, and Hood DA**. Effects of contractile activity on mitochondrial transcription factor A expression in skeletal muscle. *J Appl Physiol (1985)* 90: 389-396, 2001.

58. **Gutierrez-Martin Y, Martin-Romero FJ, and Henao F**. Store-operated calcium entry in differentiated C2C12 skeletal muscle cells. *Biochim Biophys Acta* 1711: 33-40, 2005.

59. **Han EK, McGonigal T, Butler C, Giranda VL, and Luo Y**. Characterization of Akt overexpression in MiaPaCa-2 cells: prohibitin is an Akt substrate both *in vitro* and in cells. *Anticancer Res* 28: 957-963, 2008.

60. **Han YQ, Ming SL, Wu HT, Zeng L, Ba G, Li J, Lu WF, Han J, Du QJ, Sun MM, Yang GY, Wang J, and Chu BB**. Myostatin knockout induces apoptosis in human cervical cancer cells via elevated reactive oxygen species generation. *Redox Biol* 19: 412-428, 2018.

61. **Hardee JP, Counts BR, Gao S, VanderVeen BN, Fix DK, Koh HJ, and Carson JA**. Inflammatory signalling regulates eccentric contraction-induced protein synthesis in cachectic skeletal muscle. *J Cachexia Sarcopenia Muscle* 9: 369-383, 2018.

62. **Hardee JP, Mangum JE, Gao S, Sato S, Hetzler KL, Puppa MJ, Fix DK, and Carson JA**. Eccentric contraction-induced myofiber growth in tumor-bearing mice. *J Appl Physiol (1985)* 120: 29-37, 2016.

63. **Hawley JA, and Holloszy JO**. Exercise: it's the real thing! *Nutr Rev* 67: 172-178, 2009.

64. **Henderson CA, Gomez CG, Novak SM, Mi-Mi L, and Gregorio CC**. Overview of the Muscle Cytoskeleton. *Compr Physiol* 7: 891-944, 2017.

65. **Hilber K, Galler S, Gohlsch B, and Pette D**. Kinetic properties of myosin heavy chain isoforms in single fibers from human skeletal muscle. *FEBS Lett* 455: 267-270, 1999.

66. **Hood DA, Irrcher I, Ljubicic V, and Joseph AM**. Coordination of metabolic plasticity in skeletal muscle. *J Exp Biol* 209: 2265-2275, 2006.

67. **Hood DA, Memme JM, Oliveira AN, and Triolo M**. Maintenance of Skeletal Muscle Mitochondria in Health, Exercise, and Aging. *Annu Rev Physiol* 81: 19-41, 2019.

68. **Huang SC, Wu JF, Saovieng S, Chien WH, Hsu MF, Li XF, Lee SD, Huang CY, Huang CY, and Kuo CH**. Doxorubicin inhibits muscle inflammation after eccentric exercise. *J Cachexia Sarcopenia Muscle* 8: 277-284, 2017.

69. **Hultman E, Sjoholm H, Jaderholm-Ek I, and Krynicki J**. Evaluation of methods for electrical stimulation of human skeletal muscle in situ. *Pflugers Arch* 398: 139-141, 1983.

70. **Jarvinen T, Ilonen I, Kauppi J, Salo J, and Rasanen J**. Loss of skeletal muscle mass during neoadjuvant treatments correlates with worse prognosis in esophageal cancer: a retrospective cohort study. *World J Surg Oncol* 16: 27, 2018.

71. **Johns N, Stephens NA, and Fearon KC**. Muscle wasting in cancer. *Int J Biochem Cell Biol* 45: 2215-2229, 2013.

72. **Jun I, Jeong S, and Shin H**. The stimulation of myoblast differentiation by electrically conductive sub-micron fibers. *Biomaterials* 30: 2038-2047, 2009.

73. **Kaji H, Ishibashi T, Nagamine K, Kanzaki M, and Nishizawa M**. Electrically induced contraction of C2C12 myotubes cultured on a porous membrane-based substrate with muscle tissue-like stiffness. *Biomaterials* 31: 6981-6986, 2010.

74. **Kang C, Goodman CA, Hornberger TA, and Ji LL**. PGC-1alpha overexpression by *in vivo* transfection attenuates mitochondrial deterioration of skeletal muscle caused by immobilization. *FASEB J* 29: 4092-4106, 2015.

75. **Kang C, and Ji LL**. PGC-1alpha overexpression via local transfection attenuates mitophagy pathway in muscle disuse atrophy. *Free Radic Biol Med* 93: 32-40, 2016.

76. **Kang C, and Li Ji L**. Role of PGC-1alpha signaling in skeletal muscle health and disease. *Ann N Y Acad Sci* 1271: 110-117, 2012.

77. **Kavazis AN, Smuder AJ, and Powers SK**. Effects of short-term endurance exercise training on acute doxorubicin-induced FoxO transcription in cardiac and skeletal muscle. *J Appl Physiol (1985)* 117: 223-230, 2014.

78. **Khairallah RJ, Shi G, Sbrana F, Prosser BL, Borroto C, Mazaitis MJ, Hoffman EP, Mahurkar A, Sachs F, Sun Y, Chen YW, Raiteri R, Lederer WJ, Dorsey SG, and Ward CW**. Microtubules underlie dysfunction in duchenne muscular dystrophy. *Sci Signal* 5: ra56, 2012.

79. **Kim JS, and Yi HK**. Schisandrin C enhances mitochondrial biogenesis and autophagy in C2C12 skeletal muscle cells: potential involvement of anti-oxidative mechanisms. *Naunyn Schmiedebergs Arch Pharmacol* 391: 197-206, 2018.

80. **Kinney MC, Dayanidhi S, Dykstra PB, McCarthy JJ, Peterson CA, and Lieber RL**. Reduced skeletal muscle satellite cell number alters muscle morphology after chronic stretch but allows limited serial sarcomere addition. *Muscle Nerve* 55: 384-392, 2017.

81. **Kislinger T, Gramolini AO, Pan Y, Rahman K, MacLennan DH, and Emili A**. Proteome dynamics during C2C12 myoblast differentiation. *Mol Cell Proteomics* 4: 887-901, 2005.

82. **Kontrogianni-Konstantopoulos A, Catino DH, Strong JC, and Bloch RJ**. De novo myofibrillogenesis in C2C12 cells: evidence for the independent assembly of M bands and Z disks. *Am J Physiol Cell Physiol* 290: C626-637, 2006.

83. **Lai KM, Gonzalez M, Poueymirou WT, Kline WO, Na E, Zlotchenko E, Stitt TN, Economides AN, Yancopoulos GD, and Glass DJ**. Conditional activation of akt in adult skeletal muscle induces rapid hypertrophy. *Mol Cell Biol* 24: 9295-9304, 2004.

84. **LeBlanc TW, Nipp RD, Rushing CN, Samsa GP, Locke SC, Kamal AH, Cella DF, and Abernethy AP**. Correlation between the international consensus definition of the Cancer Anorexia-Cachexia Syndrome (CACS) and patient-centered outcomes in advanced non-small cell lung cancer. *J Pain Symptom Manage* 49: 680-689, 2015.

85. **Lebrecht D, Setzer B, Ketelsen UP, Haberstroh J, and Walker UA**. Time-dependent and tissue-specific accumulation of mtDNA and respiratory chain defects in chronic doxorubicin cardiomyopathy. *Circulation* 108: 2423-2429, 2003.

86. **Lebrecht D, Setzer B, Rohrbach R, and Walker UA**. Mitochondrial DNA and its respiratory chain products are defective in doxorubicin nephrosis. *Nephrol Dial Transplant* 19: 329-336, 2004.

87. **Lee JH, Tachibana H, Morinaga Y, Fujimura Y, and Yamada K**. Modulation of proliferation and differentiation of C2C12 skeletal muscle cells by fatty acids. *Life Sci* 84: 415-420, 2009.

88. **Lenk K, Schuler G, and Adams V**. Skeletal muscle wasting in cachexia and sarcopenia: molecular pathophysiology and impact of exercise training. *J Cachexia Sarcopenia Muscle* 1: 9-21, 2010.

89. **Li YP, Chen Y, John J, Moylan J, Jin B, Mann DL, and Reid MB**. TNF-alpha acts via p38 MAPK to stimulate expression of the ubiquitin ligase atrogin1/MAFbx in skeletal muscle. *FASEB J* 19: 362-370, 2005.

90. **Loprinzi CL, Ellison NM, Goldberg RM, Michalak JC, and Burch PA**. Alleviation of cancer anorexia and cachexia: studies of the Mayo Clinic and the North Central Cancer Treatment Group. *Semin Oncol* 17: 8-12, 1990.

91. **Luo Y, and Shoichet MS**. Light-activated immobilization of biomolecules to agarose hydrogels for controlled cellular response. *Biomacromolecules* 5: 2315-2323, 2004.

92. **Maddocks M, Armstrong S, and Wilcock A**. Exercise as a supportive therapy in incurable cancer: exploring patient preferences. *Psychooncology* 20: 173-178, 2011.

93. **Maffiuletti NA, Gondin J, Place N, Stevens-Lapsley J, Vivodtzev I, and Minetto MA**. Clinical Use of Neuromuscular Electrical Stimulation for Neuromuscular Rehabilitation: What Are We Overlooking? *Arch Phys Med Rehabil* 99: 806-812, 2018.

94. **Mason C, Alfano CM, Smith AW, Wang CY, Neuhouser ML, Duggan C, Bernstein L, Baumgartner KB, Baumgartner RN, Ballard-Barbash R, and McTiernan A**. Long-term physical activity trends in breast cancer survivors. *Cancer Epidemiol Biomarkers Prev* 22: 1153-1161, 2013.

95. **Matsuyama T, Ishikawa T, Okayama T, Oka K, Adachi S, Mizushima K, Kimura R, Okajima M, Sakai H, Sakamoto N, Katada K, Kamada K, Uchiyama K, Handa O, Takagi T, Kokura S, Naito Y, and Itoh Y**. Tumor inoculation site affects the development of cancer cachexia and muscle wasting. *Int J Cancer* 137: 2558-2565, 2015.

96. **McCarthy JJ, and Esser KA**. Counterpoint: Satellite cell addition is not obligatory for skeletal muscle hypertrophy. *J Appl Physiol (1985)* 103: 1100-1102; discussion 1102-1103, 2007.

97. **McLean J, Moylan JS, and Andrade FH**. Mitochondria dysfunction in lung cancer-induced muscle wasting in C2C12 myotubes. *Front Physiol* 5: 2014.

98. **McLoon LK, Falkenberg JH, Dykstra D, and Iaizzo PA**. Doxorubicin chemomyectomy as a treatment for cervical dystonia: histological assessment after direct injection into the sternocleidomastoid muscle. *Muscle Nerve* 21: 1457-1464, 1998.

99. **McMahon DK, Anderson PA, Nassar R, Bunting JB, Saba Z, Oakeley AE, and Malouf NN**. C2C12 cells: biophysical, biochemical, and immunocytochemical properties. *Am J Physiol* 266: C1795-1802, 1994.

100. **Mijwel S, Cardinale DA, Norrbom J, Chapman M, Ivarsson N, Wengstrom Y, Sundberg CJ, and Rundqvist H**. Exercise training during chemotherapy preserves skeletal muscle fiber area, capillarization, and mitochondrial content in patients with breast cancer. *FASEB J* 32: 5495-5505, 2018.

101. **Mikkelsen UR, Agergaard J, Couppe C, Grosset JF, Karlsen A, Magnusson SP, Schjerling P, Kjaer M, and Mackey AL**. Skeletal muscle morphology and regulatory signalling in endurance-trained and sedentary individuals: The influence of ageing. *Exp Gerontol* 93: 54-67, 2017.

102. **Miller MS, Callahan DM, Tourville TW, Slauterbeck JR, Kaplan A, Fiske BR, Savage PD, Ades PA, Beynnon BD, and Toth MJ**. Moderate-intensity resistance exercise alters skeletal muscle molecular and cellular structure and function in inactive older adults with knee osteoarthritis. *J Appl Physiol (1985)* 122: 775-787, 2017.

103. **Miller RP, Tadagavadi RK, Ramesh G, and Reeves WB**. Mechanisms of Cisplatin nephrotoxicity. *Toxins (Basel)* 2: 2490-2518, 2010.

104. **Min K, Kwon OS, Smuder AJ, Wiggs MP, Sollanek KJ, Christou DD, Yoo JK, Hwang MH, Szeto HH, Kavazis AN, and Powers SK**. Increased mitochondrial emission of reactive oxygen species and calpain activation are required for doxorubicin-induced cardiac and skeletal muscle myopathy. *J Physiol* 593: 2017-2036, 2015.

105. **Mitch WE, and Goldberg AL**. Mechanisms of muscle wasting. The role of the ubiquitin-proteasome pathway. *N Engl J Med* 335: 1897-1905, 1996.

106. **Mitsui T, Umaki Y, Nagasawa M, Akaike M, Aki K, Azuma H, Ozaki S, Odomi M, and Matsumoto T**. Mitochondrial damage in patients with long-term corticosteroid therapy: development of oculoskeletal symptoms similar to mitochondrial disease. *Acta Neuropathol* 104: 260-266, 2002.

107. **Monster AW, and Chan H**. Isometric force production by motor units of extensor digitorum communis muscle in man. *J Neurophysiol* 40: 1432-1443, 1977.

108. **Morley JE, Anker SD, and von Haehling S**. Prevalence, incidence, and clinical impact of sarcopenia: facts, numbers, and epidemiology-update 2014. *J Cachexia Sarcopenia Muscle* 5: 253-259, 2014.

109. **Morvan F, Rondeau JM, Zou C, Minetti G, Scheufler C, Scharenberg M, Jacobi C, Brebbia P, Ritter V, Toussaint G, Koelbing C, Leber X, Schilb A, Witte F, Lehmann S, Koch E, Geisse S, Glass DJ, and Lach-Trifilieff E**. Blockade of activin type II receptors with a dual anti-ActRIIA/IIB antibody is critical to promote maximal skeletal muscle hypertrophy. *Proc Natl Acad Sci U S A* 114: 12448-12453, 2017.

110. **Moss FP, and Leblond CP**. Satellite cells as the source of nuclei in muscles of growing rats. *Anat Rec* 170: 421-435, 1971.

111. **Mueller TC, Bachmann J, Prokopchuk O, Friess H, and Martignoni ME**. Molecular pathways leading to loss of skeletal muscle mass in cancer cachexia--can findings from animal models be translated to humans? *BMC Cancer* 16: 75, 2016.

112. **Muller MJ, Baracos V, Bosy-Westphal A, Dulloo AG, Eckel J, Fearon KC, Hall KD, Pietrobelli A, Sorensen TI, Speakman J, Trayhurn P, Visser M, and Heymsfield SB**. Functional body composition and related aspects in research on obesity and cachexia: report on the 12th Stock Conference held on 6 and 7 September 2013 in Hamburg, Germany. *Obes Rev* 15: 640-656, 2014.

113. **Muscaritoli M, Molfino A, Gioia G, Laviano A, and Rossi Fanelli F**. The "parallel pathway": a novel nutritional and metabolic approach to cancer patients. *Intern Emerg Med* 6: 105-112, 2011.

114. **Nagamine K, Kawashima T, Ishibashi T, Kaji H, Kanzaki M, and Nishizawa M**. Micropatterning contractile C2C12 myotubes embedded in a fibrin gel. *Biotechnol Bioeng* 105: 1161-1167, 2010.

115. **Nakashima K, and Yakabe Y**. AMPK activation stimulates myofibrillar protein degradation and expression of atrophy-related ubiquitin ligases by increasing FOXO transcription factors in C2C12 myotubes. *Biosci Biotechnol Biochem* 71: 1650-1656, 2007.

116. **Navari RM**. Managing Nausea and Vomiting in Patients With Cancer: What Works. *Oncology (Williston Park)* 32: 121-125, 131, 136, 2018.

117. **Nedachi T, Fujita H, and Kanzaki M**. Contractile C2C12 myotube model for studying exercise-inducible responses in skeletal muscle. *Am J Physiol Endocrinol Metab* 295: E1191-1204, 2008.

118. **Nystrom GJ, and Lang CH**. Sepsis and AMPK Activation by AICAR Differentially Regulate FoxO-1, -3 and -4 mRNA in Striated Muscle. *Int J Clin Exp Med* 1: 50-63, 2008.

119. **Ogawa T, Furochi H, Mameoka M, Hirasaka K, Onishi Y, Suzue N, Oarada M, Akamatsu M, Akima H, Fukunaga T, Kishi K, Yasui N, Ishidoh K, Fukuoka H, and Nikawa T**. Ubiquitin ligase gene expression in healthy volunteers with 20-day bedrest. *Muscle Nerve* 34: 463-469, 2006.

120. **Okamoto T, and Machida S**. Changes in FOXO and proinflammatory cytokines in the late stage of immobilized fast and slow muscle atrophy. *Biomed Res* 38: 331-342, 2017.

121. **Orfanos Z, Godderz MP, Soroka E, Godderz T, Rumyantseva A, van der Ven PF, Hawke TJ, and Furst DO**. Breaking sarcomeres by *in vitro* exercise. *Sci Rep* 6: 19614, 2016.

122. **Pallafacchina G, Calabria E, Serrano AL, Kalhovde JM, and Schiaffino S**. A protein kinase B-dependent and rapamycin-sensitive pathway controls skeletal muscle growth but not fiber type specification. *Proc Natl Acad Sci U S A* 99: 9213-9218, 2002.

123. **Penna F, Busquets S, and Argiles JM**. Experimental cancer cachexia: Evolving strategies for getting closer to the human scenario. *Semin Cell Dev Biol* 54: 20-27, 2016.

124. **Peterson JM, Bakkar N, and Guttridge DC**. NF-kappaB signaling in skeletal muscle health and disease. *Curr Top Dev Biol* 96: 85-119, 2011.

125. **Pette D, Peuker H, and Staron RS**. The impact of biochemical methods for single muscle fibre analysis. *Acta Physiol Scand* 166: 261-277, 1999.

126. **Pigna E, Berardi E, Aulino P, Rizzuto E, Zampieri S, Carraro U, Kern H, Merigliano S, Gruppo M, Mericskay M, Li Z, Rocchi M, Barone R, Macaluso F, Di Felice V, Adamo S, Coletti D, and Moresi V**. Aerobic Exercise and Pharmacological Treatments Counteract Cachexia by Modulating Autophagy in Colon Cancer. *Sci Rep* 6: 26991, 2016.

127. **Polomano RC, Mannes AJ, Clark US, and Bennett GJ**. A painful peripheral neuropathy in the rat produced by the chemotherapeutic drug, paclitaxel. *Pain* 94: 293-304, 2001.

128. **Powers SK, Duarte JA, Le Nguyen B, and Hyatt H**. Endurance exercise protects skeletal muscle against both doxorubicin-induced and inactivity-induced muscle wasting. *Pflugers Arch* 2018.

129. **Prado CM, Baracos VE, McCargar LJ, Reiman T, Mourtzakis M, Tonkin K, Mackey JR, Koski S, Pituskin E, and Sawyer MB**. Sarcopenia as a determinant of chemotherapy toxicity and time to tumor progression in metastatic breast cancer patients receiving capecitabine treatment. *Clin Cancer Res* 15: 2920-2926, 2009.

130. **Prado CM, Sawyer MB, Ghosh S, Lieffers JR, Esfandiari N, Antoun S, and Baracos VE**. Central tenet of cancer cachexia therapy: do patients with advanced cancer have exploitable anabolic potential? *Am J Clin Nutr* 98: 1012-1019, 2013.

131. **Raven PB**. *Exercise physiology : an integrated approach*. Australia ; Belmont, CA: Wadsworth Cengage Learning, 2013, p. xxv, 504 p.

132. **Remels AH, Gosker HR, Schrauwen P, Hommelberg PP, Sliwinski P, Polkey M, Galdiz J, Wouters EF, Langen RC, and Schols AM**. TNF-alpha impairs regulation of muscle oxidative phenotype: implications for cachexia? *FASEB J* 24: 5052-5062, 2010.

133. **Reynolds THt, Merrell E, Cinquino N, Gaugler M, and Ng L**. Disassociation of insulin action and Akt/FOXO signaling in skeletal muscle of older Akt-deficient mice. *Am J Physiol Regul Integr Comp Physiol* 303: R1186-1194, 2012.

134. **Robert F, Mills JR, Agenor A, Wang D, DiMarco S, Cencic R, Tremblay ML, Gallouzi IE, Hekimi S, Wing SS, and Pelletier J**. Targeting protein synthesis in a Myc/mTOR-driven model of anorexia-cachexia syndrome delays its onset and prolongs survival. *Cancer Res* 72: 747-756, 2012.

135. **Rommel C, Bodine SC, Clarke BA, Rossman R, Nunez L, Stitt TN, Yancopoulos GD, and Glass DJ**. Mediation of IGF-1-induced skeletal myotube hypertrophy by PI(3)K/Akt/mTOR and PI(3)K/Akt/GSK3 pathways. *Nat Cell Biol* 3: 1009-1013, 2001.

136. **Rommel C, Clarke BA, Zimmermann S, Nunez L, Rossman R, Reid K, Moelling K, Yancopoulos GD, and Glass DJ**. Differentiation stage-specific inhibition of the Raf-MEK-ERK pathway by Akt. *Science* 286: 1738-1741, 1999.

137. **Rotwein P, and Wilson EM**. Distinct actions of Akt1 and Akt2 in skeletal muscle differentiation. *J Cell Physiol* 219: 503-511, 2009.

138. **Sakai H, Kimura M, Isa Y, Yabe S, Maruyama A, Tsuruno Y, Kai Y, Sato F, Yumoto T, Chiba Y, and Narita M**. Effect of acute treadmill exercise on cisplatin-induced muscle atrophy in the mouse. *Pflugers Arch* 469: 1495-1505, 2017.

139. **Samuels SE, Knowles AL, Tilignac T, Debiton E, Madelmont JC, and Attaix D**. Protein metabolism in the small intestine during cancer cachexia and chemotherapy in mice. *Cancer Res* 60: 4968-4974, 2000.

140. **Sanchez AM, Csibi A, Raibon A, Cornille K, Gay S, Bernardi H, and Candau R**. AMPK promotes skeletal muscle autophagy through activation of forkhead FoxO3a and interaction with Ulk1. *J Cell Biochem* 113: 695-710, 2012.

141. **Sandri M**. Signaling in muscle atrophy and hypertrophy. *Physiology (Bethesda)* 23: 160-170, 2008.

142. **Sandri M, Sandri C, Gilbert A, Skurk C, Calabria E, Picard A, Walsh K, Schiaffino S, Lecker SH, and Goldberg AL**. Foxo transcription factors induce the atrophy-related ubiquitin ligase atrogin-1 and cause skeletal muscle atrophy. *Cell* 117: 399-412, 2004.

143. **Sartorelli V, and Fulco M**. Molecular and cellular determinants of skeletal muscle atrophy and hypertrophy. *Sci STKE* 2004: re11, 2004.

144. **Schakman O, Gilson H, and Thissen JP**. Mechanisms of glucocorticoid-induced myopathy. *J Endocrinol* 197: 1-10, 2008.

145. **Schiaffino S, and Mammucari C**. Regulation of skeletal muscle growth by the IGF1-Akt/PKB pathway: insights from genetic models. *Skelet Muscle* 1: 4, 2011.

146. **Schiaffino S, Rossi AC, Smerdu V, Leinwand LA, and Reggiani C**. Developmental myosins: expression patterns and functional significance. *Skelet Muscle* 5: 22, 2015.

147. **Sciancalepore M, Coslovich T, Lorenzon P, Ziraldo G, and Taccola G**. Extracellular stimulation with human "noisy" electromyographic patterns facilitates myotube activity. *J Muscle Res Cell Motil* 36: 349-357, 2015.

148. **Shih A, and Jackson KC, 2nd**. Role of corticosteroids in palliative care. *J Pain Palliat Care Pharmacother* 21: 69-76, 2007.

149. **Shyh-Chang N**. Metabolic Changes During Cancer Cachexia Pathogenesis. *Adv Exp Med Biol* 1026: 233-249, 2017.

150. **Smuder AJ, Kavazis AN, Min K, and Powers SK**. Exercise protects against doxorubicin-induced oxidative stress and proteolysis in skeletal muscle. *J Appl Physiol (1985)* 110: 935-942, 2011.

151. **Stamenovic D, Mijailovich SM, Tolic-Norrelykke IM, Chen J, and Wang N**. Cell prestress. II. Contribution of microtubules. *Am J Physiol Cell Physiol* 282: C617-624, 2002.

152. **Staron RS**. Human skeletal muscle fiber types: delineation, development, and distribution. *Can J Appl Physiol* 22: 307-327, 1997.

153. **Stitt TN, Drujan D, Clarke BA, Panaro F, Timofeyva Y, Kline WO, Gonzalez M, Yancopoulos GD, and Glass DJ**. The IGF-1/PI3K/Akt pathway prevents expression of muscle atrophy-induced ubiquitin ligases by inhibiting FOXO transcription factors. *Mol Cell* 14: 395-403, 2004.

154. **Sturgeon KM, Fisher C, McShea G, Sullivan SK, Sataloff D, and Schmitz KH**. Patient preference and timing for exercise in breast cancer care. *Support Care Cancer* 26: 507-514, 2018.

155. **Su Z, Chen M, Xiao Y, Sun M, Zong L, Asghar S, Dong M, Li H, Ping Q, and Zhang C**. ROS-triggered and regenerating anticancer nanosystem: an effective strategy to subdue tumor's multidrug resistance. *J Control Release* 196: 370-383, 2014.

156. **Tan BH, Birdsell LA, Martin L, Baracos VE, and Fearon KC**. Sarcopenia in an overweight or obese patient is an adverse prognostic factor in pancreatic cancer. *Clin Cancer Res* 15: 6973-6979, 2009.

157. **Thelen MH, Simonides WS, and van Hardeveld C**. Electrical stimulation of C2C12 myotubes induces contractions and represses thyroid-hormone-dependent transcription of the fast-type sarcoplasmic-reticulum Ca2+-ATPase gene. *Biochem J* 321 (Pt 3): 845-848, 1997.

158. **Theologides A**. Generalized perturbations in host physiology caused by localized tumors. The anorexia-cachexia syndrome: a new hypothesis. *Ann N Y Acad Sci* 230: 14-22, 1974.

159. **Tisdale MJ**. Cancer cachexia. *Curr Opin Gastroenterol* 26: 146-151, 2010.

160. **Tisdale MJ**. Catabolic mediators of cancer cachexia. *Curr Opin Support Palliat Care* 2: 256-261, 2008.

161. **Tsuchida K**. Activins, myostatin and related TGF-beta family members as novel therapeutic targets for endocrine, metabolic and immune disorders. *Curr Drug Targets Immune Endocr Metabol Disord* 4: 157-166, 2004.

162. **Vainshtein A, Tryon LD, Pauly M, and Hood DA**. Role of PGC-1alpha during acute exercise-induced autophagy and mitophagy in skeletal muscle. *Am J Physiol Cell Physiol* 308: C710-719, 2015.

163. **van Norren K, Dwarkasing JT, and Witkamp RF**. The role of hypothalamic inflammation, the hypothalamic-pituitary-adrenal axis and serotonin in the cancer anorexia-cachexia syndrome. *Curr Opin Clin Nutr Metab Care* 20: 396-401, 2017.

164. **Vanhoutte G, van de Wiel M, Wouters K, Sels M, Bartolomeeussen L, De Keersmaecker S, Verschueren C, De Vroey V, De Wilde A, Smits E, Cheung KJ, De Clerck L, Aerts P, Baert D, Vandoninck C, Kindt S, Schelfhaut S, Vankerkhoven M, Troch A, Ceulemans L, Vandenbergh H, Leys S, Rondou T, Dewitte E, Maes K, Pauwels P, De Winter B, Van Gaal L, Ysebaert D, and Peeters M**. Cachexia in cancer: what is in the definition? *BMJ Open Gastroenterol* 3: e000097, 2016.

165. **Wang J, Wang F, Zhang P, Liu H, He J, Zhang C, Fan M, and Chen X**. PGC-1alpha over-expression suppresses the skeletal muscle atrophy and myofiber-type composition during hindlimb unloading. *Biosci Biotechnol Biochem* 81: 500-513, 2017.

166. **Wang Q, Lu JB, Wu B, and Hao LY**. Expression and clinicopathologic significance of proteolysis-inducing factor in non-small-cell lung cancer: an immunohistochemical analysis. *Clin Lung Cancer* 11: 346-351, 2010.

167. **Whidden MA, Smuder AJ, Wu M, Hudson MB, Nelson WB, and Powers SK**. Oxidative stress is required for mechanical ventilation-induced protease activation in the diaphragm. *J Appl Physiol (1985)* 108: 1376-1382, 2010.

168. **White J, Barro MV, Makarenkova HP, Sanger JW, and Sanger JM**. Localization of sarcomeric proteins during myofibril assembly in cultured mouse primary skeletal myotubes. *Anat Rec (Hoboken)* 297: 1571-1584, 2014.

169. **White JP, Puppa MJ, Gao S, Sato S, Welle SL, and Carson JA**. Muscle mTORC1 suppression by IL-6 during cancer cachexia: a role for AMPK. *Am J Physiol Endocrinol Metab* 304: E1042-1052, 2013.

170. **Wilkinson SB, Phillips SM, Atherton PJ, Patel R, Yarasheski KE, Tarnopolsky MA, and Rennie MJ**. Differential effects of resistance and endurance exercise in the fed state on signalling molecule phosphorylation and protein synthesis in human muscle. *J Physiol* 586: 3701-3717, 2008.

171. **Winters-Stone KM, Dobek JC, Bennett JA, Dieckmann NF, Maddalozzo GF, Ryan CW, and Beer TM**. Resistance training reduces disability in prostate cancer survivors on androgen deprivation therapy: evidence from a randomized controlled trial. *Arch Phys Med Rehabil* 96: 7-14, 2015.

172. **Wirtschafter JD, and McLoon LK**. Long-term efficacy of local doxorubicin chemomyectomy in patients with blepharospasm and hemifacial spasm. *Ophthalmology* 105: 342-346, 1998.

173. **Witkowski S, Lovering RM, and Spangenburg EE**. High-frequency electrically stimulated skeletal muscle contractions increase p70s6k phosphorylation independent of known IGF-I sensitive signaling pathways. *FEBS Lett* 584: 2891-2895, 2010.

174. **Wolfe RR**. Skeletal muscle protein metabolism and resistance exercise. *J Nutr* 136: 525S-528S, 2006.

175. **Wu CT, Liao JM, Ko JL, Lee YL, Chang HY, Wu CH, and Ou CC**. D-Methionine Ameliorates Cisplatin-Induced Muscle Atrophy via Inhibition of Muscle Degradation Pathway. *Integr Cancer Ther* 18: 1534735419828832, 2019.

176. **Xiao DY, Luo S, O'Brian K, Sanfilippo KM, Ganti A, Riedell P, Lynch RC, Liu W, Kahl BS, Cashen AF, Fehniger TA, and Carson KR**. Longitudinal Body Composition Changes in Diffuse Large B-cell Lymphoma Survivors: A Retrospective Cohort Study of United States Veterans. *J Natl Cancer Inst* 108: 2016.

177. **Yaffe D, and Saxel O**. Serial passaging and differentiation of myogenic cells isolated from dystrophic mouse muscle. *Nature* 270: 725-727, 1977.

178. **Yakovenko A, Cameron M, and Trevino JG**. Molecular therapeutic strategies targeting pancreatic cancer induced cachexia. *World J Gastrointest Surg* 10: 95-106, 2018.

179. **Yamamoto Y, Hoshino Y, Ito T, Nariai T, Mohri T, Obana M, Hayata N, Uozumi Y, Maeda M, Fujio Y, and Azuma J**. Atrogin-1 ubiquitin ligase is upregulated by doxorubicin via p38-MAP kinase in cardiac myocytes. *Cardiovasc Res* 79: 89-96, 2008.

180. **Yan Z, Lira VA, and Greene NP**. Exercise training-induced regulation of mitochondrial quality. *Exerc Sport Sci Rev* 40: 159-164, 2012.

181. **Ydfors M, Fischer H, Mascher H, Blomstrand E, Norrbom J, and Gustafsson T**. The truncated splice variants, NT-PGC-1alpha and PGC-1alpha4, increase with both endurance and resistance exercise in human skeletal muscle. *Physiol Rep* 1: e00140, 2013.

182. **Zhao J, Brault JJ, Schild A, Cao P, Sandri M, Schiaffino S, Lecker SH, and Goldberg AL**. FoxO3 coordinately activates protein degradation by the autophagic/lysosomal and proteasomal pathways in atrophying muscle cells. *Cell Metab* 6: 472-483, 2007.

183. **Zheng B, Ohkawa S, Li H, Roberts-Wilson TK, and Price SR**. FOXO3a mediates signaling crosstalk that coordinates ubiquitin and atrogin-1/MAFbx expression during glucocorticoid-induced skeletal muscle atrophy. *FASEB J* 24: 2660-2669, 2010.

Figures

FIGURE 1:

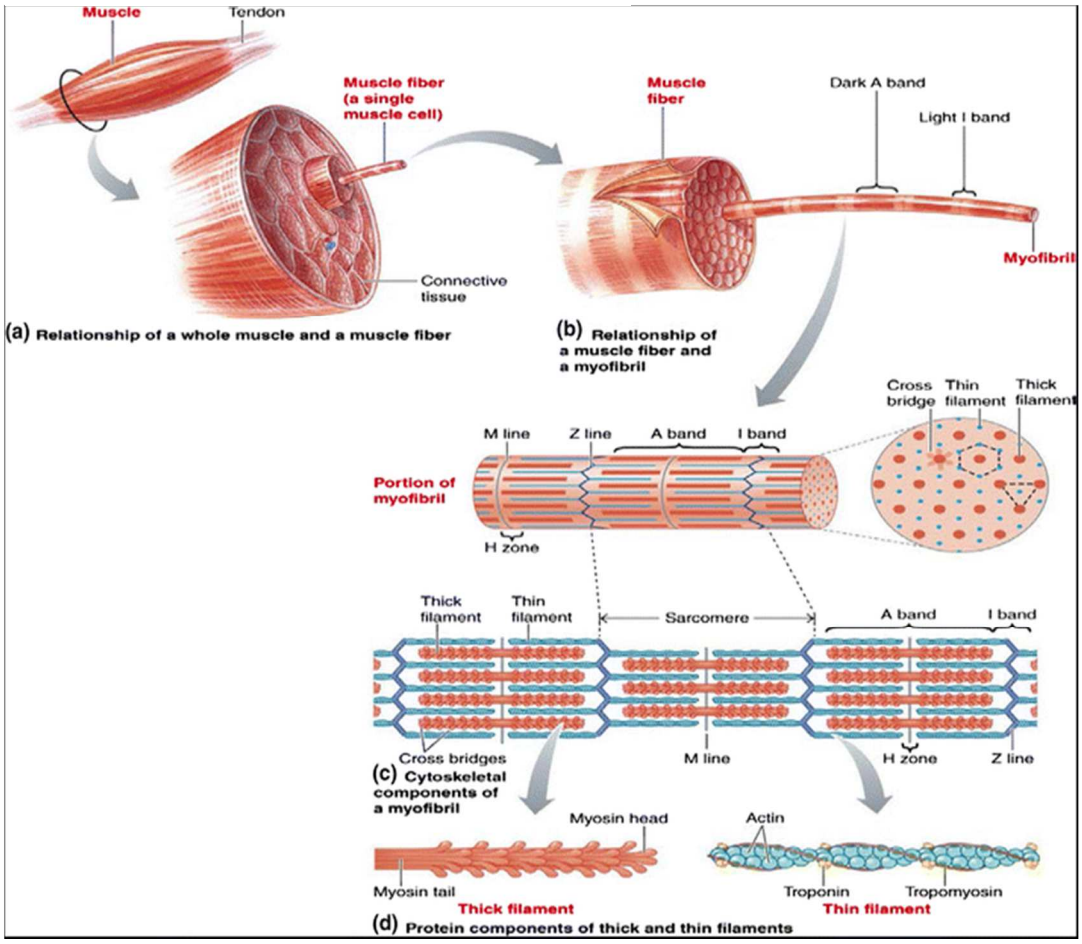

Figure 1.0.1: *Skeletal muscle structure*

Structure of skeletal muscle (From: Raven et al. Fig. 3.6) (131)

FIGURE 2:

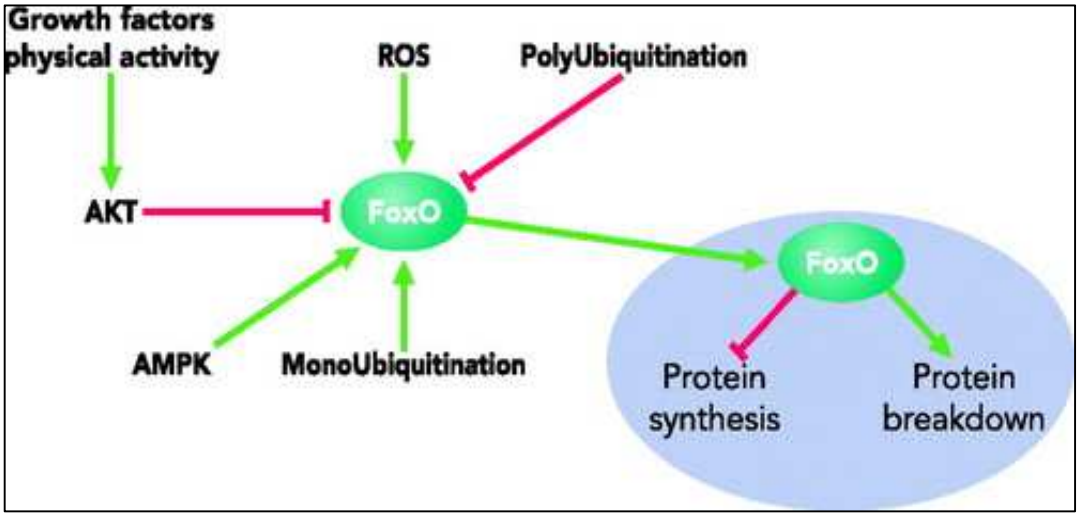

Figure 1.0.2: *Skeletal muscle Akt pathway.*

Scheme illustrating the regulation of FoxO via modulation of ROS and the Akt pathway. (From: Sandri *et al*. Fig. 3) (141)

FIGURE 3:

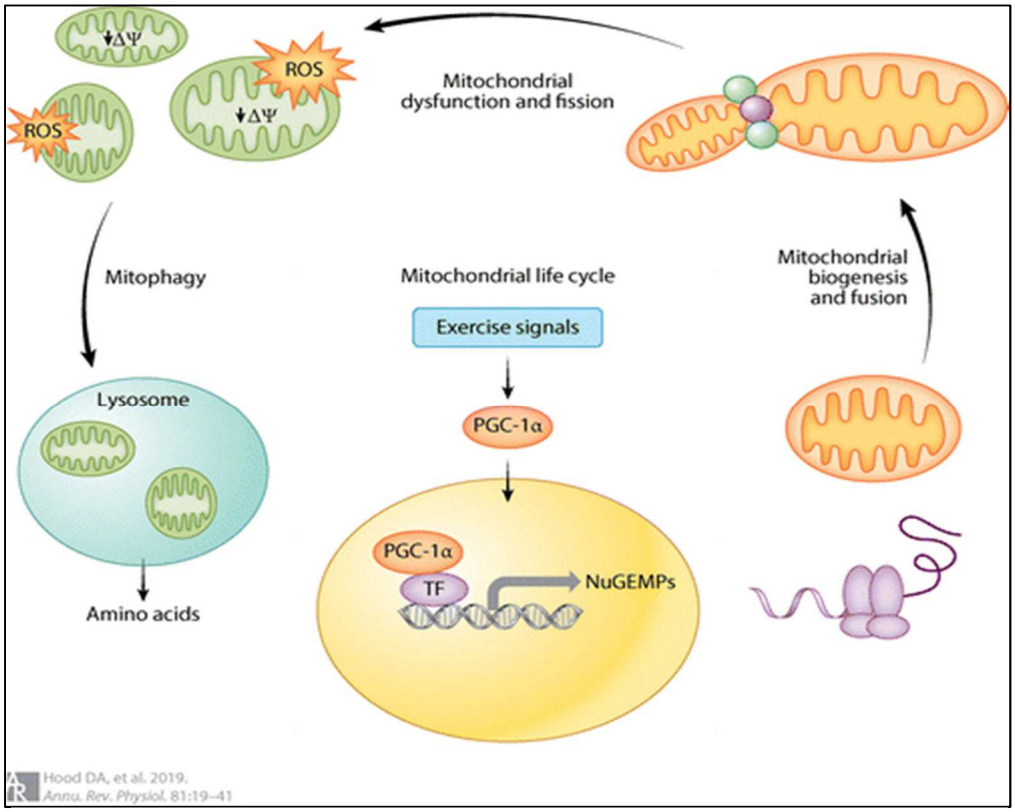

Figure 1.0.3: *Mitochondrial dynamics schematic.*

Mitochondrial regulation in skeletal muscle (From: Hood *et al*. Fig. 1) (67)

FIGURE 4:

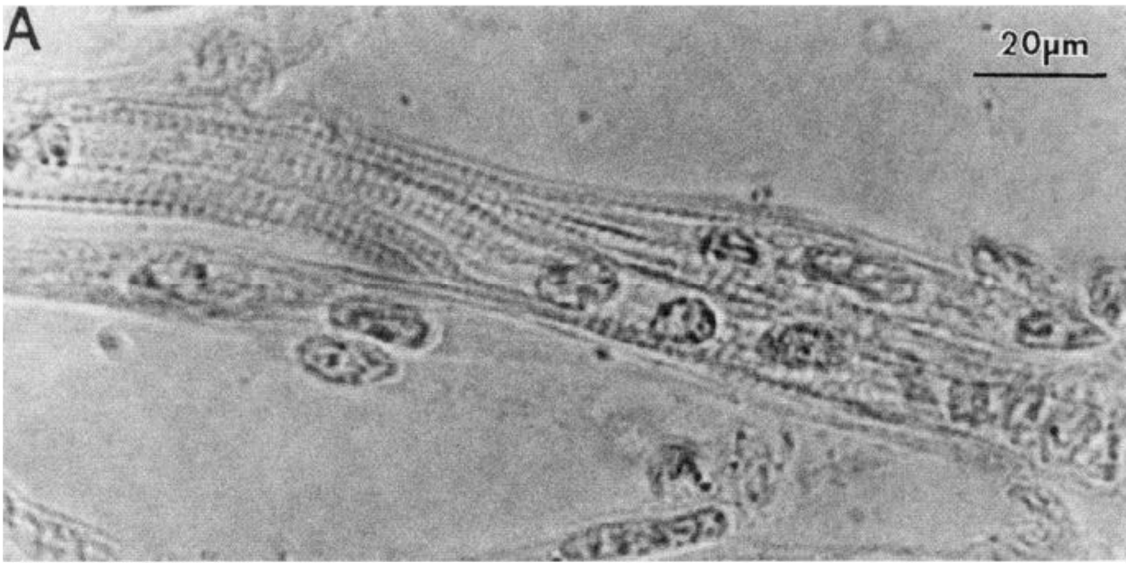

Figure 1.0.4: *light microscope image of mature C2C12 myotube*

C2C12 myotube, 8 days post starvation, photographed in culture. Striations suggest presence of well-organized myofilaments. (From: McMahon *et al*. Fig. 1A)(99)

FIGURE 5:

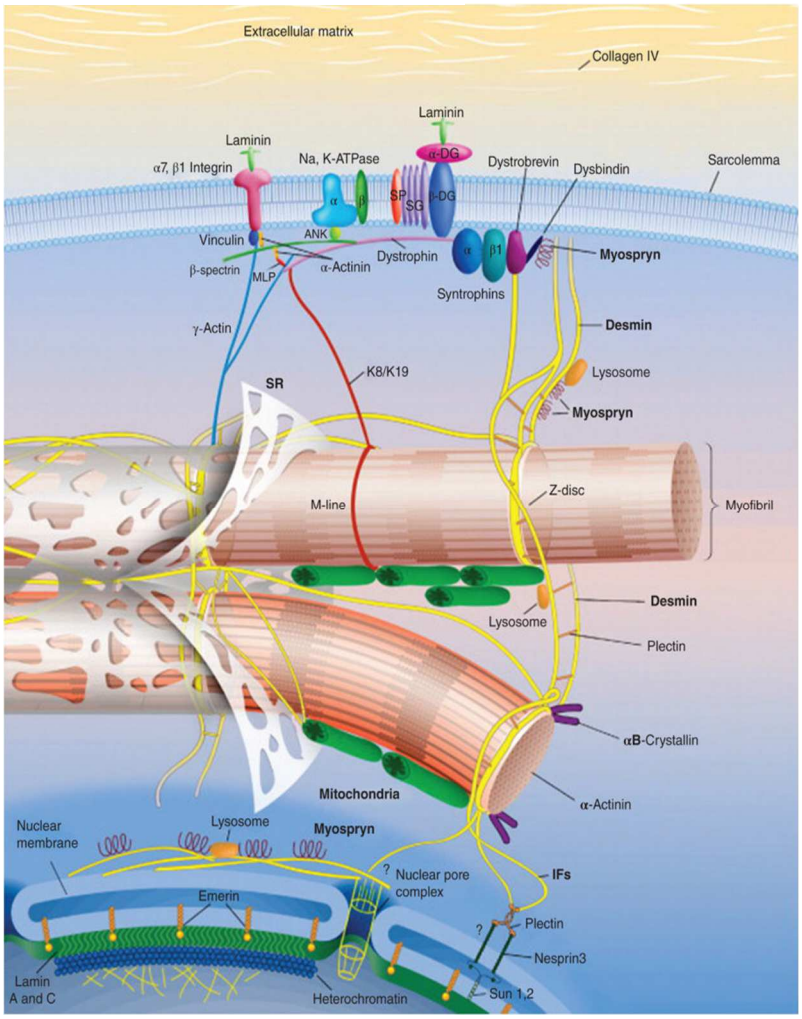

Figure 1.0.5: *Schematic representation of the intermediate filament in skeletal muscle*.

Schematic representation of the intermediate filament (IF) scaffold in striated muscle. The IF scaffold, predominantly composed of desmin (yellow), links the entire contractile apparatus to the sarcolemma and other organelles, such as the nucleus, mitochondria, lysosomes, and potentially the sarcoplasmic reticulum (SR). Desmin interacts with many other proteins including synemin, paranemin, syncoilin, and myospryn. Keratins (K8/K19) link the contractile apparatus to the sarcolemma and interact with the dystrophin-dystroglycan (DG) complex. Overall, the IF scaffold helps maintain the integrity of muscle cytoarchitecture and provide mechanical strength to the cell. Abbreviations: MLP, striated muscle-specific LIM protein; SG, sarcoglycan, From: Henderson *et al*. Fig. 3) (64)

Table 1.1: *Common properties of skeletal muscle fiber types*

	Type I	Type IIA	Type IIX
Other Names	Slow Twitch	Fast Twitch	Fast Twitch
Metabolism	Oxidative	Oxidative/Glycolytic	Glycolytic
Myosin Heavy Chain	MHC I	MHC IIa	MHC IIx
mATPase activity	Slow	Fast	Very fast
Power	Weak	Intermediate	Strong
Velocity	Slow	Fast	Very fast
Force	Low	Intermediate	High
Mitochondrial density	High	Intermediate	Low
Endurance capacity	High	Intermediate	Low
Appearance	Red	Pink	White

List of abbreviations

2-[4-(2-hydroxyethyl) piperazin-1-yl]ethanesulfonic acid	HEPES
Antioxidant response element	ARE
atrogin-1/muscle atrophy F-box	MAFbx
Autophagy Lysosome Pathway	ALP
circulating Atrophy Inducing Factor	cAIF
c-*Jun* N-terminal kinase	JNK
Conditioned Medium	CM
Cross Sectional Area	CSA
Dimethyl sulfoxide	DMSO
Dithiothreitol	DTT
Doxorubicin	DOX
Dulbecco´s Modified Eagle´s Medium	DMEM
Electron Microscopy	EM
extracellular signal-regulated kinase 1/2	ERK1/2
Fetal Bovine Serum	FBS
GABA(A) receptor-associated protein-like 1	Gabarapl1
glutathione	GSH
Hank's balanced salt solution	HBSS
Human biopsy cell line	hTCM
Interleukin 6	IL-6
Kirsten rat sarcoma viral oncogene homolog	KRAS
Lewis lung carcinoma	LLC
Lox-Stop-Lox- KRASG12D	LSL-KRASG12D
Manganese superoxide dismutase	MnSOD
mitogen-activated protein kinase	MAPK
Mouse tracheal epithelial cell	MTEC
Muscle-specific RING finger protein 1	MuRF1
Myosin Heavy Chain type I	MHC I
Myosin Heavy Chain type II	MHC II
N-acetylcysteine	NAC
Nicotinamide adenine dinucleotide phosphate	NADPH
non-small cell lung	NSCL
non-small cell lung cancer	NSCLC
Nuclear factor (erythroid-derived 2)-like 2	Nrf2
nuclear transcription factor kappa B	NFκB
Paclitaxel	TAXOL
Penicillin-Streptomycin	P/S
Peroxiredoxin 3	Prx 3

Peroxisome proliferator-activated receptor gamma coactivator 1-alpha	PGC-1α
Phosphate Buffered Saline	PBS
phosphatidylinositol 3-kinase (PI3-kinase)/protein kinase B	Akt
Proteolysis Inducing Factor	PIF
quality of life	QOL
Quantitative real time PCR	qRT-PCR/qPCR
Reactive oxygen species	ROS
sarcoplasmic reticulum	SR
small cell lung cancer	SCLC
small interfering RNA	siRNA
Sodium dodecyl sulfate polyacrylamide gel electrophoresis	SDS PAGE
superoxide dismutase	SOD
TBS-Tween	TBST
TNF receptor subtype 1	TNFR1
Tris-buffered saline	TBS
tumor necrosis factor-alpha	TNF
Tumor Necrosis Factor-α	TNFα
Ubiquitin 26S-Proteasome System	UPS
Whole Cell Lysate	WCL

CHAPTER 2: EFFECTS OF MURINE AND HUMAN LUNG TUMOR CELL CONDITIONED MEDIA ON SKELETAL MUSCLE

Blas A. Guigni[1,2], Jos van der Velden[3] , C. Matthew Kinsey[1], James A. Carson[4] and Michael J. Toth[1,2]

Departments of Medicine[1], Molecular Physiology and Biophysics[2], Pathology and Laboratory Medicine[3], College of Medicine, University of Vermont, Burlington, VT and Department of Exercise Science, University of South Carolina, Columbia, SC[4]

Correspondence to: Michael J. Toth, Ph.D.

Health Science Research Facility 126B

149 Beaumont Ave

University of Vermont

Burlington, VT 05405

Email: michael.toth@uvm.edu

Tele: (802) 656-7989

Fax: (802) 656-0747

Running Title: Tumor effects on skeletal muscle

Abstract

Tumor-secreted factors are hypothesized to cause fat and skeletal muscle wasting in cancer patients. To test this hypothesis, we examined whether tumor cells secrete factors to promote atrophy by evaluating the effects of tumor-conditioned media (CM) from murine and human lung tumor cells on cultured muscle myotubes. We evaluated two murine lung cancer cell lines that produce cachexia in mice, Lewis lung carcinoma (LLC) and $KRAS^{G12D}$ cells, and primary cell lines derived from tumor biopsies from patients with lung cancer (hTCM; n=4). We hypothesized that conditioned media from murine and human tumor cells would reduce myotube myosin content, decrease mitochondrial content and increase mitochondrial reactive oxygen species production (ROS). Treatment of myotubes differentiated for 7 days with CM from LLC and $KRAS^{G12D}$ cells did not alter myotube myosin content or mitochondrial content or ROS production. Effects of murine tumor cell CM were observed, however, when myotubes differentiated for 4 days were treated with tumor cell CM and compared to undiluted differentiation media. However, these effects were not apparent if tumor cell CM treatments were compared to control cell CM or dilution controls. Finally, CM from human lung tumor primary cell lines did not modify myosin content or mitochondrial content or ROS production compared to either undiluted differentiated media, control cell CM or dilution controls. Collectively, our results argue against the hypothesis that lung cancer cell-derived factors act directly on skeletal muscle to promote muscle wasting or mitochondrial abnormalities.

Introduction

Cancer cachexia is a syndrome characterized by unintentional loss of both fat and skeletal muscle tissue (19) that affects ~50% of patients (18, 60). Patients with solid tumors are most likely to experience muscle atrophy, particularly in advanced stages (42). Muscle wasting increases treatments side effects (15, 23, 55), decrease response to chemotherapy (29, 33, 53) and increases mortality (17). Despite these deleterious consequences, the causes of cancer cachexia remain unclear.

How tumors that are anatomically distal to skeletal muscle cause atrophy is unknown. One long-standing theory holds that factors released from tumor cells promote tissue wasting, through direct effects on the muscle or indirectly by provoking host-related factors, such as inflammatory cytokines. Data supporting this theory comes primarily from pre-clinical models (2, 37, 47). While these studies have provided a wealth of mechanistic data, their translatability to human cancer remains questionable. In animal models, tumors grow rapidly and comprise a large fraction of body mass (7). For instance, in the C26 xenoplant model, the onset of cachexia typically occurs when the tumor reaches ~5% of body mass (56), which occurs 2-4 weeks after inoculation (10, 30). Extrapolated to humans, the size of this tumor would equate to an ~8 lb. tumor in men and ~6 lb. tumor in women. Accordingly, the pathoetiology of cachexia in these pre-clinical models may be skewed disproportionately towards tumor-derived factors. In contrast, human tumors develop relatively slower and comprise <<1% of body mass. In this context, cancer cachexia in humans may be less dependent on tumor-derived factors

and/or factors derived from tumor cells may be less effective at promoting muscle wasting and cachexia.

A common model for testing the effect of tumor-derived factors on skeletal muscle involves treating cultured muscle cells with conditioned media (CM) from tumor cells (11, 21, 52, 58, 59). Conditioned media experiments provide a more focused model to examine the direct effects of tumor-derived factors on skeletal muscle. Data from these approaches using various cell lines support the notion that tumor-derived factors promote skeletal muscle atrophy (38, 63, 64, 69). In the current study, we sought to use this model to examine the effects of lung cancer cell-derived factors on skeletal muscle. We chose lung cancer because these patients experience a high prevalence of cachexia (6) and because lung cancer is a common model used for pre-clinical cancer cachexia studies. We utilized CM from two murine lung tumor cell lines: the Lewis lung carcinoma (LLC) and $KRAS^{G12D}$ cell lines. The former potently induces cachexia in mice (48, 69) and is used widely in the field. The latter contains the most frequently occurring mutation in human non-small cell lung tumors (62) and provides a near genetically identical cell line for control studies. Additionally, we report, for the first time to our knowledge, the effects of CM from primary cell lines derived from clinical biopsies of human lung tumors. We tested the effects of CM from these cells on differentiated C2C12 myotubes. Myotubes were differentiated for 7 days prior to treatment with CM, a time when they develop anatomical and physiological attributes similar to *in vivo* skeletal muscle and demonstrate atrophy in response to myotoxic chemotherapeutics, such as anthracyclines (24). Based on prior work in the field using these and other cell lines, we hypothesized that CM from murine and human tumor cells would reduce myotube myosin content, decrease

mitochondrial content and increase mitochondrial reactive oxygen species production (ROS).

Methods

Cell culture

C2C12 myoblasts (ATCC® CRL-1772™, Manassas, VA) were cultured in low glucose (1 g/L), Dulbecco's Modified Eagle's Medium (DMEM) supplemented with 10% fetal bovine serum (FBS; Gibco™ Thermo Fisher Scientific Waltham, MA) and antibiotics (50 U/ml penicillin and 50 μg/ml streptomycin). Cells were plated (2 X 10^4 cells/cm^2) on Matrigel (60 μg/cm^2; Corning, Bedford, MA) and switched to differentiation media (DM) of low serum (1% heat-inactivated FBS), high glucose (4.5 g/L) DMEM when they reached 90-100% confluence to induce differentiation, as described (32).

Lewis lung carcinoma (LLC; ATCC CRL-1642) cells, a murine lung cancer cell line that promotes cachexia in mice (46), were cultured, as described (21). Briefly, 2 X 10^5 LLC cells were plated on 10-cm diameter culture dishes in DMEM, supplemented with 10% FBS, 50 U/ml penicillin and 50 μg/ml streptomycin, and grown for 48 h to a final density of 0.8–11 X 10^6 cells per culture dish. NL20 (ATCC CRL-2503) cells were used as a control cell line for LLC cells, as they are non-tumorigenic and have been used as controls for LLC CM treatment of C2C12 myotubes previously (70). NL20 cells were grown, as described (21). Briefly, 2 X 10^5 NL20 cells were plated into 10-cm diameter culture dishes in DMEM, supplemented with 10% FBS, 50 U/ml penicillin, and 50 μg/ml streptomycin, and grown for 48 h to a final density of 0.8–11 X 10^6 cells per dish. For both LLC and NL20 cells, CM from this 48 hr growth period was collected, centrifuged to remove cell debris and stored at -80°C until use.

Primary mouse tracheal epithelial cells (MTECs) were isolated from 14 week old male and female *LSL-KRAS^{G12D}* (The Jackson Laboratory #008179), as described (28). The LSL-*KRAS^{G12D}* mice were generated by crossing *CCSP-rtTA* (The Jacksons Laboratory *CCSP-rtTA* #006222) and *TetO7-Cre* (The Jacksons Laboratory #006224) bi-transgenic mice, to create C*CSP-rtTA/TetO-Cre/LSL-KRAS^{G12D}* mice, as described (1). Cells were cultured on collagen-coated plates in DMEM/F12 media containing 10 μg/ml cholera toxin (Sigma), 2 mg/ml insulin (Roche), 2.5 mg/ml transferrin (Sigma), 12.5 mg/ml bovine pituitary extract (Invitrogen), 10 μg/ml epithelial growth factor (Calbiochem), 50 μM dexamethasone (Sigma), U/50 μg/ml p/s (Gibco), 4.5 mM L-glutamine (Invitrogen), and 1 ml Primocin (InvivoGen), as described (1). MTECs were either treated with a Cre recombinant adenovirus to activate the oncogenic KRAS mutation (Kras^{G12D}) or an empty vector (Kras^{WT}), which serves as a control cell line. Cells were then washed and cultured in serum free media for 2 days and the media was collected, centrifuged to remove cell debris and stored at -80°C until use.

To obtain human tumor cell CM, lung tumor cells obtained from patients during clinical evaluations were used to establish primary cultures, as described (43), with modifications. Briefly, tissue obtained from the biopsy was treated with elastase and DNAse, and then cultured in RPMI 1640 supplemented with L-glutamine and HEPES on collagen-coated dishes. Primary broncheal/tracheal endothelial cells (HBEC; ATCC, PCS-300-010) (2.5 × 10^5 cells/cm2) were used as a non-cancer cell line. They were cultured as adherent monolayers in minimum essential media (MEM) (Invitrogen; Carlsbad, CA) supplemented with 9% FBS (Invitrogen), 2 mM L-glutamine, 100 U penicillin and 100 μg/mL streptomycin (Sigma-Aldrich; St. Louis, MO). For both

primary tumor and HBEC cells, CM was collected following 24 hr incubation in RPMI 1640 + 9% FBS, centrifuged to remove cell debris and stored at -80°C until use.

Preparation of CM and HBSS dilution control.

One volume of tumor or control cell CM was mixed with three volumes of serum-free DMEM to treat myotubes. In all cases, serum content was standardized so that both CM diluted and undiluted DM treatments had the same final serum concentration (2.5% for LLC and NL20 cells; 1% for $Kras^{G12D}$ and $Kras^{WT}$ cells and 2.25% for human tumor and HBEC cells). We also included a dilution control to our experiments, which consisted of DM diluted 1:3 with Hank's balanced salt solution (HBSS; 1 g/L glucose). Thus, we have 4 treatment groups in each experiment: untreated controls (undiluted DM; i.e., no CM added), dilution control (1:3 dilution of HBSS:DM), non-tumorigenic/cachectic cell CM control (1:3 dilution of CM:DM) and tumor cell CM (1:3 dilution of CM:DM). In all conditions, media was changed daily during the 3-day treatment period.

Patients

Patients (76 ± 7 yr; Table 1 for details) with known or suspected lung cancer were recruited from the University of Vermont Medical Center Lung Multi-disciplinary Clinic. Written informed consent was obtained from all volunteers prior to their participation and protocols were approved by the Committees on Human Research at the University of Vermont. Tumor cells were obtained when patients underwent either clinically indicated bronchoscopy or percutaneous biopsy. Following on-site cytopathological diagnosis of cancer, one additional fine needle aspiration was performed to obtain cells.

Protein expression

Protein expression was measured by western blot. Myotubes were washed with phosphate buffered saline, lysed (50 mM Tris, 150 mM NaCl, 10% (v/v) glycerol, 0.5% IGEPAL CA-630,1 mM EDTA, containing Protease Inhibitor Cocktail (1:100, cat# P8340, Sigma) and Phosphatase Inhibitor Cocktail 3 (1:100, cat# P0044, Sigma), incubated on ice for 30 min and then centrifuged at 14,000 × g at 4 °C for 10 min. Lysate protein contents were measured (BioRad DC Protein Assay, Hercules, CA) and diluted in sample prep buffer (62.5 mM Tris-HCl, pH 6.8, 10% glycerol, 1% SDS 0.005% bromophenol blue, 5% 2-mercaptoethanol). Proteins were separated by SDS-PAGE (Bio-Rad, Hercules, CA, USA), transferred to polyvinylidene (PVDF) membranes and blocked with TBST buffer (150 mM NaCl, 0.05 % Tween-20, and 20 mM Tris-HCl, pH 7.4) containing 5% non-fatty milk or BSA. After blocking, membranes were incubated overnight with myosin primary antibody (1:20000, Sigma M4276, RRID: AB_477190). Membranes were washed for 30 min in TBST and then incubated for 1 h at room temperature in 5% milk-TBST containing Anti-Mouse IgG-Peroxidase (1:15000, Sigma A2304, RRID: AB_257993) secondary antibody with Clarity Western ECL Substrate (Bio-Rad, Hercules, CA, USA).

Myotube mitochondrial content and reactive oxygen species (ROS) production

Mitochondrial content and ROS production were measured with fluorometric dyes, as described (25). Briefly, C2C12 myotubes grown in 35 mm dishes or black-walled 96 well plates were loaded with fluorescent dyes to assess mitochondrial content (1 μM MitoTracker Green FM; 490/516 nm) and ROS production (1 μM MitoSOX Red;

510/580 nm; both Molecular Probes, Eugene, OR) 15 minutes prior to measurement. Fluorescence was measured on a microplate reader (BioTek, Winooski, VT) and the MitoSox signal was expressed relative to MitoTracker signal to control ROS production for mitochondrial content.

Statistics

Analysis of variance (ANOVA) was used to compare treatments. Most studies examining CM treatment have compared CM application to a single control condition. Thus, we also made pairwise comparisons between CM and all three control conditions using unpaired t-test.

Results

Characteristics of C2C12 myotube cultures. C2C12 myotubes were differentiated for 7 days before treatment with CM. Under our culture conditions, there is rapid growth and accumulation of myosin between d3 and d7, followed by a relative plateauing of myotube myosin content and diameter (data not shown). At d7, myotubes express myofilament proteins, including myosin, actin, and α-actinin, and organize these proteins into myofilaments (data not shown). Myofilaments and components of the excitation-contraction coupling system are functional at this time, as electrical field stimulation causes intracellular Ca^{2+} cycling and contraction, which can be prevented by pharmacological inhibition of excitation contraction coupling with the sodium channel blocker tetrodotoxin (data not shown). Thus, at this stage of differentiation, myotubes exhibit numerous hallmark characteristics of *in vivo* muscle.

LLC and Kras CM. We began by testing the effects of LLC CM, as this cell line is widely used to promote cachexia in mouse xenoplant models (4, 8, 11). In C2C12 myotubes differentiated for 7 days, we found no differences in myosin content among LLC CM, HBSS dilution control and NL20 control CM and untreated controls (Figure 1A) when analyzed via ANOVA. Moreover, because many studies only compare LLC CM to a single control, we also performed pairwise comparisons between LLC CM and different control conditions (untreated control, HBSS dilution control or NL20 control) by unpaired t-tests. There were still no effects of LLC CM on myotube myosin content with this different analytical approach. We found an effect of $Kras^{G12D}$ CM on myotube myosin content (Figure 1B), but it paradoxically increased myosin content compared to

all control conditions (P=0.002) using either ANOVA or pairwise analytical approaches (P<0.01).

Timing of CM application. Reasons for the absence of effects of CM are uncertain, but one difference between our protocol and the majority of studies in the field is that we used myotubes that were differentiated for 7 days prior to CM application. Most studies have treated myotubes at day 4 or 5 post-differentiation. Thus, we also examined the effects of CM on myotubes starting at day 4 post-differentiation. Under these conditions, we observed a 32% reduction in myosin content (P<0.05 using either ANOVA or pairwise analytical approaches) in response to LLC CM compared to untreated control (Figure 2A). However, a similar reduction in myosin content was noted with CM from the non-tumorigenic NL20 cell line (33%, P<0.05 using either ANOVA or pairwise analysis) and a trend for lower myosin content was observed in the HBSS dilution control (P=0.07 pairwise analysis, P=0.08 ANOVA) compared to untreated controls (Figure 2A). Similarly, using Kras CM administered at day 4 post-differentiation, we found a 36% reduction in myosin content with $Kras^{G12D}$ CM (P<0.05 ANOVA or pairwise analysis). However, we also observed a reduction 38% in myosin content with CM from $Kras^{WT}$ cells (P<0.05 ANOVA or pairwise analysis) and 39% reduction with the HBSS dilution control (P<0.05 ANOVA or pairwise analysis) when compared to untreated controls (Figure 2B).

Mitochondrial content and ROS production with murine CM. Recent reports have suggested a role for oxidant stress in the atrophic effect of tumor-related factors (3, 16, 20, 31, 60). Thus, we examined the effects of CM on mitochondrial content and ROS

production. LLC treatment of myotubes 7 days post-differentiation did not alter mitochondrial ROS production (Figure 3A), nor did treatment with any of the control conditions, whether we utilized ANOVA or pairwise comparisons. Mitochondrial content was also unchanged with HBSS, NL20 or LLC treatment (Figure 3B). With Kras experiments on day 7 post-differentiation myotubes, there was no change in ROS production compared to untreated controls (Figure 3C), but both $Kras^{G12D}$ ($P<0.01$ ANOVA or pairwise analysis) and $Kras^{WT}$ ($P<0.01$ ANOVA or pairwise analysis) CM increased mitochondrial content ($P<0.01$; Figure 3D) when measured with ANOVA or pairwise comparisons.

When LLC CM was applied to d4 myotubes, no changes in ROS were found (Figure 4A). However, mitochondrial content was elevated with NL20 CM ($P<0.01$ ANOVA or pairwise analysis) (Figure 4B). Kras CM increased ROS production in d4 myotubes with both $Kras^{G12D}$ ($P<0.01$) and $Kras^{WT}$ ($P<0.01$) CM (Figure 4C), but not with HBSS control dilution. Mitochondrial content was also increased by $Kras^{G12D}$ ($P<0.01$) and $Kras^{WT}$ ($P<0.01$) CM (Figure 4D) relative to untreated controls when measured with either ANOVA or pairwise analysis.

Myotube myosin content with human CM. Informed by the results of LLC and Kras studies, we decided to test CM from patient lung cancer biopsies on d7 myotubes, as we reasoned that effects of CM observed on d4 myotubes were due to growth inhibition, rather than a unique effect of tumor-derived factors on myotubes. We treated d7 myotubes with patient tumor CM from 4 patients (human tumor conditioned media; hTCM), non-cancer control cells (human bronchial epithelial cells; HBEC), HBSS

dilution controls, and untreated controls for 3 days with serum content constant among all groups. We found no effect of patient lung tumor primary cell CM on myosin content compared to untreated and saw no reduction with any of the treatment groups (Figure 5A). Similarly, we found no effect of patient lung tumor primary cell CM, non-cancer control cell CM or dilution control compared to untreated control (Figure 5B). We observed an effect of hTCM (+19%, $P<0.01$) and HBEC CM (+16%, $P<0.05$) to increase mitochondrial content compared to untreated controls, but no effect of HBSS dilution control (Figure 5C) when measured with either ANOVA or pairwise analysis.

Discussion

Conventional wisdom holds that tumors release soluble factors that act on distal skeletal muscle tissue to cause atrophy and other metabolic derangements in cancer patients. We evaluated this proposition by testing the effects of murine and human lung tumor cell CM on C2C12 myotube cultures, a common model to test for tumor cell-derived atrophic factors (11, 35, 36, 38, 44, 51, 68). Our studies included controls to account for dilution of media, factors released into media by growing cells and the timing of CM application relative to the start of differentiation. When we examined the effects of murine lung tumor cell CM 7 days post-differentiation, when myotubes express structural and functional phenotypes common to *in vivo* skeletal muscle, we found no atrophic effects of murine tumor CM on myotubes. Although murine lung tumor cell CM reduced myosin content and caused mitochondrial adaptations when applied to myotubes differentiated for 4 days compared to untreated controls, similar effects were observed with control cell CM and HBSS dilution controls. Finally, to our knowledge, we present the first report of the effect of CM from primary cultures of human lung tumor cells on cultured myotubes. Similar to murine cancer cell CM, however, we found no evidence for an effect of human tumor CM on myotubes. Our results argue against the hypothesis that factors released from tumor cells contribute to skeletal muscle atrophy and mitochondrial abnormalities.

Cultured muscle cells are a unique and valuable system that permits examination of muscle in isolation, with the ability to manipulate the extracellular environment. Despite these strengths, studies in cultured muscle cells are criticized because of the

artificial nature of this system. While a myotube is not a perfect model of a muscle fiber, how well this system models *in vivo* muscle may vary depending on its stage of differentiation. Treatment of myotubes with either murine or human tumor cell CM starting at 7 days post-differentiation had no effect on either myotube myosin content or mitochondrial content/ROS production compared to untreated controls. In fact, in the case of $KRAS^{G12D}$ cells, CM paradoxically enhanced myotube myosin and mitochondrial content compared to untreated controls. In contrast to results on 7 day differentiated myotubes, CM had effects on cells treated at 4 days post-differentiation, causing myosin depletion and some mitochondrial adaptations. The failure to observe effects at 7 days post-differentiation is unlikely related to the cell lines used, as LLC is well-proven to cause cachexia when transplanted into mice (12, 34, 45, 65) and when LLC CM has been applied to cultured myotubes (21, 36, 38, 39, 67). $KRAS^{G12D}$ is less well-described, but data from our labs (unpublished data) and others show that $KRAS^{G12D}$ mice experience muscle atrophy (40). One could argue that myotubes at this later developmental stage are recalcitrant to atrophic stimuli. However, the application of various chemotherapeutics provokes atrophy at this time (24), in agreement with studies by other laboratories on myotubes studied earlier following differentiation (22).

Our data from experiments treating 4-day differentiated myotubes with LLC and $KRAS^{G12D}$ CM argue that a dilution effect caused by the addition of the CM to standard DM impairs myotube growth. Numerous studies have shown that C2C12s are still increasing in size and myosin content from day 4 to day 7 post-differentiation (13, 14, 26, 41, 54, 57, 61). Media dilution with CM may simply starve cells of nutrients required for normal growth. A recent study by Jackman *et al.* supports this interpretation (27). In this

study, 4 -day post-differentiation myotubes were treated for 3 days with tumor cell CM and compared to untreated DM, similar to the current study. Time course data show that the effect of CM was not to induce atrophy but to impair the growth of myotubes. Our HBSS dilution control further supports the effects of the CM dilution on myotube growth. Thus, we conclude that compared to control cells maintained in undiluted DM, the effects of tumor cell CM on 4 day differentiated myotubes primarily reflects growth inhibition.

If media dilution impairs myotube growth, a more valid control would be a cell type similar to the tumor cell line, but that does not release factors that cause muscle wasting. Because the identity of these secreted factors is unknown, the selection of appropriate control cell lines is difficult. We used CM from a similar lung epithelial cell type compared to tumor cell lines. In the control for LLC CM, we used the non-tumorigenic NL20 cells (21, 49, 50, 71), which is used widely in the field as a control for LLC CM (66, 68, 69). This is not an ideal cell line because of species differences, but it is non-tumorigenic in animals and grows well under similar media conditions as LLC cells and has been used as a control for LLC CM in past studies (46, 70).

Concern about the appropriateness of the control cell line is lessened in the Kras CM experiments, where we used a Cre recombinant adenovirus to activate the oncogenic KRAS mutation ($Kras^{G12D}$) or treatment of cells with an empty vector as a control ($Kras^{WT}$). Thus, with the exception of Cre expression and transgene activation, the $Kras^{WT}$ cells are identical to $Kras^{G12D}$ cells. CM from $Kras^{WT}$ controls, therefore, should reflect the effects of nutrient depletion, secreted factors and/or metabolic by-products typical to growing cells, only differing from $Kras^{G12D}$ CM for those secreted factors that

contribute to cachexia. As with LLC CM experiments, data from these controls largely mirrored that of HBSS dilution controls and $Kras^{G12D}$ CM, further supporting the conclusion that most of the effects of tumor cell CM observed in prior work is related to a dilution effect when comparisons are made to cells maintained in untreated (i.e., undiluted) control media. Thus, our data collectively argue against the hypothesis that factors secreted from tumor cells act directly on skeletal muscle cells to provoke atrophy and mitochondrial maladaptations.

Several caveats to our studies deserve discussion. First, we are examining the direct effects of CM on skeletal muscle. Muscles contain an array of other cell types (immune cells, satellite cells, fibroblasts, etc.) that could respond to tumor-derived factors to provoke atrophy. For instance, tumor CM may mediate its effects through host inflammatory response to tumor presence, either systemically or locally within the muscle (5, 9). Our experiments did not test potential host-specific host-derived factors. Second, we used the common 1:3 dilution of DM with CM to treat the cultured myotubes. The amount of secreted factors in this dilution, and the fact that we exposed myotubes to a single bolus of the CM (media changed daily), may be insufficient to promote skeletal muscle myotube atrophy. To the first point, considering the relatively small size of most human tumors relative to the systemic circulation and interstitial fluid volumes, such a dilution would seem far in excess of what skeletal muscles are exposed to *in vivo*. To the latter point, recent studies have argued that co-culture of tumor cells and muscle myotubes is required to observe a true atrophic effect of tumor-secreted factors to cause atrophy (27). While this may be the case, as we have demonstrated with our various control conditions, appropriate control cell lines are needed to assure that

myotube atrophy is not provoked by media substrate depletion and/or accumulation of metabolic waste products. Finally, our model is uncoupled from the complex clinical condition present in cancer patients, such as pulmonary insufficiency, chemotherapeutics and muscle disuse. The effects of these clinical factors may cause skeletal muscle to be more responsive to tumor-related factors that incite muscle wasting.

In summary, we found no evidence that tumor-secreted factors influence skeletal muscle. Although the common experimental model of using 4 day differentiated myotubes for treatment yielded lower myotube myosin content compared to untreated controls, these decreases were not apparent when compared to controls for media dilution or other secreted factors, suggesting that CM effects are most likely related to media dilution and growth inhibition, rather than atrophy. Finally, to our knowledge, this is the first report of the effects of human tumor primary cell CM on cultured myotubes. Similar to results from murine tumor cell CM, we found no effect of human tumor cell CM on myotube myosin content or mitochondrial content or ROS production. Collectively, our results argue against direct effects of tumor secreted factors on skeletal muscle to cause atrophy and metabolic dysfunction.

Acknowledgments

We thank the patients who generously volunteered for these studies.

Grants

This study was funded by R01 AR065826, R21 CA191532, S10 OD017969 and P30 RR032135. B.G. was funded by a Department of Defense SMART Scholarship ID 2016-85335.

Disclosures

None.

References:

1. **Alcorn JF, Guala AS, van der Velden J, McElhinney B, Irvin CG, Davis RJ, and Janssen-Heininger YM.** Jun N-terminal kinase 1 regulates epithelial-to-mesenchymal transition induced by TGF-beta1. *J Cell Sci* 121: 1036-1045, 2008.

2. **Ando K, Takahashi F, Kato M, Kaneko N, Doi T, Ohe Y, Koizumi F, Nishio K, and Takahashi K.** Tocilizumab, a proposed therapy for the cachexia of Interleukin6-expressing lung cancer. *PLoS One* 9: e102436, 2014.

3. **Antunes D, Padrao AI, Maciel E, Santinha D, Oliveira P, Vitorino R, Moreira-Goncalves D, Colaco B, Pires MJ, Nunes C, Santos LL, Amado F, Duarte JA, Domingues MR, and Ferreira R.** Molecular insights into mitochondrial dysfunction in cancer-related muscle wasting. *Biochim Biophys Acta* 1841: 896-905, 2014.

4. **Au ED, Desai AP, Koniaris LG, and Zimmers TA.** The MEK-Inhibitor Selumetinib Attenuates Tumor Growth and Reduces IL-6 Expression but Does Not Protect against Muscle Wasting in Lewis Lung Cancer Cachexia. *Front Physiol* 7: 682, 2016.

5. **Baracos VE, Martin L, Korc M, Guttridge DC, and Fearon KCH.** Cancer-associated cachexia. *Nat Rev Dis Primers* 4: 17105, 2018.

6. **Baracos VE, Reiman T, Mourtzakis M, Gioulbasanis I, and Antoun S.** Body composition in patients with non-small cell lung cancer: a contemporary view of cancer cachexia with the use of computed tomography image analysis. *Am J Clin Nutr* 91: 1133S-1137S, 2010.

7. **Bennani-Baiti N and Walsh D.** Animal models of the cancer anorexia-cachexia syndrome. *Support Care Cancer* 19: 1451-1463, 2011.

8. **Blackwell TA, Cervenka I, Khatri B, Brown JL, Rosa-Caldwell ME, Lee DE, Perry RA, Jr., Brown LA, Haynie WS, Wiggs MP, Bottje WG, Washington TA, Kong BC, Ruas JL, and Greene NP.** Transcriptomic analysis of the development of skeletal muscle atrophy in cancer-cachexia in tumor-bearing mice. *Physiol Genomics* 50: 1071-1082, 2018.

9. **Bohnert KR, McMillan JD, and Kumar A.** Emerging roles of ER stress and unfolded protein response pathways in skeletal muscle health and disease. *J Cell Physiol* 233: 67-78, 2018.

10. **Bonetto A, Rupert JE, Barreto R, and Zimmers TA.** The Colon-26 Carcinoma Tumor-bearing Mouse as a Model for the Study of Cancer Cachexia. *J Vis Exp*, 2016.

11. **Brown JL, Lee DE, Rosa-Caldwell ME, Brown LA, Perry RA, Haynie WS, Huseman K, Sataranatarajan K, Van Remmen H, Washington TA, Wiggs MP, and Greene NP.** Protein imbalance in the development of skeletal muscle wasting in tumour-bearing mice. *J Cachexia Sarcopenia Muscle* 9: 987-1002, 2018.

12. **Brown JL, Rosa-Caldwell ME, Lee DE, Blackwell TA, Brown LA, Perry RA, Haynie WS, Hardee JP, Carson JA, Wiggs MP, Washington TA, and Greene NP.** Mitochondrial degeneration precedes the development of muscle atrophy in progression of cancer cachexia in tumour-bearing mice. *J Cachexia Sarcopenia Muscle* 8: 926-938, 2017.

13. **Chaturvedi V, Dye DE, Kinnear BF, van Kuppevelt TH, Grounds MD, and Coombe DR.** Interactions between Skeletal Muscle Myoblasts and their Extracellular Matrix Revealed by a Serum Free Culture System. *PLoS One* 10: e0127675, 2015.

14. **Cheng CS, El-Abd Y, Bui K, Hyun YE, Hughes RH, Kraus WE, and Truskey GA.** Conditions that promote primary human skeletal myoblast culture and muscle differentiation in vitro. *Am J Physiol Cell Physiol* 306: C385-395, 2014.

15. **Choi Y, Oh DY, Kim TY, Lee KH, Han SW, Im SA, Kim TY, and Bang YJ.** Skeletal Muscle Depletion Predicts the Prognosis of Patients with Advanced Pancreatic Cancer Undergoing Palliative Chemotherapy, Independent of Body Mass Index. *PLoS One* 10: e0139749, 2015.

16. **Constantinou C, Fontes de Oliveira CC, Mintzopoulos D, Busquets S, He J, Kesarwani M, Mindrinos M, Rahme LG, Argiles JM, and Tzika AA.** Nuclear magnetic resonance in conjunction with functional genomics suggests mitochondrial dysfunction in a murine model of cancer cachexia. *Int J Mol Med* 27: 15-24, 2011.

17. **Dewys WD, Begg C, Lavin PT, Band PR, Bennett JM, Bertino JR, Cohen MH, Douglass HO, Jr., Engstrom PF, Ezdinli EZ, Horton J, Johnson GJ, Moertel CG, Oken MM, Perlia C, Rosenbaum C, Silverstein MN, Skeel RT, Sponzo RW, and Tormey DC.** Prognostic effect of weight loss prior to chemotherapy in cancer patients. Eastern Cooperative Oncology Group. *Am J Med* 69: 491-497, 1980.

18. **Fearon KC.** Cancer cachexia and fat-muscle physiology. *N Engl J Med* 365: 565-567, 2011.

19. **Fearon KC, Glass DJ, and Guttridge DC.** Cancer cachexia: mediators, signaling, and metabolic pathways. *Cell Metab* 16: 153-166, 2012.

20. **Fontes-Oliveira CC, Busquets S, Toledo M, Penna F, Paz Aylwin M, Sirisi S, Silva AP, Orpi M, Garcia A, Sette A, Ines Genovese M, Olivan M, Lopez-Soriano FJ, and Argiles JM.** Mitochondrial and sarcoplasmic reticulum abnormalities in cancer cachexia: altered energetic efficiency? *Biochim Biophys Acta* 1830: 2770-2778, 2013.

21. **Gao S and Carson JA.** Lewis lung carcinoma regulation of mechanical stretch-induced protein synthesis in cultured myotubes. *Am J Physiol Cell Physiol* 310: C66-79, 2016.

22. **Gilliam LA, Moylan JS, Patterson EW, Smith JD, Wilson AS, Rabbani Z, and Reid MB.** Doxorubicin acts via mitochondrial ROS to stimulate catabolism in C2C12 myotubes. *Am J Physiol Cell Physiol* 302: C195-202, 2012.

23. **Go SI, Park MJ, Song HN, Kang MH, Park HJ, Jeon KN, Kim SH, Kim MJ, Kang JH, and Lee GW.** Sarcopenia and inflammation are independent predictors of survival in male patients newly diagnosed with small cell lung cancer. *Support Care Cancer* 24: 2075-2084, 2016.

24. **Guigni BA, Callahan DM, Tourville TW, Miller MS, Fiske B, Voigt T, Korwin-Mihavics B, Anathy V, Dittus K, and Toth MJ.** Skeletal muscle atrophy and dysfunction in breast cancer patients: role for chemotherapy-derived oxidant stress. *Am J Physiol Cell Physiol* 315: C744-C756, 2018.

25. **Guigni BA, Callahan DM, Tourville TW, Miller MS, Fiske B, Voigt T, Korwin-Mihavics B, Anathy V, Dittus K, and Toth MJ.** Skeletal Muscle Atrophy and Dysfunction in Breast Cancer Patients: Role for Chemotherapy-Derived Oxidant Stress. *Am J Physiol Cell Physiol*, 2018.

26. **Issa ME, Muruganandan S, Ernst MC, Parlee SD, Zabel BA, Butcher EC, Sinal CJ, and Goralski KB.** Chemokine-like receptor 1 regulates skeletal muscle cell myogenesis. *Am J Physiol Cell Physiol* 302: C1621-1631, 2012.

27. **Jackman RW, Floro J, Yoshimine R, Zitin B, Eiampikul M, El-Jack K, Seto DN, and Kandarian SC.** Continuous Release of Tumor-Derived Factors Improves the Modeling of Cachexia in Muscle Cell Culture. *Front Physiol* 8: 738, 2017.

28. **Jackson EL, Willis N, Mercer K, Bronson RT, Crowley D, Montoya R, Jacks T, and Tuveson DA.** Analysis of lung tumor initiation and progression using conditional expression of oncogenic K-ras. *Genes Dev* 15: 3243-3248, 2001.

29. **Johns N, Stephens NA, and Fearon KC.** Muscle wasting in cancer. *Int J Biochem Cell Biol* 45: 2215-2229, 2013.

30. **Jourdain M, Melly S, Summermatter S, and Hatakeyama S.** Mouse models of cancer-induced cachexia: Hind limb muscle mass and evoked force as readouts. *Biochem Biophys Res Commun* 503: 2415-2420, 2018.

31. **Julienne CM, Dumas JF, Goupille C, Pinault M, Berri C, Collin A, Tesseraud S, Couet C, and Servais S.** Cancer cachexia is associated with a decrease in skeletal muscle mitochondrial oxidative capacities without alteration of ATP production efficiency. *J Cachexia Sarcopenia Muscle* 3: 265-275, 2012.

32. **Langen RCJ, Schols AMWJ, Kelders MCJM, Wouters EFM, and Janssen-Heininger YMW.** Enhanced myogenic differentiation by extracellular matrix is regulated at the early stages of myogenesis. *In Vitro Cell Dev Biol Anim* 39: 163-169, 2003.

33. **Lanic H, Kraut-Tauzia J, Modzelewski R, Clatot F, Mareschal S, Picquenot JM, Stamatoullas A, Lepretre S, Tilly H, and Jardin F.** Sarcopenia is an independent prognostic factor in elderly patients with diffuse large B-cell lymphoma treated with immunochemotherapy. *Leuk Lymphoma* 55: 817-823, 2014.

34. **Lee DE, Brown JL, Rosa-Caldwell ME, Blackwell TA, Perry RA, Jr., Brown LA, Khatri B, Seo D, Bottje WG, Washington TA, Wiggs MP, Kong BW, and Greene NP.** Cancer cachexia-induced muscle atrophy: evidence for alterations in microRNAs important for muscle size. *Physiol Genomics* 49: 253-260, 2017.

35. **Lee H, Lee SJ, Bae GU, Baek NI, and Ryu JH.** Canadine from Corydalis turtschaninovii Stimulates Myoblast Differentiation and Protects against Myotube Atrophy. *Int J Mol Sci* 18, 2017.

36. **Lee HW, Baker E, Lee KM, Persinger AM, Hawkins W, and Puppa M.** Effects of low dose leucine supplementation on gastrocnemius muscle mitochondrial content and protein turnover in tumor bearing mice. *Appl Physiol Nutr Metab*, 2019.

37. **Llovera M, Garcia-Martinez C, Lopez-Soriano J, Agell N, Lopez-Soriano FJ, Garcia I, and Argiles JM.** Protein turnover in skeletal muscle of tumour-bearing transgenic mice overexpressing the soluble TNF receptor-1. *Cancer Lett* 130: 19-27, 1998.

38. **McLean JB, Moylan JS, and Andrade FH.** Mitochondria dysfunction in lung cancer-induced muscle wasting in C2C12 myotubes. *Front Physiol* 5: 503, 2014.

39. **McLean JB, Moylan JS, Horrell EM, and Andrade FH.** Proteomic analysis of media from lung cancer cells reveals role of 14-3-3 proteins in cachexia. *Front Physiol* 6: 136, 2015.

40. **Miller A, McLeod L, Alhayyani S, Szczepny A, Watkins DN, Chen W, Enriori P, Ferlin W, Ruwanpura S, and Jenkins BJ.** Blockade of the IL-6 trans-signalling/STAT3 axis suppresses cachexia in KrasWTinduced lung adenocarcinoma. *Oncogene* 36: 3059-3066, 2017.

41. **Murphy SM, Kiely M, Jakeman PM, Kiely PA, and Carson BP.** Optimization of an in vitro bioassay to monitor growth and formation of myotubes in real time. *Biosci Rep* 36, 2016.

42. **Naito T, Okayama T, Aoyama T, Ohashi T, Masuda Y, Kimura M, Shiozaki H, Murakami H, Kenmotsu H, Taira T, Ono A, Wakuda K, Imai H, Oyakawa T, Ishii T, Omori S, Nakashima K, Endo M, Omae K, Mori K, Yamamoto N, Tanuma A, and Takahashi T.** Unfavorable impact of cancer cachexia on activity of daily living and need for inpatient care in elderly patients with advanced non-small-cell lung cancer in Japan: a prospective longitudinal observational study. *BMC Cancer* 17: 800, 2017.

43. **Niederst MJ, Sequist LV, Poirier JT, Mermel CH, Lockerman EL, Garcia AR, Katayama R, Costa C, Ross KN, Moran T, Howe E, Fulton LE, Mulvey HE, Bernardo LA, Mohamoud F, Miyoshi N, VanderLaan PA, Costa DB, Jänne PA, Borger DR, Ramaswamy S, Shioda T, Iafrate AJ, Getz G, Rudin CM, Mino-Kenudson M, and Engelman JA.** RB loss in resistant EGFR mutant lung adenocarcinomas that transform to small-cell lung cancer. *Nat Commun* 6, 2015.

44. **Oraldi M, Maggiora M, Paiuzzi E, Canuto RA, and Muzio G.** CLA reduces inflammatory mediators from A427 human lung cancer cells and A427 conditioned medium promotes differentiation of C2C12 murine muscle cells. *Lipids* 48: 29-38, 2013.

45. **Paul PK, Gupta SK, Bhatnagar S, Panguluri SK, Darnay BG, Choi Y, and Kumar A.** Targeted ablation of TRAF6 inhibits skeletal muscle wasting in mice. *J Cell Biol* 191: 1395-1411, 2010.

46. **Penna F, Busquets S, and Argiles JM.** Experimental cancer cachexia: Evolving strategies for getting closer to the human scenario. *Semin Cell Dev Biol* 54: 20-27, 2016.

47. **Puppa MJ, White JP, Velazquez KT, Baltgalvis KA, Sato S, Baynes JW, and Carson JA.** The effect of exercise on IL-6-induced cachexia in the Apc (Min/+) mouse. *J Cachexia Sarcopenia Muscle* 3: 117-137, 2012.

48. **Puyol M, Martin A, Dubus P, Mulero F, Pizcueta P, Khan G, Guerra C, Santamaria D, and Barbacid M.** A synthetic lethal interaction between K-Ras oncogenes and Cdk4 unveils a therapeutic strategy for non-small cell lung carcinoma. *Cancer Cell* 18: 63-73, 2010.

49. **Schiller JH and Bittner G.** Loss of the tumorigenic phenotype with in vitro, but not in vivo, passaging of a novel series of human bronchial epithelial cell lines: possible role of an alpha 5/beta 1-integrin-fibronectin interaction. *Cancer Res* 55: 6215-6221, 1995.

50. **Schiller JH, Bittner G, Oberley TD, Kao C, Harris C, and Meisner LF.** Establishment and characterization of a SV40 T-antigen immortalized human bronchial epithelial cell line. *In Vitro Cell Dev Biol* 28A: 461-464, 1992.

51. **Seo E, Kang H, Lim OK, and Jun HS.** Supplementation with IL-6 and Muscle Cell Culture Conditioned Media Enhances Myogenic Differentiation of Adipose Tissue-Derived Stem Cells through STAT3 Activation. *Int J Mol Sci* 19, 2018.

52. **Seto DN, Kandarian SC, and Jackman RW.** A Key Role for Leukemia Inhibitory Factor in C26 Cancer Cachexia. *J Biol Chem* 290: 19976-19986, 2015.

53. **Shachar SS, Deal AM, Weinberg M, Williams GR, Nyrop KA, Popuri K, Choi SK, and Muss HB.** Body Composition as a Predictor of Toxicity in Patients Receiving Anthracycline and Taxane-Based Chemotherapy for Early-Stage Breast Cancer. *Clin Cancer Res* 23: 3537-3543, 2017.

54. **Shu L and Houghton PJ.** The mTORC2 complex regulates terminal differentiation of C2C12 myoblasts. *Mol Cell Biol* 29: 4691-4700, 2009.

55. **Sjoblom B, Gronberg BH, Wentzel-Larsen T, Baracos VE, Hjermstad MJ, Aass N, Bremnes RM, Flotten O, Bye A, and Jordhoy M.** Skeletal muscle radiodensity is prognostic for survival in patients with advanced non-small cell lung cancer. *Clin Nutr* 35: 1386-1393, 2016.

56. **Strassmann G, Fong M, Kenney JS, and Jacob CO.** Evidence for the involvement of interleukin 6 in experimental cancer cachexia. *J Clin Invest* 89: 1681-1684, 1992.

57. **Stuelsatz P, Pouzoulet F, Lamarre Y, Dargelos E, Poussard S, Leibovitch S, Cottin P, and Veschambre P.** Down-regulation of MyoD by calpain 3 promotes generation of reserve cells in C2C12 myoblasts. *J Biol Chem* 285: 12670-12683, 2010.

58. **Sun R, Zhang S, Hu W, Lu X, Lou N, Yang Z, Chen S, Zhang X, and Yang H.** Valproic acid attenuates skeletal muscle wasting by inhibiting C/EBPbeta-regulated atrogin1 expression in cancer cachexia. *Am J Physiol Cell Physiol* 311: C101-115, 2016.

59. **Sustova H, De Feudis M, Reano S, Alves Teixeira M, Valle I, Zaggia I, Agosti E, Prodam F, and Filigheddu N.** Opposing effects of 25-hydroxy- and 1alpha,25-dihydroxy-vitamin D3 on pro-cachectic cytokine- and cancer conditioned medium-induced atrophy in C2C12 myotubes. *Acta Physiol (Oxf)*: e13269, 2019.

60. **Tan BH and Fearon KC.** Cachexia: prevalence and impact in medicine. *Curr Opin Clin Nutr Metab Care* 11: 400-407, 2008.

61. **Tang J, He A, Yan H, Jia G, Liu G, Chen X, Cai J, Tian G, Shang H, and Zhao H.** Damage to the myogenic differentiation of C2C12 cells by heat stress is associated with up-regulation of several selenoproteins. *Sci Rep* 8: 10601, 2018.

62. **Timar J.** The clinical relevance of KRAS gene mutation in non-small-cell lung cancer. *Curr Opin Oncol* 26: 138-144, 2014.

63. **Tisdale MJ.** Are tumoral factors responsible for host tissue wasting in cancer cachexia? *Future Oncol* 6: 503-513, 2010.

64. **Yano CL, Ventrucci G, Field WN, Tisdale MJ, and Gomes-Marcondes MC.** Metabolic and morphological alterations induced by proteolysis-inducing factor from Walker tumour-bearing rats in C2C12 myotubes. *BMC Cancer* 8: 24, 2008.

65. **Yoshimura T, Saitoh K, Sun L, Wang Y, Taniyama S, Yamaguchi K, Uchida T, Ohkubo T, Higashitani A, Nikawa T, Tachibana K, and Hirasaka K.** Morin suppresses cachexia-induced muscle wasting by binding to ribosomal protein S10 in carcinoma cells. *Biochem Biophys Res Commun* 506: 773-779, 2018.

66. **Zhang G, Jin B, and Li YP.** C/EBPbeta mediates tumour-induced ubiquitin ligase atrogin1/MAFbx upregulation and muscle wasting. *EMBO J* 30: 4323-4335, 2011.

67. **Zhang G and Li YP.** p38beta MAPK upregulates atrogin1/MAFbx by specific phosphorylation of C/EBPbeta. *Skelet Muscle* 2: 20, 2012.

68. **Zhang G, Lin RK, Kwon YT, and Li YP.** Signaling mechanism of tumor cell-induced up-regulation of E3 ubiquitin ligase UBR2. *FASEB J* 27: 2893-2901, 2013.

69. **Zhang G, Liu Z, Ding H, Miao H, Garcia JM, and Li YP.** Toll-like receptor 4 mediates Lewis lung carcinoma-induced muscle wasting via coordinate activation of protein degradation pathways. *Sci Rep* 7: 2273, 2017.

70. **Zhang G, Liu Z, Ding H, Zhou Y, Doan HA, Sin KWT, Zhu ZJ, Flores R, Wen Y, Gong X, Liu Q, and Li YP.** Tumor induces muscle wasting in mice through releasing extracellular Hsp70 and Hsp90. *Nat Commun* 8: 589, 2017.

71. **Zhou D, Xie M, He B, Gao Y, Yu Q, He B, and Chen Q.** Microarray data re-annotation reveals specific lncRNAs and their potential functions in non-small cell lung cancer subtypes. *Mol Med Rep* 16: 5129-5136, 2017.

Figures & Tables

Figure 1:

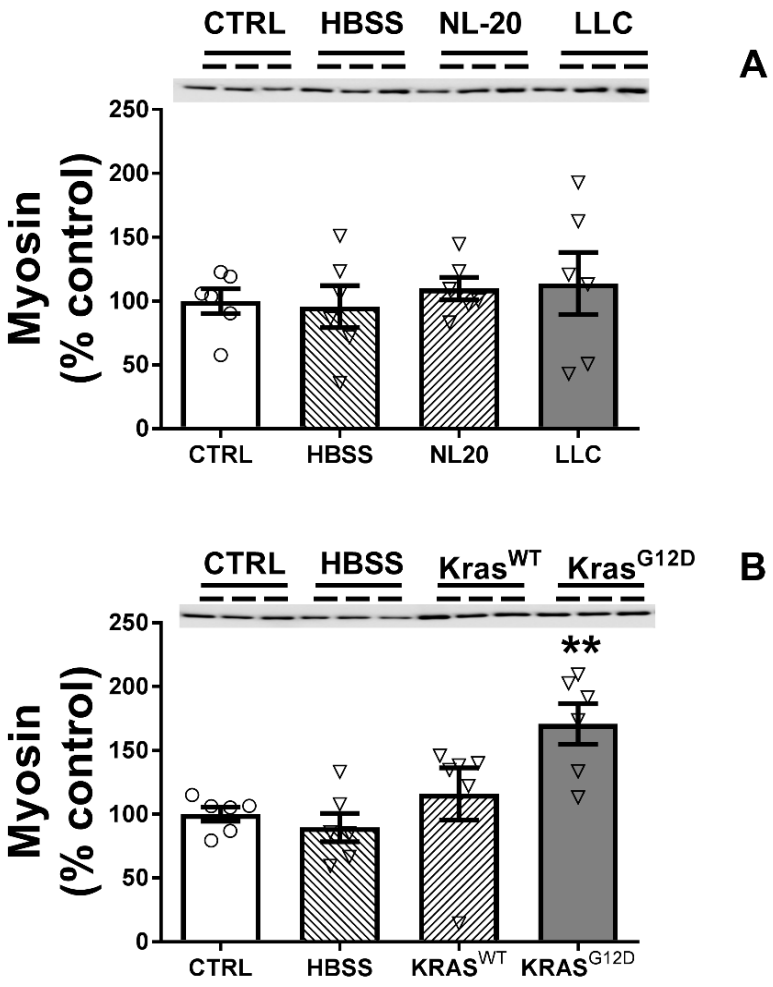

Figure 2.0.1: *The effects of murine CM on d7 myotubes.*

Figure 1. Effects of 3 d of murine LLC (A; gray bar) or KrasG12D (B; gray bar) conditioned media (CM; 1:3) treatment on myosin content in d7 differentiated myotubes compared to undiluted (CTRL; open bars), dilution (HBSS; 1:3; hatched bar) and non-tumorigenic (NL20 and KrasWT cells; 1:3; hatched bars) controls. (A) No effect of LLC CM was found compared to CTRL or non-tumorigenic NL20 or HBSS controls (n=6/bar). (B) KrasG12D CM increased myotube myosin content compared to CTRL and both KrasWT and dilution controls (n=6/bar). Representative gel images are shown at the top of panels A and B for a subset of replicates. All data are mean ± SEM, with individual data points shown with each bar. **, $P<0.01$.

Figure 2:

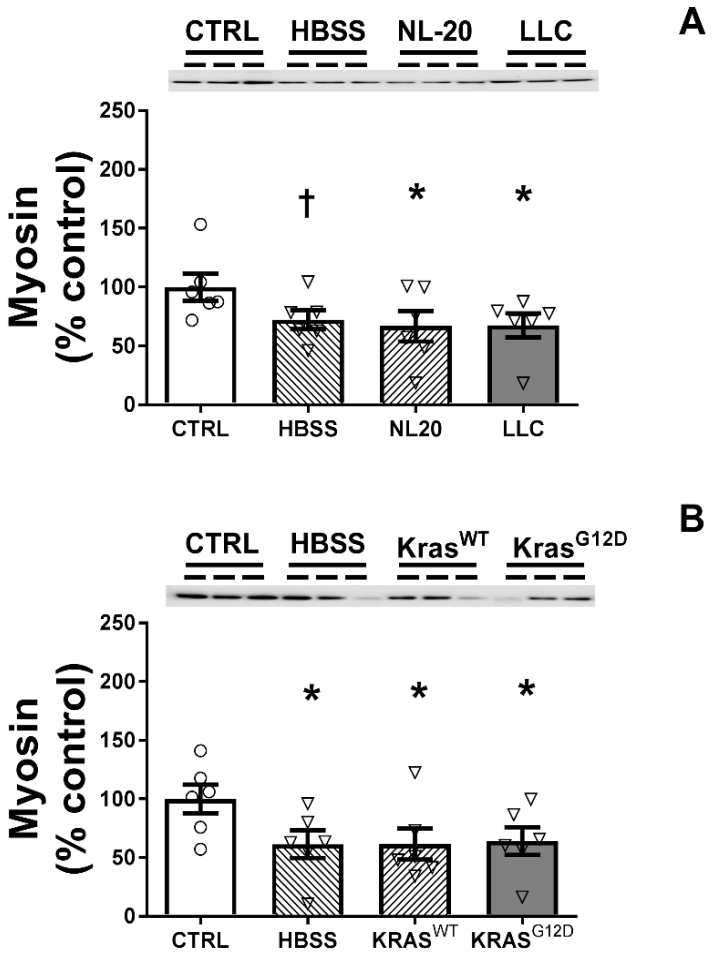

Figure 2.0.2: *The effects of murine CM on d4 myotube myosin.*

Figure 2. Effects of 3 d of murine LLC (A; gray bar) or KrasG12D (B; gray bar) conditioned media (CM; 1:3) treatment on myosin content in d4 differentiated myotubes compared to undiluted (CTRL; open bars), dilution (HBSS; 1:3; hatched bar) and non-tumorigenic (NL20 and KrasWT cells; 1:3; hatched bars) controls. (A) LLC and NL20 CM reduced and HBSS tended to reduce myotube myosin content compared to CTRL. (B) KrasG12D and KrasWT CM and HBSS reduced myotube myosin content compared to CTRL. Representative gel images are shown at the top of panels A and B for a subset of replicates. All data are mean ± SEM, with individual data points shown with each bar.*, $P<0.05$; †, $P<0.10$.

Figure 3:

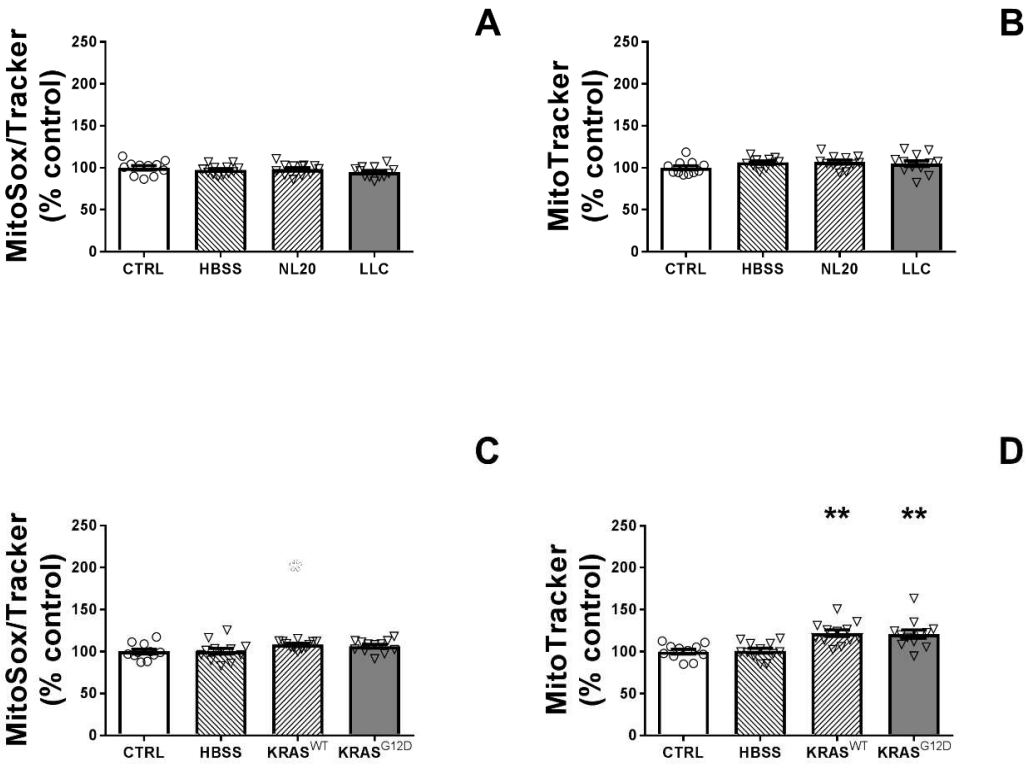

Figure 2.0.3 *The effects of murine CM on d7 myotube mitochondria*

Figure 3. Effects of 3 d of murine LLC (A and B; gray bar) or KrasG12D (C and D; gray bar) conditioned media (CM; 1:3) treatment on mitochondrial reactive oxygen species (ROS) production and mitochondrial content in d7 differentiated myotubes compared to undiluted (CTRL; open bars), dilution (HBSS; 1:3; hatched bar) and non-tumorigenic (NL20 and KrasWT cells; 1:3; hatched bars) controls. No differences were found between LLC or NL20 CM or HBSS dilution or untreated (CTRL) controls for mitochondrial ROS (A) or content (B) (n=12/bar). (C) No differences were found between KrasG12D and KrasWT CM or HBSS dilution or untreated (CTRL) controls for mitochondrial ROS (C)(n=12/bar). (D) Both KrasG12D and KrasWT CM increased mitochondrial content compared to HBSS and CTL conditions (n=12/bar). All data are mean ± SEM, with individual data points shown with each bar.**, $P<0.01$.

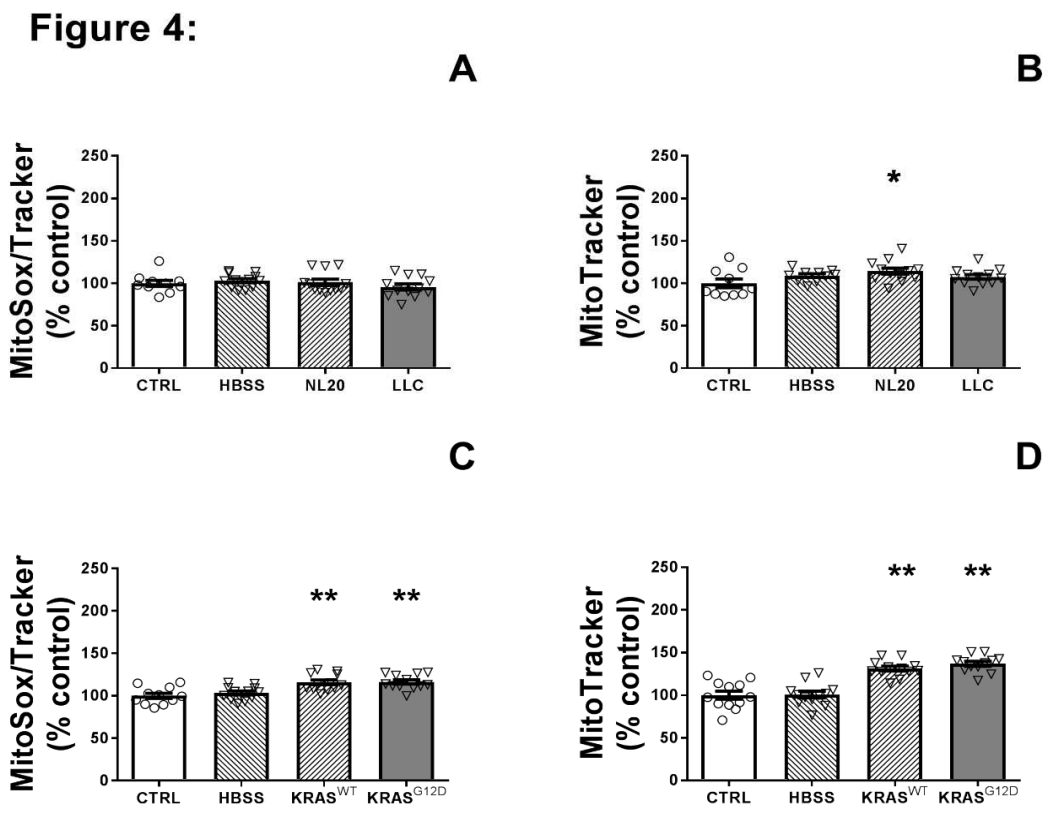

Figure 2.0.4: *The effects of murine CM on d4 myotube mitochondria.*

Figure 4. Effects of 3 d of murine LLC (A and B; gray bar) or KrasG12D (C and D; gray bar) conditioned media (CM; 1:3) treatment on mitochondrial reactive oxygen species (ROS) production and mitochondrial content in d4 differentiated myotubes compared to undiluted (CTRL; open bars), dilution (HBSS; 1:3; hatched bar) and non-tumorigenic (NL20 and KrasWT cells; 1:3; hatched bars) controls. No differences were found between LLC or NL20 CM or HBSS dilution or untreated (CTRL) controls for mitochondrial ROS (A)(n=12/bar). (B) NL20 CM increased mitochondrial content compared to LLC, HBSS or CTRL conditions (n=12/bar). Both KrasG12D and KrasWT CM increased mitochondrial ROS production (C) and content (D) compared to either HBSS dilution or untreated (CTRL) controls (n=12/bar). All data are mean ± SEM, with individual data points shown with each bar. **, $P<0.01$.

Figure 5:

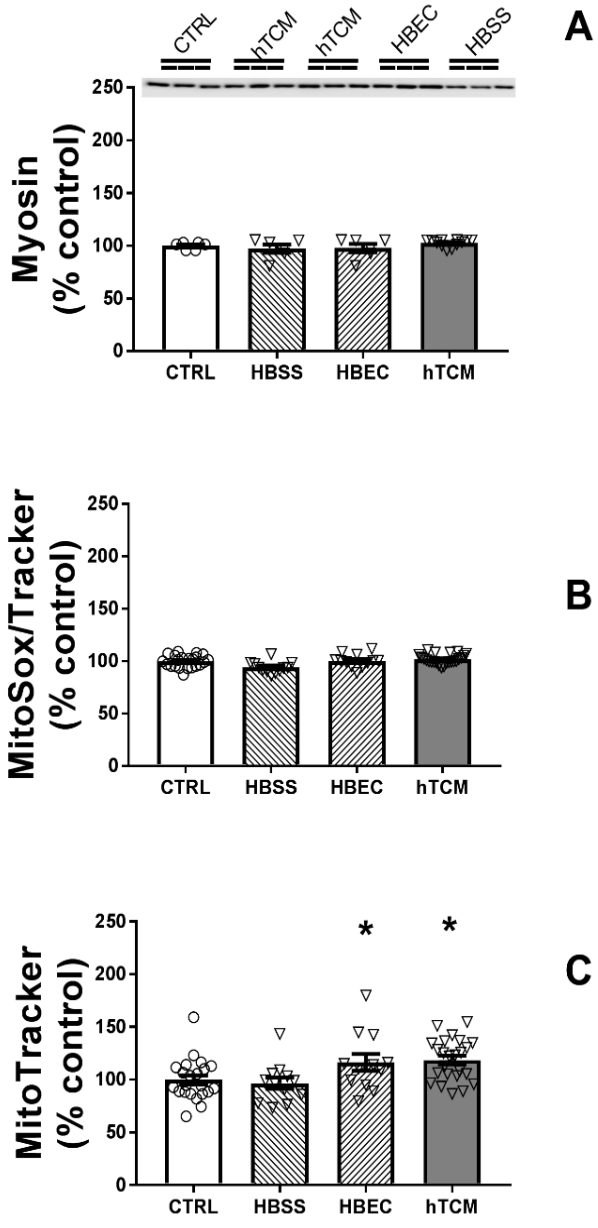

Figure 2.0.5: *The effects of human CM on d7 myotubes.*

Figure 5. Effects of 3 d of treatment with primary human tumor cell conditions media (hTCM; 1:3; gray bars) on myosin protein content (A) and mitochondrial reactive oxygen species (ROS) production (B) and content (C) in d7 differentiated myotubes compared to undiluted (CTRL), dilution (HBSS; hatched bars) and primary human bronchial epithelial cell (HBEC; 1:3 dilution; hatched bars) controls. No differences were found between treatments for myotube myosin content (A) or mitochondrial ROS production (B) (n=12-24/bar). (C) Both hTCM and HBEC increased mitochondrial content compared to HBSS dilution and untreated (CTRL) controls (n=12-24/bar). All data are mean ± SEM, with individual data points shown with each bar.*, $P<0.05$.

Table 2.1: *Physical and disease characteristics in cancer patients*

n	4
Age (yr)	76 ± 7
Sex (M/F)	1,3
BMI	23.5 ± 4
Weight loss Reported	0
Cancer Stage (I/II/III/IV)	0,1,1,1
Diagnosis (n)	
NSCLC	3
SCLC	1
Histology (n)	
Adenocarcinoma	2
Basaloid Squamous Cell	1
Neuroendocrine	1
Chemotherapeutics (n)	
Paclitaxel	1
Carboplatin	2
Pembrolizumab	1
Pemetrexed	1
Radiation (n)	1

CHAPTER 3: SKELETAL MUSCLE ATROPHY AND DYSFUNCTION IN BREAST CANCER PATIENTS: ROLE FOR CHEMOTHERAPY-DERIVED OXIDANT STRESS

Blas A. Guigni[1,2], Damien M. Callahan[1], Timothy W. Tourville[3,5], Mark S. Miller[6], Brad Fiske[1], Thomas Voigt[1], Bethany Korwin-Mihavics[4], Vikas Anathy[4], Kim Dittus[1], Michael J. Toth[1,2,3]

Departments of Medicine[1], Molecular Physiology and Biophysics[2], Orthopedics and Rehabilitation[3] and Pathology and Laboratory Medicine[4], College of Medicine, University of Vermont, Burlington, VT, Department of Rehabilitation and Movement Science[5], College of Nursing and Health Sciences, University of Vermont, Burlington, VT and Department of Kinesiology, University of Massachusetts Amherst, Amherst, MA[6]

Correspondence to: Michael J. Toth, Ph.D.

Health Science Research Facility 126B

149 Beaumont Ave

University of Vermont

Burlington, VT 05405

Email: michael.toth@uvm.edu

Tele: (802) 656-7989

Fax: (802) 656-0747.

Running Title: Skeletal muscle in breast cancer

Abstract

How breast cancer and its treatments affect skeletal muscle is not well defined. To address this question, we assessed skeletal muscle structure and protein expression in 13 women diagnosed with breast cancer, who were receiving adjuvant chemotherapy following tumor resection, and 12 non-diseased controls. Breast cancer patients showed reduced single muscle fiber cross-sectional area (CSA) and fractional content of both sub-sarcolemmal and intermyofibrillar mitochondria. Drugs commonly used in breast cancer patients (doxorubicin and paclitaxel) caused reductions in myosin expression, mitochondrial loss and increased reactive oxygen species (ROS) production in C2C12 murine myotube cell cultures, supporting a role for chemotherapeutics in the atrophic and mitochondrial phenotypes. Additionally, concurrent treatment of myotubes with mitochondrial-targeted antioxidant (MitoQ) prevented chemotherapy-induced myosin depletion, mitochondrial loss, and ROS production. In patients, reduced mitochondrial content and size, and increased expression and oxidation of peroxiredoxin 3, a mitochondrial peroxidase, were associated with reduced muscle fiber CSA. Our results suggest that chemotherapeutics may adversely affect skeletal muscle in patients and that these effects may be driven through effects of these drugs on mitochondrial content and/or ROS production.

Keywords: cachexia, mitochondria, myotube

Introduction

Cancer and its treatment can affect skeletal muscle. The most widely studied consequence is cachexia, a syndrome characterized by fat and skeletal muscle tissue depletion that typically occurs in late-stage disease (17). Most studies have evaluated skeletal muscle from patients with cancers that are prone to cachexia and model systems that mimic them. However, patients with other cancer types less prone to cachexia, or those with early-stage disease, may also experience muscle atrophy (21) and dysfunction. Despite the fact that these patients comprise the majority of cancer survivors, our understanding of the effect of these cancer types and their treatments on skeletal muscle is limited.

Breast cancer, the most commonly diagnosed cancer in the US (1), is thought to have minimal effects on skeletal muscle because patients are less prone to cachexia (16) and are typically weight-stable or gain weight during treatment (30). This constancy in body weight, however, belies reciprocal changes in body composition, specifically a gain in fat and a loss of lean tissue (21). Muscle atrophy and the resulting weakness have prognostic importance in breast cancer patients (6, 9, 60), underscoring the need to better understand the effects of this cancer type and its clinical sequelae on skeletal muscle.

In the present study, our objective was to examine skeletal muscle in patients receiving adjuvant chemotherapy following tumor resection and in healthy controls without a history of cancer. We hypothesized that cancer therapeutics might promote skeletal muscle adaptations in patients, as drugs commonly used in breast cancer, such as

anthracyclines, cause muscle wasting and dysfunction in pre-clinical models (22, 25, 43), whereas breast cancer tumors do not (27, 61). More specifically, we hypothesize that chemotherapeutics have myotoxic effects through their ability to provoke mitochondrial dysfunction and oxidative stress, as studies suggest that mitochondrial remodeling and oxidant stress promote skeletal muscle atrophy (48, 51). To begin to address this possibility, and building on pre-clinical studies showing that chemotherapeutics have effects on mitochondrial biology (3, 43), we also assessed mitochondrial content/morphology and markers of oxidative stress. Finally, we employed the C2C12 murine muscle cell line, as we could not ascribe muscle morphological and mitochondrial phenotypes in humans to chemotherapeutics because of the complex clinical background of these patients and our case-control study design. Cultured muscle cells provide a model where the singular effect of chemotherapeutics can be evaluated independent of clinical factors associated with treatment in patients, as well as effects on other tissue and organ systems. This latter point is particularly relevant to anthracyclines, which cause cardiac damage and heart failure in animal models (26), a syndrome that could affect skeletal muscle (54). Though there are the limitations of C2C12 myotube cultures, results from these experiments can be used as proof-of-principle evidence that chemotherapeutics may have effects on skeletal muscle to provoke phenotypes observed in human patients.

Methods

Subjects. Thirteen women with breast cancer were recruited. Patients were included if they had stage I, II or III, histologically documented breast cancer and were receiving or scheduled to receive chemotherapy following surgical resection. We excluded patients with prior history of cancer, other than non-melanoma skin cancer, prior chemotherapeutic use, autoimmune, vascular or neuromuscular disease or prior knee or hip replacement surgery. All patients received dexamethasone for 1 to 4 days concurrent with chemotherapy administration to prevent adverse drug reaction and diminish cancer-induced nausea and vomiting. Patients could receive a maximum dose of 12 mg on the day of chemotherapy and 4 mg per day for 3 days thereafter as symptoms necessitate. As dosing was symptom-dependent and not tracked clinically, exact doses for dexamethasone treatment are not available. Three patients were characterized as having experienced weight loss, defined as self-reported, unintentional weight loss >5% of body weight within 6 months prior to evaluation; whereas, other patients who reported little or no weight change (<5%) were characterized as weight stable. All patients were tested during adjuvant chemotherapy, prior to radiation therapy. One patient reported current tobacco use (44 pack year history). None of the patients received nutritional support or anabolic therapy or were taking medications known to influence skeletal muscle size or function aside from chemotherapeutics. One volunteer was on a stable regimen of HMG CoA reductase inhibitor, which our recent work suggests would not affect the variables assessed in this study (50).

Healthy female controls (n=12) were recruited if they were free from acute or chronic disease, based on medical screening and routine clinical/laboratory tests, and had no prior history of cancer, chronic lung or cardiovascular disease, neurological or orthopedic conditions, or other mobility-limiting ailments. Volunteers were excluded if they were a current or previous smoker or were taking medications that could influence skeletal muscle, with the exception of stable HMG CoA reductase inhibitor treatment (n=1). Plasma creatine kinase levels were within the normative range in this volunteer and she reported no muscle symptoms. Written informed consent was obtained from all volunteers prior to their participation and protocols and procedures were approved by the Committees on Human Research at the University of Vermont.

Total and regional body composition. Body weight was measured on a digital scale (ScaleTronix, Wheaton, IL). Total and regional body composition was measured by dual energy x-ray absorptiometry, as described (57).

Muscle tissue processing. Percutaneous biopsy of the vastus lateralis was performed at the mid-way point between the most proximal aspect of the patella and the inguinal fold. The skin was sterilized (2% chlorhexidine/70% isopropyl alcohol) and local anesthetic (1% lidocaine) infiltrated into the site, as described (55). A small incision (~5 mm) was made through the skin, fat and fascia and the biopsy needle (5 mm Bergstrom) advanced past the fascia into the muscle at an angle approximately 30-45° to the skin surface to position the needle roughly parallel with the muscle fascicles, as described (15), to collect long, intact bundles of fibers. Suction was applied and tissue was excised. Tissue for

electron microscopy (EM) was tied to a glass rod at a slightly stretched length and placed into glutaraldehyde/paraformaldehyde (2.5%/1%) for electron microscopy (EM). Tissue for immunohistochemistry was embedded in optimal cutting temperature medium and frozen in isopentane cooled in liquid nitrogen. Tissue was also taken for measurement of mechanical properties of skeletal muscle fibers, but those data are not presented. Remaining tissue was frozen in liquid nitrogen and stored at -80°C until analysis. In one breast cancer patient, sufficient tissue was obtained only for EM analysis.

Immunohistochemistry. Muscle fiber cross-sectional area (CSA) and myonuclear number were quantified by immunohistochemistry using rabbit anti-laminin (Abcam) and mouse anti-MHC I antibodies (DSHB), as described (11). Nuclei were stained with 4',6-diamidino-2-phenylindole (Invitrogen). CSA measurements were performed using image analysis software (NIH ImageJ, version 1.51n). Although the myonuclei count will include muscle satellite cells, these are a small fraction of the nuclei under the laminin border (<5%; (46)). For healthy controls, immunohistochemistry was available on 5 volunteers because of limited tissue.

Myosin heavy chain (MHC) content and isoform distribution. MHC content and isoform distribution were measured in tissue homogenates via gel electrophoresis, as described (58), as a marker of the relative fiber type distribution of muscle.

Electron microscopy. EM was conducted on intact (i.e., unskinned) skeletal muscle fibers to assess intermyofibrillar and sub-sarcolemmal mitochondrial area fraction,

average area and number, as estimates of mitochondrial content, and myofibrillar fractional area, as described (10).

Cell culture. Cultured murine myotubes were used to evaluate the singular effect of chemotherapy agents on skeletal muscle cell biology; primarily, mitochondrial content and oxidant production. Use of this system obviates the possible secondary effects of these drugs on muscle through effects on other organs/tissue systems (e.g., cardiac damage and failure due to doxorubicin administration (26)), which could affect skeletal muscle (54)). The C2C12 model has been used to characterize the effects of tumor-derived factors on mitochondrial oxidant production (39), effects that have been confirmed *in vivo* in pre-clinical models (7).

C2C12 myoblasts (ATCC® CRL-1772™, Manassas, VA) were cultured in low glucose (1 g/L), Dulbecco's Modified Eagle's Medium (DMEM) supplemented with 10% fetal bovine serum (FBS; Gibco™ Thermo Fisher Scientific Waltham, MA) and antibiotics (50 U/ml penicillin and 50 μg/ml streptomycin). Cells were plated (1.5 X 10^4 cells/cm^2) on Matrigel (40 μg/cm^2; Corning, Bedford, MA) and switched to low serum, high glucose (4.5 g/L) DMEM (1% heat-inactivated FBS) to induce differentiation, as generally described (34). On day 7 post-differentiation, myotubes were treated with doxorubicin (DOX), paclitaxel (TAXOL) (both Sigma, St. Louis, MO), cisplatin (CIS; Tocris, Minneapolis, MN) or respective vehicle control (DMSO for DOX and TAXOL and PBS for CIS) for 3 days. DOX dose was based on prior work (24) and serum concentrations (47). TAXOL (66) and CIS (56) doses were based on tumor intracellular levels. In all

cases, preliminary dose response studies were undertaken to obtain doses for DOX (0.2 μM), TAXOL (40 nM) and CIS (10 μM) that elicited loss of myotube myosin content over the 3 day study period. In DOX and TAXOL experiments, where increased oxidant generation was noted (Figure 5 and 6), MitoQ (MedKoo Biosciences, Morrisville, NC), a mitochondrial-targeted anti-oxidant was added concurrent with chemotherapeutics to determine whether decreasing mitochondrial oxidant stress prevents atrophy. MitoQ has a narrow therapeutic range, a characteristic that we found varied by chemotherapeutic. Accordingly, doses were 0.25 μM for DOX and 0.125 μM for TAXOL. On the final day of treatment, myotubes were harvested for protein expression via western blot or underwent mitochondrial measurements.

No genetic testing was conducted to validate the cell line. However, upon serum withdrawal, these cells fuse to form multinucleated cells (Figure 5) and express myofilament proteins, such as myosin, actin, and α-actinin (unpublished data). At day 7 post-differentiation, when chemotherapy treatment began, myotubes contain myofilaments, contract with electrical stimulation and demonstrate intracellular calcium release and reuptake (unpublished data). All of these anatomic and physiologic characteristics have been demonstrated in C2C12 myotubes previously (33, 34, 38). Additionally, we found that electrically stimulated contraction could be mitigated by blocking either sodium channels with tetrodotoxin or myosin ATPase activity with N-benzyl-p-toluene sulphonamide, with the former mitigating intracellular calcium currents and contractures and the latter only mitigating contractures (unpublished data). Here again, these characteristics of the contractile response and its sensitivity to specific

pharmacological agents have been demonstrated by others (14, 44). Thus, C2C12 myotubes demonstrate many classical phenotypes of *in vivo* skeletal muscle.

Myotube mitochondrial content and reactive oxygen species (ROS) production. Mitochondrial content and ROS production were measured with fluorometric dyes, as described (45, 64) with minor modifications. C2C12 myotubes grown in black-walled, 96-well plates were loaded with fluorescent dyes to assess mitochondrial content (1 μM MitoTracker Green FM; 490/516 nm) and ROS production (1 μM MitoSOX Red; 510/580 nm; both Molecular Probes, Eugene, OR) 15 minutes prior to measurement. Fluorescence was measured on a microplate reader (BioTek, Winooski, VT). The ROS signal (MitoSox) was expressed relative to MitoTracker signal to control for any effect of the chemotherapeutic to modify mitochondrial content. MitoTracker Green FM was chosen because its labeling of mitochondria is insensitive to membrane potential, as this could be affected by chemotherapeutics (23). To confirm co-localization of MitoTracker and MitoSox signals in myotubes, myoblasts were plated (2.5 X 10^4 cells/cm^2) on Matrigel-coated (60 μg/cm^2), 35 mm, glass bottom imaging dishes (MatTek; Ashland, MA) and differentiated following procedures described above, with the exception that media was changed daily for the first 3 days following the start of differentiation. Cells were imaged on a Nikon Ti-E inverted microscope in a heated environmental chamber, equipped with a Clara CCD camera (Andor) and Spectra X light engine.

Western blot analysis. Skeletal muscle tissue was homogenized, as described (59), in a sub-set of patients (n=9) and controls (n=11), where tissue was available. In a sub-set of

breast cancer patients (n=11), mitochondria were isolated, as described (35), and treated as below for peroxiredoxin-3 (Prx 3) assessments. Myotubes were washed with phosphate buffered saline, lysed (50 mM Tris, 150 mM NaCl, 10% (v/v) glycerol, 0.5% IGEPAL CA-630,1 mM EDTA), incubated on ice for 30 min and centrifuged. Homogenate, mitochondrial isolate, and lysate protein contents were measured (BioRad DC Protein Assay, Hercules, CA) and diluted in gel loading buffer. For Prx 3, tissue homogenates and myotube lysates were treated with N-ethylmaleimide (NEM) to prevent oxidation and/or dimerization of Prx 3 during processing and then placed in gel loading buffer with (reducing) or without DTT (non-reducing). Oxidation of Prx 3 can be used as a marker of intracellular oxidative stress (49) and mitochondria specifically, as Prx 3 is localized to mitochondria. The importance of Prx 3 in muscle is underscored by studies showing that altered expression modulates mitochondrial content, morphology, and function, as well as muscle contractility (36). Proteins separated by SDS-PAGE were, transferred to nitrocellulose (Prx 3) or polyvinylidene (PVDF; all others), blocked (either BSA, non-fat milk in Tris-buffered saline, or Odyssey Blocking buffer) and incubated overnight with Prx 3 (1:6000; Cat# LF-PA0030, Thermo Fisher), p38 (1:1000; Cat# 9112, Cell Signaling), phospho-p38 (Thr 180/Thr 182; 1:500; Cat# 4511, Cell Signaling), ERK1/2 (1:1000; Cat# 9102, Cell Signaling), phosoho-ERK1/2 (Thr 202/Thr 204; 1:500; Cat# 9106, Cell Signaling), α-tubulin (Cat# 12G10, Developmental Studies Hybridoma Bank; 0.5 μg/mL), detyrosinated α-tubulin (1:500; Cat# ab48389, Abcam), myosin fast (1:15000; Cat# M4276, Sigma) antibodies or GAPDH (1:5000; Cat# MCA4739, Biorad). Blots were washed and incubated with secondary antibodies conjugated to horseradish peroxidase and developed by chemiluminescence (Clarity Western ECL Substrate

BioRad, Hercules, CA) or the Odyssey Infrared Imaging System (for p38, ERK1/2 and tubulin analytes; IRDye 680 or IRDye 800 secondary antibodies; both LiCor, Lincoln, NE). Bands were quantified by densitometry (Quantity One; BioRad, Hercules, CA or Odyssey Application Software v3.0; LiCor, Lincoln, NE). For analysis that required running more than one gel, data were normalized to an internal loading control to permit comparisons across gels. Technicians were blinded to group assignment or treatment.

Statistics. Differences between groups were determined using unpaired t-tests. For variables with multiple observations within the same individual (e.g., single fiber CSA), a linear mixed model was used, including a between-subject effect of group assignment (control or cancer) and a repeated effect to account for variation in fiber characteristics within each individual. This effect accounts for the fact that each fiber within an individual is not independent and has some relationship to other fibers within that individual. The mixed model is preferable to taking an average value for each individual, which makes the erroneous assumption that within-subject variation is zero. Instead, the mixed model considers this within-subject variation in the derivation of within-group variance to test for fixed effects (i.e., group differences). Least squared mean and variance estimates are used to test for fixed effects in the mixed model. However, arithmetic means are displayed figuratively and in the text to correspond with individual data (or individual average data for variables with multiple observations per volunteer), the latter of which is plotted to illustrate the spread of data. For cell culture experiments, unpaired t-tests or one-way analysis of variance were used. Finally, relationships between variables were determined by Pearson correlation coefficients, with normality confirmed

by Shapiro-Wilk test. For non-normally distributed variables that remained so following data transformations (e.g., MHC II CSA), Spearman rank correlation coefficients were used. SPSS (version 23, IBM Co., Armonk, NY) was used for all statistical analysis, except mixed model analysis (SAS, version 9.4, SAS Institute Inc., Cary, NC). All data are reported as mean ± SEM, unless otherwise specified.

Results

Disease and physical characteristics. Controls were older, but groups were similar for all body size and composition variables (Table 1). Disease and treatment characteristics of patients are detailed in Table 1. Five patients reported unintentional weight loss during 6 months prior to testing (-4.0 ± 1.1 kg; range: 1 to 7 kg), with 3 (1 stage I, 1 stage II and 1 stage III) reporting >5% loss (-5.7 ± 0.7 kg). Breast cancer patients were studied an average of 59 ± 10 d into their chemotherapy regimens (range: 5-114 d).

Single muscle fiber characteristics. Breast cancer patients showed lower single muscle fiber CSA compared to controls ($P<0.05$; n=1682 and 450 fibers; Figure 1A), with lower MHC II fiber CSA ($P=0.05$; n=745 and 228 fibers) and a trend toward lower MHC I CSA ($P=0.07$; n=937 and 222 fibers). No differences in CSA were found between patients reporting weight loss and those reporting weight stability in all fibers, or MHC I or II fibers separately, ($P>0.40$; data not shown). Of note, as detailed in the *Statistics* section, statistical tests for group differences are based on the number of volunteers per group, not the total number of fibers. No differences were found in myonuclear number per fiber in MHC I or II fibers (Figure 1B). Finally, we found no differences between groups for myofibrillar fractional area by EM (Figure 1C) or myosin or actin protein in tissue homogenates (Figure 1D).

Mitochondrial content and structure. In breast cancer patients, intermyofibrillar mitochondria fractional area was lower ($P<0.03$) than controls (Figure 2A), due to smaller ($P<0.02$) average mitochondrion area (Figure 2B), with no difference in number

(control: 0.24 ± 0.03 vs. cancer: 0.29 ± 0.03 n/μm^2). Similarly, sub-sarcolemmal mitochondrial fractional area was reduced ($P<0.05$; Figure 2C) due to decreased number of mitochondria per unit area ($P<0.01$; Figure 2D), while average sub-sarcolemmal mitochondrion area showed a trend ($P=0.07$) towards being greater in cancer patients (control: 0.95 ± 0.08 vs. cancer: 1.59 ± 0.26 μm^2). Sub-sarcolemmal area did not differ between groups (control: 21.7 ± 2.3 vs. cancer: 21.7 ± 1.6 μm^2). Finally, in the breast cancer patients, reduced intermyofibrillar mitochondrial size was associated with smaller CSA in both MHC I ($r=0.792$; $P<0.01$) and II ($r=0.769$; $P<0.01$) fibers, whereas intermyofibrillar mitochondrial size was not associated with CSA in either fiber type in controls (both $P>0.50$). Reduced sub-sarcolemma mitochondrial fractional content was associated with smaller MHC II CSA in cancer patients ($r=0.743$; $P<0.01$), but not controls in either fiber type ($P>0.60$).

We examined whether differences in fiber type distribution, a marker of muscle fiber type proportion, might account for variation in mitochondrial parameters. Breast cancer patients were characterized by a lower fractional content of MHC I proteins compared to controls (35.8 ± 0.8 vs. 39.0 ± 1.2%; $P<0.05$), although neither MHC IIA (36.3 ± 0.3 vs. 35.8 ± 1.0%) nor MHC IIX (27.9 ± 0.9 vs. 25.2 ± 1.5%) differed. Variation in MHC I fractional content, however, was not associated with mitochondrial fractional content from either compartment in the whole group or either group separately. Moreover, as slopes of these relationships were shallow (range: -0.005 to 0.064), modest differences in MHC I fiber fractional content would likely not explain group differences in mitochondrial content in either compartment.

Prx 3 expression. To examine whether mitochondrial oxidant stress in cancer patients is associated with muscle fiber size, we evaluated the expression and oxidation state of the mitochondrial-targeted anti-oxidant enzyme Prx 3 in a sub-group of breast cancer patients (n=9). We found that expression of Prx 3 was negatively related to both MHC I and MHC II CSA (Figure 3A and 3B, respectively). Moreover, in mitochondrial isolates (n=11), increased amounts of oxidized Prx 3 in breast cancer patients was related to decreased CSA in MHC II fibers (Figure 3C).

To further examine whether chemotherapeutics might contribute to variation in Prx 3 expression and/or oxidation, we treated C2C12 myotubes for 3 days with DOX or TAXOL, two commonly used chemotherapeutics in our population (Table 1). DOX did not affect Prx 3 expression, whereas TAXOL reduced Prx 3 expression (Figure 3D; n=4/group). Note that the two bands shown under reducing conditions are due to the addition of NEM to prevent oxidation and/or dimerization during processing, as samples not treated with NEM showed only one band (data not shown). The above results reflect quantification of both bands. Under non-reducing conditions, we found that DOX increased oxidized Prx 3 in myotubes ($P<0.05$), as shown by increased Prx 3 dimer (Control: 100 ± 8.9 vs. DOX: 162.5 ± 11.0 vs. TAXOL: 106.7 ± 6.1%; Figure 3E). Because TAXOL reduced Prx 3 expression (Figure 3D), we calculated the relative amount of dimer in each treatment group as a function of monomer + dimer as a marker of mitochondrial oxidative stress. This did not alter the results, as oxidized Prx 3 in DOX treated myotubes remained elevated (Figure 3F; n=4/group).

Tubulin expression and detyrosination. Because mitochondrial motility and communication occur via kinesin-dependent movement along microtubules, and because taxane chemotherapeutics, which were taken by all breast cancer volunteers, alter tubulin expression and post-translational modification in skeletal muscle, we examined the effects of taxanes on tubulin expression and post-translational modification. In C2C12 myotubes, treatment with TAXOL (40 nM for 3 days; n=6) increased expression of tubulin and detyrosinated tubulin (Figure 4A). Similarly, in patients treated with therapeutic doses of taxane chemotherapeutics (n=9), we found increased tubulin and detyrosinated tubulin expression compared to controls (n=11; Figure 4B, respectively). Because TAXOL can increase ROS production in skeletal muscles, we examined whether variation in tubulin or detyrosinated tubulin correlated with mitochondrial content or morphology. The average area of intermyofibrillar mitochondria was inversely correlated to α-tubulin ($r=-0.472$; $P<0.05$) and detyrosinated tubulin ($r=-0.580$; $P<0.01$). In sub-sarcolemmal mitochondria, α-tubulin was negatively correlated to fractional content ($r=-0.558$; $P<0.05$) and number per area ($r=-0.654$; $P>0.01$) and positively related to average area ($r=0.582$; $P<0.01$).

Chemotherapy-induced atrophy and oxidant stress. To further examine the effects of chemotherapeutics on skeletal muscle cell size and mitochondrial content and ROS production, C2C12 myotubes were treated with DOX, a chemotherapeutic with well-characterized myotoxicity, or TAXOL, the most common chemotherapeutic in our cohort. Treatment with DOX or TAXOL reduced myosin content (Figure 5A; n=15 and

9, respectively). That myosin content serves as a proxy of myotube cell size was confirmed by the fact that DOX-induced changes in myotube diameter (-22 ± 7% relative to controls; n=3 wells/condition) tracked closely with changes in myosin content (-21 ± 2%; n=10). Accordingly, we utilized myosin protein content as our index of myotube size throughout our studies.

Both DOX and TAXOL caused a loss of mitochondrial content (-8 ± 2%, n=16, $P<0.01$ and -38 ± 3, n=12, $P<0.001$, respectively). Accordingly, ROS production, as reflected by MitoSox signal, was expressed per unit MitoTracker signal to control for changes in mitochondrial content. The use of MitoTracker signal to correct MitoSox signal is based on the mitochondrial targeting of both probes, which we confirmed in our preparations (Figure 6A). Both chemotherapeutics increased ROS production per unit MitoTracker signal (Figure 5B; n=12 and 11, respectively). To examine whether increased ROS production with chemotherapeutics contributes to myotube atrophy, we concurrently treated cells with the mitochondrial-targeted anti-oxidant MitoQ and observed that it prevented DOX- and TAXOL-induced loss of myosin protein content (Figure 5C and D; n=12 and 3, respectively). Additionally, MitoQ application to myotubes prevented the loss of mitochondrial content (Figure 6B and C; n=12 and 12, respectively) and prevented (DOX) or lessened (TAXOL) the increase in ROS production (Figure 6D and E; n=12 and 12, respectively).

Our prior work showed mitochondrial rarefaction (-50%) in skeletal muscle from patients with cancers that are prone to cachexia—primarily lung cancer—where platin-based

drugs were the most common chemotherapeutic (58). To explore whether they have effects similar to DOX and TAXOL, we evaluated the effects of CIS on C2C12 myotubes. CIS caused profound myosin loss (control: 100 ± 17% vs. CIS: 19 ± 4% of control; n=3; $P<0.01$), but did not increase ROS production relative to MitoTracker signal (control: 100 ± 1 vs. CIS: 98 ± 1% of control; n=12) and paradoxically increased MitoTracker signal (control: 100 ± 6 vs. CIS: 113 ± 5 of control; n=12; $P<0.01$).

Signaling pathways. Recent studies suggested that upregulation of redox-responsive signaling pathways, such as p38 and ERK1/2, may contribute to muscle atrophy with chemotherapeutic administration in pre-clinical models. However, we found no differences in the expression or phosphorylation of p38 (Figure 6A) or ERK1/2 (Figure 6B), nor the ratio of phosphorylated to total content of either, between patients (n=9) to controls (n=11). ERK1/2 data represent quantitation of both bands.

Discussion

Breast cancer patients showed evidence of muscle fiber atrophy and mitochondrial rarefaction, with reduced muscle fiber size tracking, reduced mitochondrial content and increased oxidant stress. Treatment with chemotherapeutics promoted these phenotypes in cultured muscle cells, effects that were mitigated by concomitant treatment with a mitochondrial-targeted antioxidant. These results provide seminal human data that suggest deleterious effects of cancer treatments on muscle secondary to their mitotoxic properties. That chemotherapeutics promote these adaptations provides a potential explanation for muscle atrophy in cancers not prone to cachexia or early stage patients, as well as the high prevalence of fatigue and physical disability across different cancer types (12).

Reduced skeletal muscle fiber CSA in breast cancer patients was unlikely due to weight loss, as few patients reported weight loss and fiber CSA did not differ between patients reporting weight loss and those reporting weight stability. Other groups have reported that lean tissue mass is reduced (21), but our report provides evidence of this using direct measures of muscle cell size in breast cancer patients. We emphasize this point because tissue level imaging-based measurements may not accurately reflect muscle size in patients due to effects of treatments on tissue hydration (2). Indeed, we found no differences between groups in leg muscle mass by DEXA (Table 1). Such discrepancies in humans are not unique to this study, as we (42) and others (4) have shown discordance between measures at these different anatomic levels under conditions when tissue hydration may be altered (13). Although we acknowledge that biopsy samples represent a

small amount of tissue relative to that sampled with imaging techniques, single fiber CSA measurements agree well with imaging-based whole muscle CSA under stable conditions, where muscle mass and hydration are not changing (11). This potential limitation of imaging techniques is noteworthy because most studies to date have used these approaches for defining cancer-related muscle atrophy in clinical populations.

This is the first report of skeletal muscle mitochondrial morphological adaptations in breast cancer patients, a cohort with a low prevalence of cachexia, and is consistent with our results in patients with cancers more prone to cachexia (58), albeit the reduction was not as pronounced (current study vs. (58)). While cancer (62) or chemotherapeutics (3) may reduce mitochondrial content, the fact that our patients had tumors removed surgically and that breast cancer tumors generally do not promote cachexia in pre-clinical models (27, 61) suggests chemotherapeutics as a more likely mediator. Indeed, recent pre-clinical studies showed that administration of chemotherapeutics used for colorectal tumors to mice reduced intermyofibrillar mitochondrial content secondary to decreased mitochondrion size (3), a similar morphological phenotype as in our patients. Our results also extend both pre-clinical and clinical work (58) to show mitochondrial loss in the sub-sarcolemmal compartment. Interestingly, different structural characteristics accounted for reduced mitochondrial content in sub-sarcolemmal and intermyofibrillar compartments in breast cancer patients, suggesting different mechanisms for mitochondrial remodeling in the two compartments. Considering the beneficial effect of increasing or maintaining mitochondrial content in other models of atrophy (52), therapeutics or interventions (e.g.,

exercise) that preserve or increase mitochondria may prevent muscle atrophy and weakness in cancer patients.

Chemotherapeutics may promote mitochondrial loss through their ability to provoke mitochondrial dysfunction and oxidant production, as even modest amounts of oxidant stress can promote mitophagy (20). To address this question, we utilized C2C12 myotubes to examine the singular effect of chemotherapeutics used in breast cancer patients on mitochondrial content and oxidant production. We found that chemotherapeutics caused mitochondrial loss and increased oxidant production in C2C12 myotubes. Moreover, treatment with the mitochondrial-targeted antioxidant MitoQ prevented a loss of mitochondria, further implicating ROS in mitochondrial loss. In contrast, mitochondrial content remained unchanged with CIS, another widely used chemotherapeutic that did not increase ROS production. These data provide proof-of-principle evidence that mitochondrial loss tracks with drug-induced oxidant stress.

Another potential explanation for mitochondrial loss is the effect of taxane chemotherapeutics on microtubules, as all of our patients were treated with these drugs. Microtubules form a lattice in muscle fibers and serve as tracks to support kinesin-dependent mitochondrial movement (65) and communication (29). Pre-clinical studies show that TAXOL increases the amount of tubulin and its detyrosinated form in skeletal muscle (31), which we confirmed in C2C12 murine myotubes. Our results further provide seminal data showing that taxanes at therapeutic doses used in human patients upregulate tubulin and detyrosinated tubulin levels in skeletal muscle. That taxanes may have

detrimental effects on mitochondria in patients is suggested by the negative correlations of tubulin and detyrosinated tubulin to mitochondrial content and morphology in both compartments. The mechanism whereby TAXOL affects mitochondria is not clear, but our data in cultured myotubes and that of others in intact muscle fibers suggests that TAXOL increases ROS production (Figure 4B and (32)), which could promote mitophagy (20). In support of a role for ROS in promoting mitochondrial rarefaction, we found that MitoQ prevented TAXOL-induced mitochondrial loss. Collectively, our results highlight novel mitotoxic effects of taxane chemotherapeutics in skeletal muscle.

The effect of chemotherapeutics to increase cellular oxidant stress might also promote myofiber atrophy (48). In patients, increased expression and oxidation of Prx 3, which our data and that of others (37) from cultured muscle cells suggests may result from chemotherapeutics, were associated with reduced CSA in MHC I and II fibers. Moreover, in C2C12 myotubes, concomitant treatment with the mitochondrial-targeted anti-oxidant MitoQ prevented chemotherapy-induced myosin loss. These findings are not confined to cultured muscle cells, as mitochondrial-targeted antioxidants prevent DOX-induced atrophy in rodents (43). Our data show that these effects are also apparent in cultured muscle cells for TAXOL, the most commonly used drug among our breast cancer patients. The mechanisms whereby increased cellular or mitochondrial oxidant stress promotes muscle atrophy are not well defined and we found no evidence for activation of p38 and ERK in breast cancer patients, signaling pathways that have been suggested to be associated with the atrophic effects of chemotherapeutics in pre-clinical models (3). The effects of chemotherapy may promote muscle atrophy through other signaling pathways

that are sensitive to energetic/oxidative stress created by mitochondrial adaptations, such as AMP-activated kinase (63), which can suppress protein synthesis and/or increase proteolysis.

Not all chemotherapeutics derive their myotoxic effects through mitochondrial adaptations, as we found marked myosin depletion in myotubes with CIS in the absence of increased ROS production or mitochondrial rarefaction. The lack of an effect of CIS to induce ROS production may be explained by the concentration we used, as prior work suggests that mitochondrial effects occur at higher concentrations (5). However, the concentrations in our experiments are in line with tumor intracellular levels, and we used PBS as a diluent, which yields greater DNA binding capacity and, in turn, cytotoxicity (18). Despite the lack of effect on mitochondrial content/ROS production, these data nonetheless reinforce the potential myotoxic effects of chemotherapeutics through multiple pathways.

Several limitations to our studies deserve note. First, all patients received short courses of dexamethasone concurrent with their chemotherapy (1 to 4 days for each cycle, depending on symptom severity). Glucocorticoids have well-known effects to cause muscle atrophy (53). Whether the short course of dexamethasone given to these patients would affect muscle structure or function is not known, but longer-term treatment with glucocorticoids combined with bed rest (28 days) lead to only modest changes in muscle fiber size (~11% reductions in cross-sectional area; (19)) and chronic treatment has minimal effects on mitochondrial content (28). Moreover, the atrophic effects of

glucocorticoids are generally more apparent in fast-twitch, MHC II fibers (53), whereas we found effects in both fiber types. Thus, we conclude that it is unlikely that glucocorticoids alone explain the muscle atrophy or mitochondrial rarefaction that we observed in breast cancer patients, but acknowledge that current data is insufficient to resolve what effects it might have. Second, because of the cross-sectional nature of our study, we cannot discount that muscle phenotypes observed in cancer patients are attributable to other factors separate from, or secondary to, cancer and its treatment. For example, acute (e.g., following surgical resection) or chronic physical inactivity (40), which can also induce muscle atrophy and mitochondrial adaptations, may explain these differences. During the review and revision of our manuscript, a study was published showing declines in skeletal muscle fiber size and citrate synthase activity over 16 weeks in breast cancer patients receiving chemotherapy (41), suggesting that muscle atrophy and mitochondrial adaptations occur in concert with cancer treatment. Third, controls were slightly older than cancer patients. However, most of the phenotypes noted in cancer patients (e.g., fiber atrophy, mitochondrial rarefaction) would worsen with aging, suggesting that the age difference likely lessened group differences in these measures. Fourth, myotube cultures are not a perfect model of *in vivo* skeletal muscle. While they offer a model system to evaluate the singular effects of select agents and obviate off-target effects found *in vivo* (e.g., cardiac damage/failure associated with DOX administration (26) could affect skeletal muscle size and function (54)), they do not recreate the 3D structural or functional environment of *in vivo* muscle. Nonetheless, numerous aspects of the atrophic process have been studied extensively in myotube cultures and been shown to correspond with skeletal muscle *in vivo*, such as the effects of

cancer to promote oxidant stress (7, 39). Fifth, we did not include a group of post-resection, treatment-naïve patients to further delineate the effects of chemotherapy because of practical difficulties in recruiting and studying these patients. Finally, we did not standardize for time on chemotherapeutics among patients, although it did not correlate with any outcomes that differed between groups.

In summary, our results provide evidence for skeletal muscle atrophy and mitochondrial rarefaction in breast cancer patients that may be linked to the mitotoxic effects of chemotherapeutics. From a clinical standpoint, these adaptations may contribute to muscle weakness (atrophy) and fatigue (mitochondrial). Accordingly, that chemotherapeutics have such effects on skeletal muscle provides a possible explanation for the high prevalence of fatigue and functional disability across cancer types (12), including those not typically characterized by cachexia, such as breast cancer. Given the contribution of these side effects to a poor quality of life (8) and increased mortality (6, 9, 60), interventions designed to counter these effects on muscle may help to alleviate some of the burden of the disease on patients.

Acknowledgements

We thank all the volunteers who dedicated their valuable time to these studies. The authors also wish to thank Dr. Jason Stumpff for assistance with live cell imaging and Dr. Brad Palmer for assistance with electrical field stimulation and assessment of myotube contracture and calcium cycling. The α tubulin antibody was obtained from the Developmental Studies Hybridoma Bank, created by the NICHD of the NIH, and maintained at The University of Iowa, Department of Biology.

Grants

This study was funded by a grant from the Vermont Cancer Center/Lake Champlain Cancer Research Organization, R21 CA191532 and R01 AR065826. K.D. was funded by P20 GM103644. B.G. was funded by a Department of Defense SMART Scholarship ID 2016-85335.

Disclosures

The authors declare no potential conflicts of interest

Author contributions

BAG, KD and MJT were involved in the conception and design of the experiments. DMC, MSM, TWT, VA, TV, BF, BK, BAG, KD and MJT were involved in the collection, analysis and interpretation of the data. All of the authors were involved in drafting or critically revising the manuscript and all approved the final version.

Literature cited

1. **American CS**. Cancer Facts and Figures 2015. American Cancer Society. http://www.cancer.org/acs/groups/content/@research/documents/document/acspc-047079.pdf.

2. **Aslani A, Smith RC, Allen BJ, Pavlakis N, and Levi JA**. Changes in body composition during breast cancer chemotherapy with the CMF-regimen. *Breast Cancer Res Treat* 57: 285-290, 1999.

3. **Barreto R, Waning DL, Gao H, Liu Y, Zimmers TA, and Bonetto A**. Chemotherapy-related cachexia is associated with mitochondrial depletion and the activation of ERK1/2 and p38 MAPKs. *Oncotarget* 7: 43442-43460, 2016.

4. **Bechshøft RL, Malmgaard-Clausen NM, Gliese B, Beyer N, Mackey AL, Andersen JL, Kjær M, and Holm L**. Improved skeletal muscle mass and strength after heavy strength training in very old individuals. *Exp Gerontol* 92: 96-105, 2017.

5. **Berndtsson M, Hägg M, Panaretakis T, Havelka AM, Shoshan MC, and Linder S**. Acute apoptosis by cisplatin requires induction of reactive oxygen species but is not associated with damage to nuclear DNA. *Int J Cancer* 120: 175-180, 2007.

6. **Braithwaite D, Satariano WA, Sternfeld B, Hiatt RA, Ganz PA, Kerlikowske K, Moore DH, Slattery ML, Tammemagi M, Castillo A, Melisko M, Esserman L, Weltzien EK, and Caan BJ**. Long-term prognostic role of functional limitations among women with breast cancer. *J Natl Compr Canc Netw* 102: 1468-1477, 2010.

7. **Brown JL, Rosa-Caldwell ME, Lee DE, Blackwell TA, Brown LA, Perry RA, Haynie WS, Hardee JP, Carson JA, Wiggs MP, Washington TA, and Greene NP**. Mitochondrial degeneration precedes the development of muscle atrophy in progression of cancer cachexia in tumour-bearing mice. *J Cachexia Sarcopenia Musc* 8: 926-938, 2017.

8. **Butt Z, Rosenbloom SK, Abernethy AP, Beaumont JL, Paul D, Hamptom D, Jacobsen PB, Syrjala KL, Von Roenn JH, and Cella D**. Fatigue is the most important symptom for advanced cancer patients who have had chemotherapy. *J Natl Compr Canc Netw* 6: 448-455, 2008.

9. **Caan BJ, Cespedes Feliciano EM, Prado CM, and et al.** Association of muscle and adiposity measured by computed tomography with survival in patients with nonmetastatic breast cancer. *JAMA Oncology* 2018.

10. **Callahan DM, Bedrin NG, Subramanian M, Berking J, Ades PA, Toth MJ, and Miller MS**. Age-related structural alterations in human skeletal muscle fibers and mitochondria are sex-specific: relationship to single fiber function. *J Appl Physiol* 116: 1582-1592, 2014.

11. **Callahan DM, Tourville TW, Miller MS, Hackett SB, Sharma H, Cruickshank NC, Slauterbeck JR, Savage PD, Ades PA, Maughan DW, Beynnon BD, and Toth MJ**. Chronic disuse and skeletal muscle structure in older adults: sex-specific differences and relationships to contractile function. *Am J Physiol Cell Physiol* 308: C932-C943, 2015.

12. **Cella D, Davis K, Breitbart W, Curt G, and Coalition ftF**. Cancer-related fatigue: prevalence of proposed diagnostic criteria in a United States sample of cancer survivors. *J Clin Oncol* 19: 3385-3391, 2001.

13. **Damas F, Phillips SM, Lixandrão ME, Vechin FC, Libardi CA, Roschel H, Tricoli V, and Ugrinowitsch C**. Early resistance training-induced increases in muscle cross-sectional area are concomitant with edema-induced muscle swelling. *Eur J Appl Physiol* 116: 49-56, 2016.

14. **De Deyne PG**. Formation of sarcomeres in developing myotubes: role of mechanical stretch and contractile activation. *Am J Physiol Cell Physiol* 279: C1801-C1811, 2000.

15. **Delbono O, O'Rourke KS, and Ettinger WH**. Excitation-calcium release uncoupling in aged single human skeletal muscle fibers. *J Membrane Biol* 148: 211-222, 1995.

16. **Dewys WD, Begg C, Lavin PT, Band PR, Bennett JM, Bertino JR, Cohen MH, Douglass HO, Engstrom PF, Ezdinli EZ, Horton J, Johnson GJ, Moertel CG, Oken MM, Perlia C, Rosenbaum C, Silverstein MN, Skeel RT, Sponzo RW, and Tormey DC**. Prognostic effect of weight loss prior to chemotherapy in cancer patients. *Am J Med* 69: 491-497, 1980.

17. **Fearon KCH, Glass DJ, and Guttridge DC**. Cancer cachexia: mediators, signaling and metabolic pathways. *Cell Metabolism* 16: 1-14, 2012.

18. **Fischer SJ, Benson LM, Fauq A, Naylor S, and Windebank AJ**. Cisplatin and dimethyl sulfoxide react to form an adducted compound with reduced cytotoxicity and neurotoxicity. *Neurotoxicology* 29: 444-452, 2008.

19. **Fitts RH, Romatowski JG, Peters JR, Paddon-Jones D, Wolfe RR, and Ferrando AA**. The deleterious effects of bed rest on human skeletal muscle fibers are exacerbated by hypercortisolemia and ameliorated by dietary supplementation. *Am J Physiol Cell Physiol* 293: C313-C320, 2007.

20. **Frank M, Duvezin-Caubet S, Koob S, Occhipinti A, Jagasia R, Petcherski A, Ruonala MO, Priault M, Salin B, and Reichert AS**. Mitophagy is triggered by mild oxidative stress in a mitochondrial fission dependent manner. *Biochim Biophys Acta* 1823: 2297-2310, 2012.

21. **Freedman RJ, Aziz N, Albanes D, Hartman T, Danforth D, Hill S, Sebring N, Reynolds JC, and Yanovski JA**. Weight and body composition changes during and after adjuvant chemotherapy in women with breast cancer. *J Clin Endocrinol Metab* 89: 2248-2253, 2004.

22. **Gilliam LAA, Ferreira LF, Bruton JD, Moylan JS, Westerblad H, St. Clair DK, and Reid MB**. Doxorubicin acts through tumor necrosis factor receptor subtype 1 to cause dysfunction of murine skeletal muscle. *J Appl Physiol* 107: 1935-1942, 2009.

23. **Gilliam LAA, Fisher-Wellman KH, Lin C-T, Maples JM, Cathey BL, and Neufer PD**. The anticancer agent doxorubicin disrupts mitochondrial energy metabolism and redox balance in skeletal muscle. *Free Rad Biol Med* 65: 988-996, 2013.

24. **Gilliam LAA, Moylan JS, Patterson EW, Smith JD, Wilson AS, Rabbani Z, and Reid MB**. Doxorubicin acts via mitochondrial ROS to stimulate catabolism in C2C12 myotubes. *Am J Physiol Cell Physiol* 302: C195-C202, 2012.

25. **Gouspillou G, Scheede-Bergdahl C, Spendiff S, Vuda M, Meehan B, Mlynarski H, Archer-Lahlou E, Sgarioto N, Purves-Smith FM, Konokhova Y, Rak J, Chevalier S, Taivassalo T, Hepple RT, and Jagoe RT**. Anthracycline-containing chemotherapy causes long-term impairment of mitochondrial respiration and increased reactive oxygen species release in skeletal muscle. *Sci Rep* 5: 8717, 2015.

26. **Hasenfuss G**. Animal models of human cardiovascular disease, heart failure and hypertrophy. *Cardiovasc Res* 39: 60-76, 1998.

27. **He WA, Calore F, Londhe P, Canella A, Guttridge DC, and Croce CM**. Microvesicles containing miRNAs promote muscle cell death in cancer cachexia via TLR7. *Proc Natl Acad Sci* 111: 4525-4529, 2014.

28. **Horber FF, Hoppeler H, Herren D, Claassen H, Howald H, Gerber C, and Frey FJ**. Altered skeletal muscle ultrastructure in renal transplant patients on prednisone. *Kidney International* 30: 411-416, 1986.

29. **Huang X, Sun L, Ji S, Zhao T, Zhang W, Xu J, Zhang J, Wang Y, Wang X, Franzini-Armstrong C, Zheng M, and Cheng H**. Kissing and nanotunneling mediate intermitochondrial communication in the heart. *Proc Natl Acad Sci* 110: 2846-2851, 2013.

30. **Irwin ML, McTiernan A, Baumgartner RN, Baumgartner KB, Bernstein L, Gilliland FD, and Ballard-Barbash R**. Changes in body fat and weight after a breast cancer diagnosis: influence of demographic, prognostic, and lifestyle factors. *J Clin Oncol* 23: 774-782, 2005.

31. **Kerr JP, Robison P, Shi G, Bogush AI, Kempema AM, Hexum JK, Becerra N, Harki DA, Martin SS, Raiteri R, Prosser BL, and Ward CW**. Detyrosinated microtubules modulate mechanotransduction in heart and skeletal muscle. *Nat Commun* 6: 8526, 2015.

32. **Khairallah RJ, Shi G, Sbrana F, Prosser BL, Borroto C, Mazaitis MJ, Hoffman EP, Mahurkar A, Sachs F, Sun Y, Chen Y-W, Raiteri R, Lederer WJ, Dorsey SG, and Ward CW**. Microtubules underlie dysfunction in Duchenne muscular dystrophy. *Sci Signal* 5: 10.1126/scisignal.2002829, 2012.

33. **Kontrogianni-Konstantopoulos A, Catino DH, Strong JC, and Bloch RJ**. De novo myofibrillogenesis in C2C12 cells: evidence for the independent assembly of M bands and Z disks. *Am J Physiol Cell Physiol* 290: C626-C637, 2006.

34. **Langen RCJ, Schols AMWJ, Kelders MCJM, Wouters EFM, and Janssen-Heininger YMW**. Enhanced myogenic differentiation by extracellular matrix is regulated at the early stages of myogenesis. *In Vitro Cell Dev Biol Anim* 39: 163-169, 2003.

35. **Lanza IR, and Nair KS**. Chapter 20: Functional Assessment of Isolated Mitochondria In Vitro. In: *Methods in Enzymology*, edited by William SA, and Anne NMAcademic Press, 2009, p. 349-372.

36. **Lee K-P, Shin YJ, Cho SC, Lee S-M, Bahn YJ, Kim JY, Kwon E-S, Jeong DY, Park SC, Rhee SG, Woo HA, and Kwon K-S**. Peroxiredoxin 3 has a crucial role in the contractile function of skeletal muscle by regulating mitochondrial homeostasis. *Free Rad Biol Med* 77: 298-306, 2014.

37. **Liu M-H, Zhang Y, He JUN, Tan T-P, Wu S-J, Fu H-Y, Chen Y-D, Liu JUN, Le Q-F, Hu H-J, Yuan C, and Lin X-L**. Upregulation of peroxiredoxin III in doxorubicin-induced cytotoxicity and the FoxO3a-dependent expression in H9c2 cardiac cells. *Exp Ther Med* 10: 1515-1520, 2015.

38. **Manabe Y, Miyatake S, Takagi M, Nakamura M, Okeda A, Nakano T, Hirshman MF, Goodyear LJ, and Fujii NL**. Characterization of an acute muscle contraction model using cultured C2C12 myotubes. *PLOS ONE* 7: e52592, 2013.

39. **McLean J, Moylan JS, and Andrade FH**. Mitochondria dysfunction in lung cancer-induced muscle wasting in C2C12 myotubes. *Front Physiol* 5: 2014.

40. **McTiernan A, Kooperberg C, White E, and et al.** Recreational physical activity and the risk of breast cancer in postmenopausal women: The Women's Health Initiative cohort study. *JAMA* 290: 1331-1336, 2003.

41. **Mijwel S, Cardinale DA, Norrbom J, Chapman M, Ivarsson N, Wengström Y, Sundberg CJ, and Rundqvist H**. Exercise training during chemotherapy preserves skeletal muscle fiber area, capillarization, and mitochondrial content in patients with breast cancer. *FASEB J* 0: fj.201700968R.

42. **Miller MS, Callahan DM, Tourville TW, Slauterbeck JR, Kaplan A, Fiske BR, Savage PD, Ades PA, Beynnon BD, and Toth MJ**. Moderate-intensity resistance exercise alters skeletal muscle molecular and cellular structure and function in inactive, older adults with knee osteoarthritis. *J Appl Physiol* 122: 775-787, 2017.

43. **Min K, Kwon O-S, Smuder AJ, Wiggs MP, Sollanek KJ, Christou DD, Yoo J-K, Hwang M-H, Szeto HH, Kavazis AN, and Powers SK**. Increased mitochondrial emission of reactive oxygen species and calpain activation are required for doxorubicin-induced cardiac and skeletal muscle myopathy. *J Physiol* 593: 2017-2036, 2015.

44. **Miyatake S, Bilan PJ, Pillon NJ, and Klip A**. Contracting C2C12 myotubes release CCL2 in an NF-κB-dependent manner to induce monocyte chemoattraction. *Am J Physiol Endocrinol Metab* 310: E160-E170, 2016.

45. **Montgomery MK, Osborne B, Brown SHJ, Small L, Mitchell TW, Cooney GJ, and Turner N**. Contrasting metabolic effects of medium- vs. long-chain fatty acids in skeletal muscle. *J Lipid Res* 54: 3322-3333, 2013.

46. **Petrella JK, Kim JS, Cross JM, Kosek DJ, and Bamman MM**. Efficacy of myonuclear addition may explain differential myofiber growth among resistance-trained young and older men and women. *Am J Physiol Endocrinol Metab* 291: E937-946, 2006.

47. **Piscitelli SC, Rodvold KA, Rushing DA, and Tewksbury DA**. Pharmacokinetics and pharmacodynamics of doxorubicin in patients with small cell lung cancer. *Clin Pharm Ther* 53: 555-561, 1993.

48. **Powers SK, Morton AB, Ahn B, and Smuder AJ**. Redox control of skeletal muscle atrophy. *Free Rad Biol Med* 98: 208-217, 2016.

49. **Poynton RA, and Hampton MB**. Peroxiredoxins as biomarkers of oxidative stress. *Biochim Biophys Acta* 1840: 906-912, 2014.

50. **Rengo JL, Callahan DM, Savage PD, Ades PA, and Toth MJ**. Skeletal muscle ultrastructure and function in statin-tolerant individuals. *Muscle Nerve* 53: 242-251, 2016.

51. **Romanello V, Guadagnin E, Gomes L, Roder I, Sandri C, Petersen Y, Milan G, Masiero E, Del Piccolo P, Foretz M, Scorrano L, Rudolf R, and Sandri M**. Mitochondrial fission and remodelling contributes to muscle atrophy. *EMBO J* 29: 1774-1785, 2010.

52. **Sandri M, Lin J, Handschin C, Yang W, Arany ZP, Lecker SH, Goldberg AL, and Spiegelman BM**. PGC-1α protects skeletal muscle from atrophy by suppressing FoxO3 action and atrophy-specific gene transcription. *Proc Natl Acad Sci* 103: 16260-16265, 2006.

53. **Schakman O, Kalista S, Barbé C, Loumaye A, and Thissen JP**. Glucocorticoid-induced skeletal muscle atrophy. *Int J Biochem Cell Biol* 45: 2163-2172, 2013.

54. **Simonini A, Long CS, Dudley GA, Yue P, McElhinny J, and Massie BM**. Heart failure in rats causes changes in skeletal muscle morphology and gene expression that are not explained by reduced activity. *Circulation* 79: 128-136, 1996.

55. **Tarnopolsky MA, Pearce E, Smith K, and Lach B**. Suction-modified Bergström muscle biopsy technique: Experience with 13,500 procedures. *Muscle Nerve* 43: 716-725, 2011.

56. **Tegeder I, Brautigam L, Seegel M, Al-Dam A, Turowski B, Geisslinger G, and Kovacs AF**. Cisplatin tumor concentrations after intra-arterial cisplatin infusion or embolization in patients with oral cancer. *Clin Pharm Ther* 73: 417-426, 2003.

57. **Toth MJ, Gottlieb SS, Fisher ML, and Poehlman ET**. Skeletal muscle atrophy and peak oxygen consumption in heart failure. *Am J Cardiol* 79: 1267-1269, 1997.

58. **Toth MJ, Miller MS, Callahan DM, Sweeny AP, Nunez I, Grunberg SM, Der-Torossian H, Couch ME, and Dittus K**. Molecular mechanisms underlying skeletal muscle weakness in human cancer: reduced myosin-actin cross-bridge formation and kinetics. *J Appl Physiol* 114: 858-868, 2013.

59. **Toth MJ, Ward K, vand der Velden J, Miller MS, VanBuren P, LeWinter MM, and Ades PA**. Chronic heart failure reduces Akt phosphorylation in human skeletal muscle: relationship to muscle size and function. *J Appl Physiol* 119: 892-900, 2011.

60. **Villaseñor A, Ballard-Barbash R, Baumgartner K, Baumgartner R, Bernstein L, McTiernan A, and Neuhouser M**. Prevalence and prognostic effect of sarcopenia in breast cancer survivors: the HEAL Study. *J Cancer Surviv* 6: 398-406, 2012.

61. **Waning DL, Mohammad KS, Reiken S, Xie W, Andersson DC, John S, Chiechi A, Wright LE, Umanskaya A, Niewolna M, Trivedi T, Charkhzarrin S, Khatiwada P, Wronska A, Haynes A, Benassi MS, Witzmann FA, Zhen G, Wang X, Cao X, Roodman GD, Marks AR, and Guise TA**. Excess TGF-β mediates muscle weakness associated with bone metastases in mice. *Nat Med* 21: 1262-1271, 2015.

62. **White J, Puppa M, Sato S, Gao S, Price R, Baynes J, Kostek M, Matesic L, and Carson J**. IL-6 regulation on skeletal muscle mitochondrial remodeling during cancer cachexia in the ApcMin/+ mouse. *Skelet Muscle* 2: 14, 2012.

63. **White JP, Puppa MJ, Gao S, Sato S, Welle SL, and Carson JA**. Muscle mTORC1 suppression by IL-6 during cancer cachexia: a role for AMPK. *Am J Physiol Endocrinol Metab* 304: E1042-E1052, 2013.

64. **Wojtala A, Bonora M, Malinska D, Pinton P, Duszynski J, and Wieckowski MR**. Methods to monitor ROS production by fluorescence microscopy and fluorometry. In: *Methods in Enzymology*, edited by Lorenzo G, and Guido KAcademic Press, 2014, p. 243-262.

65. **Yi M, Weaver D, and Hajnóczky G**. Control of mitochondrial motility and distribution by the calcium signal. *J Cell Biol* 167: 661, 2004.

66. **Zasadil LM, Andersen KA, Yeum D, Rocque GB, Wilke LG, Tevaarwerk AJ, Raines RT, Burkard ME, and Weaver BA**. Cytotoxicity of paclitaxel in breast cancer is due to chromosome missegregation on multipolar spindles. *Sci Transl Med* 6: 229ra243-229ra243, 2014.

Figures and tables

Figure 1:

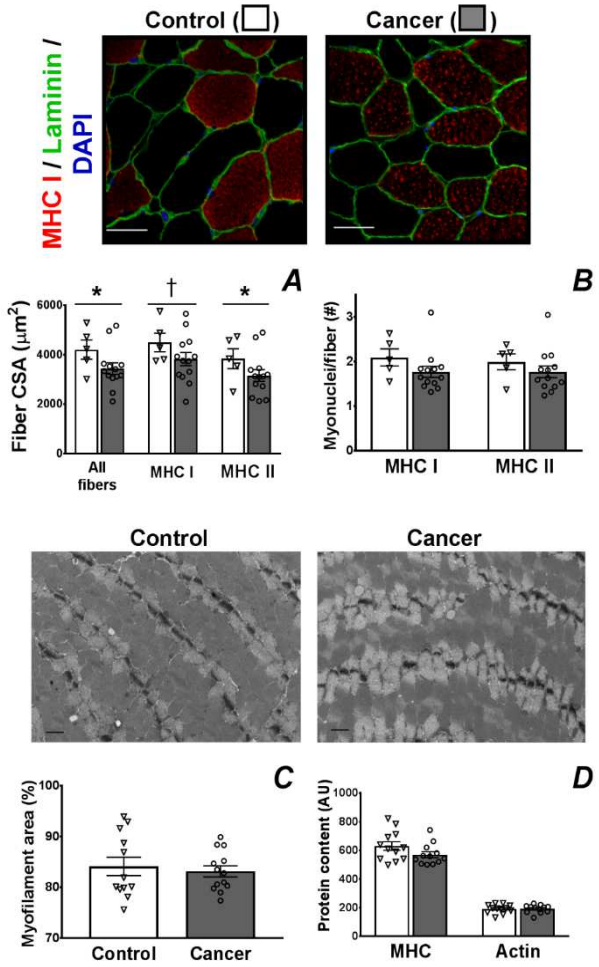

Figure 3.0.1: *Breast cancer patient skeletal muscle morphology.*

Figure 1. Skeletal muscle fiber cross-sectional area (CSA) in all fibers and myosin heavy chain (MHC) I and II fibers (A), myonuclei content in MHC I and II fibers (B), myofilament fractional area (C) and MHC and actin protein content in tissue homogenates (D) in controls (open bars) and breast cancer patients (gray bars). Data are mean ± SEM, with individual data points shown with each bar. For panels A, B and C, multiple observations within each individual were averaged to provide a single data point for each volunteer. Representative immunohistochemical images used to measure CSA and myonuclei content for control and cancer patients are shown above panels A and B, respectively. Scale bars=100 μm. Representative electron microscopy images used to measure myofilament fractional area (Panel C) for controls and cancer patients are shown above panels C and D, respectively. Scale bars=1 μm. AU, arbitrary units. *, P≤0.05; †, 0.07.

Figure 2:

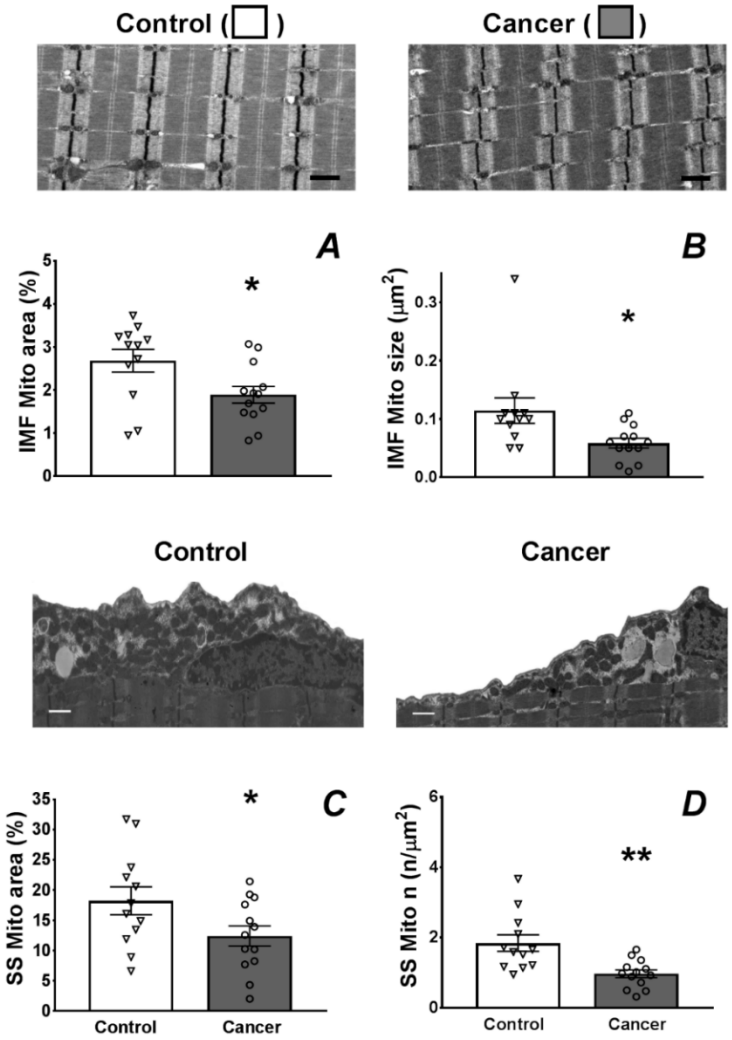

Figure 3.0.2: *Breast Cancer patient mitochondrial morphology.*

Figure 2. Skeletal muscle mitochondrial (Mito) content and structure in the intermyofibrillar (IMF) and sub-sarcolemmal (SS) compartments. Representative images for IMF mitochondrial fractional area for controls and cancer patients are shown above panels A and B, respectively, with average IMF mitochondrial fractional area (A) and average size (B) for controls (open bars) and breast cancer patients (gray bars). Representative images for SS mitochondria for controls and cancer patients are shown above panels C and D, respectively, with average SS fractional area (C) and average number (n) per unit sub-sarcolemmal area (D). Scale bars= 1 μm for all images. Data are mean ± SEM, with individual data points shown with each bar. For panels A-D, multiple observations within each individual were averaged to provide a single data point for each individual. *, $P<0.05$ and **, $P<0.01$ compared to controls.

Figure 3:

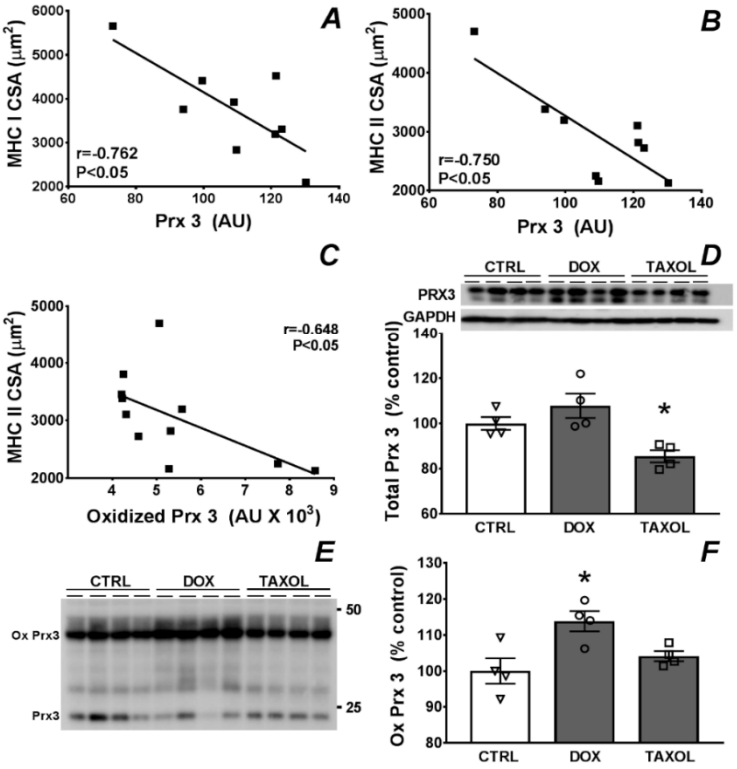

Figure 3.0.3*: Patient and C2C12 PRX3.*

Figure 3. Relationship of mitochondrial oxidant stress to myofiber size and chemotherapy administration. The relationship of MHC I (A) and MHC II (B) CSA to peroxiredoxin 3 (Prx 3) expression, and MHC II CSA (C) to oxidized Prx 3 in breast cancer patients (black squares). The r-value in A is a Pearson coefficient, while r-values in B and C are Spearman rank coefficients. For panels A and B (n=9) and C (n=11). Effects of 3 days of doxorubicin (DOX; 0.2 μM) or paclitaxel (TAXOL; 40 nM) treatment (gray bars) vs. control (Ctrl; DMSO; open bar) on C2C12 myotube Prx 3 expression (D, n=4/condition) and oxidation, with the latter being shown by Prx 3 dimers (oxidized) under non-reducing conditions, as shown in the blot in panel E. Quantitation of oxidized Prx 3 is shown in F (n=4/condition). Data in D and F are mean ± SEM, with individual data points shown with each bar. For panels A-C, multiple observations for CSA within each individual were averaged to provide a single data point for each individual. For panel D, immunoblots are shown above average data with loading control (GAPDH). Loading controls were not shown for panel E, as oxidized Prx 3 data are expressed as a fraction of total (oxidized + non-oxidized) Prx 3. *, P<0.05 compared to control conditions.

Figure 4:

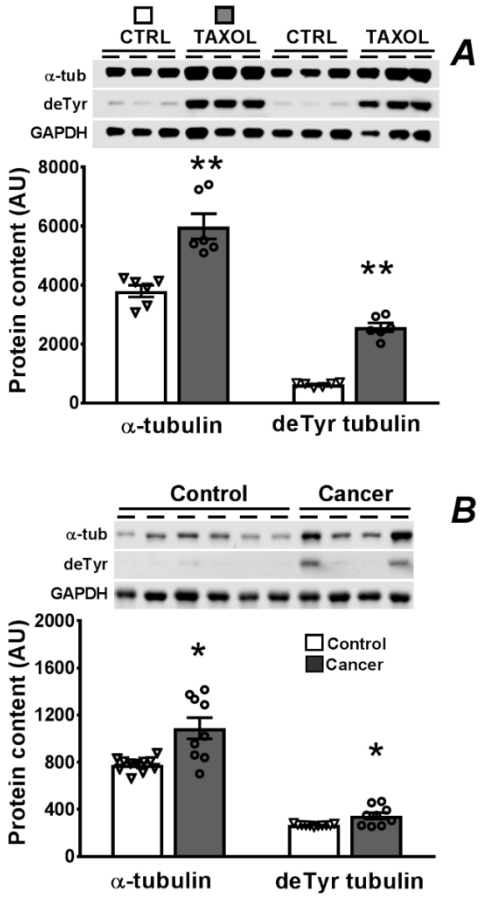

Figure 3.0.4*: Tubulin content in breast cancer patients and C2C12.*

Figure 4. α-tubulin (α-tub) and detyrosinated (deTyr) tubulin expression. α-tubulin and detyrosinated tubulin were assessed following 3 days of treatment of C2C12 myotubes (A) with vehicle (CTRL; treated with DMSO; clear bars; n=6) or TAXOL (40 nM; gray bars; n=6), and in controls (open bars; n=11) and breast cancer patients (gray bars; n=9)(B). Gels images are provided for both experiments. Data are mean ± SEM, with individual data points shown with each bar. *, $P<0.05$ and **, $P<0.01$ compared to controls.

Figure 5:

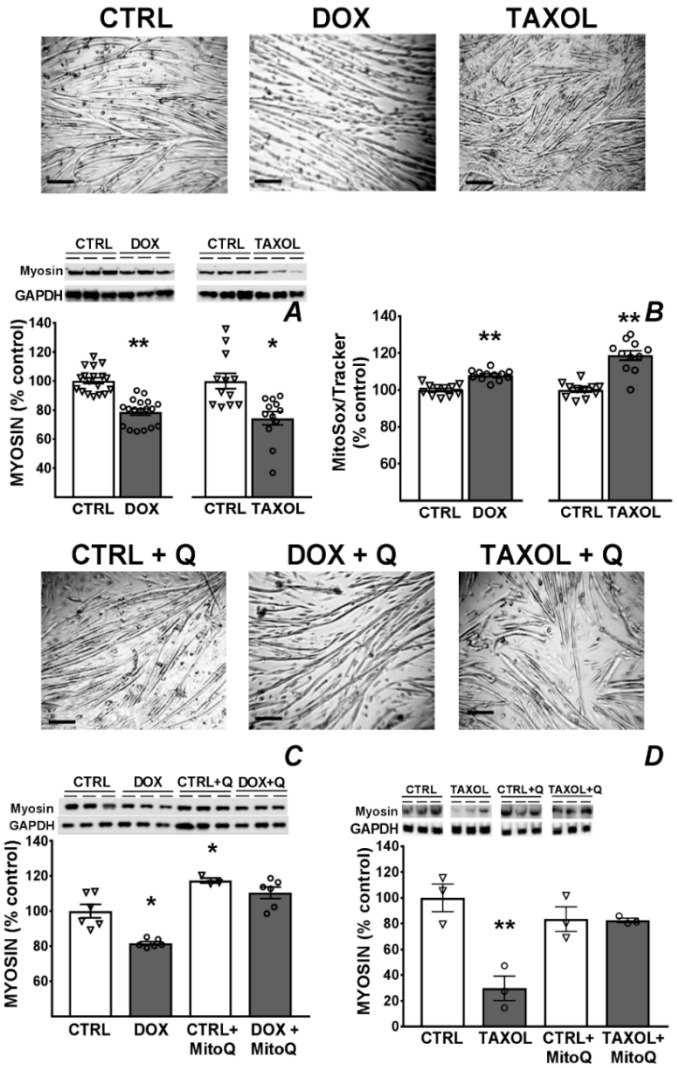

Figure 3.0.5: *Mitochondrial anti-oxidant administration on myosin content*.

Figure 5. Chemotherapeutic effects on myotube myosin content. The effects of 3 days of DOX (0.2 μM) or TAXOL (40 nM) administration (gray bars) versus vehicle (DMSO in both; CTRL; open bars) on myosin content (A) and ROS production (B), with representative images of myotubes for each experimental condition in panel A shown above (scale bar for all images=100 μm).The effects of concomitant treatment with the mitochondrial-targeted anti-oxidant MitoQ (0.25 μM for DOX and 0.125 μM for TAXOL; gray bars) to prevent myosin loss with DOX or TAXOL are shown in panels C and D, respectively, with representative images of myotubes for each experimental condition shown above (scale bar for all images=100 μm). Data are mean ± SEM, with individual data points shown with each bar. *, $P<0.05$ and **, $P<0.01$ compared to control conditions.

Figure 6:

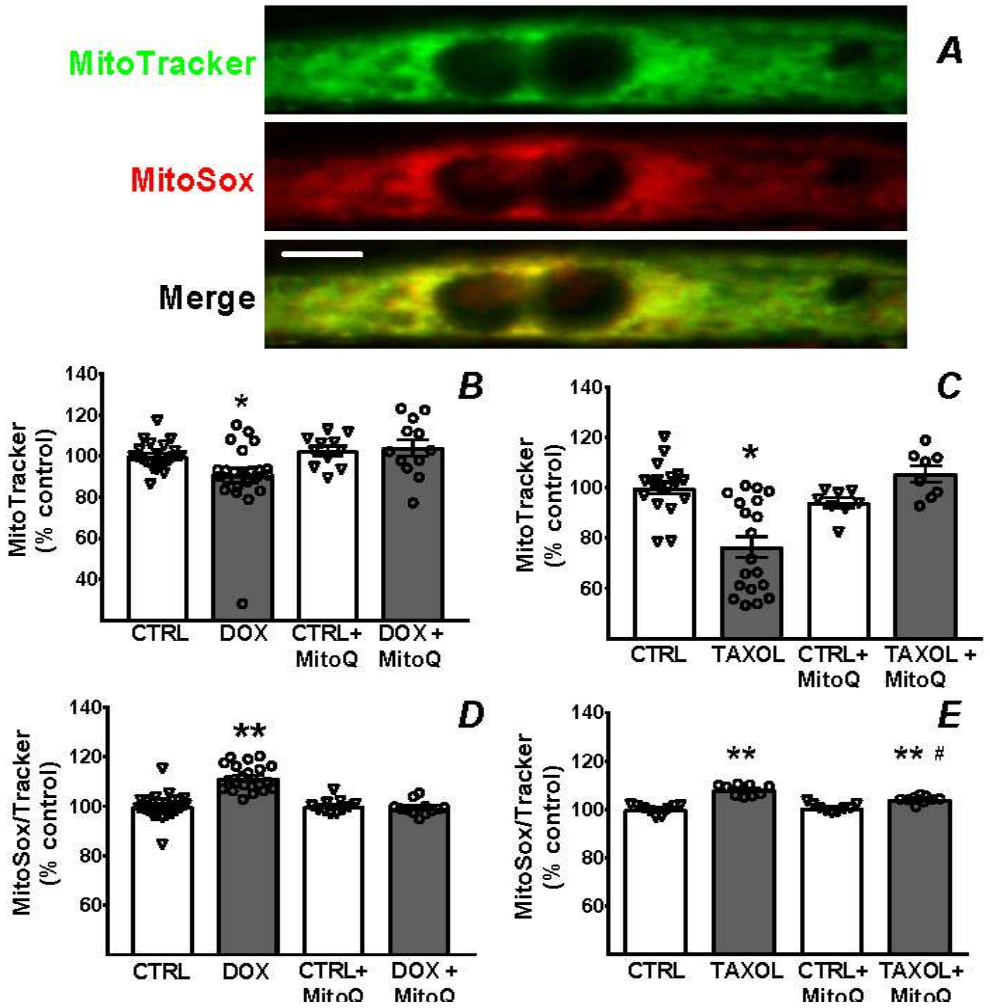

Figure 3.0.6*:* Anti-oxidant administration on ROS and mitochondrial content.

Figure 6. Effect of chemotherapeutics (gray bars) and concomitant treatment with the mitochondrial-targeted anti-oxidant MitoQ (+MitoQ; 0.25 μM for DOX and 0.125 μM for TAXOL) on mitochondrial content (B and C, respectively) and oxidant production (D and E) vs. vehicle control (DMSO; clear bars). Data are mean ± SEM, with individual data points shown with each bar. Co-localization of MitoTracker (green) and MitoSox (red) in a C2C12 murine myotube (A). Scale bar=10 μm. *, P<0.05 vs. controls; **, P<0.01 vs. controls; #, P<0.01 vs. TAXOL.

Figure 7:

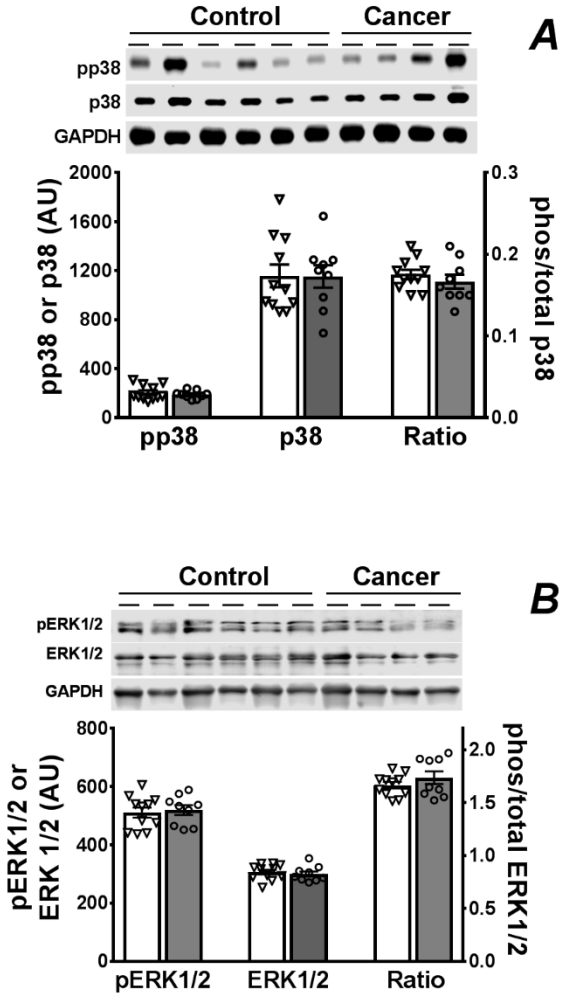

Figure 3.0.7: *Patient p38 and ERK content.*

Figure 7. p38 (A) and ERK1/2 (B) expression and phosphorylation (pp38 and pERK1/2, respectively) in tissue homogenates from controls (open bars; n=11) and breast cancer patients (gray bars; n=9). Gels images are provided for both phospho- and total protein, as well as GAPDH. The ratio measure reflects the ratio of phospho- to total protein. Data are mean ± SEM, with individual data points shown with each bar.

Table 3.3. *Physical and disease characteristics in patients.*

	Control	Cancer
n	12	13
Age (yr)	66 ± 5	57 ± 12 *
Body weight (kg)	67 ± 15	70 ± 13
Height (cm)	164 ± 5	161 ± 8
Fat mass (kg)	24 ± 12	28 ± 11
Fat-free mass (kg)	40 ± 5	40 ± 4
Fat-free mass index (kg/m^2)	15.2 ± 1.3	15.4 ± 1.6
Leg fat-free mass (kg)	13 ± 2	14 ± 2
Cancer Stage (I/II/III)	NA	7 / 2 / 4
Histology (n)		
Adenocarcinoma	NA	13
Dexamethasone (n)	NA	13
Chemotherapeutics (n)		
Taxanes	NA	13
Cyclophosphamide	NA	8
Doxorubicin	NA	5
Trastuzumab	NA	3
History of smoking (n)	NA	1
Radiation (n)	NA	0

Data are mean ± SD. * $P<0.05$. NA, not applicable to control volunteers.

List of abbreviations

CSA: Cross Sectional Area

DMSO: Dimethyl sulfoxide

DOX: Doxorubicin

EM: Electron Microscopy

MHC I: Myosin Heavy Chain type I

MHC II: Myosin Heavy Chain type II

Prx 3: Peroxiredoxin 3

ROS: Reactive Oxygen Species

TAXOL: Paclitaxel

CHAPTER 4: ELECTRICAL STIMULATION PREVENTS DELETERIOUS EFFECTS OF CHEMOTHERAPY ON CULTURED MYOTUBES

Blas A. Guigni[1,2], Dennis K. Fix[4], Joseph J. Bivona III [1], Bradley M. Palmer[2], James A. Carson[4,5], Michael J. Toth[1,2,3]

Departments of Medicine[1], Molecular Physiology and Biophysics[2] and Orthopedics and Rehabilitation[3], College of Medicine, University of Vermont, Burlington, VT; Department of Exercise Science, University of South Carolina, Columbia, SC[4] and Division of Rehabilitation Sciences, College of Health Professions, University of Tennessee Health Science Center [5]

Correspondence to: Michael J. Toth, Ph.D.
Health Science Research Facility 126B
149 Beaumont Ave
University of Vermont
Burlington, VT 05405
Email: michael.toth@uvm.edu
Tele: (802) 656-7989
Fax: (802) 656-0747

Running Title: Exercise and chemotherapy

Abstract

Muscle contraction may protect against the effects of chemotherapy to cause skeletal muscle atrophy and weakness, but the mechanisms underlying these benefits are unclear. To address this question, we utilized *in vitro* modeling of contraction and mechanotransduction in C2C12 myotubes treated with doxorubicin (DOX; 0.2 μM for 3 days). Myotubes expressed contractile proteins and organized these into functional myofilaments, as electrical field stimulation (STIM) induced intracellular calcium (Ca^{2+}) transients and contractions, both of which were prevented by inhibition of membrane depolarization. DOX treatment reduced myotube myosin content, protein synthesis, Akt (S308) and forkhead box O3a (FoxO3a; S253) phosphorylation and increased muscle ring fiber 1 (MuRF1) expression. STIM (1 h/d) prevented DOX-induced reductions in myotube myosin content and Akt and FoxO3a phosphorylation, as well as increases in MuRF1 expression, but did not prevent DOX-induced reductions in protein synthesis. Inhibition of myosin-actin interaction during STIM prevented contraction and the anti-atrophic effects of STIM without affecting Ca^{2+}cycling, suggesting the beneficial effect of STIM derives from mechanotransductive pathways. Further supporting this conclusion, mechanical stretch of myotubes recapitulated the effects of STIM to prevent DOX suppression of FoxO3a phosphorylation and upregulation of MuRF1. DOX also increased reactive oxygen species (ROS) production, which led to a decrease in mitochondrial content. While STIM did not alter DOX-induced ROS production or anti-oxidant gene expression, PGC-1α expression was induced and mitochondrial loss prevented. Our results suggest that the activation of mechanotransductive pathways that downregulate proteolysis and preserve mitochondrial content can protect against the atrophic effects of chemotherapeutics.

Keywords: cachexia, exercise, mechanotransduction

Introduction

Cancer afflicts ~1 in 2 men and 1 in 3 women (24). With improved detection and treatments, and increased incidence due to an aging populace (51), the number of individuals living with effects of cancer and its treatment will exceed 18 million by 2020 (9) and continue to grow. Cancer and its treatment have profound effects on skeletal muscle, including atrophy, impaired contractility and oxidative dysfunction (54, 55, 57), that negatively impact quality of life, treatment decisions and survival (4, 6, 10, 41) and can persist for years after treatment (35). These detrimental effects reduce quality of life and predispose to disability and cardio-metabolic disease.

Exercise can mitigate the negative effects of cancer and its associated treatment and improve long-term prognosis (21, 25, 56). Part of these benefits may derive from the positive effect of exercise on skeletal muscle. Exercise induces an array of beneficial adaptations in muscle, including improved proteostasis, energy metabolism and contractility (3, 13). Although the effects of various exercise regimens have been examined in patients (1, 29, 38), the mechanism(s) whereby exercise derives its benefits remains unknown. Knowledge of the fundamental mechanisms underlying the benefits of exercise could inform the development of more effective regimens that derive the greatest benefit with the least burden on patients. Therefore, we utilized *in vitro* exercise modeling in C2C12 myotube cultures subjected to chemotherapeutic treatment, with or without electrical field stimulation (STIM), to dissect the mechanisms underlying the beneficial effects of exercise on skeletal muscle. We hypothesized that STIM imparts its

beneficial effects, in part, via mechanotransductive signaling to upregulate protein synthesis and preserve mitochondrial health following chemotherapy application.

Methods

Cell culture. C2C12 myoblasts (ATCC® CRL-1772™, Manassas, VA) were cultured in growth media (GM), consisting of low glucose (1 g/L), Dulbecco's Modified Eagle's Medium (DMEM) supplemented with 10% fetal bovine serum (FBS; Gibco™ Thermo Fisher Scientific Waltham, MA) and antibiotics (50 U/ml penicillin and 50 μg/ml streptomycin). Cells were plated (2 X 10^4 cells/cm^2) on Matrigel (60 μg/cm^2; Corning, Bedford, MA) and switched to differentiation medium (DM) of low serum (1% heat-inactivated FBS), high glucose (4.5 g/L) DMEM when they reached 90-100% confluence, as described (36), with modifications as described (18). On day 7 post-differentiation (d7), myotubes were treated with doxorubicin (DOX) (0.2 μM) or vehicle control (DMSO in DM) for 3 d (chronic experiments). Thirty minutes after starting DOX treatment, STIM was applied using a C-Pace pulse generator (20V, 1Hz, 12ms; C-Pace 100, IonOptix, Milton MA) for 1 h each day for 3 days. At the end of each STIM bout, myotubes were washed twice with Hank's buffered salt solution (HBSS), fresh DM containing either DOX or vehicle (DMSO) were added and 23 h allowed before the next bout of STIM or measurements. In some experiments, myotubes were treated with tetrodotoxin (TTX; 10μM), a sodium channel inhibitor, or N-benzyl-p-toluene sulphonamide (BTS; 50μM), an inhibitor of myosin-actin ATPase cycling (49), during the 1 h STIM bouts. Cells were lysed and collected on d10, 23 h after the last STIM bout, to eliminate the possibility that results reflect an acute effect of the STIM intervention. In acute experiments, cells were treated with vehicle, DOX alone, STIM or STIM+DOX, as described above, to examine acute modulation of protein synthesis, expression of proteolytic mediators and signaling molecular phosphorylation, and harvested/measured

after 1 or 24 h. In another set of acute experiments, cells were treated with vehicle, DOX, cisplatin (CIS; 10 μM) or paclitaxel (TAXOL; 40 nM) without STIM, and harvested after 24 h.

A separate set of acute experiments examined the effects of mechanical stretch on C2C12 myotubes differentiated on type I collagen coated (Advanced Biomatrix, San Diego, CA) silastic membranes (GLOSS/GLOSS, 0.02 in, Specialty Manufacturing, Saginaw, MI). Silastic membranes were mounted on two friction-fit C-clamps, as previously described (14). The screw nuts were set to 30 cycles from baseline when the stretching device was assembled, as described (14). C2C12 myoblasts were suspended (~1×10^6cells/ml) and plated onto silastic membranes (~$1.5–2 \times 10^5$ cells/stretching device). The cells were grown to ~95% confluence and differentiated into myotubes using 2% horse serum. After 5 days of differentiation, cells were treated with DOX (0.2 μM) or vehicle control (DMSO in DM). A 5% stretch was supplied for a duration of 1 h and in cells receiving DOX, stretch was started 30 min following the first DOX administration, identical to STIM intervention detailed above. Following 1 h, of stretch the membranes were returned to baseline, cells washed 2x with HBSS, replaced with the fresh media with or without DOX for a duration of 23 h, when cells were lysed and collected, as described above.

Myotube size. Myotube size was assessed from myotube diameter measurements. Digital images of myotube cultures were acquired at 4X magnification. Average diameters (5 diameters per tube) of n=5 to 25 myotubes per field from n=4 random fields were measured using Image J software (NIH, Frederick, MD, USA) by an assessor blinded to treatment status.

Immunocytochemistry. Myofilament proteins were visualized by immunocytochemistry. Cells were grown on Matrigel-coated (60 μg/cm2), 35 mm, glass bottom imaging dishes (MatTek; Ashland, MA) or plastic, as detailed above, with the modification that the media was changed daily. Cells were fixed with 4% paraformaldehyde (Fisher Scientific, Atlanta, GA), permeabilized with 0.2% Triton-X 100 (Fisher) and blocked with 5% BSA in PBS for 1 h at room temperature. Cells were incubated overnight at 4°C in fast skeletal muscle myosin antibody (1:500; MY-32; Sigma) followed by secondary antibody (1:100 anti-mouse IgG, Molecular Probes) to visualize myofilaments, or 1 μM TRITC-phalloidin (Sigma) to stain actin to visualize the entire cell. Cells were imaged using a Nikon Ti-E Inverted Microscope with C2 Confocal at 40X for myofilament measures or an Olympus BX51 with Q-Imaging Retiga R6 at 10X.

Measurement of contractility and Ca^{2+} cycling. Ca^{2+} transients were recorded from d7-d10 myotubes grown on Matrigel-coated (60 μg/cm2), 35-mm, glass bottom imaging dishes (MatTek; Ashland, MA). For these experiments, cells were plated at a higher

density (2.5 X 10^4 cells/cm^2) and DMEM changed daily. C2C12 myotubes were loaded with 1 μM Fluo-2-acetoxymethyl ester (Fluo-2 AM, TefLabs, Austin, TX) for 15 min at 37°C in the dark. Cells were washed once with HBSS and placed in pre-warmed DM for 10 min. The culture dish was fitted with a custom-built insert that maintained media temperature at 37°C and contained platinum electrodes to allow STIM with biphasic pulses (20V, 1Hz, 12ms) (Myopacer, IonOptix, Westwood MA). The same experimental design used for performing intracellular Ca^{2+} recordings was applied to contractility measurements. Fluorescent signal and cell contractility were traced using an IonOptix system, as previously described (58). Ca^{2+} fluorescence was recorded with an inverted fluorescence microscope and galvo-controlled, dichroic mirror filters at 480/510 nm (Hyperswitch, IonOptix) (44). Contractions were tracked using the edge detection feature of the IonWizard data acquisition software using visible landmarks on/within the myotube. Both contraction and Fluo-2 AM fluorescence measurements were made simultaneously from the same myotube. Experiments lasted 300 sec. Transient analysis was performed using the IonWizard analysis software (IonOptix). For each test condition, data for 15-20 seconds of Ca^{2+} transients or contractions per myotube were averaged, using the pacing time as a common reference point, to derive an averaged monotonic Ca^{2+}/contractility transient. Fractional change, which indicates the percentage of peak following STIM relative to baseline, was used to quantify contractile dynamics and Ca^{2+} transients. Images of the Ca^{2+} fluorescent signal were acquired (40 frames/sec) using a spinning disk confocal microscope (Yokogawa CSU-W1). During these experiments, cells were stimulated (20V, 1Hz, 12ms) with platinum electrodes.

An additional set of experiments were performed without the measurement of Ca^{2+} fluorescence to assess contractility. To aid in the visualization of cell movement, 2 μm latex beads (1:1000, L3030; Sigma) were added to the culture dish 2 h prior to STIM. Digital video images were collected with a down-sampled field of 512 X 512 $pixels^2$ and a frame rate of 10 Hz (MyoCam-S3, IonOptix). Video images were analyzed by first establishing a hexagonal grid and tracking each local image featured within each hexagon by cross-correlation from frame to frame (Figure 2A, left panel). The displacement of a local image relative to its neighboring local images allowed for calculation of local strain (i.e., change in relative displacement between neighbors normalized to the original distance between neighbors). With each local image having six neighbors, three strains oriented at 120° to each other were measured. This orientation of strains allowed for calculation of magnitude and orientation of principal strains on a Mohr's circle similar to that based on a delta rosette strain gauge (8). Local strains are depicted as green ellipses illustrating the contraction or elongation of the local region (Figure 2A, right panel). From these assessments, relative strain was calculated.

Myotube mitochondrial content and reactive oxygen species (ROS) production. Mitochondrial content and ROS production were measured with fluorometric dyes, as described (18). Briefly, C2C12 myotubes grown in 35 mm dishes or black-walled 96 well plates were loaded with fluorescent dyes to assess mitochondrial content (1 μM MitoTracker Green FM; 490/516 nm) and ROS production (1 μM MitoSOX Red; 510/580 nm; both Molecular Probes, Eugene, OR) 15 minutes prior to measurement. Fluorescence was measured on a microplate reader (BioTek, Winooski, VT) and the MitoSox signal was expressed relative to MitoTracker signal to control ROS production for variation in mitochondrial content. We have shown that the MitoSox and MitoTracker signals co-localize (18).

Protein synthesis. Protein synthesis was measured using the SUnSET technique, as described (14). Briefly, 23 h after the last bout of STIM, stretch or control conditions, 1 μM puromycin (Sigma) was added to myotubes for 30 min prior to lysis and collection. Lysates were then analyzed by western blot, as described below.

Protein expression. Protein expression or phosphorylation was measured by western blot. Myotubes were washed with phosphate buffered saline, lysed (50 mM Tris, 150 mM NaCl, 10% (v/v) glycerol, 0.5% IGEPAL CA-630,1 mM EDTA, containing Protease Inhibitor Cocktail (1:100, cat# P8340, sigma) and Phosphatase Inhibitor Cocktail 3 (1:100, cat# P0044, sigma)), incubated on ice for 30 min and then centrifuged at 14,000 ×

g at 4 °C for 10 min. Lysate protein contents were measured (BioRad DC Protein Assay, Hercules, CA) and diluted in gel loading buffer. Proteins were separated by SDS-PAGE (Bio-Rad, Hercules, CA, USA), transferred to polyvinylidene (PVDF) membranes and blocked with Tris-buffered saline-Tween buffer (TBST; 150 mM NaCl, 0.05 % Tween-20, and 20 mM Tris-HCl, pH 7.4) containing 5% non-fatty milk or BSA. After blocking, membranes were incubated overnight with primary antibody: anti-puromycin, clone 12D10 (1:2000, Millipore MABE343, RRID:AB_2566826), myosin (1:20000,Sigma M4276, RRID:AB_477190), TRIM63/muscle ring finger 1 (MuRF-1; 1:1000, R&D Systems AF5366, RRID:AB_2208833), phospho-p70 S6 kinase (T389; 1A5; 1:1000, Cell Signaling Technology 9206, RRID:AB_2285392), p70 S6 kinase (1:1000, Cell Signaling Technology 2708, RRID:AB_390722), phospho-AMPK-alpha (T172, 1:2000, Cell Signaling Technology 2535, RRID:AB_331250), AMPK (1:2000, Cell Signaling Technology 23A3, RRID:AB_490795), phospho-Akt (T308, 1:1000, Cell Signaling 5056, RRID:AB_10695743), Akt (1:1000, Cell Signaling Technology 4691, RRID:AB_915783), phospho-FoxO3a (S413, 1:1000, Cell Signaling Technology 8174, RRID:AB_10889562), phospho-FoxO3a (S253, 1:1000, Cell Signaling Technology 9466, RRID:AB_2106674), FoxO3a (1:1000, Cell Signaling Technology 2497, RRID:AB_836876). Membranes were washed for 30 min in TBST and then incubated for 1 h at room temperature in 5% milk-TBST containing secondary antibody. For puromycin measurements, the entire lane was quantified by densitometry.

RNA isolation and quantitative real-time PCR (qPCR). Total RNA was isolated from C2C12 cells using Trizol reagent followed by a chloroform-isopropanol extraction (Invitrogen, USA), and the concentration and quality measured using a NanoDrop 2000 spectrophotometer (Thermo Fisher, Waltham MA). cDNA was synthesized from 100 ng of mRNA using the qScript Supermix reagent kit per manufacturer's instructions (Quantabio, Beverly, MA). Quantitative real-time PCR (qPCR) was performed using iTaq™ Universal SYBR® Green Supermix (BioRad, Hercules, CA) on a CFX96 Touch system (BioRad, Hercules, CA), with the relative mRNA expression calculated using the Ct ($2-\Delta\Delta Ct$) method normalized to GAPDH expression. Primer sequences are provided in Table 1.

Statistics. One- or two-way analysis of variance (ANOVA) models were used to examine differences between groups. For one-way ANOVA, time, pharmacological inhibitor of contraction (e.g., BTS or TTX) or chemotherapy were utilized as between group factors. In two-way ANOVA, chemotherapy and STIM/stretch/time were used as between-group factors. If an interaction effect was noted, pairwise comparisons (Least Significant Difference) were performed to identify the location of group differences. Relationships between variables were determined by linear regression analysis. All data were analyzed using GraphPad Software (v7; La Jolla, CA) and are presented as mean ± standard error of the mean (SEM), unless otherwise stated.

Results

Characterization of C2C12 myotubes and STIM. C2C12 myotubes were differentiated for 7 days before treatment with chemotherapy and/or STIM was started. Under our culture conditions, there was a rapid growth and accumulation of myosin between d5 and d7 (Figure 1A and B), followed by myosin content and myotube size reaching a plateau. At d7, myotubes express myofilament proteins, such as myosin (Figure 1A and 1C), actin (Figure 1A) and α-actinin (data not shown), and organize these proteins into myofilaments (Figure 1C). These myofilaments are functional, as are other components of the excitation-contraction coupling system, as STIM of d7 myotubes provokes intracellular Ca^{2+} cycling (Figure 1D, 1E and 1F; Supplemental Video 1) and contraction (Figure 1E and 1F; Supplemental Video 2). Moreover, calcium release and reuptake were synchronized with the electric pulses, and with contraction and relaxation of the myotube (Figure 1E), respectively. Finally, the degree of fractional shortening tracked with the magnitude of the intracellular Ca^{2+} transient (Figure 1F).

Myotube contractility was quantified using two techniques. The first involved manual selection and automated tracking of two cellular landmarks on myotubes using the edge tracking feature of the IonWizard software. Data from these measurements showed that myotubes contracted with a fractional strain of 3.9 ± 2.7% (n=13 myotubes; open circles in Figure 2C). These measurements, however, suffer bias from manual selection of landmarks and limitations in the precision of edge tracking. To address these limitations, we developed a novel pixel tracking image analysis approach (Figure 2A and 2B) that minimizes these biases. This approach yielded a slightly lower average fractional strain

of 2.6% ± 1.0 (n=17 myotubes; filled circles in Figure 2C). Each technique has strengths and weaknesses, but their results generally agreed. Thus, we calculated an average fractional strain from all data, which was 3.2 ± 2.0% (Figure 2C).

Myotube contraction with STIM was sensitive to modulators of excitation-contraction coupling (ECC) and myosin-actin cycling. Application of the Na^+ channel blocker TTX, which prevents membrane depolarization and all downstream ECC events, eliminated myotube intracellular Ca^{2+} cycling ($P<0.05$) and contraction ($P<0.01$; Figure 2D and Supplemental Figure 2A). Additionally, application of BTS, an inhibitor of myosin-actin interaction/ATPase activity, eliminated contraction ($P<0.01$) without diminishing Ca^{2+} cycling (Figure 2D and Supplemental Figure 2B).

STIM prevents DOX-induced myosin loss. A DOX by STIM interaction effect ($P<0.01$) was observed for myosin content, such that DOX caused a reduction in myosin content ($P<0.01$), whereas 1 h of STIM each day during DOX administration prevented loss of myosin (Figure 3A). STIM alone did not alter myotube myosin content relative to control. To confirm that STIM-induced membrane depolarization and subsequent intracellular Ca^{2+} cycling and contraction were required for this protective effect of STIM, we treated myotubes with TTX, as this eliminates intracellular Ca^{2+} cycling and contraction (Figure 2D and Supplemental Figure 2A). Treatment with TTX prevented the effects of STIM on myosin content (Figure 3B; $P<0.01$ DOX effect).

DOX and STIM effects on protein synthesis and proteolytic mediators. To examine the mechanism by which STIM prevented DOX-induced myosin loss, we measured acute (1 d) modulation of protein synthesis and expression of MuRF1, an E3 ubiquitin ligase responsible for ubiquitination of myosin (7). DOX treatment reduced protein synthesis rate (Figure 3C and 3D; $P<0.01$ DOX effect) and phosphorylation of p70S6 kinase (T389; Figure 3E; $P<0.01$ DOX effect), and STIM was unable to preserve either protein synthesis or p70S6 kinase phosphorylation in DOX-treated cells (Figure 3C, 3D and 3E, respectively).

A DOX by STIM interaction effect was noted for MuRF1 expression ($P<0.01$), such that DOX increased MuRF1 protein ($P<0.01$) and STIM prevented the DOX-induced increase in MuRF1 expression, while STIM alone did not alter MuRF1 (Figure 3F). A DOX by STIM interaction was also noted for FoxO3a phosphorylation (S253) ($P<0.01$), where DOX reduced FoxO3a phosphorylation and this reduction was prevented by STIM ($P<0.01$), while STIM alone did not alter FoxO3a phosphorylation (Figure 3G). At this same time point (1 d), STIM reduced Akt phosphorylation (S308; Supplemental Figure 2A, $P<0.01$ STIM effect), but no DOX or DOX by STIM interaction effects were noted. Because regulation of Akt may be transitory (45), we explored Akt phosphorylation early following the first STIM bout (1 h; Figure 3H). At this time point, we found a DOX by STIM interaction effect ($P<0.05$). Pairwise comparisons showed that DOX+STIM was higher than all other groups (all $P<0.05$, with the exception of $P<0.01$ for DOX).

Effects of other chemotherapeutics on protein synthesis and MuRF1 expression. We explored whether other commonly used chemotherapeutics that cause myotube myosin loss (18) alter protein synthesis and MuRF1 expression similar to DOX at 1 d post-treatment. Results showed that both CIS and TAXOL upregulate MuRF1 expression ($P<0.01$ and $P<0.05$; Figure 4A) and reduce protein synthesis ($P<0.01$ for both; Figures 4B and 4C), similar to DOX ($P<0.01$ for both panels), suggesting a common effect of numerous chemotherapeutics on myotube protein metabolism.

Role of contraction and cell stretch in mediating effects of STIM. To examine if mechanical contraction and myotube shortening explain the protective effects of STIM, we treated myotubes with BTS, an inhibitor of myosin-actin interaction that prevents myotube contraction, but does not disrupt intracellular Ca^{2+} cycling (Figure 2D and Supplemental Figure 2B), during 1 h STIM sessions. BTS blocked the effect of STIM to prevent DOX-induced myosin loss over 3 d of treatment (Figure 5A; $P<0.01$ DOX effect). To clarify whether the effects of STIM were mediated via mechanotransductive signaling, we mechanically stretched cells (5%) for 1 h during DOX or vehicle treatments. The magnitude of the stretch stimulus was chosen to match the relative strain of myotubes induced by STIM (Figure 2C). DOX by stretch interaction effects were found for MuRF1 ($P<0.01$) and FOXO3a (S253; $P<0.05$). Pairwise comparisons showed that, similar to STIM experiments (Figure 3), DOX stimulated MuRF1expression (Figure 5B; $P<0.01$) and reduced FoxO3a phosphorylation (S253; $P<0.05$; Figure 5C), and mechanical stretch prevented these alterations (Figure 5B and 5C). Stretch alone did not

alter MuRF1 expression or FoxO3a phosphorylation. In contrast to STIM, however, mechanical stretch remediated DOX-induced reductions in protein synthesis (Figures 5D and 5E; $P<0.01$ DOX by stretch interaction). These changes in protein synthesis were generally paralleled by altered p70 S6K phosphorylation of (Figure 5F), but the interaction effect was not significant ($P<0.01$ stretch effect and $P<0.01$ DOX effect).

Activation of TRPV1 with CAP does not mimic effects of STIM on myotube myosin content. Recent work identified activation of TRPV1 channels as integral to the muscle anabolic response to mechanical stimuli, that the anabolic response to stress was mimicked by the TRPV1 agonist CAP and that CAP could prevent the catabolic effects of unloading and denervation (26). Because the effects of STIM were dependent on myotube contraction (i.e., mechanotransduction; Figures 3B and 5A) and were mimicked by cell stretch (Figure 5B and 5C), we reasoned that CAP administration may mimic the effects of STIM. Initially, we performed a dose-response experiment to examine the effects of CAP (50 nM to 1 μM) for 3 d (d7-d10) on myotube myosin content. To our surprise, we found no effect of CAP on myosin content at any concentration. We chose a dose of 100 nM CAP because prior work showed that this was sufficient to activate anabolic pathways (e.g., p70S6 kinase; (26)). CAP (100 nM) did not mitigate the effect of DOX administration to reduce myotube myosin protein content (Figure 6B). To further interrogate whether a higher dose of CAP could mimic mechanotransductive signaling and protect against DOX-induced atrophy, we also treated cells with 1 μM CAP. However, this higher dose of CAP similarly did not mitigate the effects of DOX to reduce

myosin content (Figure 6C). Finally, 100 nM CAP showed a DOX by CAP interaction effect ($P<0.01$) on ROS production, but not with directionality that would be expected to mitigate myotube myosin loss. DOX increased ROS production ($P<0.01$), with an additive effect when combined with CAP (Supplemental Figure 3A). We found an effect of DOX ($P<0.01$) to reduce mitochondrial content regardless of CAP treatment (Supplemental Figure 3B).

Myotube mitochondrial ROS production, content and antioxidant gene expression. As the TRPV1 agonist CAP did not mitigate the effects of DOX, we sought other potential mechanisms underlying the protective effects of STIM on myotube myosin content. We recently showed that DOX treatment for 3 d increased myotube mitochondrial ROS production and reduced mitochondrial content, and that mitochondrial targeted anti-oxidant treatment prevented DOX-induced ROS production, mitochondrial loss and reductions in myotube myosin content (18). As exercise modulates mitochondrial biology and redox balance, we examined the effects of STIM on DOX-induced changes in mitochondrial content, ROS production, and antioxidant gene expression. One day of DOX treatment increased ROS production, and these effects were maintained after 3 d of DOX treatment (Figure 7A; $P<0.01$ DOX effect). Unlike ROS production, 1 d of DOX treatment did not reduce mitochondrial content, whereas a reduction ($P<0.01$) was apparent after 3 d of DOX treatment (Figure 7B; $P<0.01$ DOX by time interaction; 3d Control vs. 3 d DOX; $P<0.05$).

A STIM by DOX interaction effect was found on ROS production ($P<0.01$), such that STIM did not prevent DOX-induced upregulation of ROS production at 3 d (Figure 7C). In fact, both STIM groups showed increased ROS production at 3 d compared to non-STIM groups ($P<0.01$; Figure 7C). DOX alone also increased ROS production ($P<0.01$). A STIM by DOX interaction was noted for mitochondrial content ($P<0.05$), as STIM prevented DOX-induced reductions in mitochondrial content (Figure 7D). This effect of STIM to preserve mitochondrial content was accompanied by increased expression of PGC-1α ($P<0.05$ STIM effect; Figure 7E), although no effect of STIM was noted on TFAM expression. DOX upregulated TFAM expression ($P<0.01$ DOX effect).

Energetic insufficiency brought about by DOX-induced mitochondrial loss could contribute to myosin loss via upregulation of AMPK and activation of FoxO3a/MuRF1 (43). In this context, the protective effects of STIM could derive from its ability to maintain mitochondrial content (Figure 7D). To explore this possibility, we evaluated AMPK (T172) and FoxO3a (S413) phosphorylation 1 h and 1 d following the start of treatments. We found no DOX or DOX by STIM interaction effects on AMPK phosphorylation after 1 h (1.5 h post-DOX/1 h post STIM; Supplemental Figure 4A), but there was a STIM effect ($P<0.05$) 1 d following the start of treatments (Figure 7F). Thus, the pattern of AMPK phosphorylation did not match the pattern of changes in mitochondrial content (Figure 7D) or MuRF1 expression (Figure 3F). Interestingly, however, we found that FoxO3a phosphorylation at S413, a site phosphorylated by AMPK (17), 1 d following the start of treatments showed a strong trend ($P=0.06$) towards a DOX by STIM interaction effect. Pairwise comparisons showed that there was an increase ($P<0.05$) in FoxO3a phosphorylation with DOX and that STIM prevented this

increase. To further examine mechanosensitive control of FoxO3a, we examined the effect of mechanical stretch on this phosphorylation site at 1 d post-treatment and found a DOX by stretch interaction effect ($P<0.05$; Figure 7H). DOX increased FoxO3a phosphorylation relative to control and stretch control ($P<0.01$ and $P<0.05$, respectively). However, stretch did not fully remediate the increase in FoxO3a phosphorylation. In fact, FoxO3a phosphorylation was increased in the DOX + Stretch group compared to control ($P<0.05$).

Finally, we examined whether STIM upregulated antioxidant gene expression, as recent studies have suggested this possibility (22), and because we previously showed that mitochondrial targeted anti-oxidant prevents myotube myosin loss with DOX administration (18). DOX ($P<0.05$) and STIM ($P<0.01$) effects were found for expression of the redox-sensitive transcription factor Nrf2, while no effects were observed for KEAP1 (Figure 8A). DOX effects were observed for a number of antioxidant genes, including SOD1, SOD2, CAT and GCLM (all $P<0.01$). DOX by STIM interaction effects (both $P<0.05$) were found for GCLC and GPx1. In the former, DOX increased GCLC expression relative to all other groups ($P<0.05$ to $P<0.01$). In the latter, DOX increased GPx1 expression relative to all other groups ($P<0.05$). There were no effects of STIM observed for any gene, nor any DOX by STIM interaction effects.

Discussion

How muscle contraction protects skeletal muscle against the detrimental effects of chemotherapeutics (33, 40, 52, 53) is unclear. Using *in vitro* muscle contraction models, we show that the atrophic effects of DOX can be prevented by daily bouts of electrically-induced contraction. STIM prevented DOX-induced downregulation of Akt and FoxO3a phosphorylation and increased MuRF1 expression, but was unable to recover protein synthesis. STIM effects were mediated via mechanotransductive signaling, as pharmacological inhibition of myosin-actin interaction/ATPase abolished these effects and mechanical stretch mimicked the effects of STIM. Finally, STIM upregulated PGC-1α and prevented the loss of mitochondrial content. Our findings suggest that muscle contraction counters the catabolic effects of chemotherapy through effects to downregulate proteolysis and preserve mitochondrial content via mechanotransductive signaling pathways.

Contrary to our original hypothesis, the most likely mechanism to explain the beneficial effects of STIM is reductions in proteolysis, as STIM downregulated DOX-induced increases in MuRF1 expression, while protein synthesis was not rescued. How STIM modulates MuRF1 expression is suggested by Akt and FoxO3a phosphorylation data. Prior studies show that muscle stretch and contraction upregulate Akt activation (45), and our data advance these results to show that STIM-induced myotube contraction counters the effects of catabolic mediators, such as DOX, to reduce Akt phosphorylation. FoxO3a transcriptional effectiveness is regulated, in part, by its cytoplasmic-nuclear localization, which is regulated via targeted phosphorylation, particularly by Akt (48).

Correspondingly, increased Akt phosphorylation with STIM was associated with similar preservation of FoxO3a phosphorylation on the Akt site (S253). The effects of STIM to prevent DOX-induced increases in MuRF1 further suggest that these signaling events likely reduced FoxO3a transcriptional activity. Supporting the relevance of our results for *in vivo* skeletal muscle are data showing that electrical stimulation of skeletal muscle prevents disuse-induced atrophy, in part, via downregulation of MuRF1 expression (11).

One strength of our *in vitro* contraction model is that it allows us to discern whether STIM mediates these effects via mechano- or Ca^{2+} chemotransductive signaling pathways. BTS application during 1 h daily STIM bouts prevented the ability of STIM to preserve myotube myosin content in the face of DOX, implicating mechanotransductive pathways in the beneficial effects of STIM. This notion was reinforced by our results from mechanical stretch experiments, which showed similar upregulation of FoxO3a phosphorylation and decreased MuRF1 expression. These findings concur with studies showing that muscle stretch upregulates Akt (2) and reduces nuclear FoxO content and DNA binding (39). Such a mechanism may be operative *in vivo*, as recent studies show that muscle stretch diminished atrophy associated with and experimental intensive care unit stay via downregulation of MuRF1 expression, whereas it did not alter protein synthesis (42). Collectively, these data extend the role of muscle mechanotransductive signaling to include protection against catabolic stimuli, and suggest that this occurs through suppression of proteolysis, rather than preservation or upregulation of protein synthesis (59).

Building on this last point, although we attempted to match mechanical stretch to STIM by utilizing a similar relative strain, the two stimuli differed with respect to their effects on protein synthesis. Unlike STIM, stretch prevented the DOX-induced reduction in protein synthesis. The more pronounced effects of stretch on myotube protein synthesis may relate to the fact that the mechanical stretch stimulus (5%) was slightly higher than the fractional strain during STIM (~3%), as the stretch device has not been validated below 5%, while the response to ≥5% has been previously established. Additionally, STIM imparts its mechanotransductive effects through shortening of the cell while stretch is an elongation stimulus. More specifically, STIM produces stress/strain on myotubes primarily via shortening along their longitudinal axis (Supplemental Video 1), in-line with the orientation of myofilaments (Figure 1C). In contrast, the uniaxial mechanical stretch model we employed would cause multi-axial lengthening and, in turn, stress/strain, because myotubes grow in random orientations relative to the axis of stretch. This may explain differences between the two stimuli, as transverse stretch is more anabolic than uniaxial stretch (23, 34). Extrapolating from these results, one might hypothesize that a more intense mechanical stimulus than that provided by STIM may more effectively counter the deleterious effects of DOX by also preserving protein synthesis (59). Regardless of differences between STIM and stretch conditions on protein synthesis, the similarity in their ability to prevent DOX-induced modifications in Akt/FoxO3a/MuRF1 signaling underscores the importance of exercise-induced downregulation of proteolysis in prevention of chemotherapy-induced atrophy via mechanotransductive pathways.

Numerous mechanotransductive-signaling pathways could mediate the effects of STIM/stretch. We chose to examine the effect of TRPV1 antagonism with CAP because a recent report suggested that activation of TRPV1 with CAP promoted muscle anabolism and was sufficient to prevent unloading- and denervation-induced atrophy (26, 27). Moreover, activation of TRPV1 channels by CAP increases mitochondrial content and function in C2C12 myotubes and mouse muscle *in vivo* (37). However, we found that treatment of myotubes with CAP did not prevent DOX-induced atrophy, nor did it counter DOX-induced oxidant production or mitochondrial loss. Although we used a concentration of CAP (100 nM) shown to promote muscle anabolism/anti-catabolism (26, 27) and mitochondrial adaptations (37), higher concentrations (1 μM) similarly failed to prevent DOX-induced myosin loss. In fact, we found no evidence for effects of CAP on myotube myosin content throughout a range of doses. Thus, our results do not support the contention that the beneficial effects of STIM in our model are mediated via mechanotransductive signaling through activation of TRPV1 channels via CAP.

In light of the role for mitochondrial oxidant production and/or rarefaction in the deleterious effects of DOX and the protective effects of reducing oxidant stress (18), we examined whether the effects of STIM are explained by effects on mitochondrial health/redox balance. STIM preserved mitochondrial content, an effect accompanied by increased PGC-1α expression, a key mediator of mitochondrial biogenesis that is upregulated in response to muscle contraction and that protects against disuse-induced mitochondrial loss and atrophy (32, 47). In keeping with studies overexpressing PGC-1α (5, 31), STIM may prevent DOX-induced atrophy, in part, through effects on mitochondrial dynamics to maintain mitochondria content and/or function. Energetic

insufficiency brought about by mitochondrial loss would be expected to upregulate AMPK, which can phosphorylate FoxO3a (17), leading to transcription of MuRF1. However, the pattern of AMPK phosphorylation (T172) did not mirror the effects of DOX or STIM on Akt/FoxO3a/MuRF1 activation/expression. Despite this, FoxO3a phosphorylation on S413, which is regulated by AMPK, was increased by DOX and reduced to control levels by STIM. In the absence of concordance between AMPK and FoxO3a phosphorylation, we posit that STIM-induced upregulation of PGC-1α may contribute to inhibition of FoxO3a S413 phosphorylation and MuRF1 expression (20, 43, 47) and, in turn, myotube myosin loss.

As prior work from our lab and others suggest that improved redox balance prevents the deleterious effects of DOX (15, 16, 18), the beneficial effects of STIM could also be explained, in part, by its ability to reduce ROS production and/or increase anti-oxidant capacity. Contrary to the former possibility, however, STIM did not diminish the DOX-induced increase in mitochondrial ROS production. In fact, in keeping with prior work (46), STIM-induced myotube contraction increased ROS production (Figure 6C), which may partially account for the effects of STIM to upregulate Akt (19) and PGC-1α (50). Additionally, contrary to recent reports (22), our results showed that no effect on antioxidant gene expression. This may be explained by our milder STIM protocol. In our model, ROS production was increased ~20% over baseline (Figure 7C), whereas, in Horie *et al.* (22), STIM increased ROS production ~100% over baseline. Whether variation in the magnitude of STIM-induced ROS production explains differences in antioxidant gene expression, however, is unclear, as DOX alone increased antioxidant gene expression with a similar, or slightly smaller, increase in ROS production compared

to STIM alone. There were also differences in the timing of STIM between studies. We utilized 1 h of STIM, whereas Horie *et al.* observed an upregulation of antioxidant genes only after 4 h of STIM. Regardless of the explanation for differences between studies, our results suggest that the protective effects of STIM are likely not mediated via either reduced oxidant production or upregulation of antioxidant defenses.

Several limitations of our study should be acknowledged. First, responses in myotube cultures to STIM and DOX may not emulate skeletal muscle *in vivo*. However, myotubes expressed functional myofilaments, contracted in response to STIM and were sensitive to pharmacological inhibitors of ECC and myosin-actin interaction/myosin ATPase similar to *in vivo* muscle. Moreover, adaptations in protein metabolism and signaling were similar to those demonstrated *in vivo* in response to DOX and exercise (33), and these patterns mimicked those in other atrophy models (42) and with the use of electrical stimulation to protect against atrophy *in vivo* (11, 12). Thus, while this model has limitations, it is likely sufficient to study the metabolic and signaling pathways whereby muscle contraction prevents the deleterious effects of chemotherapeutics. Second, static mechanical stretch may provoke different cellular responses than the cyclical contracting myotubes with STIM (28). However, similar results to prevent upregulation of proteolytic signals via FoxO/MuRF1 were found in both models, implicating mechanotransductive signaling in the beneficial effects of STIM.

In summary, the beneficial effects of mechanotransductive signaling in C2C12 myotubes can prevent DOX-induced activation of the FoxO-MuRF1 pathway via downregulation of Akt activation. These effects of STIM may be mediated, in part, via upregulation of

PGC-1α expression, which has been shown to inhibit FoxO3a-induced expression of MuRF1 (47) and upregulates mitochondrial content. These effects of STIM parallel the benefits of neuromuscular electrical stimulation (NMES) in humans to prevent atrophy (12). NMES maintains or improves muscle size and strength in clinical populations (30), and might be a useful exercise modality in cancer patients during chemotherapy, as they are often unable to perform facility-based exercise programs because of fatigue or other logistical/clinical hurdles.

Acknowledgments

We thank Isaac Smith for technical assistance.

Grants

This study was funded by R01 AR065826, R21 CA191532, S10 OD017969 and P30 RR032135. B.G. was funded by a Department of Defense SMART Scholarship ID 2016-85335.

Disclosures

BMP is an employee of IonOptix, LLC. All other authors declare no conflicts of interest

References

1. **Adams SC, Segal RJ, McKenzie DC, Vallerand JR, Morielli AR, Mackey JR, Gelmon K, Friedenreich CM, Reid RD, and Courneya KS**. Impact of resistance and aerobic exercise on sarcopenia and dynapenia in breast cancer patients receiving adjuvant chemotherapy: a multicenter randomized controlled trial. *Breast Cancer Res Treat* 158: 497-507, 2016.

2. **Bodine SC, Stitt TN, Gonzalez M, Kline WO, Stover GL, Bauerlein R, Zlotchenko E, Scrimgeour A, Lawrence JC, Glass DJ, and Yancopoulos GD**. Akt/mTOR pathway is a crucial regulator of skeletal muscle hypertrophy and can prevent muscle atrophy in vivo. *Nat Cell Biol* 3: 1014-1019, 2001.

3. **Bowen TS, Schuler G, and Adams V**. Skeletal muscle wasting in cachexia and sarcopenia: molecular pathophysiology and impact of exercise training. *J Cachexia Sarcopenia Muscle* 6: 197-207, 2015.

4. **Braithwaite D, Satariano WA, Sternfeld B, Hiatt RA, Ganz PA, Kerlikowske K, Moore DH, Slattery ML, Tammemagi M, Castillo A, Melisko M, Esserman L, Weltzien EK, and Caan BJ**. Long-term prognostic role of functional limitations among women with breast cancer. *J Natl Compr Canc Netw* 102: 1468-1477, 2010.

5. **Brault JJ, Jespersen JG, and Goldberg AL**. Peroxisome proliferator-activated receptor gamma coactivator 1alpha or 1beta overexpression inhibits muscle protein degradation, induction of ubiquitin ligases, and disuse atrophy. *J Biol Chem* 285: 19460-19471, 2010.

6. **Brunelli A, Pompili C, Berardi R, Mazzanti P, Onofri A, Salati M, Cascinu S, and Sabbatini A**. Performance at preoperative stair-climbing test is associated with prognosis after pulmonary resection in Stage I non-small cell lung cancers. *Ann Thorac Surg* 93: 1796-1800, 2012.

7. **Cohen S, Brault JJ, Gygi SP, Glass DJ, Valenzuela DM, Gartner C, Latres E, and Goldberg AL**. During muscle atrophy, thick, but not thin, filament components are degraded by MuRF1-dependent ubiquitylation. *J Cell Biol* 185: 1083-1095, 2009.

8. **Dally JW, and Riley WF**. *Experimental stress analysis*. Knoxville, Tenn.: College House Enterprises, 2005, p. 671 p.

9. **de Moor JS, Mariotto AB, Parry C, Alfano CM, Padgett L, Kent EE, Forsythe L, Scoppa S, Hachey M, and Rowland JH**. Cancer survivors in the United States: prevalence across the survivorship trajectory and implications for care. *Cancer Epidemiol Biomarkers Prev* 22: 561-570, 2013.

10. **Dewys WD, Begg C, Lavin PT, Band PR, Bennett JM, Bertino JR, Cohen MH, Douglass HO, Engstrom PF, Ezdinli EZ, Horton J, Johnson GJ, Moertel CG, Oken MM, Perlia C, Rosenbaum C, Silverstein MN, Skeel RT, Sponzo RW, and Tormey DC**. Prognostic effect of weight loss prior to chemotherapy in cancer patients. *Am J Med* 69: 491-497, 1980.

11. **Dirks ML, Hansen D, Van Assche A, Dendale P, and Van Loon LJ**. Neuromuscular electrical stimulation prevents muscle wasting in critically ill comatose patients. *Clin Sci (Lond)* 128: 357-365, 2015.

12. **Dirks ML, Wall BT, Snijders T, Ottenbros CL, Verdijk LB, and van Loon LJ**. Neuromuscular electrical stimulation prevents muscle disuse atrophy during leg immobilization in humans. *Acta Physiol (Oxf)* 210: 628-641, 2014.

13. **Drake JC, and Yan Z**. Mitophagy in maintaining skeletal muscle mitochondrial proteostasis and metabolic health with ageing. *J Physiol* 595: 6391-6399, 2017.

14. **Gao S, and Carson JA**. Lewis lung carcinoma regulation of mechanical stretch-induced protein synthesis in cultured myotubes. *Am J Physiol Cell Physiol* 310: C66-79, 2016.

15. **Gilliam LA, Lark DS, Reese LR, Torres MJ, Ryan TE, Lin CT, Cathey BL, and Neufer PD**. Targeted overexpression of mitochondrial catalase protects against cancer chemotherapy-induced skeletal muscle dysfunction. *Am J Physiol Endocrinol Metab* 311: E293-301, 2016.

16. **Gilliam LA, Moylan JS, Patterson EW, Smith JD, Wilson AS, Rabbani Z, and Reid MB**. Doxorubicin acts via mitochondrial ROS to stimulate catabolism in C2C12 myotubes. *Am J Physiol Cell Physiol* 302: C195-202, 2012.

17. **Greer EL, Oskoui PR, Banko MR, Maniar JM, Gygi MP, Gygi SP, and Brunet A**. The energy sensor AMP-activated protein kinase directly regulates the mammalian FOXO3 transcription factor. *J Biol Chem* 282: 30107-30119, 2007.

18. **Guigni BA, Callahan DM, Tourville TW, Miller MS, Fiske B, Voigt T, Korwin-Mihavics B, Anathy V, Dittus K, and Toth MJ**. Skeletal muscle atrophy and dysfunction in breast cancer patients: role for chemotherapy-derived oxidant stress. *Am J Physiol Cell Physiol* 315: C744-C756, 2018.

19. **Higaki Y, Mikami T, Fujii N, Hirshman MF, Koyama K, Seino T, Tanaka K, and Goodyear LJ**. Oxidative stress stimulates skeletal muscle glucose uptake through a phosphatidylinositol 3-kinase-dependent pathway. *Am J Physiol Endocrinol Metab* 294: E889-897, 2008.

20. **Hindi SM, Mishra V, Bhatnagar S, Tajrishi MM, Ogura Y, Yan Z, Burkly LC, Zheng TS, and Kumar A**. Regulatory circuitry of TWEAK-Fn14 system and PGC-1alpha in skeletal muscle atrophy program. *FASEB J* 28: 1398-1411, 2014.

21. **Holmes MD, Chen WY, Feskanich D, Kroenke CH, and Colditz GA**. Physical activity and survival after breast cancer diagnosis. *JAMA* 293: 2479-2486, 2005.

22. **Horie M, Warabi E, Komine S, Oh S, and Shoda J**. Cytoprotective Role of Nrf2 in Electrical Pulse Stimulated C2C12 Myotube. *PLoS One* 10: e0144835, 2015.

23. **Hornberger TA, Armstrong DD, Koh TJ, Burkholder TJ, and Esser KA**. Intracellular signaling specificity in response to uniaxial vs. multiaxial stretch: implications for mechanotransduction. *Am J Physiol Cell Physiol* 288: C185-194, 2005.

24. **Howlader N, Noone AM, Krapcho M, Garshell J, Miller D, Altekruse SF, Kosary CL, Yu M, Ruhl J, Tatalovich Z, Mariotto A, Lewis DR, Chen HS, Feuer EJ, and Cronin KA**. SEER Cancer Statistics Review, 1975-2012, National Cancer Institute. http://seer.cancer.gov/csr/1975_2011/results_merged/topic_lifetime_risk_diagnosis.pdf.

25. **Irwin ML, McTiernan A, Manson JE, Thomson CA, Sternfeld B, Stefanick ML, Wactawski-Wende J, Craft L, Lane D, Martin LW, and Chlebowski R**. Physical activity and survival in postmenopausal women with breast cancer: results from the Women's Health Initiative. *Cancer Prev Res* 4: 522-529, 2011.

26. **Ito N, Ruegg UT, Kudo A, Miyagoe-Suzuki Y, and Takeda S**. Activation of calcium signaling through Trpv1 by nNOS and peroxynitrite as a key trigger of skeletal muscle hypertrophy. *Nat Med* 19: 101-106, 2013.

27. **Ito N, Ruegg UT, Kudo A, Miyagoe-Suzuki Y, and Takeda S**. Capsaicin mimics mechanical load-induced intracellular signaling events: involvement of TRPV1-mediated calcium signaling in induction of skeletal muscle hypertrophy. *Channels (Austin)* 7: 221-224, 2013.

28. **Ito Y, Obara K, Ikeda R, Ishii M, Tanabe Y, Ishikawa T, and Nakayama K**. Passive stretching produces Akt- and MAPK-dependent augmentations of GLUT4 translocation and glucose uptake in skeletal muscles of mice. *Pflugers Arch* 451: 803-813, 2006.

29. **Jee H, Chang JE, and Yang EJ**. Positive Prehabilitative Effect of Intense Treadmill Exercise for Ameliorating Cancer Cachexia Symptoms in a Mouse Model. *J Cancer* 7: 2378-2387, 2016.

30. **Jones S, Man WD, Gao W, Higginson IJ, Wilcock A, and Maddocks M**. Neuromuscular electrical stimulation for muscle weakness in adults with advanced disease. *Cochrane Database Syst Rev* 10: CD009419, 2016.

31. **Kang C, Goodman CA, Hornberger TA, and Ji LL**. PGC-1alpha overexpression by in vivo transfection attenuates mitochondrial deterioration of skeletal muscle caused by immobilization. *FASEB J* 29: 4092-4106, 2015.

32. **Kang C, O'Moore KM, Dickman JR, and Ji LL**. Exercise activation of muscle peroxisome proliferator-activated receptor-gamma coactivator-1alpha signaling is redox sensitive. *Free Radic Biol Med* 47: 1394-1400, 2009.

33. **Kavazis AN, Smuder AJ, and Powers SK**. Effects of short-term endurance exercise training on acute doxorubicin-induced FoxO transcription in cardiac and skeletal muscle. *J Appl Physiol (1985)* 117: 223-230, 2014.

34. **Kumar A, Chaudhry I, Reid MB, and Boriek AM**. Distinct signaling pathways are activated in response to mechanical stress applied axially and transversely to skeletal muscle fibers. *J Biol Chem* 277: 46493-46503, 2002.

35. **Lakoski SG, Barlow CE, Koelwyn GJ, Hornsby WE, Hernandez J, DeFina LF, Radford NB, Thomas SM, Herndon JE, II, Peppercorn J, Douglas PS, and Jones LW**. The influence of adjuvant therapy on cardiorespiratory fitness in early-stage breast cancer seven years after diagnosis: the Cooper Center Longitudinal Study. *Breast Cancer Res Treat* 138: 909-916, 2013.

36. **Langen RCJ, Schols AMWJ, Kelders MCJM, Wouters EFM, and Janssen-Heininger YMW**. Enhanced myogenic differentiation by extracellular matrix is regulated at the early stages of myogenesis. *In Vitro Cell Dev Biol Anim* 39: 163-169, 2003.

37. **Luo Z, Ma L, Zhao Z, He H, Yang D, Feng X, Ma S, Chen X, Zhu T, Cao T, Liu D, Nilius B, Huang Y, Yan Z, and Zhu Z**. TRPV1 activation improves exercise endurance and energy metabolism through PGC-1alpha upregulation in mice. *Cell Res* 22: 551-564, 2012.

38. **Maddocks M, Murton AJ, and Wilcock A**. Therapeutic exercise in cancer cachexia. *Crit Rev Oncog* 17: 285-292, 2012.

39. **Pardo PS, Lopez MA, and Boriek AM**. FOXO transcription factors are mechanosensitive and their regulation is altered with aging in the respiratory pump. *Am J Physiol Cell Physiol* 294: C1056-1066, 2008.

40. **Powers SK, Duarte JA, Le Nguyen B, and Hyatt H**. Endurance exercise protects skeletal muscle against both doxorubicin-induced and inactivity-induced muscle wasting. *Pflugers Arch* 471: 441-453, 2019.

41. **Prado CMM, Baracos VE, McCargar LJ, Reiman T, Mortzakis M, Tonkin K, Mackey JR, Koski S, Pituskin E, and Sawyer MB**. Sarcopenia as a determinant of chemotherapy toxicity and time to tumor progression in metastatic breast cancer patients receiving capecitabine treatment. *Clin Cancer Res* 15: 2920-2926, 2009.

42. **Renaud G, Llano-Diez M, Ravara B, Gorza L, Feng HZ, Jin JP, Cacciani N, Gustafson AM, Ochala J, Corpeno R, Li M, Hedstrom Y, Ford GC, Nair KS, and Larsson L**. Sparing of muscle mass and function by passive loading in an experimental intensive care unit model. *J Physiol* 591: 1385-1402, 2013.

43. **Romanello V, Guadagnin E, Gomes L, Roder I, Sandri C, Petersen Y, Milan G, Masiero E, Del Piccolo P, Foretz M, Scorrano L, Rudolf R, and Sandri M**. Mitochondrial fission and remodelling contributes to muscle atrophy. *EMBO J* 29: 1774-1785, 2010.

44. **Runte KE, Bell SP, Selby DE, Haussler TN, Ashikaga T, LeWinter MM, Palmer BM, and Meyer M**. Relaxation and the Role of Calcium in Isolated Contracting Myocardium From Patients With Hypertensive Heart Disease and Heart Failure With Preserved Ejection Fraction. *Circ Heart Fail* 10: 2017.

45. **Sakamoto K, Aschenbach WG, Hirshman MF, and Goodyear LJ**. Akt signaling in skeletal muscle: regulation by exercise and passive stretch. *Am J Physiol Endocrinol Metab* 285: E1081-1088, 2003.

46. **Sakellariou GK, Vasilaki A, Palomero J, Kayani A, Zibrik L, McArdle A, and Jackson MJ**. Studies of mitochondrial and nonmitochondrial sources implicate nicotinamide adenine dinucleotide phosphate oxidase(s) in the increased skeletal muscle superoxide generation that occurs during contractile activity. *Antioxid Redox Signal* 18: 603-621, 2013.

47. **Sandri M, Lin J, Handschin C, Yang W, Arany ZP, Lecker SH, Goldberg AL, and Spiegelman BM**. PGC-1alpha protects skeletal muscle from atrophy by suppressing FoxO3 action and atrophy-specific gene transcription. *Proc Natl Acad Sci U S A* 103: 16260-16265, 2006.

48. **Schachter TN, Shen T, Liu Y, and Schneider MF**. Kinetics of nuclear-cytoplasmic translocation of Foxo1 and Foxo3A in adult skeletal muscle fibers. *Am J Physiol Cell Physiol* 303: C977-990, 2012.

49. **Shaw MA, Ostap EM, and Goldman YE**. Mechanism of inhibition of skeletal muscle actomyosin by N-benzyl-p-toluenesulfonamide. *Biochemistry* 42: 6128-6135, 2003.

50. **Silveira LR, Pilegaard H, Kusuhara K, Curi R, and Hellsten Y**. The contraction induced increase in gene expression of peroxisome proliferator-activated receptor (PPAR)-gamma coactivator 1alpha (PGC-1alpha), mitochondrial uncoupling protein 3 (UCP3) and hexokinase II (HKII) in primary rat skeletal muscle cells is dependent on reactive oxygen species. *Biochim Biophys Acta* 1763: 969-976, 2006.

51. **Smith BD, Smith GL, Hurria A, Hortobagyi GN, and Buchholz TA**. Future of cancer incidence in the United States: burdens upon an aging, changing nation. *J Clin Oncol* 27: 2758-2765, 2009.

52. **Smuder AJ, Kavazis AN, Min K, and Powers SK**. Exercise protects against doxorubicin-induced markers of autophagy signaling in skeletal muscle. *J Appl Physiol (1985)* 111: 1190-1198, 2011.

53. **Smuder AJ, Kavazis AN, Min K, and Powers SK**. Exercise protects against doxorubicin-induced oxidative stress and proteolysis in skeletal muscle. *J Appl Physiol (1985)* 110: 935-942, 2011.

54. **Tisdale M**. Mechanisms of cancer cachexia. *Physiol Rev* 89: 381 - 410, 2009.

55. **Toth MJ, Miller MS, Callahan DM, Sweeny AP, Nunez I, Grunberg SM, Der-Torossian H, Couch ME, and Dittus K**. Molecular mechanisms underlying skeletal muscle weakness in human cancer: reduced myosin-actin cross-bridge formation and kinetics. *J Appl Physiol* 114: 858-868, 2013.

56. **Velthuis MJ, Agasi-Idenburg SC, Aufdemkampe G, and Wittink HM**. The effect of physical exercise on cancer-related fatigue during cancer treatment: a meta-analysis of randomised controlled trials. *Clin Oncol* 22: 208-221, 2010.

57. **White JP, Baltgalvis KA, Puppa MJ, Sato S, Baynes JW, and Carson JA**. Muscle oxidative capacity during IL-6-dependent cancer cachexia. *Am J Physiol* 300: R201-R211, 2011.

58. **Yi T, Vick JS, Vecchio MJ, Begin KJ, Bell SP, Delay RJ, and Palmer BM**. Identifying cellular mechanisms of zinc-induced relaxation in isolated cardiomyocytes. *Am J Physiol Heart Circ Physiol* 305: H706-715, 2013.

59. **You JS, Anderson GB, Dooley MS, and Hornberger TA**. The role of mTOR signaling in the regulation of protein synthesis and muscle mass during immobilization in mice. *Dis Model Mech* 8: 1059-1069, 2015.

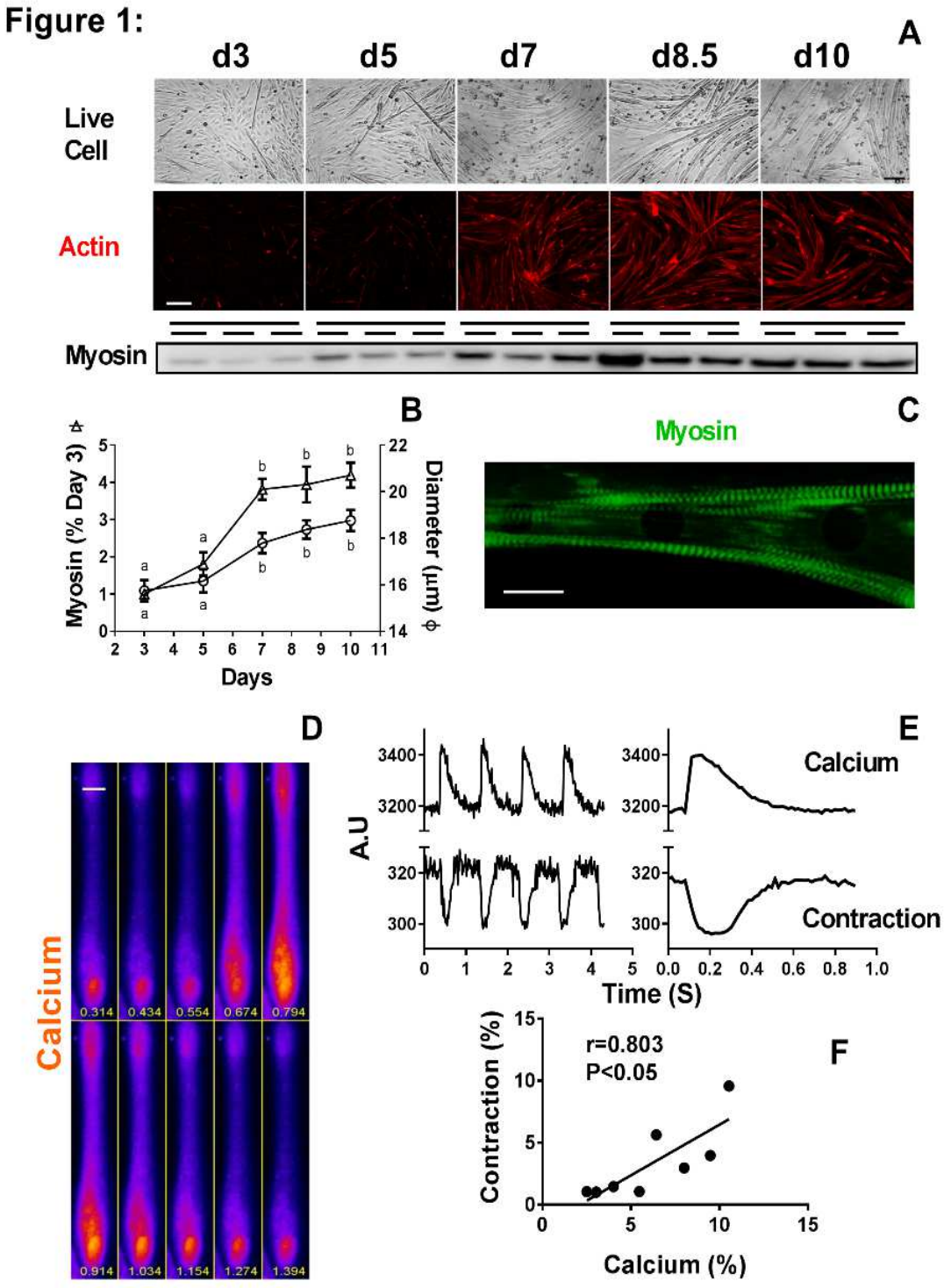

Figure 4.0.1: *Myotube morphology and dynamics*.

Figure 1. C2C12 murine myotube morphology, protein expression, Ca2+ cycling and contraction. (A) Content and morphology of myotubes at d3, d5, d7, d8.5 and d10 are shown (scale bar=25 μm; top panels) and following fixation and staining of actin with TRITC-labeled phalloidin (scale bar=200 μm; middle panels), with corresponding representative gel bands for fast myosin expression at each time point (bottom panel). (B) Average myotube myosin (open triangles) expression and diameters (open circles) are shown for d3 (n=9 and 107), d5 (n=9 and 116), d7 (n=9 and 177), d8.5 (n=9 and 186) and d10 (n=9 and 146, respectively). Differences between days are denoted with different letters (all differences are $P<0.01$ using one-way ANOVA). (C) Myofilament formation in d7 myotube using anti-fast myosin antibody (green) in d7 myotubes (scale bar=25 μm). (D) Pseudo colored images of intracellular Ca2+ cycling in d7 myotube measured by Fluo-2 AM in response to 20V, 12 ms pulses at 1Hz. Time signatures for each image are provided at the bottom of each panel (frame rate=40/s, scale bar=10 μm). The time sequence starts in the upper left corner image, runs from right to left, ending in the bottom right image. (E) Raw Fluo-2 AM fluorescence signal, showing intracellular Ca2+ release (+ excursion) and reuptake (- excursion; top panels), and contractions (- excursion) and relaxations (+ excursion; bottom panels) for several excitation-contraction cycles (left side) and the average of 15 contraction cycles (right side) in response to 20V, 12 ms pulses at 1Hz. (F) Relationship between the relative magnitude of intracellular Ca2+ cycling and contraction measures simultaneously in d7 myotubes (n=8)..

Figure 2:

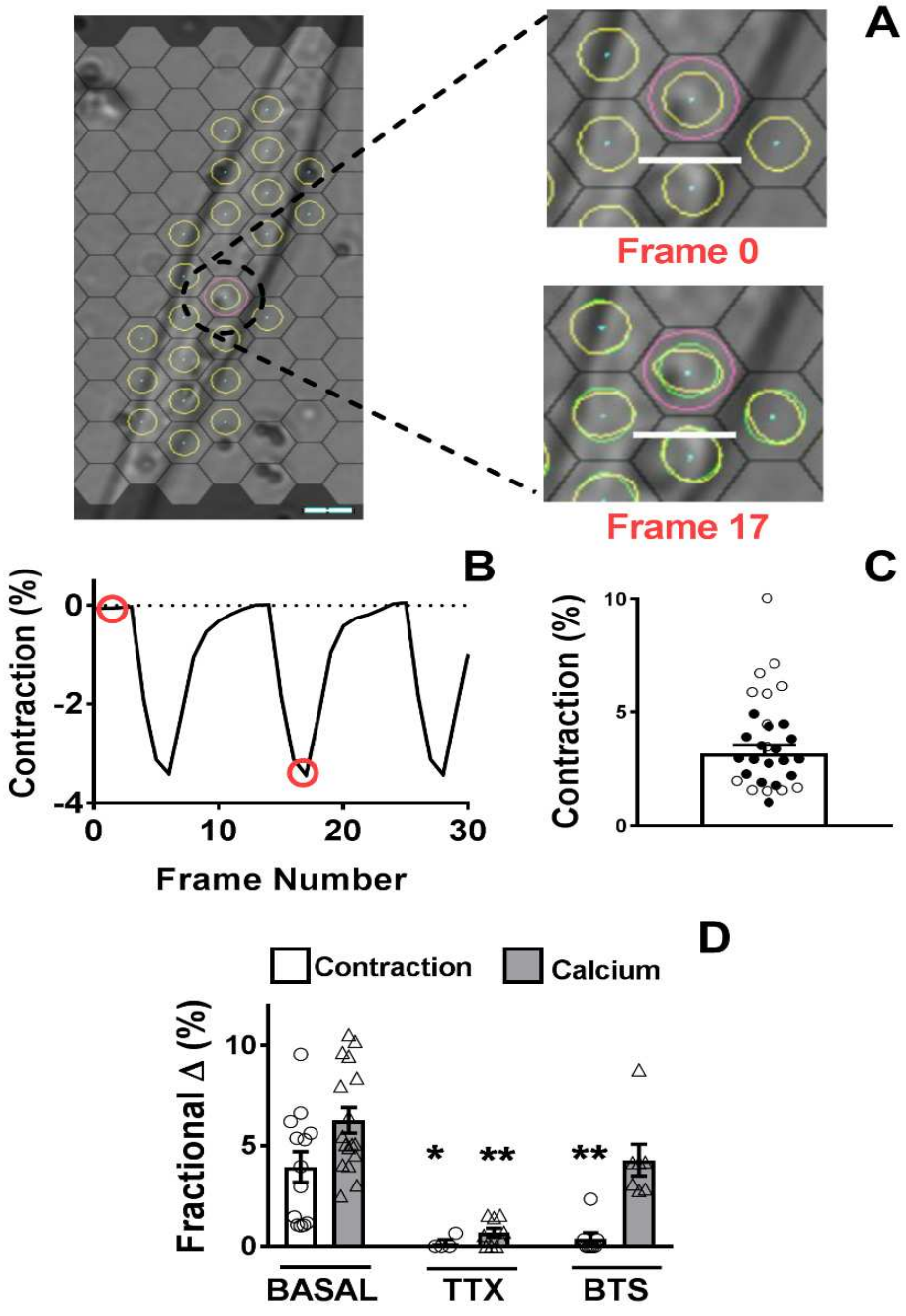

Figure 4.0.2: *Myotube contractile dynamics and intracellular Ca2+ cycling.*

Figure 2. Contractile dynamics and intracellular Ca2+ cycling in d7-d10 C2C12 myotubes. (A) Digital images of C2C12 myotube at rest with hexagonal grid overlay (scale bar=10 μm; left panel). A blowup of the circled hexagon is provided for baseline (Frame 0) and during the peak of contraction (Frame 17) to illustrate contraction monitoring by pixel tracking (right panel). Yellow colored ellipses show trackable image contrast, with green ellipses tracking local pixel strains and negative displacements signifying contractions. (B) Negative displacements of one hexagonal grid showing several contraction cycles. (C) Fractional strain of n=30 myotubes measured with edge tracking of manually selected myotube features/landmarks (open circles) and pixel tracking approach described above and in the Methods section (closed circles). Data are mean ± SEM, with individual data points shown. (D) Average fractional change (Δ) in contraction and intracellular Ca2+ cycling under basal conditions (n=14 and 17, respectively), following TTX (n=8 and 7, respectively) and BTS administration (n=5 and 9, respectively). *, $P<0.05$ and **, $P<0.01$ compared to its respective basal conditions using one-way ANOVA.

Figure 3:

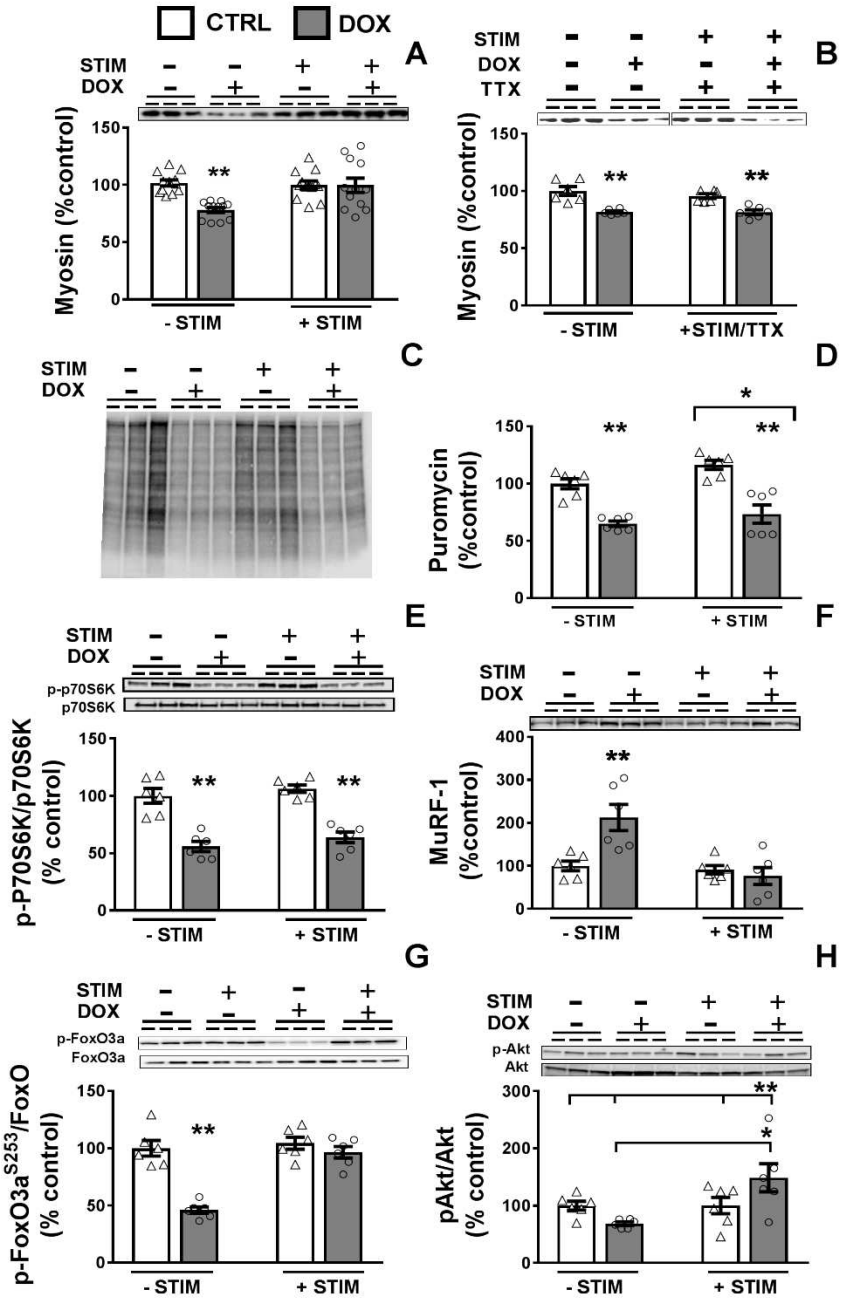

Figure 4 0.3*: STIM molecular changes.*

Figure 3. Effects of doxorubicin (DOX; 0.2 μM; gray bars) or vehicle (DMSO; CTRL; open bars) administration, with or without electrical field stimulation (±STIM; 20V, 12 ms pulses at 1Hz for 1 hr/d), on myotube myosin content, protein synthesis, markers of proteolysis and signaling molecule expression/phosphorylation. (A) DOX administration (3 d) reduces myosin content and STIM prevents this reduction (n=12/bar; $P<0.01$ DOX by STIM interaction). (B) Application of tetrodotoxin (TTX; 10μM) during 1 h STIM bouts mitigates its protective effects on myotube myosin content (n=6/bar; $P<0.01$ DOX effect). (C) Representative gel image of protein synthesis measurements using incorporation of puromycin into protein, as described in Methods section, for a sub-set of replicates in 1 d DOX/STIM experiments. (D) DOX administration (1 d) reduces myotube protein synthesis and STIM fails to prevent this reduction (n=6/bar; $P<0.01$ DOX effect and $P<0.05$ STIM effect). (E) DOX administration (1 d) reduces phosphorylation of p70 S6 kinase (p-p70S6k; S308) and STIM fails to prevent this reduction (n=6/bar; $P<0.01$ DOX effect). (F) DOX administration (1 d) increases MuRF1 expression and STIM prevents this increase (n=6/bar; $P<0.01$ DOX by STIM interaction). (G) DOX administration (1 d) decreased FoxO3a phosphorylation (p-FoxO3a; S253) and STIM prevents this decrease (n=6/bar; $P<0.01$ DOX by STIM interaction). (H) Phosphorylation of Akt (S308) was higher in STIM + DOX compared to all groups ($P<0.05$), except DOX, where $P<0.01$ (n=6/bar; $P<0.05$ DOX by STIM interaction). Representative gel images are shown at the top of panels A, B, E, F, G and H for a subset of replicates. All data are mean ± SEM, with individual data points shown with each bar. *, $P<0.05$ and **, $P<0.01$ in figures to denote either DOX effects (panels B, D and E) or DOX by STIM interaction effects with a single group differing from other groups (panels A, F, G and H) using two-way ANOVA.

Figure 4:

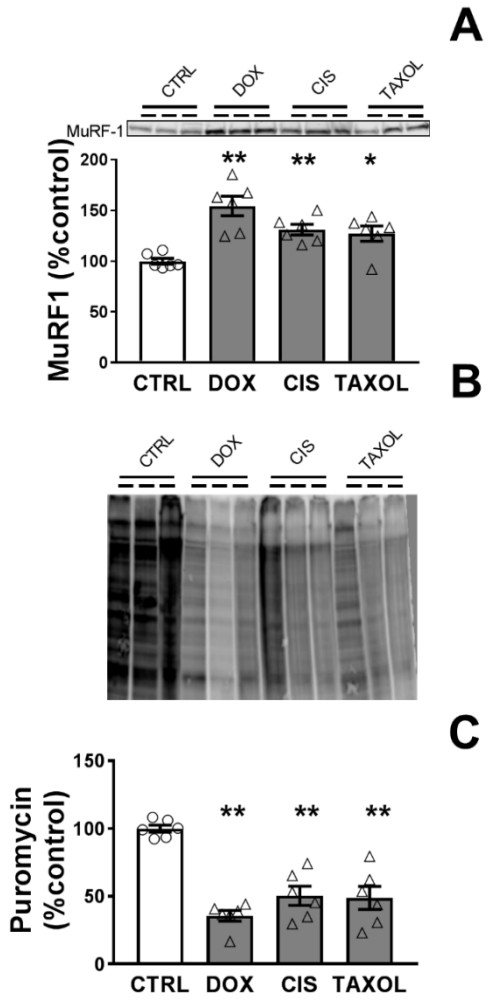

Figure 4.0.4*: Chemotherapy molecular changes.*

Figure 4. Effects of 1 d of administration of common chemotherapeutics: doxorubicin (DOX), cisplatin (CIS) and paclitaxel (TAXOL), or vehicle (DMSO; CTRL; open bars) on MuRF1 expression and protein synthesis. (A) All chemotherapeutics increased MuRF1 expression (n=6/bar). (B) Representative gel image of protein synthesis measurements using incorporation of puromycin into protein, as described in Methods section, for a sub-set of replicates with chemotherapy administration. (B) Administration of all chemotherapeutics reduced myotube protein synthesis (n=6/bar). All data are mean ± SEM, with individual data points shown with each bar. *, $P<0.05$ and **, $P<0.01$ compared to control conditions via one-way ANOVA.

Figure 5:

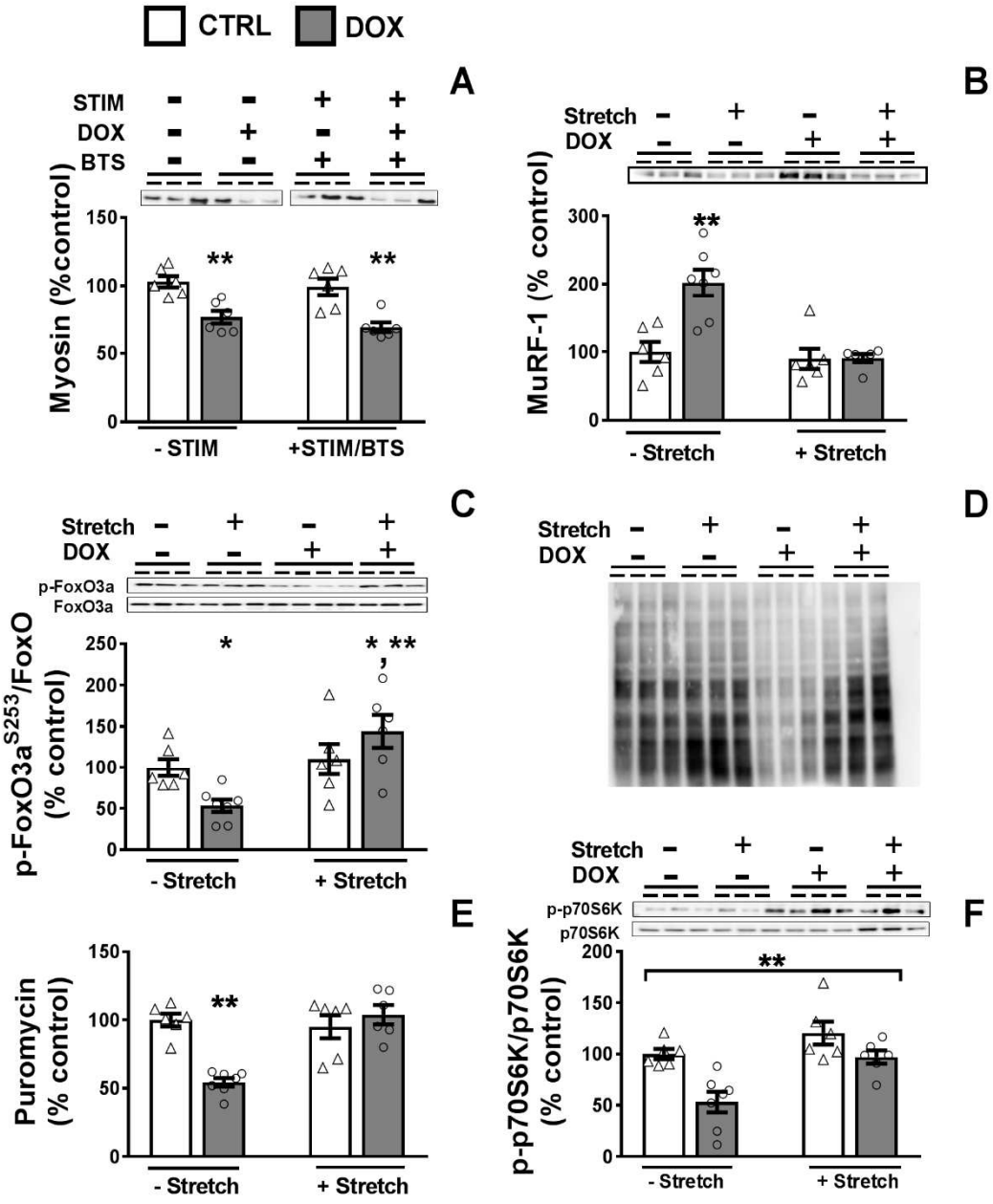

Figure 4.0.5: *Stretch molecular changes.*

Figure 5. Effects of doxorubicin (DOX; 0.2 μM; gray bars) or vehicle (DMSO; CTRL; open bars) administration, with or without electrical field stimulation (±STIM; 20V, 12 ms pulses at 1Hz for 1 h/d) and application of pharmacological inhibitor of myosin-actin contraction/ATPase (1 h/d during STIM), or mechanical stretch (±Stretch; 5% for 1 h/d), on myotube myosin content, protein synthesis and markers of proteolysis. (A) Application of N-benzyl-p-toluene sulphonamide (BTS; 50μM) during STIM bouts over 3 d of DOX administration mitigates the protective effects of STIM on myotube myosin content (n=6/bar; $P<0.01$ DOX effect). (B) Application of 5% stretch prevents increases in MuRF1 expression (n=6/bar, except DOX, where n=7 for all stretch experiments; $P<0.01$ DOX by Stretch interaction) and (C) reductions in phosphorylation of FoxO3a (S253; $P<0.05$ DOX by Stretch interaction) associated with 1 d of DOX administration. For panel C, DOX was lower than all other groups ($P<0.05$) and DOX+Stretch was higher than all groups at $P<0.05$, except DOX, where $P<0.01$. (D) Representative gel image of protein synthesis measurements using incorporation of puromycin into protein, as described in Methods section, for a sub-set of replicates with 1 d DOX administration with or without 5% mechanical stretch for 1 h. (E) DOX administration reduces protein synthesis ($P<0.01$ DOX by Stretch interaction). (F) For phosphorylation of p70 S6 kinase (p-p70S6k; T308), DOX ($P<0.01$) and Stretch ($P<0.01$) effects were significant, but not DOX by Stretch interaction effect. Data are mean ± SEM, with individual data points shown with each bar. *, $P<0.05$ and **, $P<0.01$ for DOX (panel A) or DOX by Stretch interaction effects (panels B, C, E and F), with pairwise differences detailed above, as determined by two-way ANOVA.

Figure 6:

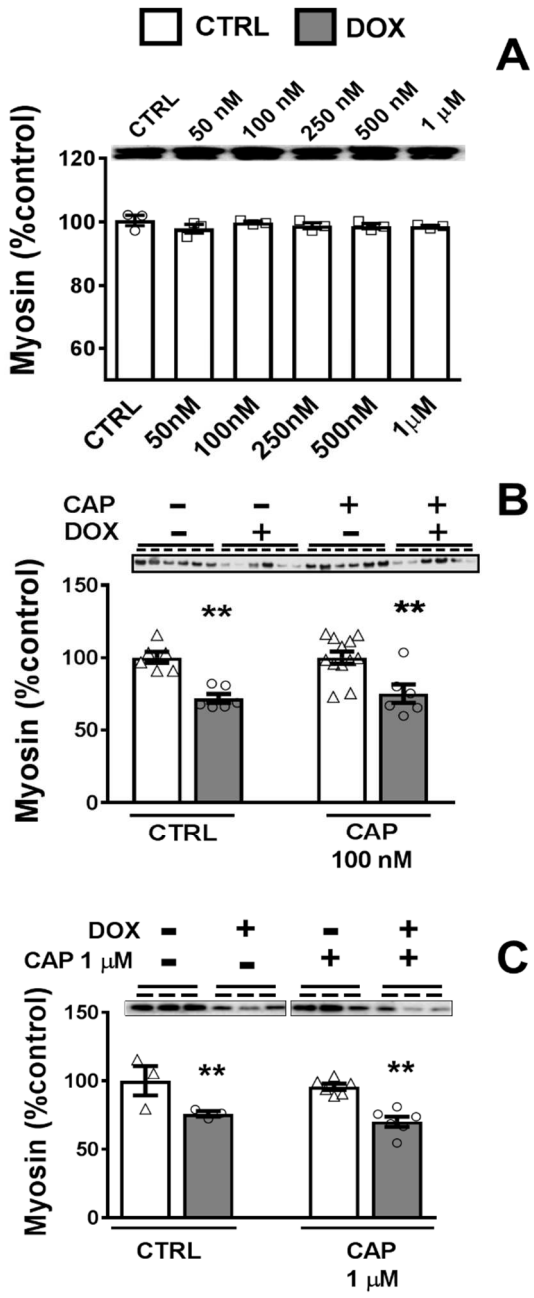

Figure 4.0.6: *Capsaicin effects on myosin content.*

Figure 6. Effects of capsaicin (CAP) or doxorubicin (DOX; 0.2 μM) administration, with or without capsaicin administration (CAP), on myotube myosin content. (A) Dose-response effects of 3 d of CAP administration (50nM, 100nM, 250nM, 500nM, 1μM) vs. DMSO vehicle CTRL on myotube myosin content (n=3/bar; one-way ANOVA). (B) Treatment with CAP (100 nM) was unable to prevent the effect of 3 d of DOX administration to reduce myotube myosin protein content (n=6/bar; $P<0.01$ DOX effect; two-way ANOVA). (C) Similar results were found with administration of high concentration CAP (1 μM) (n=6/bar, except control bars, which are n=3/bar; $P<0.01$ DOX effect; two-way ANOVA). Representative gel images are shown at the top of panels A, B and C for a sub-set of replicates. Note that the representative gel at the top of the panel for a sub-set of replicates was run on a 7.5% gel, which caused separation of myosin isoforms. Both bands were quantified. Data are mean ± SEM, with individual data points shown with each bar. *, $P<0.05$ and **, $P<0.01$ compared to vehicle control (panel A) or to denote DOX effects.

Figure 7:

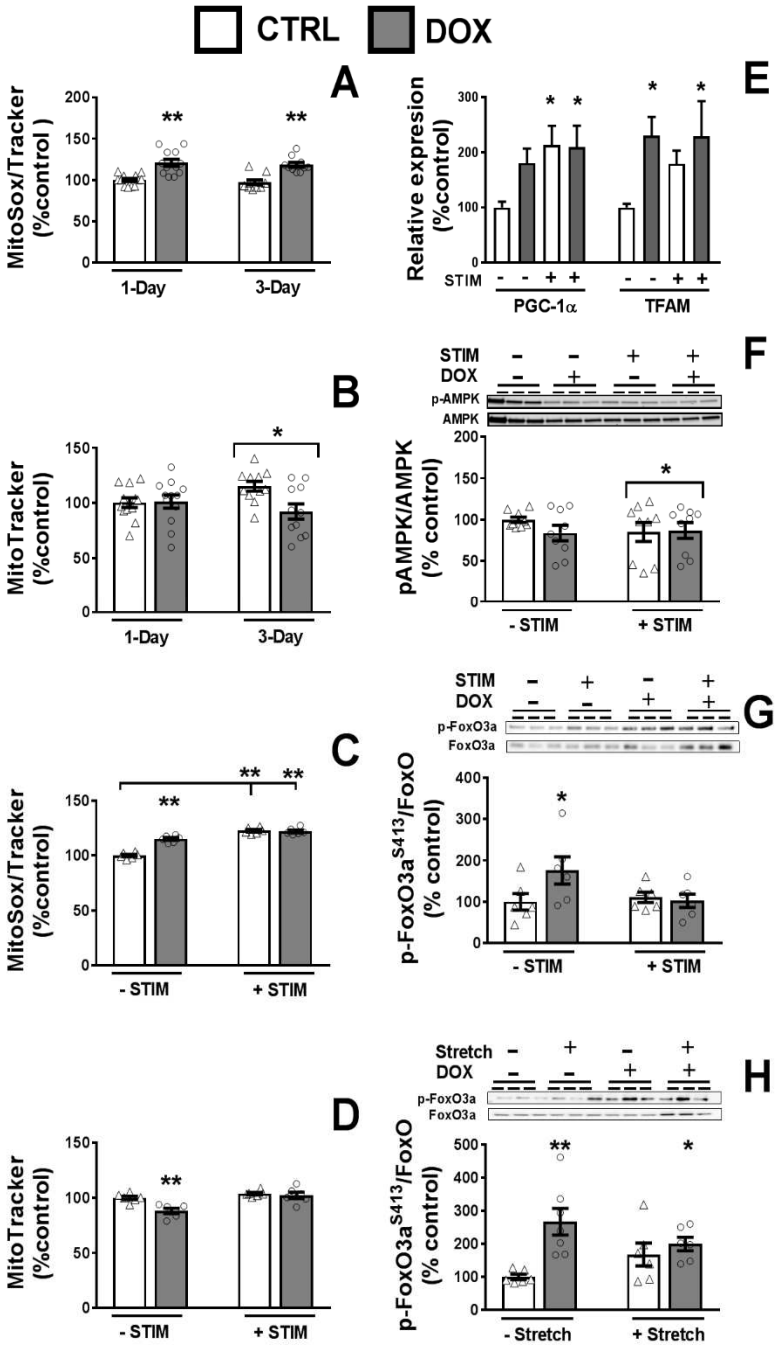

Figure 4.0.7: *STIM induced mitochondrial changes.*

Figure 7. Effects of doxorubicin (DOX; 0.2 μM; gray bars) or vehicle (DMSO; open bars) administration, with or without electrical field stimulation (±STIM; 20V, 12 ms pulses at 1Hz for 1 h/d) or a 5% static stretch, on mitochondrial reactive oxygen species (ROS) production, mitochondrial content and anti-oxidant gene expression. (A) 1 and 3 d of DOX administration increases myotube mitochondrial ROS production per unit mitochondria measured with MitoSox and MitoTracker fluorescent dyes, respectively (n=12/bar; $P<0.01$ DOX effect). (B) 3 d of DOX administration, but not 1 d, reduces myotube mitochondrial content measured by MitoTracker fluorescent dye (n=22/bar; $P<0.05$ DOX by time interaction). (C) DOX ($P<0.01$) and STIM (both STIM and DOX+STIM; $P<0.01$) increased mitochondrial ROS production during 3 d of DOX administration relative to controls (n=6/bar; $P<0.01$ DOX by STIM interaction). (D) STIM prevented DOX-induced mitochondrial loss (n=6/bar; $P<0.05$ DOX by STIM interaction). (E) 3 d of STIM upregulated PGC-1α alone and with DOX treatment ($P<0.05$ STIM effect), whereas DOX increased TFAM (n=6/bar; $P<0.01$ DOX effect). (F) No DOX by STIM interaction for 1 d but a STIM effect ($P<0.05$) was noted on phosphorylation of AMPK (p-AMPK; T172; n=9/bar). (G) DOX administration (1 d) increases FoxO3a phosphorylation (p-FoxO3a; S413; $P<0.05$) and STIM prevents this increase (n=6/bar; $P=0.06$ DOX by STIM interaction). (H) DOX administration (1 d) increases FoxO3a phosphorylation (p-FoxO3a; S413; $P<0.06$ DOX by STIM interaction; $P<0.05$ DOX higher than all other groups). (H) DOX increased FoxO3a phosphorylation (S413; $P<0.05$) and mechanical stretch was unable to fully reduce this increase (n=6/bar, except DOX, where n=7; $P<0.05$ DOX by Stretch interaction). Data are mean ± SEM, with individual data points shown with each bar. *, $P<0.05$; ** and $P<0.01$ for DOX or DOX by time/STIM/Stretch interaction effects, with pairwise differences detailed above using two-way ANOVA.

Figure 8:

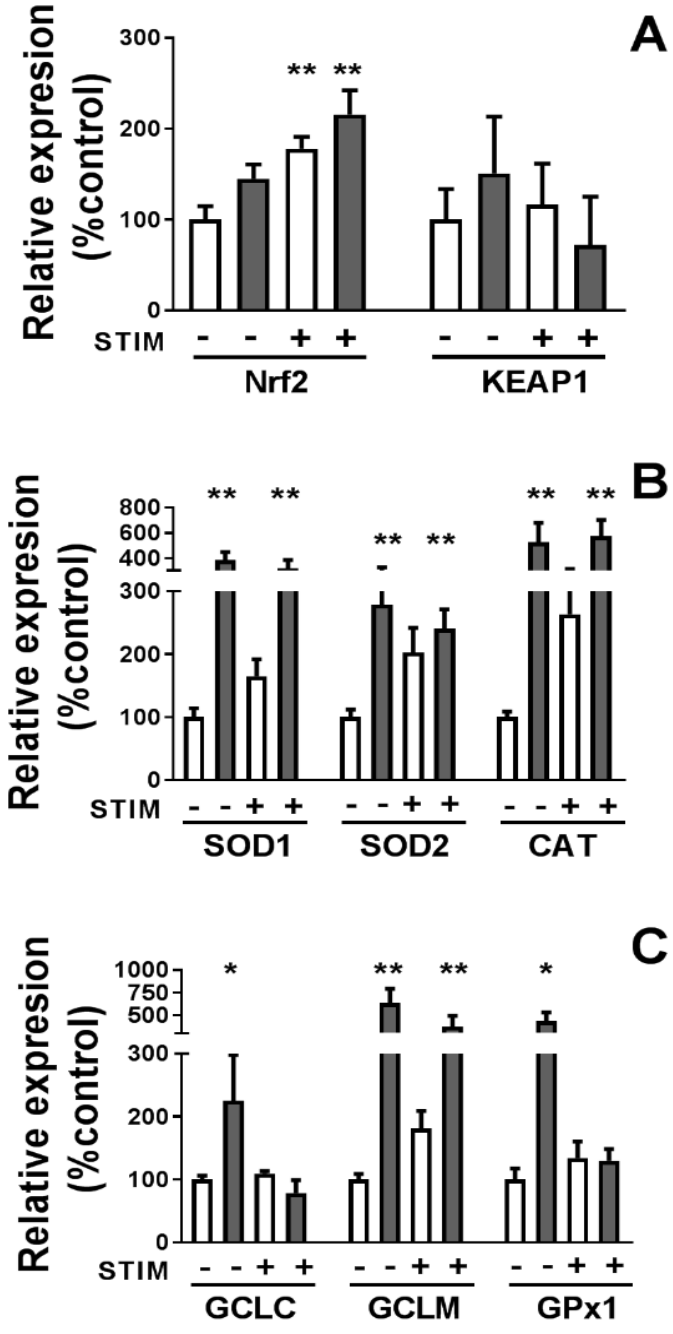

Figure 4.0.8: *Antioxidant enzyme expression.*

Figure 8. Effects of doxorubicin (DOX; 0.2 μM; gray bars) or vehicle (DMSO; open bars) administration, with or without electrical field stimulation (STIM; 20V, 12 ms pulses at 1Hz for 1 h/d), on anti-oxidant gene expression. (A) 3 d STIM and DOX both increased Nrf2 expression (n=6/bar; $P<0.05$ DOX effect and $P<0.01$ STIM effect), but had no effect on KEAP1 (n=3/bar). (B) DOX increased SOD1, SOD2 and CAT expression, independent of STIM (n=6/bar; $P<0.01$ DOX effect). (C) DOX upregulated GCLM, independent of STIM ($P<0.01$ DOX effect) and DOX alone upregulated GCLC and GPx1 ($P<0.05$ DOX by STIM interaction) (n=6/bar). Data are mean ± SEM, with individual data points shown with each bar. *, $P<0.05$ and ** $P<0.01$ for DOX or DOX by STIM interactions, with pairwise comparisons noted above using two-way ANOVA.

Table 4.4: *Primer sequences for gene expression analysis.*

Gene	Forward 5' to 3'	Reverse 5' to 3'
Cat	CGAGGGTCACGAACTGTGTC	GGTCACCCACGATATCACCA
Gclc	ATCTGCAAAGGCGGCAAC	ACTCCTCTGCAGCTGGCTC
Gclm	AGTTGGAGCAGCTGTATCAG	TTTAGCAAAGGCAGTCAAA
Gpx1	CCTCAAGTACGTCCGACCTG	CAATGTCGTTGCGGCACACC
Sod1	ATGGGTTCCACGTCCATCAG	TGCCCAGGTCTCCAACA
Sod2	GAGAATCTCAGTGCTCACTC	GGAACCCTAAATGCTGCCA
Ppargc1a (PGC-1α)	AAACCACACCCACAG GATCAG	TCTTCGCTTTATTGCTCGA
Tfam	CACCCAGATGCAAAACTTTC	CTGCTCTTTATACTTGCTCA
Keap1	TGGCCAAGCAAGAGGAGTTC	GGCTGATGAGGGTCACCAG
Nfe2l2	CGAGATATACGCAGGAGAGG	GCTCGACAATGTTCTCCAGC
GAPDH	ACGACCCCTTCATTGACCTC	TTCACACCCATCACAAACAT

Cat, catalase; Gclc, glutamate cysteine ligase catalytic subunit; Gclm, glutamate cysteine ligase modulating subunit; Gpx1, glutathione peroxidase; Sod1/Sod2, superoxide dismutase 1/2; Ppargc1a, peroxisome proliferator-activated receptor gamma coactivator 1-alpha; Tfam, transcription factor A mitochondrial; Keap1, kelch-like ECH-associated protein; Nfe2l2, nuclear factor erythroid 2 like 2; GAPDH, glyceraldehyde phosphate dehydrogenase.

Supplemental figures

Supplemental Figure 1:

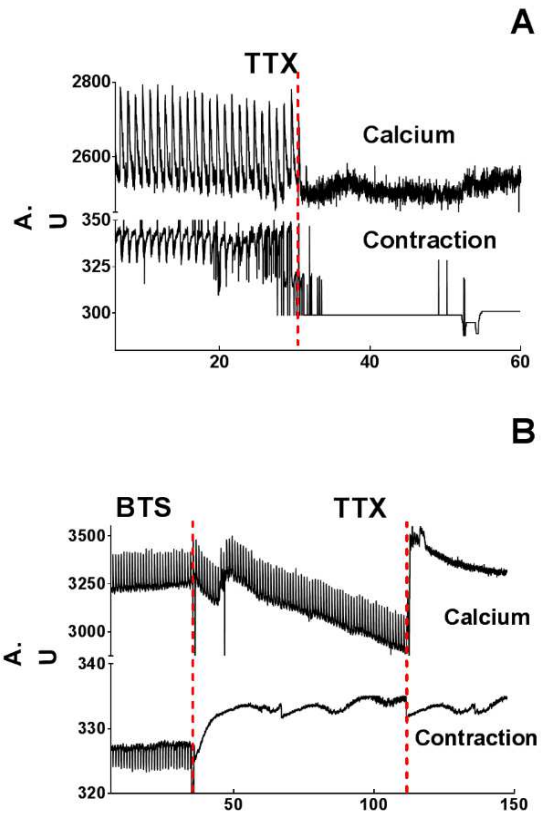

Supplemental Figure 4.0.1*: Raw tracings of Fluo-2 AM-derived intracellular Ca2+ cycling and contractions.*

Supplemental Figure 1. (A) Raw tracings of Fluo-2 AM-derived intracellular Ca2+ cycling (top portion of panel) and contractions (bottom portion of panel) of myotube during 20V, 12 ms STIM at 1Hz and its response to tetrodotoxin (TTX; 10µM; red dotted line), showing cessation of all Ca2+ cycling and contraction. Note that random spikes of contractile activity of the myotube upon application and following TTX are due to debris floating through the field where cellular landmarks were chosen to track contractile activity. These are most prevalent upon initial application of TTX due to fluid shear effects. (B) Raw tracings of Fluo-2 AM-derived intracellular Ca2+ cycling (top portion of panel) and contractions (bottom portion of panel) of myotube during 20V, 12 ms STIM at 1Hz and its response to N-benzyl-p-toluene sulphonamide (BTS; 50µM; 1st red dotted line), followed by tetrodotoxin (TTX; 10µM; 2nd dotted red line). This tracing shows that BTS causes cessation of contraction without altering Ca2+ cycling, with the latter being abolished by TTX.

Supplemental Figure 2:

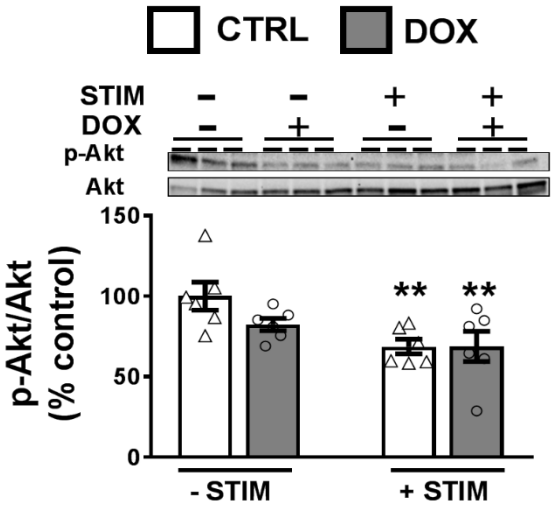

Supplemental Figure 4.0.2: *Effects of 1d doxorubicin treatment on p-Akt.*

Supplemental Figure 2. Effects of 1 d of doxorubicin (DOX; 0.2 μM; gray bars) or vehicle (DMSO; open bars) administration, with or without electrical field stimulation (STIM; 20V, 12 ms pulses at 1Hz for 1 h/d) on Akt phosphorylation. STIM reduced phosphorylation of Akt (p-Akt; T308) after 1 d ($P<0.01$ STIM effect). Representative gel images of p-Akt and total Akt expression are shown at the top of the panel for a sub-set of replicates. All data are mean ± SEM, with individual data points shown with each bar. *, $P<0.05$ for STIM effect by two-way ANOVA.

Supplemental Figure 3:

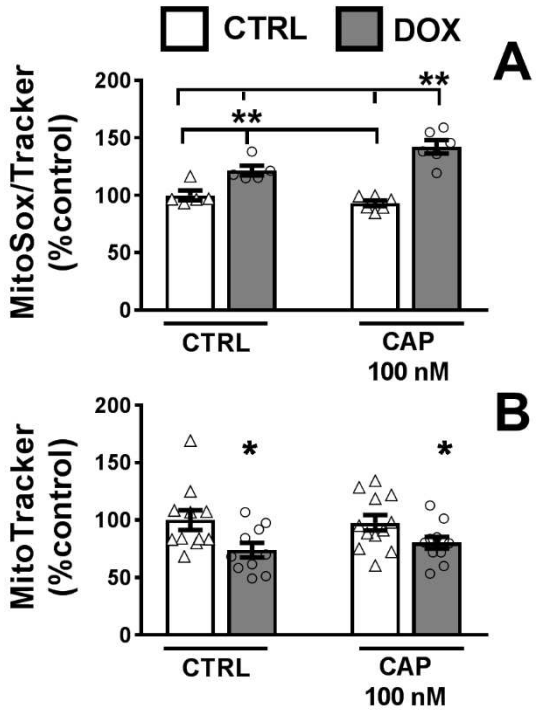

Supplemental Figure 4.0.3: *Effects of DOX and CAP on mitochondria.*

Supplemental Figure 3. Effects of doxorubicin (DOX; 0.2 μM) administration, with or without capsaicin administration (CAP; 100 nM), on mitochondrial ROS production and content. *A*) CAP administration was unable to mitigate the effects of 3 d of DOX administration to increase ROS production (n=6/bar; P<0.01 DOX effect) or (*B*) prevent the loss of mitochondrial content (n=10/bar; P<0.01 DOX effect). All data are mean ± SEM, with individual data points shown with each bar. *, P<0.05 and **, P<0.01 for DOX effects by two-way ANOVA.

Supplemental Figure 4:

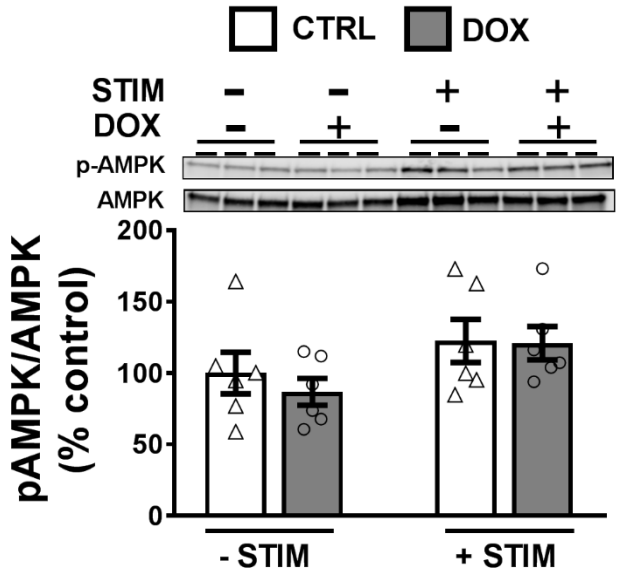

Supplemental Figure 4 0.4: *Effects of 1hr DOX treatment on p-AMPK.*

Supplemental Figure 4. Effects of 1 hour of doxorubicin (DOX; 0.2 μM; gray bars) or vehicle (DMSO; open bars) administration, with or without electrical field stimulation (STIM; 20V, 12 ms pulses at 1Hz for 1 h/d) on AMPK phosphorylation. (A) No effect of DOX or STIM for 1 h was found on phosphorylation of AMPK (p-AMPK; T172). Representative gel images of p-AMPK and total AMPK expression are shown at the top of the panel for a sub-set of replicates. All data are mean ± SEM, with individual data points shown with each bar.

Supplemental videos

Supplementalal Video 1 10um scale.avi

Supplemental Video 4.0.1: *Intracellular Ca2+ cycling in d7 myotube.*

Supplemental Video 1. Pseudocolor video of intracellular Ca^{2+} cycling in d7 myotube measured by Fluo-2 AM in response to 20V, 12 ms pulses at 1Hz. Time signatures for each image are provided at the bottom (frame rate=40/s, scale bar=10 μm).

supplemental video 2 10um scale.avi

Supplemental Video 4.0.2: *Contractile dynamics in d7 C2C12 myotubes.*

Supplemental Video 2. Contractile dynamics in d7 C2C12 myotubes with 2 μm latex beads (1:1000) in response to 20V, 12 ms pulses at 1Hz. Time signatures provided at the bottom (frame rate=10/s, scale bar=10 μm).

CHAPTER 5: COMPREHENSIVE DISCUSSION

Introduction

There is a consensus that cancer-related muscle wasting might be caused by multiple tumor factors, host-derived factors, and cancer treatments (5). Muscle wasting is a primary marker for serious clinical consequences such as physical impairment, increased morbidity, and increased mortality. Although studies into the cause of cancer-related muscle atrophy have spanned multiple decades, clinical trials addressing them individually have proven ineffective (1, 8, 9), and little is known about the mechanisms and effects of various cancers and their treatments on skeletal muscle. The overall aim of this dissertation was to identify and understand the mediators of muscle wasting in cancer patients and to examine the role of muscle contraction to help maintain muscle size and function. To address these questions we studied two different populations of cancer patients (lung and breast cancer) to tease out the effects of tumor-derived factors or chemotherapeutics to cause atrophy and used an *in vitro* skeletal muscle system to elucidate the mechanism by which muscle contraction may be beneficial.

Regulation of skeletal muscle mass

In the first part of this dissertation, our goal was to identify and understand the mediators of muscle wasting in cancer patients. We utilized an *in vitro* skeletal muscle system to examine the effects of tumor factors from patients and chemotherapies used in treatment to directly affect skeletal muscle mass. Our methodology involved treating

myotubes differentiated to the point that they showed stable myosin contact/myotube size, expressed myofilament proteins and arranged these into functioning sarcomeres. Of note, studies in the cancer cachexia field that have examined tumor-related factors using myotube cultures often compare conditioned media treated cells with non-treated controls. We found these studies insufficiently controlled and added dilution and non-cancer cell controls.

When we examined murine and patient tumor conditioned media (CM) to promote atrophy and affect mitochondrial health on fully mature myotubes, we found no effect of the CM. Collectively, our results argue against the hypothesis that there is a direct effect of tumor derived factors to cause atrophy and/or perturb mitochondrial health. We could recapitulate findings from other labs that tumor-conditioned media caused reduced myotube myosin content, but our dilution and non-cancer cell controls suggest that these results are most likely related to CM inhibiting myotube growth.

In breast cancer patients undergoing chemotherapy treatment, we observed reduced single muscle fiber CSA, mitochondrial content and increased oxidative stress. Cancer patients are often treated with chemotherapy, whose side effects are at times underestimated. Applying our *in vitro* model to test the effects of chemotherapy to directly affect skeletal muscle cells, we found similar phenotypes of muscle atrophy, mitochondrial rarefaction and increased ROS production. Moreover, diminishing mitochondrial ROS stress with a mitochondrial-targeted anti-oxidant was sufficient to prevent myotube atrophy.

There are limitations of our cell culture findings in both of the aforementioned studies. Thus, we have outlined several future experiments to address these limitations.

For conditioned media experiments, the bolus treatment protocol that we used does not simulate conditions found *in vivo,* where muscle is exposed to ongoing kinetics of constant tumor secretion of factors that could influence muscle. This could be remedied by the application of a "trasnwell" co-culture model, where human tumor cells are placed in the same chamber as mature myotubes allowing the media to be shared between both cell types. The primary outcomes for this experiment would be myosin content, mitochondrial ROS and mitochondrial content. However, this constant and high concentration of CM may provide an exaggeratedly high level of tumor-related factors for muscle, similar to animal models, where tumors exceed 5% of their mass before cachexia is seen. Thus, while this type of transwell approach may better reproduce the kinetics of tumor secreted factors, it still suffers the problem of supraphysiological doses of those factors.

Perhaps more importantly, CM from a monolayer of cultured tumor cells may not adequately reflect tumor production of secreted factors to cause the phenotype seen in xenograft models (2-4). That is, tumors exist in a three-dimensional environment *in vivo* and there is evidence that monolayers of cells do not reflect the behavior of solid, 3D tumors. Cancer organoids are cancer cells grown in a 3D system with near-physiological architectures that are reported to retain specific functions of the parent tumors. Using this technique of growing tumor cells *in vitro,* lung cancer patients biopsied cells can be grown into organoids and the CM collected for the bolus experimental model on mature C2C12 myotubes. This organoid system can also be applied to recapitulate drug responses of

tumors when treated with cisplatin (CIS), paclitaxel (TAXOL) or doxorubicin (DOX), the CM can be collected for treatment of mature C2C12 myotubes. The primary outcomes for these sets of experiments would be myotube myosin content and mitochondrial health. Use of organoid cultures of human tumors would provide the most clinically relevant system for preclinical evaluation of the effects of tumor-related factors on myotubes (12, 14).

As previously mentioned, non-muscle host factors may contribute to muscle wasting in cancer patients, as skeletal muscle atrophy in pre-clinical models are often associated with heightened inflammatory mediators and upregulation of inflammatory signaling in skeletal muscle. This is also characterized by recruitment of immune cells to skeletal muscle. The origins of cytokines are still debated, but an alternative hypothesis in the field is that tumor-derived factors may contribute to muscle wasting by inciting host immune responses (6). Indeed, the presence of the tumor itself causes the body to produce an acute phase response (11), and macrophages appear to be the source of some of the principal mediators of cachexia, such as TNF-α or IL6 (7). Conducting *in vitro* co-culture experiments such as described by Venter *et al* (13), to investigate the effects of stimulating macrophages with tumor conditioned media on cultured muscle could be used to increase our understanding of these cellular interactions The communication between nonmyogenic cells, such as macrophages and fibroblasts are crucial for skeletal muscle (13). Designing a co-culture experiment in which macrophages are in close proximity to mature C2C12 myotubes and treated with either standard patient CM (monolayer) or organoid CM may yield results that better emulate the phenotype described in patients, with primary outcomes of myosin content and mitochondrial health. This same

experiment could also be conducted with tumor cells that have been activated with chemotherapy, where the activated CM is used to treat the co-culture system.

A primary outcome for many of these proposed experiments have been mitochondrial health. Mitochondria sustain the energy required for normal muscle homeostasis. However, the role of mitochondria extends beyond energy homeostasis in muscle. With our model, we were able to inhibit the negative effects of DOX and TAXOL to cause atrophy, mitochondrial ROS and mitochondrial loss, by treating the mature myotubes with the antioxidant compound MitoQ. The coupling mechanisms between redox homeostasis, mitochondrial morphology and muscle size are still unclear. Mitochondria are able to change their morphology by undergoing either fusion to form elongated interconnected networks, or fission to generate fragmented disconnected mitochondria. Healthy mitochondrial dynamics are required for mitochondrial biogenesis via PGC-1a, for the quality-control of the organelles, and may play a role in apoptosis, redox homeostasis and mitochondrial dynamics. Designing experiments that identify and test these important mediators will be important to further elucidate how chemotherapy-induced modifications in mitochondrial content and function contribute to muscle atrophy during cancer treatment. Such experiments would include treating mature myotubes with DOX or other oxidants looking for the activation, expression and content of mitochondrial morphology regulators such as Optic Atrophy 1 (Opa1, fusion) which is inhibited by S-nitrosylation and increased by denitrosylation, and Dynamin-1-related protein (Drp1, Fission) whose activity is regulated by ROS via S-nitrosylation, leading to increased fission. Increased mitochondrial fission has been linked with skeletal muscle atrophy and experiments that test for this connection may provide more insight into the

interplay between ROS, mitochondrial fission/loss and skeletal muscle health. One such experiment would be to utilize a pharmacological inhibitor of Dpr1 such as mdivi-1 in cultured muscle when treated with DOX to prevent atrophy by reducing mitochondrial fission. The primary outcomes of these experiments would be myosin content and Drp1 content/phosphorylation/RNA, along with mitochondrial ROS measurements. A genetic approach can also be used. Using the C2C12 cell line, it is possible to generate a Drp1 knockdown (KD) model in mature myotubes. This KD model can then be tested with chemotherapies such as DOX, and evaluated for protection of mitochondrial health and further validated in an *in vivo* knockout model along with western blots for patients Drp1 for confirmation of phenotype clinically. Similar experiments can be performed with the overexpression of PGC-1α, if mitochondrial biogenesis is important, it should prevent the deleterious effects of DOX and other chemotherapies

Exercise

We established an experimental protocol to simulate some of the exercise-induced changes in gene and protein expression in cultured muscle cell using myotube contraction via electrical stimulation (STIM). However, three bouts of STIM on cultured cells may not completely reflect the complexity and time-dependent adaptation of skeletal muscle to exercise as *in vivo*. The determination of protein levels, enzymatic activity and functional read-outs might differ between the cells in culture and muscle *in vivo*. Testing these effects in an *in vivo* model may further support the results from the cell culture experiments. Using standard wildtype mice experiments with DOX can be performed with STIM on one leg, with the contralateral leg serving as a control. The outcomes for

these experiments would be muscle size measured by CSA, mitochondrial ROS measured by Amplex red assay, and mitochondrial content measured with electron microscopy. Secondary outcomes would include western blots for mitochondrial dynamics (Drp1, OPA1), antioxidant enzymes and PGC-1α content. We can further apply this in patients by utilizing neuromuscular electoral stimulation (NMES) with protocols informed by cell and animal studies, using the same metrics for primary and secondary outcomes.

In any case, the cell culture experimental system allows the delineation of molecular mechanisms important for the contracting muscle fiber that cannot be performed on muscle *in vivo*. In the future, this model system will have to be adapted and refined such as with co-cultures, but also importantly, with validation of the mechanical stress stimulus we previously reported. This would be achieved by applying a cyclical mechanical stretch with or without DOX matching the *in vitro* STIM protocol of 1Hz for 1 hour, but limiting the strain to 3.5% as reported by our studies. With this stretch system we can further delve into the mechanisms of the mechanical forces involved in maintaining muscle mass.

Calcium signaling has been reported as an important mediator of muscle health. Our studies with STIM has diminished their importance in this model of mechanotransduction with the negative results of the transient receptor potential cation channel subfamily V member 1 (TrpV1) agonist capsaicin and the BTS experiments. However, stretch activated calcium channels have also been implicated as an important signaling aspect of mechanical stretch. Using pharmacological inhibitors, such as GsMTX4, of these stretch activated calcium channels, might help rule out their importance, by showing no

inhibition in the effects of STIM or stretch to prevent atrophy. Further, applying BTS during stretch may solidify the importance of mechanical activation of mechano sensitive proteins by blocking the anti-atrophic effects of stretch.

Calcium release occurs during excitation-contraction coupling (ECC) and our data shows that STIM works via this system to induce contracture in cultured muscle cells. However, specifically targeting the main channel of calcium release in the cells has not been fully characterized. Ryanodine receptors (RyRs) are an important component of ECC that can be targeted. There are evidence that RyR agonist can be utilized to induce calcium and have been linked with anti-atrophic effects. We suspect this is due to coupled contractures, and utilizing RyR agonist Caffeine at 4mM and 4-Chloro-m-cresol (4CmC) we can elucidate these mechanisms. With the IonOptix system that we have previously demonstrated, experiments can be performed to test the calcium and contracture dynamics of these agonists on C2C12 mature myotubes with and without DOX. We can also apply inhibitors of ECC such as the myosin ATPase inhibitor BTS and the sodium channel blocker TTX as previously described, to validate the effects to caffeine and 4CMC to target the RyR and the importance of contracture in their beneficial effects. The primary outcomes for these experiments would be myotube myosin content and mitochondrial health with the secondary outcomes of mitochondrial fusion and fission dynamics.

A common phenotype of cancer patients is muscle weakness and fatigue. Muscle atrophy and intrinsic weakness likely contribute to these symptoms, but the nature of these muscle functional deficits remain unknown. Our lab has collected data showing that

single muscle fibers from cancer patients are not inherently weaker than matched controls. Thus, impaired myofilament contractility does not appear to be the cause of weakness. An alternative mediator is impairments in ECC, in particular secondary to chemotherapy-induced ROS production. We can delve deeper into the effects of chemotherapy to perturb calcium responses and contracture dynamics. Overnight treatment with chemotherapies like DOX (0.2μM to 1μM) on mature myotubes might yield a reduction in response to STIM or a reduction in the fractional strain of the contracture. Moreover, we can then examine the importance of mitochondrial health or ROS to affect these calcium and contracture dynamics. Using the previously described MitoQ at 0.25μM, to inhibit mitochondrial ROS, during DOX treatment may prevent any deleterious effects of DOX to alter myotube ECC and/or contracture dynamics. Using the C2C12 cell line, it is possible to generate a PGC-1a knockdown (KD) model in mature myotubes. This KD model can then be tested with chemotherapies such as DOX, during electrical stimulation, and evaluated for any loss of anti-atrophic effects of exercise via loss of mitochondrial health and further validated in an *in vivo* knockout model along with western blots for patients Drp1and Pgc-1a for confirmation of phenotype clinically.

The studies discussed have been designed around the murine C2C12 skeletal muscle cell line. This is a transformed cell line that may not fully match *in vivo* muscle, therefore conducting all these studies on primary human muscle cells may provide a clearer picture of the changes in patient muscle. There are commercially available Human Skeletal Muscle Myoblasts, which can be used as a consistent control cell line to conduct all experiments mentioned. However, the most relevant option is to use primary human myoblasts from muscle biopsies which are a valuable resource for modeling human

muscle disease *in vitro*. Human skeletal muscle biopsies often contain extensive populations of non-myogenic cells, such as adipocytes and fibroblasts, adding to the complexity of isolating primary cells from patients. Thus, developing proper isolation techniques such as those published by Spinazzola *et al* (10) will be important before they can be utilized for modelling studies. Besides exercise, molecules acting as exercise mimetics might also be of interest in the attempt to counteract the adverse side effects of chemotherapeutical agents. This would most likely occur when such adverse effects are mostly reversible and mainly involve preventing mitochondrial impairment.

Conclusion

Performing clinical trials in cancer patients with muscle wasting is very challenging and high drop-out rates are common. Well-designed preclinical models still have a vital role to play in screening different potential myoprotective treatments and guiding the selection of the best candidates for more detailed clinical testing. Experiments using cultured myotubes are a key step in investigating the direct effects of catabolic agents and to determine the protective effect of anti-muscle atrophy treatments. Typically, experimental outcomes employ measurements of myotube morphology (e.g., fiber diameter) and we have expanded this to include myosin content and the expression levels of anabolic and catabolic mediators in muscle. Several approaches to improve the modeling of muscle in an *in vitro* setting have been described. These have included the use of two or three-dimensional systems, co-culturing techniques, and use of electrical stimulation. Ideally, attempts would be made to test myotube responses that combine several features of the *in vivo* milieu to study disease-related muscle atrophy.

Cancer-related skeletal muscle wasting is a complex syndrome with multiple contributing factors and signaling pathways. Increasing our knowledge of the mechanisms involved in muscle wasting, and how mechanical stimulation prevents this will help point the way to developing treatments. This work makes important contributions to the field by informing the direction and design of future clinical interventions in the management of cancer-related muscle atrophy. In conclusion, our findings have uncovered previously unknown relationships that will inform clinical best practice and improve patient outcome.

References

1. **Argiles JM, Lopez-Soriano FJ, Stemmler B, and Busquets S**. Novel targeted therapies for cancer cachexia. *Biochem J* 474: 2663-2678, 2017.

2. **Au ED, Desai AP, Koniaris LG, and Zimmers TA**. The MEK-Inhibitor Selumetinib Attenuates Tumor Growth and Reduces IL-6 Expression but Does Not Protect against Muscle Wasting in Lewis Lung Cancer Cachexia. *Front Physiol* 7: 682, 2016.

3. **Blackwell TA, Cervenka I, Khatri B, Brown JL, Rosa-Caldwell ME, Lee DE, Perry RA, Jr., Brown LA, Haynie WS, Wiggs MP, Bottje WG, Washington TA, Kong BC, Ruas JL, and Greene NP**. Transcriptomic analysis of the development of skeletal muscle atrophy in cancer-cachexia in tumor-bearing mice. *Physiol Genomics* 50: 1071-1082, 2018.

4. **Brown JL, Lee DE, Rosa-Caldwell ME, Brown LA, Perry RA, Haynie WS, Huseman K, Sataranatarajan K, Van Remmen H, Washington TA, Wiggs MP, and Greene NP**. Protein imbalance in the development of skeletal muscle wasting in tumour-bearing mice. *J Cachexia Sarcopenia Muscle* 9: 987-1002, 2018.

5. **Fearon K, Strasser F, Anker SD, Bosaeus I, Bruera E, Fainsinger RL, Jatoi A, Loprinzi C, MacDonald N, Mantovani G, Davis M, Muscaritoli M, Ottery F, Radbruch L, Ravasco P, Walsh D, Wilcock A, Kaasa S, and Baracos VE**. Definition and classification of cancer cachexia: an international consensus. *Lancet Oncol* 12: 489-495, 2011.

6. **Gordon JN, Green SR, and Goggin PM**. Cancer cachexia. *QJM* 98: 779-788, 2005.

7. **Langstein HN, and Norton JA**. Mechanisms of cancer cachexia. *Hematol Oncol Clin North Am* 5: 103-123, 1991.

8. **Mantovani G, and Madeddu C**. Cancer cachexia: medical management. *Support Care Cancer* 18: 1-9, 2010.

9. **Patel JD, Pereira JR, Chen J, Liu J, Guba SC, John WJ, Orlando M, Scagliotti G, and Bonomi PD**. Relationship between efficacy outcomes and weight gain during treatment of advanced, non-squamous, non-small-cell lung cancer patients. *Ann Oncol* 27: 1612-1619, 2016.

10. **Spinazzola JM, and Gussoni E**. Isolation of Primary Human Skeletal Muscle Cells. *Bio Protoc* 7: 2017.

11. **Tisdale MJ**. Tumor-host interactions. *J Cell Biochem* 93: 871-877, 2004.

12. **Tsai S, McOlash L, Palen K, Johnson B, Duris C, Yang Q, Dwinell MB, Hunt B, Evans DB, Gershan J, and James MA**. Development of primary human pancreatic cancer organoids, matched stromal and immune cells and 3D tumor microenvironment models. *BMC Cancer* 18: 335, 2018.

13. **Venter C, and Niesler C**. A triple co-culture method to investigate the effect of macrophages and fibroblasts on myoblast proliferation and migration. *Biotechniques* 64: 52-58, 2018.

14. **Xu H, Lyu X, Yi M, Zhao W, Song Y, and Wu K**. Organoid technology and applications in cancer research. *J Hematol Oncol* 11: 116, 2018.

COMPREHENSIVE BIBLIOGRAPHY

Adams, S. C., Segal, R. J., McKenzie, D. C., Vallerand, J. R., Morielli, A. R., Mackey, J. R., . . . Courneya, K. S. (2016). Impact of resistance and aerobic exercise on sarcopenia and dynapenia in breast cancer patients receiving adjuvant chemotherapy: a multicenter randomized controlled trial. *Breast Cancer Res Treat, 158*(3), 497-507. doi:10.1007/s10549-016-3900-2

Al-Nassan, S., & Fujino, H. (2018). Exercise preconditioning attenuates atrophic mediators and preserves muscle mass in acute sepsis. *Gen Physiol Biophys, 37*(4), 433-441. doi:10.4149/gpb_2018001

Alcorn, J. F., Guala, A. S., van der Velden, J., McElhinney, B., Irvin, C. G., Davis, R. J., & Janssen-Heininger, Y. M. (2008). Jun N-terminal kinase 1 regulates epithelial-to-mesenchymal transition induced by TGF-beta1. *J Cell Sci, 121*(Pt 7), 1036-1045. doi:10.1242/jcs.019455

American, C. S. (2016). Cancer Facts and Figures 2015. Retrieved from http://www.cancer.org/acs/groups/content/@research/documents/document/acspc-047079.pdf

Ando, K., Takahashi, F., Kato, M., Kaneko, N., Doi, T., Ohe, Y., . . . Takahashi, K. (2014). Tocilizumab, a proposed therapy for the cachexia of Interleukin6-expressing lung cancer. *PLoS One, 9*(7), e102436. doi:10.1371/journal.pone.0102436

Antunes, D., Padrao, A. I., Maciel, E., Santinha, D., Oliveira, P., Vitorino, R., . . . Ferreira, R. (2014). Molecular insights into mitochondrial dysfunction in cancer-related muscle wasting. *Biochim Biophys Acta, 1841*(6), 896-905. doi:10.1016/j.bbalip.2014.03.004

Aoyagi, T., Terracina, K. P., Raza, A., Matsubara, H., & Takabe, K. (2015). Cancer cachexia, mechanism and treatment. *World J Gastrointest Oncol, 7*(4), 17-29. doi:10.4251/wjgo.v7.i4.17

Argiles, J. M., Busquets, S., Stemmler, B., & Lopez-Soriano, F. J. (2014). Cancer cachexia: understanding the molecular basis. *Nat Rev Cancer, 14*(11), 754-762. doi:10.1038/nrc3829

Argiles, J. M., Lopez-Soriano, F. J., Stemmler, B., & Busquets, S. (2017). Novel targeted therapies for cancer cachexia. *Biochem J, 474*(16), 2663-2678. doi:10.1042/BCJ20170032

Asano, T., Ishizuka, T., Morishima, K., & Yawo, H. (2015). Optogenetic induction of contractile ability in immature C2C12 myotubes. *Sci Rep, 5*, 8317. doi:10.1038/srep08317

Aslani, A., Smith, R. C., Allen, B. J., Pavlakis, N., & Levi, J. A. (1999). Changes in body composition during breast cancer chemotherapy with the CMF-regimen. *Breast Cancer Res Treat, 57*(3), 285-290. doi:10.1023/a:1006220510597

Atherton, P. J., & Smith, K. (2012). Muscle protein synthesis in response to nutrition and exercise. *J Physiol, 590*(5), 1049-1057. doi:10.1113/jphysiol.2011.225003

Au, E. D., Desai, A. P., Koniaris, L. G., & Zimmers, T. A. (2016). The MEK-Inhibitor Selumetinib Attenuates Tumor Growth and Reduces IL-6 Expression but Does Not Protect against Muscle Wasting in Lewis Lung Cancer Cachexia. *Front Physiol, 7*, 682. doi:10.3389/fphys.2016.00682

Aust, S., Knogler, T., Pils, D., Obermayr, E., Reinthaller, A., Zahn, L., . . . Polterauer, S. (2015). Skeletal Muscle Depletion and Markers for Cancer Cachexia Are Strong Prognostic Factors in Epithelial Ovarian Cancer. *PLoS One, 10*(10), e0140403. doi:10.1371/journal.pone.0140403

Aversa, Z., Costelli, P., & Muscaritoli, M. (2017). Cancer-induced muscle wasting: latest findings in prevention and treatment. *Ther Adv Med Oncol, 9*(5), 369-382. doi:10.1177/1758834017698643

Baehr, L. M., Furlow, J. D., & Bodine, S. C. (2011). Muscle sparing in muscle RING finger 1 null mice: response to synthetic glucocorticoids. *J Physiol, 589*(Pt 19), 4759-4776. doi:10.1113/jphysiol.2011.212845

Baracos, V. E., Martin, L., Korc, M., Guttridge, D. C., & Fearon, K. C. H. (2018). Cancer-associated cachexia. *Nat Rev Dis Primers, 4*, 17105. doi:10.1038/nrdp.2017.105

Baracos, V. E., Reiman, T., Mourtzakis, M., Gioulbasanis, I., & Antoun, S. (2010). Body composition in patients with non-small cell lung cancer: a contemporary view of cancer cachexia with the use of computed tomography image analysis. *Am J Clin Nutr, 91*(4), 1133S-1137S. doi:10.3945/ajcn.2010.28608C

Bardwell, W. A., & Ancoli-Israel, S. (2008). Breast Cancer and Fatigue. *Sleep Med Clin, 3*(1), 61-71. doi:10.1016/j.jsmc.2007.10.011

Barreto, R., Waning, D. L., Gao, H., Liu, Y., Zimmers, T. A., & Bonetto, A. (2016). Chemotherapy-related cachexia is associated with mitochondrial depletion and the activation of ERK1/2 and p38 MAPKs. *Oncotarget, 7*(28), 43442-43460. doi:10.18632/oncotarget.9779

Batchelor, T. T., Taylor, L. P., Thaler, H. T., Posner, J. B., & DeAngelis, L. M. (1997). Steroid myopathy in cancer patients. *Neurology, 48*(5), 1234-1238.

Bax, L., Staes, F., & Verhagen, A. (2005). Does neuromuscular electrical stimulation strengthen the quadriceps femoris? A systematic review of randomised controlled trials. *Sports Med, 35*(3), 191-212. doi:10.2165/00007256-200535030-00002

Bechshøft, R. L., Malmgaard-Clausen, N. M., Gliese, B., Beyer, N., Mackey, A. L., Andersen, J. L., . . . Holm, L. (2017). Improved skeletal muscle mass and strength after heavy strength training in very old individuals. *Exp Gerontol, 92*(Supplement C), 96-105. doi:https://doi.org/10.1016/j.exger.2017.03.014

Bennani-Baiti, N., & Walsh, D. (2011). Animal models of the cancer anorexia-cachexia syndrome. *Supportive Care in Cancer, 19*, 1451-1463.

Berndtsson, M., Hägg, M., Panaretakis, T., Havelka, A. M., Shoshan, M. C., & Linder, S. (2007). Acute apoptosis by cisplatin requires induction of reactive oxygen species but is not associated with damage to nuclear DNA. *Int J Cancer, 120*(1), 175-180. doi:10.1002/ijc.22132

Blackwell, T. A., Cervenka, I., Khatri, B., Brown, J. L., Rosa-Caldwell, M. E., Lee, D. E., . . . Greene, N. P. (2018). Transcriptomic analysis of the development of skeletal muscle atrophy in cancer-cachexia in tumor-bearing mice. *Physiol Genomics, 50*(12), 1071-1082. doi:10.1152/physiolgenomics.00061.2018

Blau, H. M., Chiu, C. P., & Webster, C. (1983). Cytoplasmic activation of human nuclear genes in stable heterocaryons. *Cell, 32*(4), 1171-1180.

Blau, H. M., Pavlath, G. K., Hardeman, E. C., Chiu, C. P., Silberstein, L., Webster, S. G., . . . Webster, C. (1985). Plasticity of the differentiated state. *Science, 230*(4727), 758-766.

Bodine, S. C., & Baehr, L. M. (2014). Skeletal muscle atrophy and the E3 ubiquitin ligases MuRF1 and MAFbx/atrogin-1. *Am J Physiol Endocrinol Metab, 307*(6), E469-484. doi:10.1152/ajpendo.00204.2014

Bodine, S. C., & Furlow, J. D. (2015). Glucocorticoids and Skeletal Muscle. *Adv Exp Med Biol, 872*, 145-176. doi:10.1007/978-1-4939-2895-8_7

Bodine, S. C., Latres, E., Baumhueter, S., Lai, V. K., Nunez, L., Clarke, B. A., . . . Glass, D. J. (2001). Identification of ubiquitin ligases required for skeletal muscle atrophy. *Science, 294*(5547), 1704-1708. doi:10.1126/science.1065874

Bodine, S. C., Stitt, T. N., Gonzalez, M., Kline, W. O., Stover, G. L., Bauerlein, R., . . . Yancopoulos, G. D. (2001). Akt/mTOR pathway is a crucial regulator of skeletal muscle hypertrophy and can prevent muscle atrophy in vivo. *Nat Cell Biol, 3*(11), 1014-1019. doi:10.1038/ncb1101-1014

Bohnert, K. R., McMillan, J. D., & Kumar, A. (2018). Emerging roles of ER stress and unfolded protein response pathways in skeletal muscle health and disease. *J Cell Physiol, 233*(1), 67-78. doi:10.1002/jcp.25852

Bonaldo, P., & Sandri, M. (2013). Cellular and molecular mechanisms of muscle atrophy. *Dis Model Mech, 6*(1), 25-39. doi:10.1242/dmm.010389

Bonetto, A., Rupert, J. E., Barreto, R., & Zimmers, T. A. (2016). The Colon-26 Carcinoma Tumor-bearing Mouse as a Model for the Study of Cancer Cachexia. *J Vis Exp*(117). doi:10.3791/54893

Braithwaite, D., Satariano, W. A., Sternfeld, B., Hiatt, R. A., Ganz, P. A., Kerlikowske, K., . . . Caan, B. J. (2010). Long-term prognostic role of functional limitations among women with breast cancer. *J Natl Compr Canc Netw, 102*(19), 1468-1477. doi:10.1093/jnci/djq344

Braun, D., Gupta, D., & Staren, E. (2011). Quality of life assessment as a predictor of survival in non-small cell lung cancer. *BMC Cancer, 11*(1), 353.

Broome, S. C., Woodhead, J. S. T., & Merry, T. L. (2018). Mitochondria-Targeted Antioxidants and Skeletal Muscle Function. *Antioxidants (Basel), 7*(8). doi:10.3390/antiox7080107

Brown, D. M., Parr, T., & Brameld, J. M. (2012). Myosin heavy chain mRNA isoforms are expressed in two distinct cohorts during C2C12 myogenesis. *J Muscle Res Cell Motil, 32*(6), 383-390. doi:10.1007/s10974-011-9267-4

Brown, J. C., & Schmitz, K. H. (2015). Weight lifting and appendicular skeletal muscle mass among breast cancer survivors: a randomized controlled trial. *Breast Cancer Res Treat, 151*(2), 385-392. doi:10.1007/s10549-015-3409-0

Brown, J. L., Lee, D. E., Rosa-Caldwell, M. E., Brown, L. A., Perry, R. A., Haynie, W. S., . . . Greene, N. P. (2018). Protein imbalance in the development of skeletal muscle wasting in tumour-bearing mice. *J Cachexia Sarcopenia Muscle, 9*(5), 987-1002. doi:10.1002/jcsm.12354

Brown, J. L., Rosa-Caldwell, M. E., Lee, D. E., Blackwell, T. A., Brown, L. A., Perry, R. A., . . . Greene, N. P. (2017). Mitochondrial degeneration precedes the development of muscle atrophy in progression of cancer cachexia in tumour-bearing mice. *J Cachexia Sarcopenia Muscle, 8*(6), 926-938. doi:10.1002/jcsm.12232

Brown, J. L., Rosa-Caldwell, M. E., Lee, D. E., Brown, L. A., Perry, R. A., Shimkus, K. L., . . . Greene, N. P. (2017). PGC-1alpha4 gene expression is suppressed by the IL-6-MEK-ERK 1/2 MAPK signalling axis and altered by resistance exercise, obesity and muscle injury. *Acta Physiol (Oxf), 220*(2), 275-288. doi:10.1111/apha.12826

Brown, J. L., Rosa-Caldwell, M. E., Lee, D. E., Blackwell, T. A., Brown, L. A., Perry, R. A., . . . Greene, N. P. (2017). Mitochondrial degeneration precedes the development of muscle atrophy in progression of cancer cachexia in tumour-bearing mice. *J Cachexia Sarcopenia Musc, 8*(6), 926-938. doi:10.1002/jcsm.12232

Brunelli, A., Pompili, C., Berardi, R., Mazzanti, P., Onofri, A., Salati, M., . . . Sabbatini, A. (2012). Performance at preoperative stair-climbing test is associated with prognosis after pulmonary resection in Stage I non-small cell lung cancers. *Ann Thorac Surg, 93*(6), 1796-1800. doi:10.1016/j.athoracsur.2012.02.068

Butt, Z., Rosenbloom, S. K., Abernethy, A. P., Beaumont, J. L., Paul, D., Hamptom, D., . . . Cella, D. (2008). Fatigue is the most important symptom for advanced cancer patients who have had chemotherapy. *J Natl Compr Canc Netw, 6*, 448-455.

Caan, B. J., Cespedes Feliciano, E. M., Prado, C. M., & et al. (2018). Association of muscle and adiposity measured by computed tomography with survival in patients with nonmetastatic breast cancer. *JAMA Oncology*. doi:10.1001/jamaoncol.2018.0137

Callahan, D. M., Bedrin, N. G., Subramanian, M., Berking, J., Ades, P. A., Toth, M. J., & Miller, M. S. (2014). Age-related structural alterations in human skeletal muscle fibers and mitochondria are sex-specific: relationship to single fiber function. *J Appl Physiol, 116*, 1582-1592.

Callahan, D. M., Tourville, T. W., Miller, M. S., Hackett, S. B., Sharma, H., Cruickshank, N. C., . . . Toth, M. J. (2015). Chronic disuse and skeletal muscle structure in older adults: sex-specific differences and relationships to contractile function. *Am J Physiol Cell Physiol, 308*(11), C932-C943.

Carty, A., McCormack, K., Coughlan, G. F., Crowe, L., & Caulfield, B. (2012). Increased aerobic fitness after neuromuscular electrical stimulation training in adults with spinal cord injury. *Arch Phys Med Rehabil, 93*(5), 790-795. doi:10.1016/j.apmr.2011.10.030

Caulfield, B., Prendergast, A., Rainsford, G., & Minogue, C. (2013). Self directed home based electrical muscle stimulation training improves exercise tolerance and strength in healthy elderly. *Conf Proc IEEE Eng Med Biol Soc, 2013*, 7036-7039. doi:10.1109/EMBC.2013.6611178

Cella, D., Davis, K., Breitbart, W., Curt, G., & Coalition, f. t. F. (2001). Cancer-related fatigue: prevalence of proposed diagnostic criteria in a United States sample of cancer survivors. *J Clin Oncol, 19*(14), 3385-3391.

Chatterjee, K., Zhang, J., Honbo, N., & Karliner, J. S. (2010). Doxorubicin cardiomyopathy. *Cardiology, 115*(2), 155-162. doi:10.1159/000265166

Chaturvedi, V., Dye, D. E., Kinnear, B. F., van Kuppevelt, T. H., Grounds, M. D., & Coombe, D. R. (2015). Interactions between Skeletal Muscle Myoblasts and their Extracellular Matrix Revealed by a Serum Free Culture System. *PLoS One, 10*(6), e0127675. doi:10.1371/journal.pone.0127675

Chen, C., Ju, R., Zhu, L., Li, J., Chen, W., Zhang, D. C., . . . Guo, L. (2017). Carboxyamidotriazole alleviates muscle atrophy in tumor-bearing mice by inhibiting NF-kappaB and activating SIRT1. *Naunyn Schmiedebergs Arch Pharmacol, 390*(4), 423-433. doi:10.1007/s00210-017-1345-8

Chen, C. Y., Liu, T. Z., Chen, C. H., Wu, C. C., Cheng, J. T., Yiin, S. J., . . . Chern, C. L. (2007). Isoobtusilactone A-induced apoptosis in human hepatoma Hep G2 cells is mediated via increased NADPH oxidase-derived reactive oxygen species (ROS) production and the mitochondria-associated apoptotic mechanisms. *Food Chem Toxicol, 45*(7), 1268-1276. doi:10.1016/j.fct.2007.01.008

Cheng, C. S., El-Abd, Y., Bui, K., Hyun, Y. E., Hughes, R. H., Kraus, W. E., & Truskey, G. A. (2014). Conditions that promote primary human skeletal myoblast culture and muscle differentiation in vitro. *Am J Physiol Cell Physiol, 306*(4), C385-395. doi:10.1152/ajpcell.00179.2013

Choi, Y., Oh, D. Y., Kim, T. Y., Lee, K. H., Han, S. W., Im, S. A., . . . Bang, Y. J. (2015). Skeletal Muscle Depletion Predicts the Prognosis of Patients with Advanced Pancreatic Cancer Undergoing Palliative Chemotherapy, Independent of Body Mass Index. *PLoS One, 10*(10), e0139749. doi:10.1371/journal.pone.0139749

Clarke, B. A., Drujan, D., Willis, M. S., Murphy, L. O., Corpina, R. A., Burova, E., . . . Glass, D. J. (2007). The E3 Ligase MuRF1 degrades myosin heavy chain protein in dexamethasone-treated skeletal muscle. *Cell Metab, 6*(5), 376-385. doi:10.1016/j.cmet.2007.09.009

Cohen, S., Brault, J. J., Gygi, S. P., Glass, D. J., Valenzuela, D. M., Gartner, C., . . . Goldberg, A. L. (2009). During muscle atrophy, thick, but not thin, filament components are degraded by MuRF1-dependent ubiquitylation. *J Cell Biol, 185*(6), 1083-1095. doi:10.1083/jcb.200901052

Collinsworth, A. M., Zhang, S., Kraus, W. E., & Truskey, G. A. (2002). Apparent elastic modulus and hysteresis of skeletal muscle cells throughout differentiation. *Am J Physiol Cell Physiol, 283*(4), C1219-1227. doi:10.1152/ajpcell.00502.2001

Constantinou, C., Fontes de Oliveira, C. C., Mintzopoulos, D., Busquets, S., He, J., Kesarwani, M., . . . Tzika, A. A. (2011). Nuclear magnetic resonance in conjunction with functional genomics suggests mitochondrial dysfunction in a murine model of cancer cachexia. *Int J Mol Med, 27*(1), 15-24. doi:10.3892/ijmm.2010.557

Costelli, P., Muscaritoli, M., Bossola, M., Penna, F., Reffo, P., Bonetto, A., . . . Rossi Fanelli, F. (2006). IGF-1 is downregulated in experimental cancer cachexia. *Am J Physiol Regul Integr Comp Physiol, 291*(3), R674-683. doi:10.1152/ajpregu.00104.2006

Courneya, K. S., & Friedenreich, C. M. (2001). Framework PEACE: an organizational model for examining physical exercise across the cancer experience. *Ann Behav Med, 23*(4), 263-272. doi:10.1207/S15324796ABM2304_5

Crilly, M. J., Tryon, L. D., Erlich, A. T., & Hood, D. A. (2016). The role of Nrf2 in skeletal muscle contractile and mitochondrial function. *J Appl Physiol (1985), 121*(3), 730-740. doi:10.1152/japplphysiol.00042.2016

Crognale, D., Vito, G. D., Grosset, J. F., Crowe, L., Minogue, C., & Caulfield, B. (2013). Neuromuscular electrical stimulation can elicit aerobic exercise response without undue discomfort in healthy physically active adults. *J Strength Cond Res, 27*(1), 208-215. doi:10.1519/JSC.0b013e318252f5e5

Cunningham, J. T., Rodgers, J. T., Arlow, D. H., Vazquez, F., Mootha, V. K., & Puigserver, P. (2007). mTOR controls mitochondrial oxidative function through a YY1-PGC-1alpha transcriptional complex. *Nature, 450*(7170), 736-740. doi:10.1038/nature06322

Cuthbertson, D. J., Babraj, J., Smith, K., Wilkes, E., Fedele, M. J., Esser, K., & Rennie, M. (2006). Anabolic signaling and protein synthesis in human skeletal muscle after dynamic shortening or lengthening exercise. *Am J Physiol Endocrinol Metab, 290*(4), E731-738. doi:10.1152/ajpendo.00415.2005

Dally, J. W., & Riley, W. F. (2005). *Experimental stress analysis* (4th ed.). Knoxville, Tenn.: College House Enterprises.

Damas, F., Phillips, S. M., Lixandrão, M. E., Vechin, F. C., Libardi, C. A., Roschel, H., . . . Ugrinowitsch, C. (2016). Early resistance training-induced increases in muscle cross-sectional area are concomitant with edema-induced muscle swelling. *European Journal of Applied Physiology, 116*(1), 49-56. doi:10.1007/s00421-015-3243-4

Damrauer, J. S., Stadler, M. E., Acharyya, S., Baldwin, A. S., Couch, M. E., & Guttridge, D. C. (2018). Chemotherapy-induced muscle wasting: association with NF-kappaB and cancer cachexia. *Eur J Transl Myol, 28*(2), 7590. doi:10.4081/ejtm.2018.7590

De Deyne, P. G. (2000). Formation of sarcomeres in developing myotubes: role of mechanical stretch and contractile activation. *Am J Physiol Cell Physiol, 279*(6), C1801-C1811.

de Moor, J. S., Mariotto, A. B., Parry, C., Alfano, C. M., Padgett, L., Kent, E. E., . . . Rowland, J. H. (2013). Cancer survivors in the United States: prevalence across the survivorship trajectory and implications for care. *Cancer Epidemiol Biomarkers Prev, 22*(4), 561-570. doi:10.1158/1055-9965.epi-12-1356

Delbono, O., O'Rourke, K. S., & Ettinger, W. H. (1995). Excitation-calcium release uncoupling in aged single human skeletal muscle fibers. *J Membrane Biol, 148*, 211-222.

Dewys, W. D., Begg, C., Lavin, P. T., Band, P. R., Bennett, J. M., Bertino, J. R., . . . Tormey, D. C. (1980). Prognostic effect of weight loss prior to chemotherapy in cancer patients. *Am J Med, 69*, 491-497.

Dewys, W. D., Begg, C., Lavin, P. T., Band, P. R., Bennett, J. M., Bertino, J. R., . . . Tormey, D. C. (1980). Prognostic effect of weight loss prior to chemotherapy in cancer patients. Eastern Cooperative Oncology Group. *Am J Med, 69*(4), 491-497.

Ding, H., Jiang, N., Liu, H., Liu, X., Liu, D., Zhao, F., . . . Zhang, Y. (2010). Response of mitochondrial fusion and fission protein gene expression to exercise in rat skeletal muscle. *Biochim Biophys Acta, 1800*(3), 250-256. doi:10.1016/j.bbagen.2009.08.007

Ding, H., Zhang, G., Sin, K. W., Liu, Z., Lin, R. K., Li, M., & Li, Y. P. (2017). Activin A induces skeletal muscle catabolism via p38beta mitogen-activated protein kinase. *J Cachexia Sarcopenia Muscle, 8*(2), 202-212. doi:10.1002/jcsm.12145

Dirks, M. L., Hansen, D., Van Assche, A., Dendale, P., & Van Loon, L. J. (2015). Neuromuscular electrical stimulation prevents muscle wasting in critically ill comatose patients. *Clin Sci (Lond), 128*(6), 357-365. doi:10.1042/CS20140447

Dirks, M. L., Wall, B. T., Snijders, T., Ottenbros, C. L., Verdijk, L. B., & van Loon, L. J. (2014). Neuromuscular electrical stimulation prevents muscle disuse atrophy during leg immobilization in humans. *Acta Physiol (Oxf), 210*(3), 628-641. doi:10.1111/apha.12200

Dittus, K. L., Lakoski, S. G., Savage, P. D., Kokinda, N., Toth, M. J., Stevens, D., . . . Ades, P. A. (2015). Exercise-based oncology rehabilitation: leveraging the cardiac rehabilitation model. *J Cardiopulm Rehabil Prev, 35*, 130-139.

Egan, B., & Zierath, J. R. (2013). Exercise metabolism and the molecular regulation of skeletal muscle adaptation. *Cell Metab, 17*(2), 162-184. doi:10.1016/j.cmet.2012.12.012

Engler, A. J., Griffin, M. A., Sen, S., Bonnemann, C. G., Sweeney, H. L., & Discher, D. E. (2004). Myotubes differentiate optimally on substrates with tissue-like stiffness: pathological implications for soft or stiff microenvironments. *J Cell Biol, 166*(6), 877-887. doi:10.1083/jcb.200405004

Ewer, M. S., & Ewer, S. M. (2010). Cardiotoxicity of anticancer treatments: what the cardiologist needs to know. *Nat Rev Cardiol, 7*(10), 564-575. doi:10.1038/nrcardio.2010.121

Fearon, K., Arends, J., & Baracos, V. (2013). Understanding the mechanisms and treatment options in cancer cachexia. *Nat Rev Clin Oncol, 10*(2), 90-99. doi:10.1038/nrclinonc.2012.209

Fearon, K., Strasser, F., Anker, S. D., Bosaeus, I., Bruera, E., Fainsinger, R. L., . . . Baracos, V. E. (2011). Definition and classification of cancer cachexia: an international consensus. *Lancet Oncol, 12*(5), 489-495. doi:10.1016/S1470-2045(10)70218-7

Fearon, K. C. (2011). Cancer cachexia and fat-muscle physiology. *N Engl J Med, 365*(6), 565-567. doi:10.1056/NEJMcibr1106880

Fearon, K. C., Glass, D. J., & Guttridge, D. C. (2012). Cancer cachexia: mediators, signaling, and metabolic pathways. *Cell Metab, 16*(2), 153-166. doi:10.1016/j.cmet.2012.06.011

Fearon, K. C. H., Glass, D. J., & Guttridge, D. C. (2012). Cancer cachexia: mediators, signaling and metabolic pathways. *Cell Metabolism, 16*, 1-14.

Fermoselle, C., García-Arumí, E., Puig-Vilanova, E., Andreu, A. L., Urtreger, A. J., de Kier Joffé, E. D. B., . . . Barreiro, E. (2013). Mitochondrial dysfunction and therapeutic approaches in respiratory and limb muscles of cancer cachectic mice. *Exp Physiol, 98*(9), 1349-1365. doi:10.1113/expphysiol.2013.072496

Fielitz, J., Kim, M. S., Shelton, J. M., Latif, S., Spencer, J. A., Glass, D. J., . . . Olson, E. N. (2007). Myosin accumulation and striated muscle myopathy result from the loss of muscle RING finger 1 and 3. *J Clin Invest, 117*(9), 2486-2495. doi:10.1172/JCI32827

Fischer, S. J., Benson, L. M., Fauq, A., Naylor, S., & Windebank, A. J. (2008). Cisplatin and dimethyl sulfoxide react to form an adducted compound with reduced cytotoxicity and neurotoxicity. *NeuroToxicology, 29*(3), 444-452. doi:https://doi.org/10.1016/j.neuro.2008.02.010

Fitts, R. H., Romatowski, J. G., Peters, J. R., Paddon-Jones, D., Wolfe, R. R., & Ferrando, A. A. (2007). The deleterious effects of bed rest on human skeletal muscle fibers are exacerbated by hypercortisolemia and ameliorated by dietary supplementation. *Am J Physiol Cell Physiol, 293*(1), C313-C320. doi:10.1152/ajpcell.00573.2006

Fix, D. K., Hardee, J. P., Gao, S., VanderVeen, B. N., Velazquez, K. T., & Carson, J. A. (2018). Role of gp130 in basal and exercise-trained skeletal muscle mitochondrial quality control. *J Appl Physiol (1985), 124*(6), 1456-1470. doi:10.1152/japplphysiol.01063.2017

Flint, T. R., Janowitz, T., Connell, C. M., Roberts, E. W., Denton, A. E., Coll, A. P., . . . Fearon, D. T. (2016). Tumor-Induced IL-6 Reprograms Host Metabolism to Suppress Anti-tumor Immunity. *Cell Metab, 24*(5), 672-684. doi:10.1016/j.cmet.2016.10.010

Fluck, M., & Hoppeler, H. (2003). Molecular basis of skeletal muscle plasticity--from gene to form and function. *Rev Physiol Biochem Pharmacol, 146*, 159-216. doi:10.1007/s10254-002-0004-7

Fogelman, D. R., Morris, J., Xiao, L., Hassan, M., Vadhan, S., Overman, M., . . . Wang, X. S. (2017). A predictive model of inflammatory markers and patient-reported symptoms for cachexia in newly diagnosed pancreatic cancer patients. *Support Care Cancer, 25*(6), 1809-1817. doi:10.1007/s00520-016-3553-z

Foletta, V. C., White, L. J., Larsen, A. E., Leger, B., & Russell, A. P. (2011). The role and regulation of MAFbx/atrogin-1 and MuRF1 in skeletal muscle atrophy. *Pflugers Arch, 461*(3), 325-335. doi:10.1007/s00424-010-0919-9

Fong, Y., Lowry, S. F., & Cerami, A. (1988). Cachetin/TNF: a macrophage protein that induces cachexia and shock. *JPEN J Parenter Enteral Nutr, 12*(6 Suppl), 72S-77S.

Fontes-Oliveira, C. C., Busquets, S., Toledo, M., Penna, F., Paz Aylwin, M., Sirisi, S., . . . Argiles, J. M. (2013). Mitochondrial and sarcoplasmic reticulum abnormalities in cancer cachexia: altered energetic efficiency? *Biochim Biophys Acta, 1830*(3), 2770-2778. doi:10.1016/j.bbagen.2012.11.009

Formigli, L., Meacci, E., Sassoli, C., Squecco, R., Nosi, D., Chellini, F., . . . Zecchi-Orlandini, S. (2007). Cytoskeleton/stretch-activated ion channel interaction regulates myogenic differentiation of skeletal myoblasts. *J Cell Physiol, 211*(2), 296-306. doi:10.1002/jcp.20936

Frank, M., Duvezin-Caubet, S., Koob, S., Occhipinti, A., Jagasia, R., Petcherski, A., . . . Reichert, A. S. (2012). Mitophagy is triggered by mild oxidative stress in a mitochondrial fission dependent manner. *Biochim Biophys Acta, 1823*(12), 2297-2310. doi:http://dx.doi.org/10.1016/j.bbamcr.2012.08.007

Freedman, R. J., Aziz, N., Albanes, D., Hartman, T., Danforth, D., Hill, S., . . . Yanovski, J. A. (2004). Weight and body composition changes during and after adjuvant chemotherapy in women with breast cancer. *J Clin Endocrinol Metab, 89*(5), 2248-2253. doi:doi:10.1210/jc.2003-031874

Fry, C. S., Drummond, M. J., Glynn, E. L., Dickinson, J. M., Gundermann, D. M., Timmerman, K. L., . . . Rasmussen, B. B. (2011). Aging impairs contraction-induced human skeletal muscle mTORC1 signaling and protein synthesis. *Skelet Muscle, 1*(1), 11. doi:10.1186/2044-5040-1-11

Fujita, H., Nedachi, T., & Kanzaki, M. (2007). Accelerated de novo sarcomere assembly by electric pulse stimulation in C2C12 myotubes. *Exp Cell Res, 313*(9), 1853-1865. doi:10.1016/j.yexcr.2007.03.002

Gajsek, N., Jevsek, M., Mars, T., Mis, K., Pirkmajer, S., Brecelj, J., & Grubic, Z. (2008). Synaptogenetic mechanisms controlling postsynaptic differentiation of the neuromuscular junction are nerve-dependent in human and nerve-independent in mouse C2C12 muscle cultures. *Chem Biol Interact, 175*(1-3), 50-57. doi:10.1016/j.cbi.2008.05.027

Galanti, G., Stefani, L., & Gensini, G. (2013). Exercise as a prescription therapy for breast and colon cancer survivors. *Int J Gen Med, 6*, 245-251. doi:10.2147/IJGM.S42720

Gao, S., & Carson, J. A. (2016). Lewis lung carcinoma regulation of mechanical stretch-induced protein synthesis in cultured myotubes. *Am J Physiol Cell Physiol, 310*(1), C66-79. doi:10.1152/ajpcell.00052.2015

Garrison, J. A., McCune, J. S., Livingston, R. B., Linden, H. M., Gralow, J. R., Ellis, G. K., & West, H. L. (2003). Myalgias and arthralgias associated with paclitaxel. *Oncology (Williston Park), 17*(2), 271-277; discussion 281-272, 286-278.

Gilliam, L. A., Ferreira, L. F., Bruton, J. D., Moylan, J. S., Westerblad, H., St Clair, D. K., & Reid, M. B. (2009). Doxorubicin acts through tumor necrosis factor receptor subtype 1 to cause dysfunction of murine skeletal muscle. *J Appl Physiol (1985), 107*(6), 1935-1942. doi:10.1152/japplphysiol.00776.2009

Gilliam, L. A., Lark, D. S., Reese, L. R., Torres, M. J., Ryan, T. E., Lin, C. T., . . . Neufer, P. D. (2016). Targeted overexpression of mitochondrial catalase protects against cancer chemotherapy-induced skeletal muscle dysfunction. *Am J Physiol Endocrinol Metab, 311*(2), E293-301. doi:10.1152/ajpendo.00540.2015

Gilliam, L. A., Moylan, J. S., Patterson, E. W., Smith, J. D., Wilson, A. S., Rabbani, Z., & Reid, M. B. (2012). Doxorubicin acts via mitochondrial ROS to stimulate catabolism in C2C12 myotubes. *Am J Physiol Cell Physiol, 302*(1), C195-202. doi:10.1152/ajpcell.00217.2011

Gilliam, L. A., & St Clair, D. K. (2011). Chemotherapy-induced weakness and fatigue in skeletal muscle: the role of oxidative stress. *Antioxid Redox Signal, 15*(9), 2543-2563. doi:10.1089/ars.2011.3965

Gilliam, L. A. A., Ferreira, L. F., Bruton, J. D., Moylan, J. S., Westerblad, H., St. Clair, D. K., & Reid, M. B. (2009). Doxorubicin acts through tumor necrosis factor receptor subtype 1 to cause dysfunction of murine skeletal muscle. *J Appl Physiol, 107*(6), 1935-1942. doi:10.1152/japplphysiol.00776.2009

Gilliam, L. A. A., Fisher-Wellman, K. H., Lin, C.-T., Maples, J. M., Cathey, B. L., & Neufer, P. D. (2013). The anticancer agent doxorubicin disrupts mitochondrial energy metabolism and redox balance in skeletal muscle. *Free Rad Biol Med, 65*(0), 988-996. doi:http://dx.doi.org/10.1016/j.freeradbiomed.2013.08.191

Gilliam, L. A. A., Moylan, J. S., Patterson, E. W., Smith, J. D., Wilson, A. S., Rabbani, Z., & Reid, M. B. (2012). Doxorubicin acts via mitochondrial ROS to stimulate catabolism in C2C12 myotubes. *Am J Physiol Cell Physiol, 302*(1), C195-C202. doi:10.1152/ajpcell.00217.2011

Glass, D. J. (2003). Signalling pathways that mediate skeletal muscle hypertrophy and atrophy. *Nat Cell Biol, 5*(2), 87-90. doi:10.1038/ncb0203-87

Go, S. I., Park, M. J., Song, H. N., Kang, M. H., Park, H. J., Jeon, K. N., . . . Lee, G. W. (2016). Sarcopenia and inflammation are independent predictors of survival in male patients newly diagnosed with small cell lung cancer. *Support Care Cancer, 24*(5), 2075-2084. doi:10.1007/s00520-015-2997-x

Gordon, J. W., Rungi, A. A., Inagaki, H., & Hood, D. A. (2001). Effects of contractile activity on mitochondrial transcription factor A expression in skeletal muscle. *J Appl Physiol (1985), 90*(1), 389-396. doi:10.1152/jappl.2001.90.1.389

Gouspillou, G., Scheede-Bergdahl, C., Spendiff, S., Vuda, M., Meehan, B., Mlynarski, H., . . . Jagoe, R. T. (2015). Anthracycline-containing chemotherapy causes long-term impairment of mitochondrial respiration and increased reactive oxygen species release in skeletal muscle. *Sci Rep, 5*, 8717. doi:10.1038/srep08717

Guigni, B. A., Callahan, D. M., Tourville, T. W., Miller, M. S., Fiske, B., Voigt, T., . . . Toth, M. J. (2018a). Skeletal Muscle Atrophy and Dysfunction in Breast Cancer Patients: Role for Chemotherapy-Derived Oxidant Stress. *Am J Physiol Cell Physiol*. doi:10.1152/ajpcell.00002.2018

Guigni, B. A., Callahan, D. M., Tourville, T. W., Miller, M. S., Fiske, B., Voigt, T., . . . Toth, M. J. (2018b). Skeletal muscle atrophy and dysfunction in breast cancer patients: role for chemotherapy-derived oxidant stress. *Am J Physiol Cell Physiol, 315*(5), C744-C756. doi:10.1152/ajpcell.00002.2018

Gutierrez-Martin, Y., Martin-Romero, F. J., & Henao, F. (2005). Store-operated calcium entry in differentiated C2C12 skeletal muscle cells. *Biochim Biophys Acta, 1711*(1), 33-40. doi:10.1016/j.bbamem.2005.02.017

Han, E. K., McGonigal, T., Butler, C., Giranda, V. L., & Luo, Y. (2008). Characterization of Akt overexpression in MiaPaCa-2 cells: prohibitin is an Akt substrate both in vitro and in cells. *Anticancer Res, 28*(2A), 957-963.

Han, Y. Q., Ming, S. L., Wu, H. T., Zeng, L., Ba, G., Li, J., . . . Chu, B. B. (2018). Myostatin knockout induces apoptosis in human cervical cancer cells via elevated reactive oxygen species generation. *Redox Biol, 19*, 412-428. doi:10.1016/j.redox.2018.09.009

Hardee, J. P., Counts, B. R., Gao, S., VanderVeen, B. N., Fix, D. K., Koh, H. J., & Carson, J. A. (2018). Inflammatory signalling regulates eccentric contraction-induced protein synthesis in cachectic skeletal muscle. *J Cachexia Sarcopenia Muscle, 9*(2), 369-383. doi:10.1002/jcsm.12271

Hardee, J. P., Mangum, J. E., Gao, S., Sato, S., Hetzler, K. L., Puppa, M. J., . . . Carson, J. A. (2016). Eccentric contraction-induced myofiber growth in tumor-bearing mice. *J Appl Physiol (1985), 120*(1), 29-37. doi:10.1152/japplphysiol.00416.2015

Hasenfuss, G. (1998). Animal models of human cardiovascular disease, heart failure and hypertrophy. *Cardiovasc Res, 39*, 60-76.

Hawley, J. A., & Holloszy, J. O. (2009). Exercise: it's the real thing! *Nutr Rev, 67*(3), 172-178. doi:10.1111/j.1753-4887.2009.00185.x

He, W. A., Calore, F., Londhe, P., Canella, A., Guttridge, D. C., & Croce, C. M. (2014). Microvesicles containing miRNAs promote muscle cell death in cancer cachexia via TLR7. *Proc Natl Acad Sci, 111*(12), 4525-4529. doi:10.1073/pnas.1402714111

Henderson, C. A., Gomez, C. G., Novak, S. M., Mi-Mi, L., & Gregorio, C. C. (2017). Overview of the Muscle Cytoskeleton. *Compr Physiol, 7*(3), 891-944. doi:10.1002/cphy.c160033

Higaki, Y., Mikami, T., Fujii, N., Hirshman, M. F., Koyama, K., Seino, T., . . . Goodyear, L. J. (2008). Oxidative stress stimulates skeletal muscle glucose uptake through a phosphatidylinositol 3-kinase-dependent pathway. *Am J Physiol Endocrinol Metab, 294*(5), E889-897. doi:10.1152/ajpendo.00150.2007

Hilber, K., Galler, S., Gohlsch, B., & Pette, D. (1999). Kinetic properties of myosin heavy chain isoforms in single fibers from human skeletal muscle. *FEBS Lett, 455*(3), 267-270.

Hindi, S. M., Mishra, V., Bhatnagar, S., Tajrishi, M. M., Ogura, Y., Yan, Z., . . . Kumar, A. (2014). Regulatory circuitry of TWEAK-Fn14 system and PGC-1alpha in skeletal muscle atrophy program. *FASEB J, 28*(3), 1398-1411. doi:10.1096/fj.13-242123

Holmes, M. D., Chen, W. Y., Feskanich, D., Kroenke, C. H., & Colditz, G. A. (2005). Physical activity and survival after breast cancer diagnosis. *JAMA, 293*(20), 2479-2486. doi:10.1001/jama.293.20.2479

Hood, D. A., Irrcher, I., Ljubicic, V., & Joseph, A. M. (2006). Coordination of metabolic plasticity in skeletal muscle. *J Exp Biol, 209*(Pt 12), 2265-2275. doi:10.1242/jeb.02182

Hood, D. A., Memme, J. M., Oliveira, A. N., & Triolo, M. (2019). Maintenance of Skeletal Muscle Mitochondria in Health, Exercise, and Aging. *Annu Rev Physiol, 81*, 19-41. doi:10.1146/annurev-physiol-020518-114310

Horber, F. F., Hoppeler, H., Herren, D., Claassen, H., Howald, H., Gerber, C., & Frey, F. J. (1986). Altered skeletal muscle ultrastructure in renal transplant patients on prednisone. *Kidney International, 30*(3), 411-416. doi:10.1038/ki.1986.199

Horie, M., Warabi, E., Komine, S., Oh, S., & Shoda, J. (2015). Cytoprotective Role of Nrf2 in Electrical Pulse Stimulated C2C12 Myotube. *PLoS One, 10*(12), e0144835. doi:10.1371/journal.pone.0144835

Hornberger, T. A. (2011). Mechanotransduction and the regulation of mTORC1 signaling in skeletal muscle. *Int J Biochem Cell Biol, 43*(9), 1267-1276. doi:10.1016/j.biocel.2011.05.007

Hornberger, T. A., Armstrong, D. D., Koh, T. J., Burkholder, T. J., & Esser, K. A. (2005). Intracellular signaling specificity in response to uniaxial vs. multiaxial stretch: implications for mechanotransduction. *Am J Physiol Cell Physiol, 288*(1), C185-194. doi:10.1152/ajpcell.00207.2004

Howlader, N., Noone, A. M., Krapcho, M., Garshell, J., Miller, D., Altekruse, S. F., . . . Cronin, K. A. (2015). SEER Cancer Statistics Review, 1975-2012, National Cancer Institute. Retrieved from http://seer.cancer.gov/csr/1975_2011/results_merged/topic_lifetime_risk_diagnosis.pdf

Huang, S. C., Wu, J. F., Saovieng, S., Chien, W. H., Hsu, M. F., Li, X. F., . . . Kuo, C. H. (2017). Doxorubicin inhibits muscle inflammation after eccentric exercise. *J Cachexia Sarcopenia Muscle, 8*(2), 277-284. doi:10.1002/jcsm.12148

Huang, X., Sun, L., Ji, S., Zhao, T., Zhang, W., Xu, J., . . . Cheng, H. (2013). Kissing and nanotunneling mediate intermitochondrial communication in the heart. *Proc Natl Acad Sci, 110*(8), 2846-2851. doi:10.1073/pnas.1300741110

Hultman, E., Sjoholm, H., Jaderholm-Ek, I., & Krynicki, J. (1983). Evaluation of methods for electrical stimulation of human skeletal muscle in situ. *Pflugers Arch, 398*(2), 139-141.

Irwin, M. L., McTiernan, A., Baumgartner, R. N., Baumgartner, K. B., Bernstein, L., Gilliland, F. D., & Ballard-Barbash, R. (2005). Changes in body fat and weight after a breast cancer diagnosis: influence of demographic, prognostic, and lifestyle factors. *J Clin Oncol, 23*(4), 774-782. doi:doi:10.1200/JCO.2005.04.036

Irwin, M. L., McTiernan, A., Manson, J. E., Thomson, C. A., Sternfeld, B., Stefanick, M. L., . . . Chlebowski, R. (2011). Physical activity and survival in postmenopausal women with breast cancer: results from the Women's Health Initiative. *Cancer Prev Res, 4*(4), 522-529. doi:10.1158/1940-6207.capr-10-0295

Issa, M. E., Muruganandan, S., Ernst, M. C., Parlee, S. D., Zabel, B. A., Butcher, E. C., . . . Goralski, K. B. (2012). Chemokine-like receptor 1 regulates skeletal muscle cell myogenesis. *Am J Physiol Cell Physiol, 302*(11), C1621-1631. doi:10.1152/ajpcell.00187.2011

Ito, N., Ruegg, U. T., Kudo, A., Miyagoe-Suzuki, Y., & Takeda, S. (2013a). Activation of calcium signaling through Trpv1 by nNOS and peroxynitrite as a key trigger of skeletal muscle hypertrophy. *Nat Med, 19*(1), 101-106. doi:10.1038/nm.3019

Ito, N., Ruegg, U. T., Kudo, A., Miyagoe-Suzuki, Y., & Takeda, S. (2013b). Capsaicin mimics mechanical load-induced intracellular signaling events: involvement of TRPV1-mediated calcium signaling in induction of skeletal muscle hypertrophy. *Channels (Austin), 7*(3), 221-224. doi:10.4161/chan.24583

Ito, Y., Obara, K., Ikeda, R., Ishii, M., Tanabe, Y., Ishikawa, T., & Nakayama, K. (2006). Passive stretching produces Akt- and MAPK-dependent augmentations of GLUT4 translocation and glucose uptake in skeletal muscles of mice. *Pflugers Arch, 451*(6), 803-813. doi:10.1007/s00424-005-1512-5

Jackman, R. W., Floro, J., Yoshimine, R., Zitin, B., Eiampikul, M., El-Jack, K., . . . Kandarian, S. C. (2017). Continuous Release of Tumor-Derived Factors Improves the Modeling of Cachexia in Muscle Cell Culture. *Front Physiol, 8*, 738. doi:10.3389/fphys.2017.00738

Jackson, E. L., Willis, N., Mercer, K., Bronson, R. T., Crowley, D., Montoya, R., . . . Tuveson, D. A. (2001). Analysis of lung tumor initiation and progression using conditional expression of oncogenic K-ras. *Genes Dev, 15*(24), 3243-3248. doi:10.1101/gad.943001

Jarvinen, T., Ilonen, I., Kauppi, J., Salo, J., & Rasanen, J. (2018). Loss of skeletal muscle mass during neoadjuvant treatments correlates with worse prognosis in esophageal cancer: a retrospective cohort study. *World J Surg Oncol, 16*(1), 27. doi:10.1186/s12957-018-1327-4

Jatoi, A., Hillman, S., Stella, P., Mailliard, J., Sloan, J., Vanone, S., . . . Jett, J. (2003). Daily activities: exploring their spectrum and prognostic impact in older, chemotherapy-treated lung cancer patients. *Supportive Care in Cancer, 11*(7), 460-464. doi:10.1007/s00520-003-0449-5

Jee, H., Chang, J. E., & Yang, E. J. (2016). Positive Prehabilitative Effect of Intense Treadmill Exercise for Ameliorating Cancer Cachexia Symptoms in a Mouse Model. *J Cancer, 7*(15), 2378-2387. doi:10.7150/jca.17162

Johns, N., Stephens, N. A., & Fearon, K. C. (2013). Muscle wasting in cancer. *Int J Biochem Cell Biol, 45*(10), 2215-2229. doi:10.1016/j.biocel.2013.05.032

Jones, L. W., Courneya, K. S., Mackey, J. R., Muss, H. B., Pituskin, E. N., Scott, J. M., . . . Haykowsky, M. (2012). Cardiopulmonary function and age-related decline across the breast cancer survivorship continuum. *J Clin Oncol, 30*(20), 2530-2537. doi:10.1200/jco.2011.39.9014

Jones, L. W., Eves, N. D., Haykowsky, M., Freedland, S. J., & Mackey, J. R. (2009). Exercise intolerance in cancer and the role of exercise therapy to reverse dysfunction. *Lancet Oncol, 10*(6), 598-605. doi:10.1016/s1470-2045(09)70031-2

Jones, L. W., Hornsby, W. E., Goetzinger, A., Forbes, L. M., Sherrard, E. L., Quist, M., . . . Abernethy, A. P. (2012). Prognostic significance of functional capacity and exercise behavior in patients with metastatic non-small cell lung cancer. *Lung Cancer, 76*(2), 248-252. doi:10.1016/j.lungcan.2011.10.009

Jones, S., Man, W. D., Gao, W., Higginson, I. J., Wilcock, A., & Maddocks, M. (2016). Neuromuscular electrical stimulation for muscle weakness in adults with advanced disease. *Cochrane Database Syst Rev, 10*, CD009419. doi:10.1002/14651858.CD009419.pub3

Jourdain, M., Melly, S., Summermatter, S., & Hatakeyama, S. (2018). Mouse models of cancer-induced cachexia: Hind limb muscle mass and evoked force as readouts. *Biochem Biophys Res Commun, 503*(4), 2415-2420. doi:10.1016/j.bbrc.2018.06.170

Julienne, C., Dumas, J.-F., Goupille, C., Pinault, M., Berri, C., Collin, A., . . . Servais, S. (2012). Cancer cachexia is associated with a decrease in skeletal muscle mitochondrial oxidative capacities without alteration of ATP production efficiency. *Journal of Cachexia, Sarcopenia and Muscle, 3*(4), 265-275. doi:10.1007/s13539-012-0071-9

Julienne, C. M., Dumas, J. F., Goupille, C., Pinault, M., Berri, C., Collin, A., . . . Servais, S. (2012). Cancer cachexia is associated with a decrease in skeletal muscle mitochondrial oxidative capacities without alteration of ATP production efficiency. *J Cachexia Sarcopenia Muscle, 3*(4), 265-275. doi:10.1007/s13539-012-0071-9

Jun, I., Jeong, S., & Shin, H. (2009). The stimulation of myoblast differentiation by electrically conductive sub-micron fibers. *Biomaterials, 30*(11), 2038-2047. doi:10.1016/j.biomaterials.2008.12.063

Juvet, L. K., Thune, I., Elvsaas, I. K. O., Fors, E. A., Lundgren, S., Bertheussen, G., . . . Oldervoll, L. M. (2017). The effect of exercise on fatigue and physical functioning in breast cancer patients during and after treatment and at 6 months follow-up: A meta-analysis. *Breast, 33*, 166-177. doi:10.1016/j.breast.2017.04.003

Kaji, H., Ishibashi, T., Nagamine, K., Kanzaki, M., & Nishizawa, M. (2010). Electrically induced contraction of C2C12 myotubes cultured on a porous membrane-based substrate with muscle tissue-like stiffness. *Biomaterials, 31*(27), 6981-6986. doi:10.1016/j.biomaterials.2010.05.071

Kang, C., Goodman, C. A., Hornberger, T. A., & Ji, L. L. (2015). PGC-1alpha overexpression by in vivo transfection attenuates mitochondrial deterioration of skeletal muscle caused by immobilization. *FASEB J, 29*(10), 4092-4106. doi:10.1096/fj.14-266619

Kang, C., & Ji, L. L. (2016). PGC-1alpha overexpression via local transfection attenuates mitophagy pathway in muscle disuse atrophy. *Free Radic Biol Med, 93*, 32-40. doi:10.1016/j.freeradbiomed.2015.12.032

Kang, C., & Li Ji, L. (2012). Role of PGC-1alpha signaling in skeletal muscle health and disease. *Ann N Y Acad Sci, 1271*, 110-117. doi:10.1111/j.1749-6632.2012.06738.x

Kang, C., O'Moore, K. M., Dickman, J. R., & Ji, L. L. (2009). Exercise activation of muscle peroxisome proliferator-activated receptor-gamma coactivator-1alpha signaling is redox sensitive. *Free Radic Biol Med, 47*(10), 1394-1400. doi:10.1016/j.freeradbiomed.2009.08.007

Kavazis, A. N., Smuder, A. J., & Powers, S. K. (2014). Effects of short-term endurance exercise training on acute doxorubicin-induced FoxO transcription in cardiac and skeletal muscle. *J Appl Physiol (1985), 117*(3), 223-230. doi:10.1152/japplphysiol.00210.2014

Kemmler, W., Bebenek, M., Engelke, K., & von Stengel, S. (2014). Impact of whole-body electromyostimulation on body composition in elderly women at risk for sarcopenia: the Training and ElectroStimulation Trial (TEST-III). *Age (Dordr), 36*(1), 395-406. doi:10.1007/s11357-013-9575-2

Kerr, J. P., Robison, P., Shi, G., Bogush, A. I., Kempema, A. M., Hexum, J. K., . . . Ward, C. W. (2015). Detyrosinated microtubules modulate mechanotransduction in heart and skeletal muscle. *Nat Commun, 6*, 8526. doi:10.1038/ncomms9526

Khairallah, R. J., Shi, G., Sbrana, F., Prosser, B. L., Borroto, C., Mazaitis, M. J., . . . Ward, C. W. (2012). Microtubules underlie dysfunction in Duchenne muscular dystrophy. *Sci Signal, 5*(236), 10.1126/scisignal.2002829. doi:10.1126/scisignal.2002829

Khairallah, R. J., Shi, G., Sbrana, F., Prosser, B. L., Borroto, C., Mazaitis, M. J., . . . Ward, C. W. (2012). Microtubules underlie dysfunction in duchenne muscular dystrophy. *Sci Signal, 5*(236), ra56. doi:10.1126/scisignal.2002829

Kim, J. S., & Yi, H. K. (2018). Schisandrin C enhances mitochondrial biogenesis and autophagy in C2C12 skeletal muscle cells: potential involvement of anti-oxidative mechanisms. *Naunyn Schmiedebergs Arch Pharmacol, 391*(2), 197-206. doi:10.1007/s00210-017-1449-1

Kinney, M. C., Dayanidhi, S., Dykstra, P. B., McCarthy, J. J., Peterson, C. A., & Lieber, R. L. (2017). Reduced skeletal muscle satellite cell number alters muscle morphology after chronic stretch but allows limited serial sarcomere addition. *Muscle Nerve, 55*(3), 384-392. doi:10.1002/mus.25227

Kislinger, T., Gramolini, A. O., Pan, Y., Rahman, K., MacLennan, D. H., & Emili, A. (2005). Proteome dynamics during C2C12 myoblast differentiation. *Mol Cell Proteomics, 4*(7), 887-901. doi:10.1074/mcp.M400182-MCP200

Kontrogianni-Konstantopoulos, A., Catino, D. H., Strong, J. C., & Bloch, R. J. (2006). De novo myofibrillogenesis in C2C12 cells: evidence for the independent assembly of M bands and Z disks. *Am J Physiol Cell Physiol, 290*(2), C626-637. doi:10.1152/ajpcell.00442.2005

Kontrogianni-Konstantopoulos, A., Catino, D. H., Strong, J. C., & Bloch, R. J. (2006). De novo myofibrillogenesis in C2C12 cells: evidence for the independent assembly of M bands and Z disks. *Am J Physiol Cell Physiol, 290*(2), C626-C637. doi:10.1152/ajpcell.00442.2005

Kumar, A., Chaudhry, I., Reid, M. B., & Boriek, A. M. (2002). Distinct signaling pathways are activated in response to mechanical stress applied axially and transversely to skeletal muscle fibers. *J Biol Chem, 277*(48), 46493-46503. doi:10.1074/jbc.M203654200

Lai, K. M., Gonzalez, M., Poueymirou, W. T., Kline, W. O., Na, E., Zlotchenko, E., . . . Glass, D. J. (2004). Conditional activation of akt in adult skeletal muscle induces rapid hypertrophy. *Mol Cell Biol, 24*(21), 9295-9304. doi:10.1128/MCB.24.21.9295-9304.2004

Lakoski, S. G., Barlow, C. E., Koelwyn, G. J., Hornsby, W. E., Hernandez, J., DeFina, L. F., . . . Jones, L. W. (2013). The influence of adjuvant therapy on cardiorespiratory fitness in early-stage breast cancer seven years after diagnosis: the Cooper Center Longitudinal Study. *Breast Cancer Res Treat, 138*(3), 909-916. doi:10.1007/s10549-013-2478-1

Langen, R. C. J., Schols, A. M. W. J., Kelders, M. C. J. M., Wouters, E. F. M., & Janssen-Heininger, Y. M. W. (2003). Enhanced myogenic differentiation by extracellular matrix is regulated at the early stages of myogenesis. *In Vitro Cell Dev Biol Anim, 39*(3), 163-169. doi:10.1007/s11626-003-0011-2

Lanic, H., Kraut-Tauzia, J., Modzelewski, R., Clatot, F., Mareschal, S., Picquenot, J. M., . . . Jardin, F. (2014). Sarcopenia is an independent prognostic factor in elderly patients with diffuse large B-cell lymphoma treated with immunochemotherapy. *Leuk Lymphoma, 55*(4), 817-823. doi:10.3109/10428194.2013.816421

Lanza, I. R., & Nair, K. S. (2009). Chapter 20: Functional Assessment of Isolated Mitochondria In Vitro. In S. A. William & N. M. Anne (Eds.), *Methods in Enzymology* (Vol. 457, pp. 349-372): Academic Press.

LeBlanc, T. W., Nipp, R. D., Rushing, C. N., Samsa, G. P., Locke, S. C., Kamal, A. H., . . . Abernethy, A. P. (2015). Correlation between the international consensus definition of the Cancer Anorexia-Cachexia Syndrome (CACS) and patient-centered outcomes in advanced non-small cell lung cancer. *J Pain Symptom Manage, 49*(4), 680-689. doi:10.1016/j.jpainsymman.2014.09.008

Lebrecht, D., Setzer, B., Ketelsen, U. P., Haberstroh, J., & Walker, U. A. (2003). Time-dependent and tissue-specific accumulation of mtDNA and respiratory chain defects in chronic doxorubicin cardiomyopathy. *Circulation, 108*(19), 2423-2429. doi:10.1161/01.CIR.0000093196.59829.DF

Lebrecht, D., Setzer, B., Rohrbach, R., & Walker, U. A. (2004). Mitochondrial DNA and its respiratory chain products are defective in doxorubicin nephrosis. *Nephrol Dial Transplant, 19*(2), 329-336.

Lee, D. E., Brown, J. L., Rosa-Caldwell, M. E., Blackwell, T. A., Perry, R. A., Jr., Brown, L. A., . . . Greene, N. P. (2017). Cancer cachexia-induced muscle atrophy: evidence for alterations in microRNAs important for muscle size. *Physiol Genomics, 49*(5), 253-260. doi:10.1152/physiolgenomics.00006.2017

Lee, H., Lee, S. J., Bae, G. U., Baek, N. I., & Ryu, J. H. (2017). Canadine from Corydalis turtschaninovii Stimulates Myoblast Differentiation and Protects against Myotube Atrophy. *Int J Mol Sci, 18*(12). doi:10.3390/ijms18122748

Lee, H. W., Baker, E., Lee, K. M., Persinger, A. M., Hawkins, W., & Puppa, M. (2019). Effects of low dose leucine supplementation on gastrocnemius muscle mitochondrial content and protein turnover in tumor bearing mice. *Appl Physiol Nutr Metab*. doi:10.1139/apnm-2018-0765

Lee, I. H., Lee, Y. J., Seo, H., Kim, Y. S., Nam, J. O., Jeon, B. D., & Kwon, T. D. (2018). Study of muscle contraction induced by electrical pulse stimulation and nitric oxide in C2C12 myotube cells. *J Exerc Nutrition Biochem, 22*(1), 22-28. doi:10.20463/jenb.2018.0004

Lee, J. H., Tachibana, H., Morinaga, Y., Fujimura, Y., & Yamada, K. (2009). Modulation of proliferation and differentiation of C2C12 skeletal muscle cells by fatty acids. *Life Sci, 84*(13-14), 415-420. doi:10.1016/j.lfs.2009.01.004

Lee, K.-P., Shin, Y. J., Cho, S. C., Lee, S.-M., Bahn, Y. J., Kim, J. Y., . . . Kwon, K.-S. (2014). Peroxiredoxin 3 has a crucial role in the contractile function of skeletal muscle by regulating mitochondrial homeostasis. *Free Rad Biol Med, 77*, 298-306. doi:https://doi.org/10.1016/j.freeradbiomed.2014.09.010

Lenk, K., Schuler, G., & Adams, V. (2010). Skeletal muscle wasting in cachexia and sarcopenia: molecular pathophysiology and impact of exercise training. *J Cachexia Sarcopenia Muscle, 1*(1), 9-21. doi:10.1007/s13539-010-0007-1

Li, Y. P., Chen, Y., John, J., Moylan, J., Jin, B., Mann, D. L., & Reid, M. B. (2005). TNF-alpha acts via p38 MAPK to stimulate expression of the ubiquitin ligase atrogin1/MAFbx in skeletal muscle. *FASEB J, 19*(3), 362-370. doi:10.1096/fj.04-2364com

Liu, M.-H., Zhang, Y., He, J. U. N., Tan, T.-P., Wu, S.-J., Fu, H.-Y., . . . Lin, X.-L. (2015). Upregulation of peroxiredoxin III in doxorubicin-induced cytotoxicity and the FoxO3a-dependent expression in H9c2 cardiac cells. *Exp Ther Med, 10*(4), 1515-1520. doi:10.3892/etm.2015.2693

Livak, K. J., & Schmittgen, T. D. (2001). Analysis of relative gene expression data using real-time quantitative PCR and the 2(-Delta Delta C(T)) Method. *Methods, 25*(4), 402-408. doi:10.1006/meth.2001.1262

Llovera, M., Garcia-Martinez, C., Lopez-Soriano, J., Agell, N., Lopez-Soriano, F. J., Garcia, I., & Argiles, J. M. (1998). Protein turnover in skeletal muscle of tumour-bearing transgenic mice overexpressing the soluble TNF receptor-1. *Cancer Lett, 130*(1-2), 19-27.

Loprinzi, C. L., Ellison, N. M., Goldberg, R. M., Michalak, J. C., & Burch, P. A. (1990). Alleviation of cancer anorexia and cachexia: studies of the Mayo Clinic and the North Central Cancer Treatment Group. *Semin Oncol, 17*(6 Suppl 9), 8-12.

Luo, Y., & Shoichet, M. S. (2004). Light-activated immobilization of biomolecules to agarose hydrogels for controlled cellular response. *Biomacromolecules, 5*(6), 2315-2323. doi:10.1021/bm0495811

Luo, Z., Ma, L., Zhao, Z., He, H., Yang, D., Feng, X., . . . Zhu, Z. (2012). TRPV1 activation improves exercise endurance and energy metabolism through PGC-1alpha upregulation in mice. *Cell Res, 22*(3), 551-564. doi:10.1038/cr.2011.205

Maddocks, M., Armstrong, S., & Wilcock, A. (2011). Exercise as a supportive therapy in incurable cancer: exploring patient preferences. *Psychooncology, 20*(2), 173-178. doi:10.1002/pon.1720

Maddocks, M., Murton, A. J., & Wilcock, A. (2012). Therapeutic exercise in cancer cachexia. *Crit Rev Oncog, 17*(3), 285-292.

Maffiuletti, N. A., Gondin, J., Place, N., Stevens-Lapsley, J., Vivodtzev, I., & Minetto, M. A. (2018). Clinical Use of Neuromuscular Electrical Stimulation for Neuromuscular Rehabilitation: What Are We Overlooking? *Arch Phys Med Rehabil, 99*(4), 806-812. doi:10.1016/j.apmr.2017.10.028

Manabe, Y., Miyatake, S., Takagi, M., Nakamura, M., Okeda, A., Nakano, T., . . . Fujii, N. L. (2012). Characterization of an acute muscle contraction model using cultured C2C12 myotubes. *PLoS One, 7*(12), e52592. doi:10.1371/journal.pone.0052592

Manabe, Y., Miyatake, S., Takagi, M., Nakamura, M., Okeda, A., Nakano, T., . . . Fujii, N. L. (2013). Characterization of an acute muscle contraction model using cultured C2C12 myotubes. *PLoS ONE, 7*(12), e52592. doi:10.1371/journal.pone.0052592

Mantovani, G., & Madeddu, C. (2010). Cancer cachexia: medical management. *Support Care Cancer, 18*(1), 1-9. doi:10.1007/s00520-009-0722-3

Mason, C., Alfano, C. M., Smith, A. W., Wang, C. Y., Neuhouser, M. L., Duggan, C., . . . McTiernan, A. (2013). Long-term physical activity trends in breast cancer survivors. *Cancer Epidemiol Biomarkers Prev, 22*(6), 1153-1161. doi:10.1158/1055-9965.EPI-13-0141

Matsuyama, T., Ishikawa, T., Okayama, T., Oka, K., Adachi, S., Mizushima, K., . . . Itoh, Y. (2015). Tumor inoculation site affects the development of cancer cachexia and muscle wasting. *Int J Cancer, 137*(11), 2558-2565. doi:10.1002/ijc.29620

McCarthy, J. J., & Esser, K. A. (2007). Counterpoint: Satellite cell addition is not obligatory for skeletal muscle hypertrophy. *J Appl Physiol (1985), 103*(3), 1100-1102; discussion 1102-1103. doi:10.1152/japplphysiol.00101.2007a

McLean, J., Moylan, J. S., & Andrade, F. H. (2014). Mitochondria dysfunction in lung cancer-induced muscle wasting in C2C12 myotubes. *Front Physiol, 5*. doi:10.3389/fphys.2014.00503

McLean, J. B., Moylan, J. S., & Andrade, F. H. (2014). Mitochondria dysfunction in lung cancer-induced muscle wasting in C2C12 myotubes. *Front Physiol, 5*, 503. doi:10.3389/fphys.2014.00503

McLean, J. B., Moylan, J. S., Horrell, E. M., & Andrade, F. H. (2015). Proteomic analysis of media from lung cancer cells reveals role of 14-3-3 proteins in cachexia. *Front Physiol, 6*, 136. doi:10.3389/fphys.2015.00136

McLoon, L. K., Falkenberg, J. H., Dykstra, D., & Iaizzo, P. A. (1998). Doxorubicin chemomyectomy as a treatment for cervical dystonia: histological assessment after direct injection into the sternocleidomastoid muscle. *Muscle Nerve, 21*(11), 1457-1464.

McMahon, D. K., Anderson, P. A., Nassar, R., Bunting, J. B., Saba, Z., Oakeley, A. E., & Malouf, N. N. (1994). C2C12 cells: biophysical, biochemical, and immunocytochemical properties. *Am J Physiol, 266*(6 Pt 1), C1795-1802. doi:10.1152/ajpcell.1994.266.6.C1795

McTiernan, A., Kooperberg, C., White, E., & et al. (2003). Recreational physical activity and the risk of breast cancer in postmenopausal women: The Women's Health Initiative cohort study. *JAMA, 290*(10), 1331-1336. doi:10.1001/jama.290.10.1331

Mijwel, S., Cardinale, D. A., Norrbom, J., Chapman, M., Ivarsson, N., Wengstrom, Y., . . . Rundqvist, H. (2018). Exercise training during chemotherapy preserves skeletal muscle fiber area, capillarization, and mitochondrial content in patients with breast cancer. *FASEB J, 32*(10), 5495-5505. doi:10.1096/fj.201700968R

Mijwel, S., Cardinale, D. A., Norrbom, J., Chapman, M., Ivarsson, N., Wengström, Y., . . . Rundqvist, H. Exercise training during chemotherapy preserves skeletal muscle fiber area, capillarization, and mitochondrial content in patients with breast cancer. *FASEB J, 0*(0), fj.201700968R. doi:10.1096/fj.201700968R

Mikkelsen, U. R., Agergaard, J., Couppe, C., Grosset, J. F., Karlsen, A., Magnusson, S. P., . . . Mackey, A. L. (2017). Skeletal muscle morphology and regulatory signalling in endurance-trained and sedentary individuals: The influence of ageing. *Exp Gerontol, 93*, 54-67. doi:10.1016/j.exger.2017.04.001

Miller, A., McLeod, L., Alhayyani, S., Szczepny, A., Watkins, D. N., Chen, W., . . . Jenkins, B. J. (2017). Blockade of the IL-6 trans-signalling/STAT3 axis suppresses cachexia in Kras-induced lung adenocarcinoma. *Oncogene, 36*(21), 3059-3066. doi:10.1038/onc.2016.437

Miller, K. L., Kocak, Z., Kahn, D., Zhou, S.-M., Baydush, A., Hollis, D., . . . Marks, L. B. (2005). Preliminary report of the 6-minute walk test as a predictor of radiation-induced pulmonary toxicity. *Int J Radiation Oncology Biol Phys, 62*(4), 1009-1013. doi:10.1016/j.ijrobp.2004.12.054

Miller, M. S., Callahan, D. M., Tourville, T. W., Slauterbeck, J. R., Kaplan, A., Fiske, B. R., . . . Toth, M. J. (2017). Moderate-intensity resistance exercise alters skeletal muscle molecular and cellular structure and function in inactive older adults with knee osteoarthritis. *J Appl Physiol (1985), 122*(4), 775-787. doi:10.1152/japplphysiol.00830.2016

Miller, M. S., Callahan, D. M., Tourville, T. W., Slauterbeck, J. R., Kaplan, A., Fiske, B. R., . . . Toth, M. J. (2017). Moderate-intensity resistance exercise alters skeletal muscle molecular and cellular structure and function in inactive, older adults with knee osteoarthritis. *J Appl Physiol, 122*, 775-787.

Miller, R. P., Tadagavadi, R. K., Ramesh, G., & Reeves, W. B. (2010). Mechanisms of Cisplatin nephrotoxicity. *Toxins (Basel), 2*(11), 2490-2518. doi:10.3390/toxins2112490

Min, K., Kwon, O.-S., Smuder, A. J., Wiggs, M. P., Sollanek, K. J., Christou, D. D., . . . Powers, S. K. (2015). Increased mitochondrial emission of reactive oxygen species and calpain activation are required for doxorubicin-induced cardiac and skeletal muscle myopathy. *J Physiol, 593*(8), 2017-2036. doi:10.1113/jphysiol.2014.286518

Min, K., Kwon, O. S., Smuder, A. J., Wiggs, M. P., Sollanek, K. J., Christou, D. D., . . . Powers, S. K. (2015). Increased mitochondrial emission of reactive oxygen species and calpain activation are required for doxorubicin-induced cardiac and skeletal muscle myopathy. *J Physiol, 593*(8), 2017-2036. doi:10.1113/jphysiol.2014.286518

Mitch, W. E., & Goldberg, A. L. (1996). Mechanisms of muscle wasting. The role of the ubiquitin-proteasome pathway. *N Engl J Med, 335*(25), 1897-1905. doi:10.1056/NEJM199612193352507

Mitsui, T., Umaki, Y., Nagasawa, M., Akaike, M., Aki, K., Azuma, H., . . . Matsumoto, T. (2002). Mitochondrial damage in patients with long-term corticosteroid therapy: development of oculoskeletal symptoms similar to mitochondrial disease. *Acta Neuropathol, 104*(3), 260-266. doi:10.1007/s00401-002-0553-5

Miyatake, S., Bilan, P. J., Pillon, N. J., & Klip, A. (2016). Contracting C2C12 myotubes release CCL2 in an NF-κB-dependent manner to induce monocyte chemoattraction. *Am J Physiol Endocrinol Metab, 310*(2), E160-E170. doi:10.1152/ajpendo.00325.2015

Monster, A. W., & Chan, H. (1977). Isometric force production by motor units of extensor digitorum communis muscle in man. *J Neurophysiol, 40*(6), 1432-1443. doi:10.1152/jn.1977.40.6.1432

Montgomery, M. K., Osborne, B., Brown, S. H. J., Small, L., Mitchell, T. W., Cooney, G. J., & Turner, N. (2013). Contrasting metabolic effects of medium- vs. long-chain fatty acids in skeletal muscle. *J Lipid Res, 54*, 3322-3333. doi:10.1194/jlr.M040451

Morley, J. E., Anker, S. D., & von Haehling, S. (2014). Prevalence, incidence, and clinical impact of sarcopenia: facts, numbers, and epidemiology-update 2014. *J Cachexia Sarcopenia Muscle, 5*(4), 253-259. doi:10.1007/s13539-014-0161-y

Morvan, F., Rondeau, J. M., Zou, C., Minetti, G., Scheufler, C., Scharenberg, M., . . . Lach-Trifilieff, E. (2017). Blockade of activin type II receptors with a dual anti-ActRIIA/IIB antibody is critical to promote maximal skeletal muscle hypertrophy. *Proc Natl Acad Sci U S A, 114*(47), 12448-12453. doi:10.1073/pnas.1707925114

Moss, F. P., & Leblond, C. P. (1971). Satellite cells as the source of nuclei in muscles of growing rats. *Anat Rec, 170*(4), 421-435. doi:10.1002/ar.1091700405

Mueller, T. C., Bachmann, J., Prokopchuk, O., Friess, H., & Martignoni, M. E. (2016). Molecular pathways leading to loss of skeletal muscle mass in cancer cachexia--can findings from animal models be translated to humans? *BMC Cancer, 16*, 75. doi:10.1186/s12885-016-2121-8

Muller, M. J., Baracos, V., Bosy-Westphal, A., Dulloo, A. G., Eckel, J., Fearon, K. C., . . . Heymsfield, S. B. (2014). Functional body composition and related aspects in research on obesity and cachexia: report on the 12th Stock Conference held on 6 and 7 September 2013 in Hamburg, Germany. *Obes Rev, 15*(8), 640-656. doi:10.1111/obr.12187

Murphy, S. M., Kiely, M., Jakeman, P. M., Kiely, P. A., & Carson, B. P. (2016). Optimization of an in vitro bioassay to monitor growth and formation of myotubes in real time. *Biosci Rep, 36*(3). doi:10.1042/BSR20160036

Muscaritoli, M., Molfino, A., Gioia, G., Laviano, A., & Rossi Fanelli, F. (2011). The "parallel pathway": a novel nutritional and metabolic approach to cancer patients. *Intern Emerg Med, 6*(2), 105-112. doi:10.1007/s11739-010-0426-1

Nagamine, K., Kawashima, T., Ishibashi, T., Kaji, H., Kanzaki, M., & Nishizawa, M. (2010). Micropatterning contractile C2C12 myotubes embedded in a fibrin gel. *Biotechnol Bioeng, 105*(6), 1161-1167. doi:10.1002/bit.22636

Naito, T., Okayama, T., Aoyama, T., Ohashi, T., Masuda, Y., Kimura, M., . . . Takahashi, T. (2017). Unfavorable impact of cancer cachexia on activity of daily living and need for inpatient care in elderly patients with advanced non-small-cell lung cancer in Japan: a prospective longitudinal observational study. *BMC Cancer, 17*(1), 800. doi:10.1186/s12885-017-3795-2

Nakashima, K., & Yakabe, Y. (2007). AMPK activation stimulates myofibrillar protein degradation and expression of atrophy-related ubiquitin ligases by increasing FOXO transcription factors in C2C12 myotubes. *Biosci Biotechnol Biochem, 71*(7), 1650-1656.

Navari, R. M. (2018). Managing Nausea and Vomiting in Patients With Cancer: What Works. *Oncology (Williston Park), 32*(3), 121-125, 131, 136.

Nedachi, T., Fujita, H., & Kanzaki, M. (2008). Contractile C2C12 myotube model for studying exercise-inducible responses in skeletal muscle. *Am J Physiol Endocrinol Metab, 295*(5), E1191-1204. doi:10.1152/ajpendo.90280.2008

Niederst, M. J., Sequist, L. V., Poirier, J. T., Mermel, C. H., Lockerman, E. L., Garcia, A. R., . . . Engelman, J. A. (2015). RB loss in resistant EGFR mutant lung adenocarcinomas that transform to small-cell lung cancer. *Nat Commun, 6*. doi:10.1038/ncomms7377

Nystrom, G. J., & Lang, C. H. (2008). Sepsis and AMPK Activation by AICAR Differentially Regulate FoxO-1, -3 and -4 mRNA in Striated Muscle. *Int J Clin Exp Med, 1*(1), 50-63.

Ogawa, T., Furochi, H., Mameoka, M., Hirasaka, K., Onishi, Y., Suzue, N., . . . Nikawa, T. (2006). Ubiquitin ligase gene expression in healthy volunteers with 20-day bedrest. *Muscle Nerve, 34*(4), 463-469. doi:10.1002/mus.20611

Okamoto, T., & Machida, S. (2017). Changes in FOXO and proinflammatory cytokines in the late stage of immobilized fast and slow muscle atrophy. *Biomed Res, 38*(6), 331-342. doi:10.2220/biomedres.38.331

Oraldi, M., Maggiora, M., Paiuzzi, E., Canuto, R. A., & Muzio, G. (2013). CLA reduces inflammatory mediators from A427 human lung cancer cells and A427 conditioned medium promotes differentiation of C2C12 murine muscle cells. *Lipids, 48*(1), 29-38. doi:10.1007/s11745-012-3734-6

Orfanos, Z., Godderz, M. P., Soroka, E., Godderz, T., Rumyantseva, A., van der Ven, P. F., . . . Furst, D. O. (2016). Breaking sarcomeres by in vitro exercise. *Sci Rep, 6*, 19614. doi:10.1038/srep19614

Paillard, T. (2018). Muscle plasticity of aged subjects in response to electrical stimulation training and inversion and/or limitation of the sarcopenic process. *Ageing Res Rev, 46*, 1-13. doi:10.1016/j.arr.2018.05.002

Pallafacchina, G., Calabria, E., Serrano, A. L., Kalhovde, J. M., & Schiaffino, S. (2002). A protein kinase B-dependent and rapamycin-sensitive pathway controls skeletal muscle growth but not fiber type specification. *Proc Natl Acad Sci U S A, 99*(14), 9213-9218. doi:10.1073/pnas.142166599

Pardo, P. S., Lopez, M. A., & Boriek, A. M. (2008). FOXO transcription factors are mechanosensitive and their regulation is altered with aging in the respiratory pump. *Am J Physiol Cell Physiol, 294*(4), C1056-1066. doi:10.1152/ajpcell.00270.2007

Parry, C., Kent, E. E., Mariotto, A. B., Alfano, C. M., & Rowland, J. H. (2011). Cancer survivors: a booming population. *Cancer Epidemiol Biomarkers Prev, 20*(10), 1996-2005. doi:10.1158/1055-9965.epi-11-0729

Patel, J. D., Pereira, J. R., Chen, J., Liu, J., Guba, S. C., John, W. J., . . . Bonomi, P. D. (2016). Relationship between efficacy outcomes and weight gain during treatment of advanced, non-squamous, non-small-cell lung cancer patients. *Ann Oncol, 27*(8), 1612-1619. doi:10.1093/annonc/mdw211

Paul, P. K., Gupta, S. K., Bhatnagar, S., Panguluri, S. K., Darnay, B. G., Choi, Y., & Kumar, A. (2010). Targeted ablation of TRAF6 inhibits skeletal muscle wasting in mice. *J Cell Biol, 191*(7), 1395-1411. doi:10.1083/jcb.201006098

Penna, F., Busquets, S., & Argiles, J. M. (2016). Experimental cancer cachexia: Evolving strategies for getting closer to the human scenario. *Semin Cell Dev Biol, 54*, 20-27. doi:10.1016/j.semcdb.2015.09.002

Peterson, J. M., Bakkar, N., & Guttridge, D. C. (2011). NF-kappaB signaling in skeletal muscle health and disease. *Curr Top Dev Biol, 96*, 85-119. doi:10.1016/B978-0-12-385940-2.00004-8

Petrella, J. K., Kim, J. S., Cross, J. M., Kosek, D. J., & Bamman, M. M. (2006). Efficacy of myonuclear addition may explain differential myofiber growth among resistance-trained young and older men and women. *Am J Physiol Endocrinol Metab, 291*(5), E937-946.

Pette, D., Peuker, H., & Staron, R. S. (1999). The impact of biochemical methods for single muscle fibre analysis. *Acta Physiol Scand, 166*(4), 261-277. doi:10.1046/j.1365-201x.1999.00568.x

Pigna, E., Berardi, E., Aulino, P., Rizzuto, E., Zampieri, S., Carraro, U., . . . Moresi, V. (2016). Aerobic Exercise and Pharmacological Treatments Counteract Cachexia by Modulating Autophagy in Colon Cancer. *Sci Rep, 6*, 26991. doi:10.1038/srep26991

Pin, F., Busquets, S., Toledo, M., Camperi, A., Lopez-Soriano, F. J., Costelli, P., . . . Penna, F. (2015). Combination of exercise training and erythropoietin prevents cancer-induced muscle alterations. *Oncotarget, 6*(41), 43202-43215. doi:10.18632/oncotarget.6439

Piscitelli, S. C., Rodvold, K. A., Rushing, D. A., & Tewksbury, D. A. (1993). Pharmacokinetics and pharmacodynamics of doxorubicin in patients with small cell lung cancer. *Clin Pharm Ther, 53*(5), 555-561. doi:10.1038/clpt.1993.69

Polomano, R. C., Mannes, A. J., Clark, U. S., & Bennett, G. J. (2001). A painful peripheral neuropathy in the rat produced by the chemotherapeutic drug, paclitaxel. *Pain, 94*(3), 293-304.

Powers, S. K., Duarte, J. A., Le Nguyen, B., & Hyatt, H. (2018). Endurance exercise protects skeletal muscle against both doxorubicin-induced and inactivity-induced muscle wasting. *Pflugers Arch*. doi:10.1007/s00424-018-2227-8

Powers, S. K., Duarte, J. A., Le Nguyen, B., & Hyatt, H. (2019). Endurance exercise protects skeletal muscle against both doxorubicin-induced and inactivity-induced muscle wasting. *Pflugers Arch, 471*(3), 441-453. doi:10.1007/s00424-018-2227-8

Powers, S. K., Morton, A. B., Ahn, B., & Smuder, A. J. (2016). Redox control of skeletal muscle atrophy. *Free Rad Biol Med, 98*, 208-217. doi:http://dx.doi.org/10.1016/j.freeradbiomed.2016.02.021

Poynton, R. A., & Hampton, M. B. (2014). Peroxiredoxins as biomarkers of oxidative stress. *Biochim Biophys Acta, 1840*(2), 906-912. doi:https://doi.org/10.1016/j.bbagen.2013.08.001

Prado, C. M., Baracos, V. E., McCargar, L. J., Reiman, T., Mourtzakis, M., Tonkin, K., . . . Sawyer, M. B. (2009). Sarcopenia as a determinant of chemotherapy toxicity and time to tumor progression in metastatic breast cancer patients receiving capecitabine treatment. *Clin Cancer Res, 15*(8), 2920-2926. doi:10.1158/1078-0432.CCR-08-2242

Prado, C. M., Sawyer, M. B., Ghosh, S., Lieffers, J. R., Esfandiari, N., Antoun, S., & Baracos, V. E. (2013). Central tenet of cancer cachexia therapy: do patients with advanced cancer have exploitable anabolic potential? *Am J Clin Nutr, 98*(4), 1012-1019. doi:10.3945/ajcn.113.060228

Prado, C. M. M., Baracos, V. E., McCargar, L. J., Reiman, T., Mortzakis, M., Tonkin, K., . . . Sawyer, M. B. (2009). Sarcopenia as a determinant of chemotherapy toxicity and time to tumor progression in metastatic breast cancer patients receiving capecitabine treatment. *Clin Cancer Res, 15*, 2920-2926.

Puppa, M. J., White, J. P., Velazquez, K. T., Baltgalvis, K. A., Sato, S., Baynes, J. W., & Carson, J. A. (2012). The effect of exercise on IL-6-induced cachexia in the Apc (Min/+) mouse. *J Cachexia Sarcopenia Muscle, 3*(2), 117-137. doi:10.1007/s13539-011-0047-1

Puyol, M., Martin, A., Dubus, P., Mulero, F., Pizcueta, P., Khan, G., . . . Barbacid, M. (2010). A synthetic lethal interaction between K-Ras oncogenes and Cdk4 unveils a therapeutic strategy for non-small cell lung carcinoma. *Cancer Cell, 18*(1), 63-73. doi:10.1016/j.ccr.2010.05.025

Raven, P. B. (2013). *Exercise physiology : an integrated approach*. Australia ; Belmont, CA: Wadsworth Cengage Learning.

Reeve, B. B., Potosky, A. L., Smith, A. W., Han, P. K., Hays, R. D., Davis, W. W., . . . Clauser, S. B. (2009). Impact of cancer on health-related quality of life of older Americans. *J Natl Compr Canc Netw, 101*(12), 860-868. doi:10.1093/jnci/djp123

Remels, A. H., Gosker, H. R., Schrauwen, P., Hommelberg, P. P., Sliwinski, P., Polkey, M., . . . Schols, A. M. (2010). TNF-alpha impairs regulation of muscle oxidative phenotype: implications for cachexia? *FASEB J, 24*(12), 5052-5062. doi:10.1096/fj.09-150714

Renaud, G., Llano-Diez, M., Ravara, B., Gorza, L., Feng, H. Z., Jin, J. P., . . . Larsson, L. (2013). Sparing of muscle mass and function by passive loading in an experimental intensive care unit model. *J Physiol, 591*(5), 1385-1402. doi:10.1113/jphysiol.2012.248724

Rengo, J. L., Callahan, D. M., Savage, P. D., Ades, P. A., & Toth, M. J. (2016). Skeletal muscle ultrastructure and function in statin-tolerant individuals. *Muscle Nerve, 53*, 242-251. doi:10.1002/mus.24722

Reynolds, T. H. t., Merrell, E., Cinquino, N., Gaugler, M., & Ng, L. (2012). Disassociation of insulin action and Akt/FOXO signaling in skeletal muscle of older Akt-deficient mice. *Am J Physiol Regul Integr Comp Physiol, 303*(11), R1186-1194. doi:10.1152/ajpregu.00358.2012

Robert, F., Mills, J. R., Agenor, A., Wang, D., DiMarco, S., Cencic, R., . . . Pelletier, J. (2012). Targeting protein synthesis in a Myc/mTOR-driven model of anorexia-cachexia syndrome delays its onset and prolongs survival. *Cancer Res, 72*(3), 747-756. doi:10.1158/0008-5472.CAN-11-2739

Romanello, V., Guadagnin, E., Gomes, L., Roder, I., Sandri, C., Petersen, Y., . . . Sandri, M. (2010). Mitochondrial fission and remodelling contributes to muscle atrophy. *EMBO J, 29*(10), 1774-1785. doi:10.1038/emboj.2010.60

Romanello, V., Guadagnin, E., Gomes, L., Roder, I., Sandri, C., Petersen, Y., . . . Sandri, M. (2010). Mitochondrial fission and remodelling contributes to muscle atrophy. *EMBO J, 29*, 1774-1785.

Rommel, C., Bodine, S. C., Clarke, B. A., Rossman, R., Nunez, L., Stitt, T. N., . . . Glass, D. J. (2001). Mediation of IGF-1-induced skeletal myotube hypertrophy by PI(3)K/Akt/mTOR and PI(3)K/Akt/GSK3 pathways. *Nat Cell Biol, 3*(11), 1009-1013. doi:10.1038/ncb1101-1009

Rommel, C., Clarke, B. A., Zimmermann, S., Nunez, L., Rossman, R., Reid, K., . . . Glass, D. J. (1999). Differentiation stage-specific inhibition of the Raf-MEK-ERK pathway by Akt. *Science, 286*(5445), 1738-1741.

Rotwein, P., & Wilson, E. M. (2009). Distinct actions of Akt1 and Akt2 in skeletal muscle differentiation. *J Cell Physiol, 219*(2), 503-511. doi:10.1002/jcp.21692

Runte, K. E., Bell, S. P., Selby, D. E., Haussler, T. N., Ashikaga, T., LeWinter, M. M., . . . Meyer, M. (2017). Relaxation and the Role of Calcium in Isolated Contracting Myocardium From Patients With Hypertensive Heart Disease and Heart Failure With Preserved Ejection Fraction. *Circ Heart Fail, 10*(8). doi:10.1161/CIRCHEARTFAILURE.117.004311

Sakai, H., Kimura, M., Isa, Y., Yabe, S., Maruyama, A., Tsuruno, Y., . . . Narita, M. (2017). Effect of acute treadmill exercise on cisplatin-induced muscle atrophy in the mouse. *Pflugers Arch, 469*(11), 1495-1505. doi:10.1007/s00424-017-2045-4

Sakellariou, G. K., Vasilaki, A., Palomero, J., Kayani, A., Zibrik, L., McArdle, A., & Jackson, M. J. (2013). Studies of mitochondrial and nonmitochondrial sources implicate nicotinamide adenine dinucleotide phosphate oxidase(s) in the increased skeletal muscle superoxide generation that occurs during contractile activity. *Antioxid Redox Signal, 18*(6), 603-621. doi:10.1089/ars.2012.4623

Samuels, S. E., Knowles, A. L., Tilignac, T., Debiton, E., Madelmont, J. C., & Attaix, D. (2000). Protein metabolism in the small intestine during cancer cachexia and chemotherapy in mice. *Cancer Res, 60*(17), 4968-4974.

Sanchez, A. M., Csibi, A., Raibon, A., Cornille, K., Gay, S., Bernardi, H., & Candau, R. (2012). AMPK promotes skeletal muscle autophagy through activation of forkhead FoxO3a and interaction with Ulk1. *J Cell Biochem, 113*(2), 695-710. doi:10.1002/jcb.23399

Sandri, M. (2008). Signaling in muscle atrophy and hypertrophy. *Physiology (Bethesda), 23*, 160-170. doi:10.1152/physiol.00041.2007

Sandri, M., Lin, J., Handschin, C., Yang, W., Arany, Z. P., Lecker, S. H., . . . Spiegelman, B. M. (2006). PGC-1alpha protects skeletal muscle from atrophy by suppressing FoxO3 action and atrophy-specific gene transcription. *Proc Natl Acad Sci U S A, 103*(44), 16260-16265. doi:10.1073/pnas.0607795103

Sandri, M., Lin, J., Handschin, C., Yang, W., Arany, Z. P., Lecker, S. H., . . . Spiegelman, B. M. (2006). PGC-1α protects skeletal muscle from atrophy by suppressing FoxO3 action and atrophy-specific gene transcription. *Proc Natl Acad Sci, 103*(44), 16260-16265. doi:10.1073/pnas.0607795103

Sandri, M., Sandri, C., Gilbert, A., Skurk, C., Calabria, E., Picard, A., . . . Goldberg, A. L. (2004). Foxo transcription factors induce the atrophy-related ubiquitin ligase atrogin-1 and cause skeletal muscle atrophy. *Cell, 117*(3), 399-412.

Sartorelli, V., & Fulco, M. (2004). Molecular and cellular determinants of skeletal muscle atrophy and hypertrophy. *Sci STKE, 2004*(244), re11. doi:10.1126/stke.2442004re11

Schakman, O., Gilson, H., & Thissen, J. P. (2008). Mechanisms of glucocorticoid-induced myopathy. *J Endocrinol, 197*(1), 1-10. doi:10.1677/JOE-07-0606

Schakman, O., Kalista, S., Barbé, C., Loumaye, A., & Thissen, J. P. (2013). Glucocorticoid-induced skeletal muscle atrophy. *Int J Biochem Cell Biol, 45*(10), 2163-2172. doi:http://dx.doi.org/10.1016/j.biocel.2013.05.036

Schiaffino, S., & Mammucari, C. (2011). Regulation of skeletal muscle growth by the IGF1-Akt/PKB pathway: insights from genetic models. *Skelet Muscle, 1*(1), 4. doi:10.1186/2044-5040-1-4

Schiaffino, S., Rossi, A. C., Smerdu, V., Leinwand, L. A., & Reggiani, C. (2015). Developmental myosins: expression patterns and functional significance. *Skelet Muscle, 5*, 22. doi:10.1186/s13395-015-0046-6

Schiller, J. H., & Bittner, G. (1995). Loss of the tumorigenic phenotype with in vitro, but not in vivo, passaging of a novel series of human bronchial epithelial cell lines: possible role of an alpha 5/beta 1-integrin-fibronectin interaction. *Cancer Res, 55*(24), 6215-6221.

Schiller, J. H., Bittner, G., Oberley, T. D., Kao, C., Harris, C., & Meisner, L. F. (1992). Establishment and characterization of a SV40 T-antigen immortalized human bronchial epithelial cell line. *In Vitro Cell Dev Biol, 28A*(7-8), 461-464.

Schmidt, M. E., Chang-Claude, J., Seibold, P., Vrieling, A., Heinz, J., Flesch-Janys, D., & Steindorf, K. (2015). Determinants of long-term fatigue in breast cancer survivors: results of a prospective patient cohort study. *Psychooncology, 24*(1), 40-46. doi:10.1002/pon.3581

Sciancalepore, M., Coslovich, T., Lorenzon, P., Ziraldo, G., & Taccola, G. (2015). Extracellular stimulation with human "noisy" electromyographic patterns facilitates myotube activity. *J Muscle Res Cell Motil, 36*(4-5), 349-357. doi:10.1007/s10974-015-9424-2

Seo, E., Kang, H., Lim, O. K., & Jun, H. S. (2018). Supplementation with IL-6 and Muscle Cell Culture Conditioned Media Enhances Myogenic Differentiation of Adipose Tissue-Derived Stem Cells through STAT3 Activation. *Int J Mol Sci, 19*(6). doi:10.3390/ijms19061557

Seto, D. N., Kandarian, S. C., & Jackman, R. W. (2015). A Key Role for Leukemia Inhibitory Factor in C26 Cancer Cachexia. *J Biol Chem, 290*(32), 19976-19986. doi:10.1074/jbc.M115.638411

Shachar, S. S., Deal, A. M., Weinberg, M., Williams, G. R., Nyrop, K. A., Popuri, K., . . . Muss, H. B. (2017). Body Composition as a Predictor of Toxicity in Patients Receiving Anthracycline and Taxane-Based Chemotherapy for Early-Stage Breast Cancer. *Clin Cancer Res, 23*(14), 3537-3543. doi:10.1158/1078-0432.CCR-16-2266

Shaw, M. A., Ostap, E. M., & Goldman, Y. E. (2003). Mechanism of inhibition of skeletal muscle actomyosin by N-benzyl-p-toluenesulfonamide. *Biochemistry, 42*(20), 6128-6135. doi:10.1021/bi026964f

Shih, A., & Jackson, K. C., 2nd. (2007). Role of corticosteroids in palliative care. *J Pain Palliat Care Pharmacother, 21*(4), 69-76.

Shu, L., & Houghton, P. J. (2009). The mTORC2 complex regulates terminal differentiation of C2C12 myoblasts. *Mol Cell Biol, 29*(17), 4691-4700. doi:10.1128/MCB.00764-09

Shyh-Chang, N. (2017). Metabolic Changes During Cancer Cachexia Pathogenesis. *Adv Exp Med Biol, 1026*, 233-249. doi:10.1007/978-981-10-6020-5_11

Silveira, L. R., Pilegaard, H., Kusuhara, K., Curi, R., & Hellsten, Y. (2006). The contraction induced increase in gene expression of peroxisome proliferator-activated receptor (PPAR)-gamma coactivator 1alpha (PGC-1alpha), mitochondrial uncoupling protein 3 (UCP3) and hexokinase II (HKII) in primary rat skeletal muscle cells is dependent on reactive oxygen species. *Biochim Biophys Acta, 1763*(9), 969-976. doi:10.1016/j.bbamcr.2006.06.010

Simonini, A., Long, C. S., Dudley, G. A., Yue, P., McElhinny, J., & Massie, B. M. (1996). Heart failure in rats causes changes in skeletal muscle morphology and gene expression that are not explained by reduced activity. *Circulation, 79*, 128-136.

Sjoblom, B., Gronberg, B. H., Wentzel-Larsen, T., Baracos, V. E., Hjermstad, M. J., Aass, N., . . . Jordhoy, M. (2016). Skeletal muscle radiodensity is prognostic for survival in patients with advanced non-small cell lung cancer. *Clin Nutr, 35*(6), 1386-1393. doi:10.1016/j.clnu.2016.03.010

Smith, B. D., Smith, G. L., Hurria, A., Hortobagyi, G. N., & Buchholz, T. A. (2009). Future of cancer incidence in the United States: burdens upon an aging, changing nation. *J Clin Oncol, 27*(17), 2758-2765. doi:10.1200/jco.2008.20.8983

Smuder, A. J., Kavazis, A. N., Min, K., & Powers, S. K. (2011a). Exercise protects against doxorubicin-induced markers of autophagy signaling in skeletal muscle. *J Appl Physiol (1985), 111*(4), 1190-1198. doi:10.1152/japplphysiol.00429.2011

Smuder, A. J., Kavazis, A. N., Min, K., & Powers, S. K. (2011b). Exercise protects against doxorubicin-induced oxidative stress and proteolysis in skeletal muscle. *J Appl Physiol (1985), 110*(4), 935-942. doi:10.1152/japplphysiol.00677.2010

Stamenovic, D., Mijailovich, S. M., Tolic-Norrelykke, I. M., Chen, J., & Wang, N. (2002). Cell prestress. II. Contribution of microtubules. *Am J Physiol Cell Physiol, 282*(3), C617-624. doi:10.1152/ajpcell.00271.2001

Staron, R. S. (1997). Human skeletal muscle fiber types: delineation, development, and distribution. *Can J Appl Physiol, 22*(4), 307-327.

Stitt, T. N., Drujan, D., Clarke, B. A., Panaro, F., Timofeyva, Y., Kline, W. O., . . . Glass, D. J. (2004). The IGF-1/PI3K/Akt pathway prevents expression of muscle atrophy-induced ubiquitin ligases by inhibiting FOXO transcription factors. *Mol Cell, 14*(3), 395-403.

Strassmann, G., Fong, M., Kenney, J. S., & Jacob, C. O. (1992). Evidence for the involvement of interleukin 6 in experimental cancer cachexia. *J Clin Invest, 89*, 1681-1684.

Stuelsatz, P., Pouzoulet, F., Lamarre, Y., Dargelos, E., Poussard, S., Leibovitch, S., . . . Veschambre, P. (2010). Down-regulation of MyoD by calpain 3 promotes generation of reserve cells in C2C12 myoblasts. *J Biol Chem, 285*(17), 12670-12683. doi:10.1074/jbc.M109.063966

Sturgeon, K. M., Fisher, C., McShea, G., Sullivan, S. K., Sataloff, D., & Schmitz, K. H. (2018). Patient preference and timing for exercise in breast cancer care. *Support Care Cancer, 26*(2), 507-514. doi:10.1007/s00520-017-3856-8

Su, Z., Chen, M., Xiao, Y., Sun, M., Zong, L., Asghar, S., . . . Zhang, C. (2014). ROS-triggered and regenerating anticancer nanosystem: an effective strategy to subdue tumor's multidrug resistance. *J Control Release, 196*, 370-383. doi:10.1016/j.jconrel.2014.09.020

Sun, R., Zhang, S., Hu, W., Lu, X., Lou, N., Yang, Z., . . . Yang, H. (2016). Valproic acid attenuates skeletal muscle wasting by inhibiting C/EBPbeta-regulated atrogin1 expression in cancer cachexia. *Am J Physiol Cell Physiol, 311*(1), C101-115. doi:10.1152/ajpcell.00344.2015

Sustova, H., De Feudis, M., Reano, S., Alves Teixeira, M., Valle, I., Zaggia, I., . . . Filigheddu, N. (2019). Opposing effects of 25-hydroxy- and 1alpha,25-dihydroxy-vitamin D3 on pro-cachectic cytokine- and cancer conditioned medium-induced atrophy in C2C12 myotubes. *Acta Physiol (Oxf)*, e13269. doi:10.1111/apha.13269

Tan, B. H., Birdsell, L. A., Martin, L., Baracos, V. E., & Fearon, K. C. (2009). Sarcopenia in an overweight or obese patient is an adverse prognostic factor in pancreatic cancer. *Clin Cancer Res, 15*(22), 6973-6979. doi:10.1158/1078-0432.CCR-09-1525

Tan, B. H., & Fearon, K. C. (2008). Cachexia: prevalence and impact in medicine. *Curr Opin Clin Nutr Metab Care, 11*(4), 400-407. doi:10.1097/MCO.0b013e328300ecc1

Tang, J., He, A., Yan, H., Jia, G., Liu, G., Chen, X., . . . Zhao, H. (2018). Damage to the myogenic differentiation of C2C12 cells by heat stress is associated with up-regulation of several selenoproteins. *Sci Rep, 8*(1), 10601. doi:10.1038/s41598-018-29012-6

Tarnopolsky, M. A., Pearce, E., Smith, K., & Lach, B. (2011). Suction-modified Bergström muscle biopsy technique: Experience with 13,500 procedures. *Muscle Nerve, 43*(5), 716-725. doi:10.1002/mus.21945

Tegeder, I., Brautigam, L., Seegel, M., Al-Dam, A., Turowski, B., Geisslinger, G., & Kovacs, A. F. (2003). Cisplatin tumor concentrations after intra-arterial cisplatin infusion or embolization in patients with oral cancer. *Clin Pharm Ther, 73*, 417-426.

Thelen, M. H., Simonides, W. S., & van Hardeveld, C. (1997). Electrical stimulation of C2C12 myotubes induces contractions and represses thyroid-hormone-dependent transcription of the fast-type sarcoplasmic-reticulum Ca2+-ATPase gene. *Biochem J, 321 (Pt 3)*, 845-848.

Theologides, A. (1974). Generalized perturbations in host physiology caused by localized tumors. The anorexia-cachexia syndrome: a new hypothesis. *Ann N Y Acad Sci, 230*, 14-22.

Thirupathi, A., & Pinho, R. A. (2018). Effects of reactive oxygen species and interplay of antioxidants during physical exercise in skeletal muscles. *J Physiol Biochem, 74*(3), 359-367. doi:10.1007/s13105-018-0633-1

Timar, J. (2014). The clinical relevance of KRAS gene mutation in non-small-cell lung cancer. *Curr Opin Oncol, 26*(2), 138-144. doi:10.1097/CCO.0000000000000051

Tisdale, M. (2009). Mechanisms of cancer cachexia. *Physiol Rev, 89*, 381 - 410.

Tisdale, M. J. (2008). Catabolic mediators of cancer cachexia. *Curr Opin Support Palliat Care, 2*(4), 256-261.

Tisdale, M. J. (2010a). Are tumoral factors responsible for host tissue wasting in cancer cachexia? *Future Oncol, 6*(4), 503-513. doi:10.2217/fon.10.20

Tisdale, M. J. (2010b). Cancer cachexia. *Curr Opin Gastroenterol, 26*(2), 146-151. doi:10.1097/MOG.0b013e3283347e77

Toth, M. J., Gottlieb, S. S., Fisher, M. L., & Poehlman, E. T. (1997). Skeletal muscle atrophy and peak oxygen consumption in heart failure. *Am J Cardiol, 79*, 1267-1269.

Toth, M. J., Miller, M. S., Callahan, D. M., Sweeny, A. P., Nunez, I., Grunberg, S. M., . . . Dittus, K. (2013). Molecular mechanisms underlying skeletal muscle weakness in human cancer: reduced myosin-actin cross-bridge formation and kinetics. *J Appl Physiol, 114*, 858-868. doi:10.1152/japplphysiol.01474.2012

Toth, M. J., Ward, K., vand der Velden, J., Miller, M. S., VanBuren, P., LeWinter, M. M., & Ades, P. A. (2011). Chronic heart failure reduces Akt phosphorylation in human skeletal muscle: relationship to muscle size and function. *J Appl Physiol, 119*, 892-900.

Tsai, S., McOlash, L., Palen, K., Johnson, B., Duris, C., Yang, Q., . . . James, M. A. (2018). Development of primary human pancreatic cancer organoids, matched stromal and immune cells and 3D tumor microenvironment models. *BMC Cancer, 18*(1), 335. doi:10.1186/s12885-018-4238-4

Tsuchida, K. (2004). Activins, myostatin and related TGF-beta family members as novel therapeutic targets for endocrine, metabolic and immune disorders. *Curr Drug Targets Immune Endocr Metabol Disord, 4*(2), 157-166.

Tzika, A. A., Fontes-Oliveria, C. C., Shestova, A. A., Constantinou, C., Psychogios, N., Righi, V., . . . Argiles, J. M. (2013). Skeletal muscle mitochondrial uncoupling in a murine cancer cachexia model. *Int J Oncol, 43*, 886-894.

Vainshtein, A., Tryon, L. D., Pauly, M., & Hood, D. A. (2015). Role of PGC-1alpha during acute exercise-induced autophagy and mitophagy in skeletal muscle. *Am J Physiol Cell Physiol, 308*(9), C710-719. doi:10.1152/ajpcell.00380.2014

van Norren, K., Dwarkasing, J. T., & Witkamp, R. F. (2017). The role of hypothalamic inflammation, the hypothalamic-pituitary-adrenal axis and serotonin in the cancer anorexia-cachexia syndrome. *Curr Opin Clin Nutr Metab Care, 20*(5), 396-401. doi:10.1097/MCO.0000000000000401

Vanhoutte, G., van de Wiel, M., Wouters, K., Sels, M., Bartolomeeussen, L., De Keersmaecker, S., . . . Peeters, M. (2016). Cachexia in cancer: what is in the definition? *BMJ Open Gastroenterol, 3*(1), e000097. doi:10.1136/bmjgast-2016-000097

Velthuis, M. J., Agasi-Idenburg, S. C., Aufdemkampe, G., & Wittink, H. M. (2010). The effect of physical exercise on cancer-related fatigue during cancer treatment: a meta-analysis of randomised controlled trials. *Clin Oncol, 22*(3), 208-221. doi:http://dx.doi.org/10.1016/j.clon.2009.12.005

Villaseñor, A., Ballard-Barbash, R., Baumgartner, K., Baumgartner, R., Bernstein, L., McTiernan, A., & Neuhouser, M. (2012). Prevalence and prognostic effect of sarcopenia in breast cancer survivors: the HEAL Study. *J Cancer Surviv, 6*(4), 398-406. doi:10.1007/s11764-012-0234-x

Wang, J., Wang, F., Zhang, P., Liu, H., He, J., Zhang, C., . . . Chen, X. (2017). PGC-1alpha over-expression suppresses the skeletal muscle atrophy and myofiber-type composition during hindlimb unloading. *Biosci Biotechnol Biochem, 81*(3), 500-513. doi:10.1080/09168451.2016.1254531

Wang, Q., Lu, J. B., Wu, B., & Hao, L. Y. (2010). Expression and clinicopathologic significance of proteolysis-inducing factor in non-small-cell lung cancer: an immunohistochemical analysis. *Clin Lung Cancer, 11*(5), 346-351. doi:10.3816/CLC.2010.n.044

Wang, X., Hu, S., & Liu, L. (2017). Phosphorylation and acetylation modifications of FOXO3a: Independently or synergistically? *Oncol Lett, 13*(5), 2867-2872. doi:10.3892/ol.2017.5851

Waning, D. L., Mohammad, K. S., Reiken, S., Xie, W., Andersson, D. C., John, S., . . . Guise, T. A. (2015). Excess TGF-β mediates muscle weakness associated with bone metastases in mice. *Nat Med, 21*(11), 1262-1271. doi:10.1038/nm.3961

Whidden, M. A., Smuder, A. J., Wu, M., Hudson, M. B., Nelson, W. B., & Powers, S. K. (2010). Oxidative stress is required for mechanical ventilation-induced protease activation in the diaphragm. *J Appl Physiol (1985), 108*(5), 1376-1382. doi:10.1152/japplphysiol.00098.2010

White, J., Barro, M. V., Makarenkova, H. P., Sanger, J. W., & Sanger, J. M. (2014). Localization of sarcomeric proteins during myofibril assembly in cultured mouse primary skeletal myotubes. *Anat Rec (Hoboken), 297*(9), 1571-1584. doi:10.1002/ar.22981

White, J., Puppa, M., Sato, S., Gao, S., Price, R., Baynes, J., . . . Carson, J. (2012). IL-6 regulation on skeletal muscle mitochondrial remodeling during cancer cachexia in the ApcMin/+ mouse. *Skelet Muscle, 2*(1), 14.

White, J. P., Baltgalvis, K. A., Puppa, M. J., Sato, S., Baynes, J. W., & Carson, J. A. (2011). Muscle oxidative capacity during IL-6-dependent cancer cachexia. *Am J Physiol, 300*(2), R201-R211. doi:10.1152/ajpregu.00300.2010

White, J. P., Puppa, M. J., Gao, S., Sato, S., Welle, S. L., & Carson, J. A. (2013). Muscle mTORC1 suppression by IL-6 during cancer cachexia: a role for AMPK. *Am J Physiol Endocrinol Metab, 304*(10), E1042-E1052.

White, J. P., Puppa, M. J., Gao, S., Sato, S., Welle, S. L., & Carson, J. A. (2013). Muscle mTORC1 suppression by IL-6 during cancer cachexia: a role for AMPK. *Am J Physiol Endocrinol Metab, 304*(10), E1042-1052. doi:10.1152/ajpendo.00410.2012

Wilkinson, S. B., Phillips, S. M., Atherton, P. J., Patel, R., Yarasheski, K. E., Tarnopolsky, M. A., & Rennie, M. J. (2008). Differential effects of resistance and endurance exercise in the fed state on signalling molecule phosphorylation and protein synthesis in human muscle. *J Physiol, 586*(15), 3701-3717. doi:10.1113/jphysiol.2008.153916

Winters-Stone, K. M., Dobek, J. C., Bennett, J. A., Dieckmann, N. F., Maddalozzo, G. F., Ryan, C. W., & Beer, T. M. (2015). Resistance training reduces disability in prostate cancer survivors on androgen deprivation therapy: evidence from a randomized controlled trial. *Arch Phys Med Rehabil, 96*(1), 7-14. doi:10.1016/j.apmr.2014.08.010

Wirtschafter, J. D., & McLoon, L. K. (1998). Long-term efficacy of local doxorubicin chemomyectomy in patients with blepharospasm and hemifacial spasm. *Ophthalmology, 105*(2), 342-346.

Witkowski, S., Lovering, R. M., & Spangenburg, E. E. (2010). High-frequency electrically stimulated skeletal muscle contractions increase p70s6k phosphorylation independent of known IGF-I sensitive signaling pathways. *FEBS Lett, 584*(13), 2891-2895. doi:10.1016/j.febslet.2010.05.003

Wojtala, A., Bonora, M., Malinska, D., Pinton, P., Duszynski, J., & Wieckowski, M. R. (2014). Methods to monitor ROS production by fluorescence microscopy and fluorometry. In G. Lorenzo & K. Guido (Eds.), *Methods in Enzymology* (Vol. Volume 542, pp. 243-262): Academic Press.

Wolfe, R. R. (2006). Skeletal muscle protein metabolism and resistance exercise. *J Nutr, 136*(2), 525S-528S. doi:10.1093/jn/136.2.525S

Wu, C. T., Liao, J. M., Ko, J. L., Lee, Y. L., Chang, H. Y., Wu, C. H., & Ou, C. C. (2019). D-Methionine Ameliorates Cisplatin-Induced Muscle Atrophy via Inhibition of Muscle Degradation Pathway. *Integr Cancer Ther, 18*, 1534735419828832. doi:10.1177/1534735419828832

Xiao, D. Y., Luo, S., O'Brian, K., Sanfilippo, K. M., Ganti, A., Riedell, P., . . . Carson, K. R. (2016). Longitudinal Body Composition Changes in Diffuse Large B-cell Lymphoma Survivors: A Retrospective Cohort Study of United States Veterans. *J Natl Cancer Inst, 108*(11). doi:10.1093/jnci/djw145

Xu, H., Lyu, X., Yi, M., Zhao, W., Song, Y., & Wu, K. (2018). Organoid technology and applications in cancer research. *J Hematol Oncol, 11*(1), 116. doi:10.1186/s13045-018-0662-9

Yaffe, D., & Saxel, O. (1977). Serial passaging and differentiation of myogenic cells isolated from dystrophic mouse muscle. *Nature, 270*(5639), 725-727.

Yakovenko, A., Cameron, M., & Trevino, J. G. (2018). Molecular therapeutic strategies targeting pancreatic cancer induced cachexia. *World J Gastrointest Surg, 10*(9), 95-106. doi:10.4240/wjgs.v10.i9.95

Yamamoto, Y., Hoshino, Y., Ito, T., Nariai, T., Mohri, T., Obana, M., . . . Azuma, J. (2008). Atrogin-1 ubiquitin ligase is upregulated by doxorubicin via p38-MAP kinase in cardiac myocytes. *Cardiovasc Res, 79*(1), 89-96. doi:10.1093/cvr/cvn076

Yan, Z., Lira, V. A., & Greene, N. P. (2012). Exercise training-induced regulation of mitochondrial quality. *Exerc Sport Sci Rev, 40*(3), 159-164. doi:10.1097/JES.0b013e3182575599

Yano, C. L., Ventrucci, G., Field, W. N., Tisdale, M. J., & Gomes-Marcondes, M. C. (2008). Metabolic and morphological alterations induced by proteolysis-inducing factor from Walker tumour-bearing rats in C2C12 myotubes. *BMC Cancer, 8*, 24. doi:10.1186/1471-2407-8-24

Ydfors, M., Fischer, H., Mascher, H., Blomstrand, E., Norrbom, J., & Gustafsson, T. (2013). The truncated splice variants, NT-PGC-1alpha and PGC-1alpha4, increase with both endurance and resistance exercise in human skeletal muscle. *Physiol Rep, 1*(6), e00140. doi:10.1002/phy2.140

Yi, M., Weaver, D., & Hajnóczky, G. (2004). Control of mitochondrial motility and distribution by the calcium signal. *J Cell Biol, 167*(4), 661.

Yi, T., Vick, J. S., Vecchio, M. J., Begin, K. J., Bell, S. P., Delay, R. J., & Palmer, B. M. (2013). Identifying cellular mechanisms of zinc-induced relaxation in isolated cardiomyocytes. *Am J Physiol Heart Circ Physiol, 305*(5), H706-715. doi:10.1152/ajpheart.00025.2013

Yoshimura, T., Saitoh, K., Sun, L., Wang, Y., Taniyama, S., Yamaguchi, K., . . . Hirasaka, K. (2018). Morin suppresses cachexia-induced muscle wasting by binding to ribosomal protein S10 in carcinoma cells. *Biochem Biophys Res Commun, 506*(4), 773-779. doi:10.1016/j.bbrc.2018.10.184

You, J. S., Anderson, G. B., Dooley, M. S., & Hornberger, T. A. (2015). The role of mTOR signaling in the regulation of protein synthesis and muscle mass during immobilization in mice. *Dis Model Mech, 8*(9), 1059-1069. doi:10.1242/dmm.019414

Zasadil, L. M., Andersen, K. A., Yeum, D., Rocque, G. B., Wilke, L. G., Tevaarwerk, A. J., . . . Weaver, B. A. (2014). Cytotoxicity of paclitaxel in breast cancer is due to chromosome missegregation on multipolar spindles. *Sci Transl Med, 6*(229), 229ra243-229ra243. doi:10.1126/scitranslmed.3007965

Zhang, G., Jin, B., & Li, Y. P. (2011). C/EBPbeta mediates tumour-induced ubiquitin ligase atrogin1/MAFbx upregulation and muscle wasting. *EMBO J, 30*(20), 4323-4335. doi:10.1038/emboj.2011.292

Zhang, G., & Li, Y. P. (2012). p38beta MAPK upregulates atrogin1/MAFbx by specific phosphorylation of C/EBPbeta. *Skelet Muscle, 2*(1), 20. doi:10.1186/2044-5040-2-20

Zhang, G., Lin, R. K., Kwon, Y. T., & Li, Y. P. (2013). Signaling mechanism of tumor cell-induced up-regulation of E3 ubiquitin ligase UBR2. *FASEB J, 27*(7), 2893-2901. doi:10.1096/fj.12-222711

Zhang, G., Liu, Z., Ding, H., Miao, H., Garcia, J. M., & Li, Y. P. (2017). Toll-like receptor 4 mediates Lewis lung carcinoma-induced muscle wasting via coordinate activation of protein degradation pathways. *Sci Rep, 7*(1), 2273. doi:10.1038/s41598-017-02347-2

Zhang, G., Liu, Z., Ding, H., Zhou, Y., Doan, H. A., Sin, K. W. T., . . . Li, Y. P. (2017). Tumor induces muscle wasting in mice through releasing extracellular Hsp70 and Hsp90. *Nat Commun, 8*(1), 589. doi:10.1038/s41467-017-00726-x

Zhang, Y., Uguccioni, G., Ljubicic, V., Irrcher, I., Iqbal, S., Singh, K., . . . Hood, D. A. (2014). Multiple signaling pathways regulate contractile activity-mediated PGC-1alpha gene expression and activity in skeletal muscle cells. *Physiol Rep, 2*(5). doi:10.14814/phy2.12008

Zhao, J., Brault, J. J., Schild, A., Cao, P., Sandri, M., Schiaffino, S., . . . Goldberg, A. L. (2007). FoxO3 coordinately activates protein degradation by the autophagic/lysosomal and proteasomal pathways in atrophying muscle cells. *Cell Metab, 6*(6), 472-483. doi:10.1016/j.cmet.2007.11.004

Zheng, B., Ohkawa, S., Li, H., Roberts-Wilson, T. K., & Price, S. R. (2010). FOXO3a mediates signaling crosstalk that coordinates ubiquitin and atrogin-1/MAFbx expression during glucocorticoid-induced skeletal muscle atrophy. *FASEB J, 24*(8), 2660-2669. doi:10.1096/fj.09-151480

Zhou, D., Xie, M., He, B., Gao, Y., Yu, Q., He, B., & Chen, Q. (2017). Microarray data re-annotation reveals specific lncRNAs and their potential functions in non-small cell lung cancer subtypes. *Mol Med Rep, 16*(4), 5129-5136. doi:10.3892/mmr.2017.7244